TO

MY PARENTS
MY WIFE
AND MY CHILDREN

ACKNOWLEDGEMENTS

The author wishes to express his gratitude to Professor G V Jeffreys and Dr C J Mumford for their supervision, encouragement, continual help and constructive criticism throughout the course of this work.

The author also wishes to thank Mr N Roberts and the entire staff of the Workshop, Analytical Laboratory and Stores, Mr J Holloway for his assistance with photographic work and Miss Ann Ferry for diligent typing of this thesis.

Particular gratitude is due to my parents for their encouragement and financial help and to my wife for her understanding, encouragement and moral help.

Finally, thanks are due to Basrah University, Iraq for their financial support.

THE UNIVERSITY OF ASTON IN BIRMINGHAM

"Mass Transfer Characteristics of Large Oscillating Drops"

Mustafa Muhammed Rida Malalah Al-Faize February 1986

SUMMARY

The literature related to mass transfer of solute from large, oscillating drops in liquid-liquid systems has been critically reviewed.

A thermostatically-controlled spray column, provided with mirrors, was used to study the hydrodynamics and mass transfer characteristics of single large oscillating drops and drop pairs ascending through water. Up to 25%w/w of acetone was dissolved in toluene, which facilitated investigation of the effect of physical properties upon the frequency and amplitude of drop oscillation and the mass transfer rate. Glass or ptfe nozzles were used to create single, or pairs of, drops ($d \geq 5$mm) and their behaviour was investigated, during formation, and during travel. The frequency of droplet oscillation, area change, amplitude and vertical velocities were recorded using either video or high speed cine photography.

The range of shapes of large oscillating drops ($d \geq 6$mm) and drop pairs were geometrically indefinable and the mode of oscillation was 2, 3 or 4. The frequency of oscillation of drop pairs was best correlated by

$$\omega^2 = 2.8\,(We)^{0.40}\,Q$$

but both the amplitude and frequency of oscillation of droplet pairs were less than for single drops.

Published correlations for overall mass transfer coefficients during formation, underestimated the experimental coefficients by 22% for single drops and 55% for drop pairs. A new model formulated for the overall mass transfer coefficient, with the droplet surface area expressed as a function of time of formation,

$$A = \int_0^t (C + a_1 x + a_2 x^2)\,dt$$

correlated overall mass transfer coefficients for drop pairs within 5%.

Experimental data for single oscillating drops and drop pairs during travel confirmed the limitations of existing models. An enhancement of overall mass transfer coefficient of up to 88% was observed due to collision-rebound effects with drop pairs. A new correlation was developed to account for the effect of drop interactions.

$$k_d = 1.32\,(We)^{0.177}\,(Re)^{0.190}\,(\omega_{corr}\,D_d)^{0.5}$$

Agreement within 9% was obtained between experimental overall mass transfer coefficients and those predicted from theory where k_d was predicted from this correlation and k_c from Garner and Tayeban's correlation for oscillating drops.

Key words: Oscillating Drops, Liquid-Liquid Extraction

CONTENTS

Page No.

Page No.

LIST OF FIGURES

Figure No. Page No.

LIST OF TABLES

CHAPTER ONE

INTRODUCTION

Liquid-liquid extraction, and other operations which require a knowledge of droplet behaviour during a process of mass transfer, have become increasingly important in recent years. The droplet formation, droplet motion and solute transfer mechanisms involved may however be complex. For example liquid-liquid extraction entails the dispersion of one liquid as a swarm of droplets with a distribution of sizes into a continuous phase followed by solute transfer to, or from, the droplets during their residence time in a contactor. This is followed by separation of the dispersed phase by flocculation and a combination of interdrop and drop-interface coalescence.

Extraction is classified as an 'indirect' mass transfer operation because it utilizes the addition of a foreign substance, the solvent, which is immiscible, or only partially miscible, with both phases. Mass transfer between the phases is invariably facilitated by dispersion of either phase in the form of drops in order to establish conditions for a high mass transfer rate. The process depends upon the driving force ΔC, ie. the non-equilibrium distribution of the solute to be separated, which varies with the movement through the continuous phase and may be reduced by axial mixing.

For a given driving force a high rate of mass transfer depends principally on the dispersion providing a large interfacial area per unit volume, and upon a high overall mass transfer coefficient.

$$N_A = K\,A\,\Delta C \qquad (1.1)$$

N_A is the rate of solute transfer in moles per unit time. K is the overall mass transfer coefficient which is dependent on the series resistance to diffusion inside the drop, outside the drop and possibly at the interface, and is expressed mathematically by:

$$\frac{1}{K_d} = \frac{1}{k_d} + \frac{m}{k_c} \tag{1.2}$$

and,

$$\frac{1}{K_c} = \frac{1}{k_c} + \frac{1}{m' k_d} \tag{1.3}$$

where m, m', are the distribution coefficients. To maximise the rate of mass transfer an attempt is generally made to create a large interfacial area A. The total interfacial area depends upon the drop size distribution and the dispersed phase hold-up since the interfacial area per unit volume is given by

$$a = \frac{6x}{d_{32}} \tag{1.4}$$

where x is the hold-up and d_{32} the specific surface diameter. The total interfacial area is given by

$$A = aV \tag{1.5}$$

where V is the extractor volume.However whilst sub-division into microsize droplets can create an enormous interfacial area, such a fine dispersion creates difficulties for recovery of the phases. Furthermore droplet mass transfer mechanisms become less favourable with decreasing drop size. Therefore there is an optimum drop size below which the characteristics of the dispersion become undesirable.

In gravity columns which are the subject of this study the rate of mass transfer varies during the three distinct stages in the life of any drop namely, drop formation, drop movement through the continuous phase and finally drop coalescence at the interface. A knowledge of the behaviour of the droplet during formation is important for two reasons:

a) A considerable amount of extraction may occur during formation due to the generation of new interfacial area, and

b) In the absence of further drop break-up due to turbulence or impact with packings, or coalescence effects, the surface area which will be available during the rise (or fall) of the drop is determined by the size of the droplet which separates from a nozzle or perforated distributor during formation.

Unfortunately there is little agreement between the results of various workers on the prediction of the overall mass transfer coefficient during drop formation, due in part to the difficulty in establishing a suitable experimental technique and also to the difficulty of accounting for the effects of interfacial area and turbulence changes.

Drops rising, or falling, show several interesting phenomena as they pass through the continuous phase. The liquid inside may remain stagnant or possess internal circulation, or the drops may deform and oscillate. The terminal velocity and mass transfer rate are both related to these phenomena. The terminal velocity of rise, or fall, is the constant velocity the drop will attain when the forces inside and outside are balanced. As the drop size increases a point is reached at which the drop flattens, because of the action of frontal drag, which tends to flatten it to an ellipsoidal shape. However because of the interfacial tension, which tends to retain it in a spherical shape, the drop starts to oscillate, particularly in a low viscosity continuous phase. Such oscillations greatly increase the rate of mass and heat transfer between the moving drop and its field fluid.

When a drop travels through a continuous phase it develops a wake; these wakes are usually invisible and their existence has tended to be neglected. The drop Reynolds number has a marked effect on the characteristics. At high Reynolds number ~ 800, when the drop oscillates vigorously, wake shedding is predominant.

Many investigators have studied the frequency and amplitude of droplet oscillation, but there is no widely-accepted correlation for these phenomena, especially when mass transfer is taking place which is the practical situation. Furthermore, all the work to date has been with single, uniform, large oscillating liquid drops and not with a number of uniform-sized, large oscillating liquid drops, ie. a situation approximating more closely to the swarms in practical columns.

The present study followed Al Hassan's (1) work on mass transfer from large oscillating single droplets, with the intention of extending it to the interactions between multiple large oscillating drops. Such interactions may arise from collision of any adjacent drops which travel together, or collision and coalescence of any pair of drops in parallel, or transmission of the effects between drops less than some critical distance apart. Such phenomena have been considered and studied experimentally, to assist the understanding of gravity column operation and, eventually, to, lead to more accurate design methods. A novel contribution has also been made to the prediction of mass transfer coefficient during droplet formation as a function of interfacial area generation. The interpretation of mass transfer mechanisms during travel may eventually be applicable to more complex columns, eg. packed or perforated plate columns, but not to agitated contactors since the drop sizes are too small.

CHAPTER 2

DROPLET HYDRODYNAMICS IN LIQUID-LIQUID SYSTEMS

The hydrodynamic characteristics of droplets have an important effect upon mass transfer rates. Previous workers have found that Reynolds number alone is insufficient to classify the different behaviour of drops during their travel in the continuous phase. Therefore, Weber, Strouhal, Schmidt and Sherwood numbers, or other groups of physical properties (Table 2.1) may also be included to characterise the drop's behaviour. The effect of different values of these dimensionless groups on the behaviour of drops is explained in Chapter 3.

Previous workers reported that complex interactions and other property characteristics should be considered, in addition to Reynolds number, in order to classify the hydrodynamic state of drops. However droplet Reynolds number has been used as a rough guide to the hydrodynamic state of drops as follows;

i) Stagnant, or rigid droplets when $Re < 1.0$
ii) Circulating droplets when $1.0 \leq Re \leq 200$
iii) Oscillating droplets when $Re \geq 200$

The situation in any practical extractor is therefore complicated since a drop-size distribution may be present which includes drops in each regime (2, 3). In the present investigation, to study the mass transfer in a spray column based on droplet phenomena, it was necessary to create individual drops or drop pairs, repetitively from the same nozzles, so the drop size formed remained equal within each experiment. Hence the drops were in only one of the above hydrodynamic states.

Table 2.1 Dimensionless groups related to droplet behaviour

Dimensionless Groups	Definition
Reynolds Number	$Re = \frac{V d_e \rho}{\mu_c}$
Modified Reynolds Number	$\bar{R}e = \frac{\rho_c \omega d_e^2}{\mu_c}$
Schmidt Number	$Sc = \frac{\mu}{\rho D}$
Sherwood Number	$Sh = \frac{k d_e}{D}$
Strouhal Number	$S_r = \frac{\omega d_e}{V}$
Weber Number	$We = \frac{d_e V^2 \rho}{\sigma}$
Galileo Number	$Ga = \frac{d_e^3 \rho^2 g}{\mu^2}$
Peclet Number	$Pe = \frac{d_e V}{D}$
Eotvos Number	$Eo = \frac{g \Delta \rho d^2{}_e}{\sigma}$
Morton Number	$M = \frac{g \mu^4 \Delta \rho}{\rho^2 \sigma^3}$
Ohnesorge Number	$Oh = (\frac{\mu_d}{\rho_d \sigma d_e})^{0.5}$

2.1 STAGNANT DROPLETS

Stagnant droplets are generally very small droplets, usually < 1mm in diameter, which exhibit no internal circulation when moving through a low viscosity continuous phase. In most cases, liquid drops of small diameter move faster than rigid spheres of the same size and density, because of;

a. The lower drag coefficient for a liquid drop than for a rigid sphere.

b. The mobility of the liquid drop surface.

Stokes (4) solved the equation of motion for a rigid sphere in a Newtonian field-fluid (Figure 2.3). The net drag force obtained from this solution is given by;

$$F = 3\pi d \mu_c V \tag{2.1}$$

Two-thirds of the total drag force results from shear stress exerted by the continuous phase fluid at the surface; the remaining one-third is due to form drag.

The drag coefficient is defined as:

$$C_D = \frac{F/A}{0.5 \rho_c V^2} \tag{2.2}$$

From Equation 2.1 and 2.2 this gives:

$$C_D = \frac{24}{d V \rho_c / \mu_c} \tag{2.3}$$

$$= \frac{24}{Re} \tag{2.4}$$

Small droplets < 1.0mm in diameter are spherical in shape, ie. the internal liquid is stagnant, and the terminal velocity can be estimated from the equation of motion of solid spheres (5). The terminal velocity increases steadily with increasing diameter.

However many workers found that the equation of motion for solid spheres does not explain the motion of liquid drops even when they are spherical, because of the mobility of the drop surface. Hadamard (6), Rybezynski (7) and later Boussinesq (8) reported that the velocity of the drop whose interface is mobile:

$$V = \left[\frac{\mu_d + \mu_c}{\mu_d + 0.67\,\mu_c} \right] V_{\text{stokes}} \tag{2.5}$$

Therefore the velocity depends upon the viscosity of both phases:

$$V = 1.50\, V_{\text{Stokes}} \text{ when } \mu_d << \mu_c$$

eg. gas bubble rising in a liquid.

$$V = 1.23\, V_{\text{Stokes}} \text{ when } \mu_d = \mu_c$$

eg. liquid drop rising in a liquid.

$$V = V_{\text{Stokes}} \text{ when } \mu_d >> \mu_c$$

eg. liquid drop falling through a gas.

2.2 CIRCULATING DROPLETS

The essential differences between a rigid and fluid sphere are the internal circulation and mobile interface associated with the latter. The total interfacial area for mass transfer from a rigid sphere to the surrounding fluid phase remains constant except for slight changes due to sublimation or dissolution. However interfacial area is continuously created on the upstream half of a circulating fluid sphere and continuously destroyed on the downstream hemisphere (Figure 2.1). Other investigators (9, 10) showed that circulating drops move more rapidly than the equivalent solid spheres. The presence of very small traces of impurities which are surface active may inhibit internal circulation (11, 12). The circulation inside the drops is also greatly affected by Reynolds

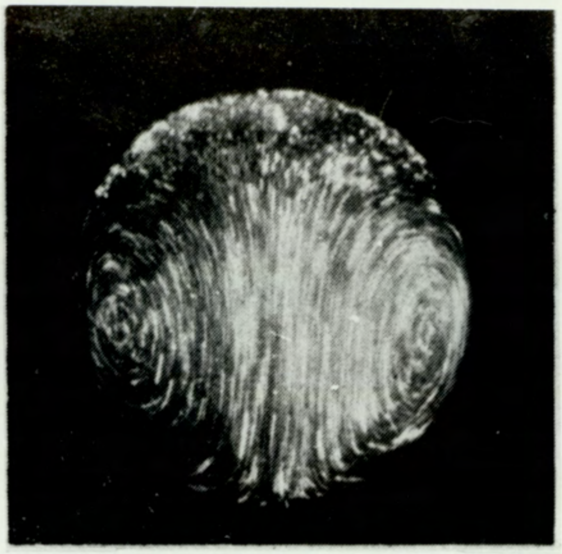

Drop Diameter 1.21cm
Falling Speed 0.62cm/sec
Exposure 1 sec

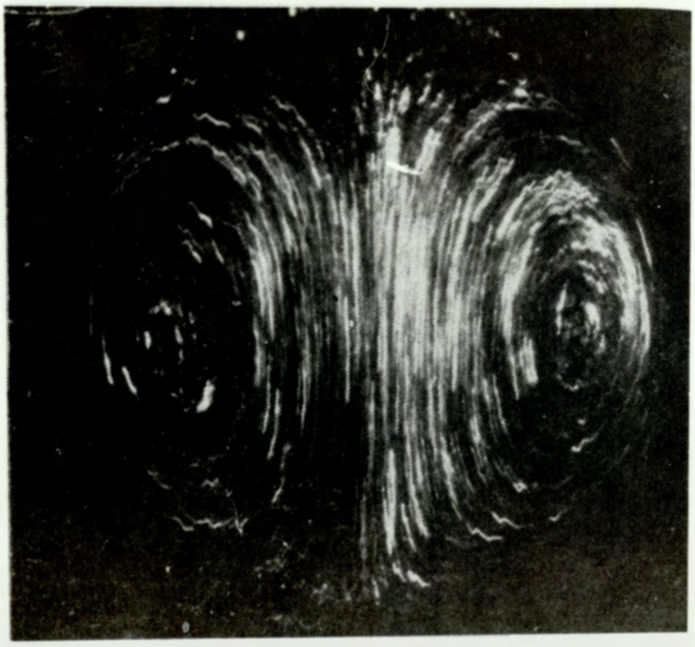

Drop Diameter 1.77cm
Falling Speed 1.16cm/sec
Exposure 1/2sec

Fig. 2.1 Internal circulation in a water drop falling through castor oil (99).

number (ie. it may start at any value of Re ≤ 200), depending upon;

i) Viscosities of continuous and dispersed phases.

ii) Interfacial tension between the two phases.

iii) Drop diameter.

Harriott (13) found that the circulation velocity increased with the diameter of the drop, and with the ratio of external to internal viscosity. Droplets of a given system did not circulate below a certain size.

Circulation will be damped out with the following factors;

i) Reynolds number > 200, when a turbulent flow regime exists and oscillations start.

ii) Higher values of interfacial tension.

iii) The presence of very small traces of impurities.

Bond and Newton (14) presented a relation for the critical size at which circulation begins. They also found that, whilst small bubbles and drops followed Stoke's Law, with increasing diameter there was a rather sharp increase in velocity towards the Hadmard-Rybezynski value. They (14) proposed that terminal circulation could only occur for $E_O > 4$, known as the "Bond Criterion". This proposal gave fair agreement with observed bubble or drop sizes for which the terminal velocity was midway between Stokes and Hadmard-Rybezynski values.

Boussinesq (15) considered the lack of internal circulation in bubbles and drops to be due to an interfacial monolayer which acts as a viscous membrane. For limited droplet viscosities and interfacial tension ranges, Garner and Skelland (16) developed a modified Reynolds number (Table 2.1) which must be exceeded in order for circulation to start.

Kintner et al (17) used a tapered tube in order to follow the behaviour of drops by recording the semi-vectorial velocities. They found that internal circulation was slowly damped out as the interface changed its character and became more contaminated. The concept by Hadamard and Rybezynski (6, 7) of a fully-circulating fluid sphere has been the basis for comparison of all work subsequently published. They reported that the fluid sphere terminal velocity should be up to 50% higher than that of a rigid sphere of the same size and density.

2.3 OSCILLATING DROPLETS

As drop size is increased beyond the laminar-flow region, generally at a drop diameter of about 3.0mm and when the Reynolds number exceeds 200, the drop flattens and assumes;

a) An "ellipsoidal" shape. The term ellipsoidal generally refers to drops which are oblate with a convex interface around the entire surface (Figure 4.2).

or b) A "spherical-cap" or "ellipsoidal-cap" shape. Such large drops may resemble segments cut from spheres or from oblate spheroids of low eccentricity. In these cases the terms "spherical-cap" and "ellipsoidal-cap" are used (Figure 4.1).

Such droplet shapes are unstable in a field of low viscosity and therefore the drop begins to oscillate.

To show the different shapes of the drops rising, or falling freely, in an infinite medium, Figure 2.2, Grace (18) and Grace et al (19) proposed a graphical correlation in terms of the Eotvos number (E_o), Morton number (M) and Reynolds number (Re). The cause of the onset of this oscillation is not yet fully understood. However Gunn (20) suggested that oscillations would start when the periodic force produced by the detachment of wake eddies was of a frequency to self-excite vibrations. Droplet oscillations are not necessarily restricted to oblate-prolate, or spherical-oblate oscillation as in Figure 2.2. As droplet size increases beyond the point where oscillations begin, the droplet oscillation tends towards a more random fluctuation in shape.

Garner and Tayeban (21), found that for a given droplet size, the extent of oscillation is greater for a system with a low value of continuous phase viscosity. Garner and Haycock (22) found that the period of oscillation for a liquid-liquid system

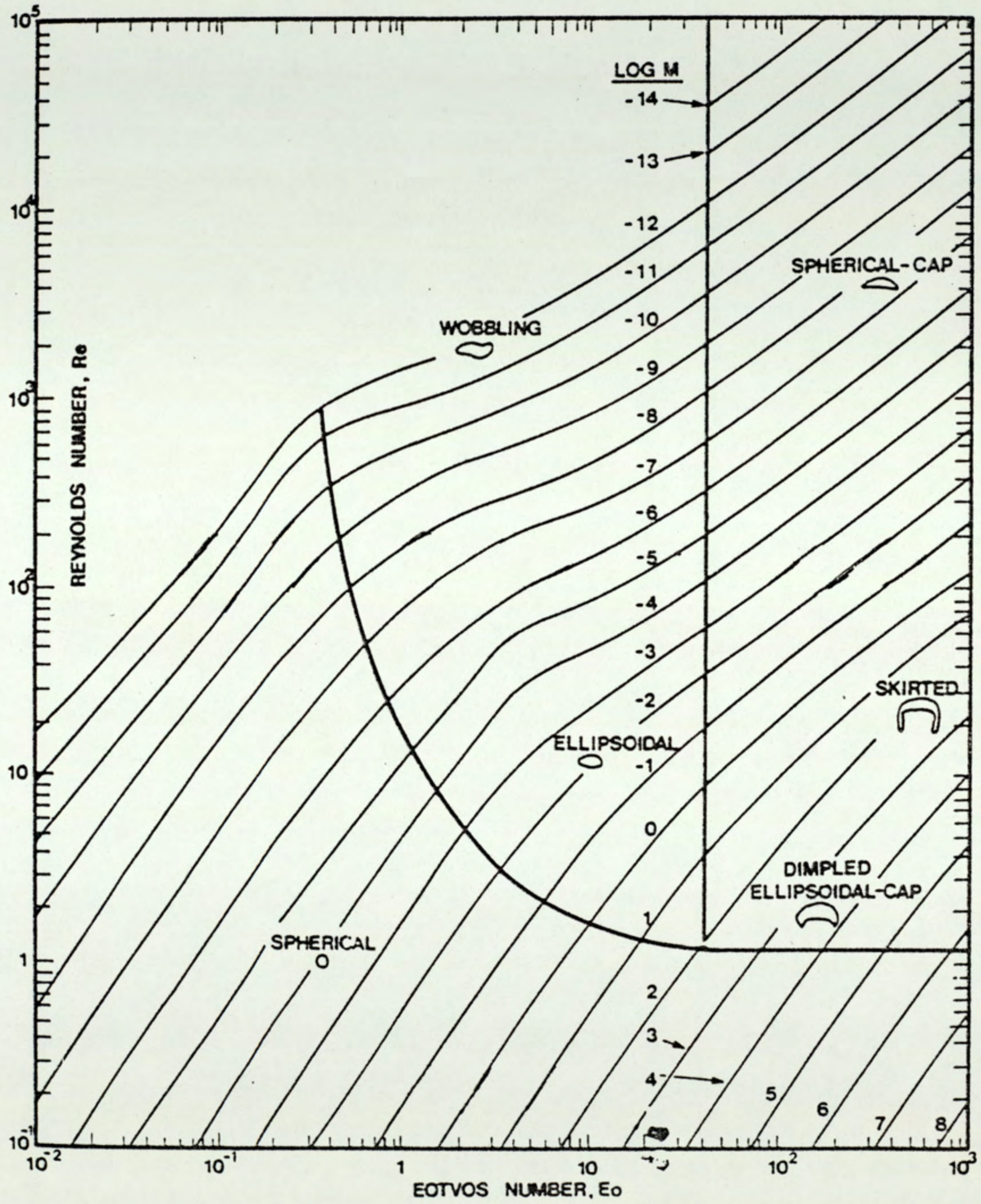

Fig. 2.2 Shape regimes for bubbles and drops in unhindered gravitational motion through liquids (19).

depends upon its physical properties, in particular the densities of both phases. Johnson and Hamielec (23) reported that once oscillations were set up in drops the effective diffusivities were as much as 52 times greater than the molecular value. Garner and Skelland (16) reported that the rate of mass transfer of an oscillating nitro-benzene drop in water was 100% greater than for an equivalent stagnant drop. Oscillation may be initiated by the tearing-away of the droplet from the forming device, or by intermittent shedding of vortices from the droplet wakes (24, 25). This conflicts with Winnikow et al's (26) observation that droplet oscillation started at some distance from the nozzle, and this distance decreased as the droplet size increased.

Rayleigh (29) proposed the following expression for frequency of oscillation:

$$a_n = b_n \cos \omega t \tag{2.6}$$

$$\omega^2 = \frac{n\,(n-1)\,(n+1)\,\sigma}{\rho_d\, r^3{}_d} \tag{2.7}$$

where n is the mode of oscillation and a values of n = 0 or 1 correspond to rigid body motion. Later Foote (27) found a good agreement with Rayleigh's theory for small amplitude oscillations, and by taking the same amplitude for each mode described the four lowest normal modes of vibration, Figure 2.4. Lamb (28) modified the solution of Rayleigh (29) for the general case of a continuous phase fluid of any density, and obtained,

$$\omega^2 = \frac{n\,(n+1)\,(n-1)\,(n+2)\sigma}{[(n+1)\,\rho_d + n\rho_c]\, r_d{}^3} \tag{2.8}$$

Schroeder and Kintner (30) studied nineteen liquid-liquid systems and introduced an amplitude factor into the Lamb equation. They reported that the discrepancy between their results and those predicted was not due to wall effects, viscosity, or velocity of fall, but to the amplitude of oscillation. They also observed that the oscillation did not damp out, contrary to the reports of many workers (5, 31, 32). Their modification for the frequency of oscillation is:

$$\omega^2 = \frac{n\,\sigma\,b_1}{r^3_d}\left[\frac{(n+1)(n-1)(n+2)}{[(n+1)\rho_d + n\rho_c]}\right] \tag{2.9}$$

where;

$$b_1 = 1 - \left[\frac{d_{max} - d_{min}}{2d_{avg}}\right] \tag{2.10}$$

The empirical correlation for "b_1" was:

$$b_1 = \frac{de^{0.225}}{1.242} \tag{2.11}$$

They also reported that, the presence of a vortex trail acted as a driving force for oscillation frequency. The experimental data of Davies (33) and Winnikow and Chao (26) demonstrate that the frequency of oscillation and the frequency of wake vortex shedding approach each other quite closely at high Reynolds number. Many investigators have used Weber number as a guide to distinguish between oscillating and non-oscillating liquid drops, Table 2.2.

Table 2.2 Values of Weber number at which drops commence oscillation

Author and Reference	Weber Number
Hartunian et al (34)	1.59
Winnikow et al (26)	4.75
Hu and Kintner (35)	4.46
Edge and Grant (36)	4.08

Finally Edge and Grant (36) used a transition Ohnesorge number to predict the transition from non-oscillating to oscillating drops based on the relationship.

$$de_t = \frac{0.162}{(\Delta\rho/\rho_d)^{0.5}} \tag{2.12}$$

Their experimental results were correlated by the empirical equation:

$$\frac{(\omega^* - \omega)}{(\omega^* - \omega)_t} = \frac{de_t}{d_e^2} \tag{2.13}$$

where ω* is predicted from Lamb's equation (2.9) and

$$(\omega^* - \omega)_t = 2.65 \left[\frac{\Delta\rho}{\rho_d}\right]^{0.8} \text{cycles/sec} \tag{2.14}$$

2.4 VELOCITY OF MOVING DROPS

The terminal velocity of drops has been measured by many investigators but, owing to the difficulty of obtaining accurate data, the results are conflicting.

Bond (37) and Bond and Newton (14) have shown that for a small drop 1.0mm in diameter, the rate of descent is very close to the value for rigid spheres given by Stoke's Law. After a certain size however the rate of descent deviates from Stoke's Law and approximates more closely to that predicted by Hadamard (6), and Rybezynski (7) who applied a correction taking into account viscosity and surface tension.

Hu and Kintner (35) studied the fall of 10 different organic liquid drops through water and presented a correlation of their data with Weber group, the Reynolds number between (10-2200) and the friction factor (Equation 2.19). The kind of motion the drop experiences critically affects the rates of mass and heat transfer between the phases. However there is little mention in the literature of droplet hydrodynamics when mass transfer is taking place.

Any quantitative hydrodynamic consideration of a drop moving in a liquid field starts with the Navier-Stokes equations of motion. For a 'rigid' liquid these equations reduce to:

$$V_{Stokes} = \frac{d^2}{18\,\mu_c}(\rho_d - \rho_c)\,g \qquad (2.15)$$

For a spherical drop moving in a liquid field where the boundary is not rigid the velocity is represented by equation 2.5.

Licht and Narasimhamurty (38) have confirmed the correlation of Hu and Kintner (35) with 10% error due to the methods of timing employed and the different physical properties of the liquids used. A typical plot of terminal velocity of rise, or fall, of a drop of oil in water is shown in Figure 2.3. For very pure systems, the relevant curve is ABCD, with poor internal circulation of the smallest drop (region 'A'). At 'B' and 'C' the drop fluid circulates freely internally, and the drop moves considerably faster than a rigid sphere, due to the mobility of the drop phase. After region 'C' the velocity decreases due to oscillation and deformation. Thorson et al (39) presented terminal velocities for high interfacial tension systems for Re at 40 to 900, and proposed the following formula:

$$V = \frac{6.5}{1.65 - \left(\dfrac{\Delta\rho}{\rho_d}\right)} \left. \sqrt{\frac{\sigma}{(3\,\rho_d + 2\,\rho_c)}} \middle/ \sqrt{d} \right. \qquad (2.16)$$

Droplets travel in helical spirals when the Reynolds number is above 300, because of the induction of alternate detachment of vortices at the rear of the drop (40). This deviation will be less for large drops.

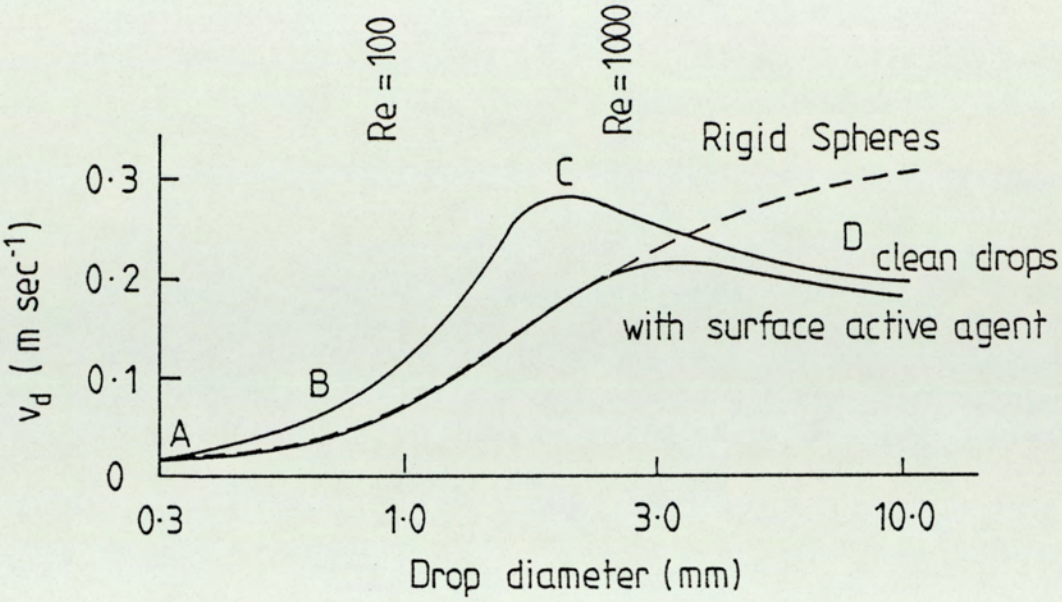

Figure 2·3 Terminal Velocity of Rise, or Fall, of a Drop of Oil in Water. (33)

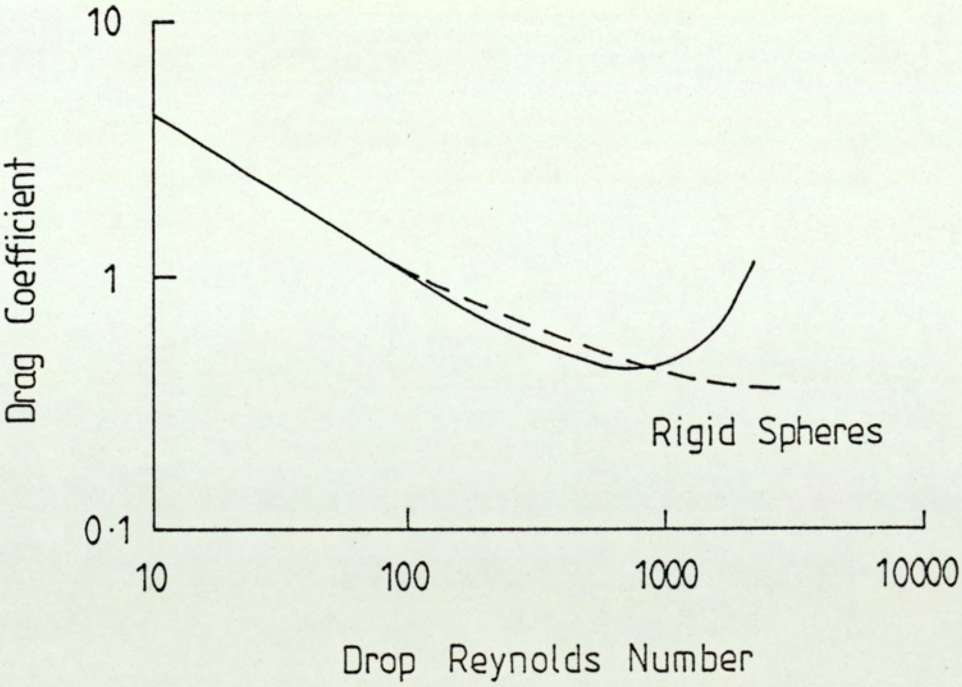

Figure 2·4 Drag Curve for Liquid Drops

Recently Mekasut et al (41) reported that Vignes (42) correlation best fitted their results for terminal velocities of drops of carbon tetrachloride falling through an aqueous continuous phase with iodine transferring to the droplet phase. They (41) reported a decrease in the mass transfer coefficient of up to 58% due to the presence of Teepol (0.05cm^3/L), and a reduction in the frequency of oscillation of up to 37%. The Vignes correlation is,

$$V = \frac{d}{42}\left[\frac{g\,\Delta\rho}{\rho_c}\right]^{2/3}\left[\frac{\rho_c}{\mu_c}\right]^{1/3}\left[1 - \frac{E_o}{6}\right] \qquad (2.17)$$

This correlation also gave a better prediction of droplet velocity than that obtained from Hu and Kintner's correlation (35).

2.4.1. Effects of Drag

Most conditions involving drops in liquid-liquid extractors are far above the upper limit for application of the preceding equations (2.15 and 2.5). A drop moving through a liquid at a velocity such that the viscous forces could be termed negligible cannot exist. Thus drop motion in liquid extractors involves both viscous and inertial terms, and the Navier-Stokes equations cannot then be solved. Hence, Kintner (43) presented the drag coefficient for a liquid sphere in the form:

$$C_D = \frac{4}{3}\,\frac{\Delta\rho}{\rho_c}\,\frac{gd}{V^2} \qquad (2.18)$$

in which d is the diameter of the sphere.

For an oblate ellipsoidal drop the minor axis of the ellipsoid (d_V) is the appropriate length to use in the drag coefficient equation (19). A plot of drag coefficient versus Reynolds number is shown in Figure 2.4 in which the equivalent spherical diameter is the length term used in both the drag coefficient and the Reynolds number. The drag coefficient is less for a rigid sphere than for a liquid drop of the same size and density. This is the result of the mobility of the drop surface, which is carried from the forward stagnation point to the rear by shear, and also because the drop contents circulate internally. The result of Hu and Kinter's (35) correlation was a plot of log (C_DWe $P^{0.15}$) against log (Re $P^{0.15}$) where "P" is a dimensionless physical property group:

$$P = \frac{\rho_c \sigma_i^3}{g\,\mu^4}\;\frac{\rho_c}{\Delta\rho} = \frac{3}{4}\;\frac{(\mathrm{Re})^4}{C_D\,(\mathrm{We})^3} \tag{2.19}$$

Equation 2.19 was found to be limited in application to low continuous phase viscosity systems (44) of about <5.0 cP. The above Hu and Kinter equation has been extended by Johnson et al (45) for use with a system of continuous phase viscosity up to 20 cP by dividing the ordinator by $(\mu_c/\mu_w)^{0.14}$. It was reported that the effect of density on fall velocity is greater than the effect of surface tension (45).

Winnikow and Chao (26) reported that the peculiar up-turn of the drag coefficient curve, Figure 2.4, at a certain value of Reynolds number is also exhibited by rigid two and three-dimensional bodies and by air bubbles which do not oscillate in very viscous liquids. They also reported that the rapid increase in drag coefficient is due to the combined effect of drop oscillation and pressure drag increase as a consequence of the change in the wake structure. Others consider that the minimum in the drag coefficient versus Reynolds number relation results from an increase of eccentricity and not the onset of oscillation (170).

2.4.2. Wake Formation and Hydrodynamics

To study mass transfer from a drop it is essential to know the characteristics of the boundary layer around it. To the rear of the drop there is naturally an invisible wake and many investigators have studied this phenomenon with, and without, mass transfer for non-oscillating and oscillating liquid drops (46, 12). The wakes were rendered visible by the dissolution of an aniline dye from the drops as they passed through the continuous phase. A boundary separation was observed as a ring on the rear surface of the drop, particularly with oscillating drops.

Most of the mass transfer from the drop to the continuous phase occurs into the boundary layer forward of the separation ring and travels in this layer around the wake to the trailing filament. Mass transfer of solute from the drop to the wake, and then to the continuous phase, depends upon solute concentration.

A large number of modes of wake shedding have been described by Yeheskel et al (47) who grouped them into three ranges of Reynolds number and drag coefficients of the droplets. In Range A, for drops Re < 150, the only shedding of elements of the wake is from the straight or wavy tail of the wake. In Range B, for drop Re between 150 to 800 wake shedding was cyclic, from alternate sides of an oscillating wake, without oscillation of the droplets themselves. The drag coefficient was lower than that for solid spheres, and decreased with increasing Reynolds number. In Range C, for drop Re > 800 random wake shedding occurred with oscillation of the droplets and drag coefficient increased sharply with increasing Reynolds number.

The ratio of wake volume to drop volume was also reported, in general, to be independent of drop size and interfacial tension and to be a linear function of $\Delta\rho/\rho_c$. This work was extended to a study of vertical and horizontal assemblages of droplets (48). It was also found that the relative wake volume, was about one third of that of a single drop for a vertical assemblage, and about twice for horizontal assemblages.

Magarvey et al (10) observed, and classified, wakes behind liquid drops falling through quiescent water and noted the approximate ranges of Reynolds number corresponding to the transition from one wake configuration to the next. The wake classification and corresponding range of Reynolds number are given in Table 2.3.

Winnikow et al (26), contrary to Margarvey et al (10), reported that the nature of the trail depends not only on the Reynolds number but also upon other physical properties of the continuous and dispersed phase fluids. For example the volume of the wake depends on the rate of vorticity generation and diffusion, and for fluid spheroids the mechanics of vorticity generation are strongly influenced by the interfacial tension. Interfacial tension would probably have been affected by the aniline dye used by Magarvey et al (10).

Wakes were classified into two classes; one for non-oscillating drops characterised by the vortex threads and the other for oscillating droplets characterised by the periodic discharge of vorticity. Garner and Grafton (49) studied mass transfer in fluid flow from a solid sphere and reported the existence of a toroidal vortex for Reynolds number <150 which is in agreement with Winnikow's (26) observation for liquid droplets in the absence of mass transfer.

Considerably less work has been described for open turbulent wakes, although some excellent photographs have been published (50, 51). Wake shedding appears to be responsible for the wobbling motion often exhibited by spherical-cap bubbles with Reynolds number <150.

Table 2.3 Classification of wake as a function of Reynolds number

Class	Range of (Re)	Nature of Trail
I	0-210	Single trail
II	210-270	Double trail
III	270-290	Double trail with waves
IV	290-410	Procession of vortex loops
V	290-700	Double row of vortex rings
VI	700-2500	Irregular wake

2.5 SHAPE OF MOVING DROPS

The shape of a liquid drop moving in a liquid continuous phase is determined by the forces acting along its surface. The shape is dependent upon the balance between the fluid dynamic pressure exerted because of the relative velocity between the drop and continuous phase and the interfacial forces which tend to retain the drop as a sphere (52)

At low Reynolds numbers (due either to a high viscosity of the continuous phase or a small droplet size) region (A) of Figure 2.3, the drops are usually spherical or distorted to such a small degree that their eccentricity is not observable. At high Reynolds number, the inertial forces tend to cause distortion from the spherical shape. As the Reynolds number is increased droplet oscillation will begin and ultimately if it is increased further drop breakup will occur. In low viscosity fields, such as water, the drop will first be distorted to a general oblate-ellipsoidal shape as in region B Figure 2.3. Kintner (43) reported that drop distortion can be classified according to the viscosity of the continuous phase. The eccentricity of a non-oscillating, ellipsoidal drop increases with drop size. The interfacial area of such a non-oscillating drop can be estimated from (52);

$$A = \frac{\pi}{2} d_h^2 + \frac{d_v d_h}{\sqrt{E^2 - 1}} \ln (E + \sqrt{E^2 - 1}) \qquad (2.20)$$

The ratio of the area of an oblate spheriod to that of a sphere of equal volume (21) is;

$$\frac{A}{As} = \frac{1}{2} E^{2/3} + \frac{1}{E^{1/3}\sqrt{E^2 - 1}} [\ln (E + \sqrt{E^2 - 1})] \qquad (2.21)$$

where

$$E = \frac{d_h}{d_v}$$

The area ratio of equation 2.21 does not significantly exceed unity until an eccentricity of 1.5 is attained. Attempts by Heertjes et al (53) to study the variation of eccentricity of an oscillating drop proved unsuccessful, so that an average eccentricity was applied but the results show considerable scatter.

Winnikow et al (26) performed dimensional analysis and reported that the physical properties influencing droplet deformation could be represented by a modified Weber number,

$$\bar{We} = \frac{V^2 de\, \Delta\rho}{\sigma} \tag{2.22}$$

the Froude number,

$$Fr = \frac{V^2}{g\, d_e} \tag{2.23}$$

and the fluid property parameter. Klee and Treybal (11) studied eleven liquid-liquid systems and showed that the eccentricity was related to $(\Delta\rho^{0.5}/\sigma)$. Wellek et al (52) investigated the effects of various physical properties, drop size, and drop velocity upon drop shape for non-oscillating liquid drops falling through a stationary continuous phase; 45 systems were studied with continuous phase viscosities varying from 0.3-46.0 centipoise and interfacial tensions varying from 0.3-42.0 dyne/cm. Correlations were proposed involving the Weber number, Eotvos number, and viscosity ratio; separate correlations were proposed depending upon the continuous phase viscosity;

$$E = 1 + 0.091\, We^{0.95} \tag{2.24}$$

$$E = 1 + 0.093\, We^{0.98}\ \mu^{0.07} \tag{2.25}$$

$$E = 1 + 0.129\, E_o \tag{2.26}$$

$$E = 1 + 0.163\, E_o^{0.757} \tag{2.27}$$

Correlations with We were accurate over the range of viscosities 0.3-46.0 cp, and correlations with E_o were reasonably accurate for the low and moderate viscosities, ie. 0.3-0.8 cp and 0.8-2.5 cp respectively, but not for high viscosities of 2.5-46.0 cp.

These correlations enabled the prediction of the eccentricity of non-oscillating drops over a Reynolds number range of 6.0-1345 with an average deviation of 6%-8%.

2.6 EFFECTS OF IMPURITIES

Many investigators have confirmed that minute traces of solid or liquid impurities have a serious effect on experimental results (45, 24, 54). Therefore much of the experimental data reported in the literature is of limited value, due to the absence of complete specifications regarding the purity of the chemicals used. Chemicals of dubious purity, such as tap water, must be avoided and distilled de-ionised water to a set specification should be used. The presence of a contaminant can eliminate internal circulation, thereby significantly increasing the drag and drastically reducing overall mass transfer and heat transfer rates. Stringent precautions are necessary to ensure clean apparatus before starting an experiment. However impurities in different percentages are present in any practical liquid-liquid extraction operation. For this reason, the Hadmard-Rybezynski theory is seldom obeyed in practice, although it serves as an important limiting case. Contaminants with the greatest retarding effect are those which are insoluble in either phase or with high surface pressures (55).

The first attempt to account for surface contamination in creeping flow of bubbles and drops was made by Frumkin and Levich (56, 57) who assumed that the contaminant was soluble in the continuous phase and distributed over the interface. The form of the concentration distribution was controlled by one of three rate limiting steps:

a. Adsorption - desorption kinetics;

b. Diffusion in the continuous phase;

c. Surface diffusion in the interface.

Kintner (43) reported a comparison of other workers data (35, 38, 45) on the rate of fall of drops of carbon tetrachloride through water. Fair agreement was noted among the data for very small spherical drops and for very large drops. However in the intermediate region, which includes the size of most interest, the disagreement was greatest. This was attributed to the presence of surface-active agents of a type that can segregate near the interface. This may cause a change in surface viscosity which inhibits circulation and causes the drops to act more like rigid bodies.

Lochiel (58) studied the influence of surface-active agents on droplet oscillation and on mass transfer, and found that a trace of impurity lowered the frequency and amplitude of oscillations; such a reduction in oscillation reduced mass transfer rates. The influence of impurities also decreases with increasing viscosity of the continuous phase.

Based on the above, the materials of construction of some of the recirculating apparatus described in the literature (including aluminium tanks or piping, or packed pumps and gaskets) could introduce enough impurities to affect the experimental results.

2.7 WALL EFFECTS

The majority of the data on terminal velocity of drops have been determined in vertical, cylindrical, glass tubes of limited size. A wall correction factor is necessary in order to interpret such data in terms of a drop moving in an infinite medium. This correction factor is a function of the diameter ratio (DR) which is the ratio between the droplet diameter and the diameter of the container. For an interface free of surface-active contaminants, Haberman and Sayre (59) obtained approximate solutions for a circulating sphere travelling in steady motion along the axis of a cylindrical tube. As (DR) increased, the presence of the walls caused droplet deformation, elongation occurring in the vertical direction to yield approximately prolate-ellipsoid shapes. The correlation (59) gave an accurate prediction of the wall correction at low Re when DR $\cong$ 0.5 or less although significant droplet deformation had occurred.

A drop of specified volume may not have the same type of motion in cylinders of different diameter. If the drop is small enough it will be spherical in shape and in the absence of the wall effect its velocity will be that of an equivalent rigid sphere, as shown by the plot of drag coefficient versus Reynolds number, Figure 2.4. All studies of drops have been carried out in containers of finite dimensions; hence wall effects have always been present to a greater or lesser extent. However, few workers have set out to determine wall effects directly using a series of different columns of varying diameters. The general aim was to determine the influence of DR on terminal velocity.

Kintner et al (43) and Strom et al (60) studied the influence of DR on terminal velocities in the range $E_o < 40$ and $Re > 1$ for drops of intermediate size. They concluded that unbounded drops tended to be flattened in the horizontal direction, whilst the containing walls tend to cause elongation. Hence the resulting shape may not deviate greatly from a sphere. Their experimental results were represented by

$$\frac{U_T}{U_\alpha} = [1 - (DR)^2)]^{3/2} \tag{2.28}$$

This relation has proved useful for systems in which the field fluid was stationary and is recommended for drops with $E_o < 40$, $Re > 200$ and $DR \leq 0.6$.

Generally all previous investigators are in agreement that droplet Reynolds number and the presence of adjacent drops have an effect on droplet hydrodynamics. However no results have been published on the phenomena under conditions involving mass transfer between the dispersed phase droplet and a continuous phase.

CHAPTER THREE

INTERPHASE MASS TRANSFER

In liquid-liquid extraction two immiscible, or partially miscible, phases are brought into contact in order to allow transfer of solute between them. The rate of solute diffusion between the phases depends on the concentration gradient in both phases. The concentration difference between the two phases is also an indication of the departure from equilibrium. The concentration gradients and the rate of diffusion both fall to zero at equilibrium.

Bird (61) summarised several mechanisms by which mass transfer can occur:

1. Ordinary diffusion, which results from a concentration gradient.
2. Thermal diffusion, which results from a temperature gradient.
3. Pressure diffusion, which results from a hydrostatic pressure gradient.
4. Forced diffusion, which results from differences in the external forces acting upon the different species present.
5. Mass transfer by forced convection, which results from the overall motion of the fluid, produced by the expenditure of energy upon it.
6. Mass transfer by free convection, which results from the overall motion of the fluid.
7. Turbulent mass transfer, which results from the motion of eddies through the fluid.
8. Interface mass transfer, which results from the non-equilibrium condition at an interface.

To describe the various mechanisms of mass transfer in flow systems it is necessary to develop basic differential equations of fluid systems with diffusion. These are the "equations of change", comprising the equations of continuity for each chemical species, the equations of motion and the equations of energy balance. These relations provide the starting point for the study of diffusion in laminar and turbulent flow systems and for simultaneous heat and mass transfer. Bird (61) reported that, for mass transfer studies the equations of continuity are the most important and the method of solution of the diffusion equations depends upon the system. He concluded that for simple systems analytical solutions may frequently be worked out. For somewhat more complex systems the basic differential equation may be solved by semi-analytical approximation procedures or by numerical methods. For very complex systems dimensional analysis, coupled with experimental data, has to be employed.

However the classification of systems as "simple" or "complex" is not easy. For example a binary system which would be characterised as "simple" may require numerical analysis to solve the differential equations describing mass transfer if the equilibrium relationship is non-linear.

3.1 FUNDAMENTALS OF MASS TRANSFER

When the velocity distribution and the rate of eddy diffusion are unknown, and the mass transfer rate cannot be predicted directly, then it is generally expressed in terms of an overall mass transfer coefficient K, defined by;

$$N = K A \Delta C \tag{1.1}$$

The concentration difference ΔC represents the total difference from the beginning to the end of the diffusion path. The coefficient therefore includes the characteristics of the laminar and turbulent flow regions of the fluid and the molecular and eddy diffusivities. Several different mechanisms have been proposed to describe conditions in the vicinity of the interface, the more important of which will be considered below.

3.1.1. The Two Film Theory

The earliest film theory developed by Lewis (62, 63) provides the simplest illustration of the meaning of mass transfer coefficients. When a fluid is in turbulent flow past a solid surface, since fluid velocity is zero at the surface itself, there must be a viscous layer or film in the fluid adjacent to the surface. Whitman (64) assumed that turbulence in the two phases dies out near the interface and that the entire resistance to transfer resides in two films on either side of the interface in which transfer occurs by molecular diffusion. For this model to be valid the effective film would have to be very thin so that the quantity of solute within it is small relative to the amount passing through it, or the concentration gradient would have to be set up quickly. The resistance to mass transfer in each phase is represented by the reciprocal of the individual film coefficient and the resistances are additive:

$$\frac{1}{K_d} = \frac{1}{k_d} + \frac{m}{k_c} \tag{1.2}$$

or

$$\frac{1}{K_c} = \frac{1}{k_c} + \frac{1}{m'k_d} \tag{1.3}$$

Equilibrium at the interface requires equal values of chemical potential in the liquids at the interface and, consequently, no resistance to transfer across the interface.

3.1.2. Penetration Theory

The Penetration Theory is simply the expression for the rate of molecular diffusion into an infinite slab with the boundary conditions of uniform concentration at $\theta = 0$ and a constant surface concentration for $\theta > 0$. By integration of Fick's Second Law, the instantaneous rate of mass transfer is:

$$N_{A\theta} = \sqrt{\frac{D_A}{\pi \theta}}(C_{A1} - C_{A2}) \tag{3.1}$$

Higbie (65) applied this equation to gas absorption in a liquid, and predicted that diffusing molecules would not reach the other side of a thin layer at very short contact times. Higbie's equation has been applied to absorption in short-wetted wall columns, liquid jets, and other devices designed to obtain measurable contact times. The time-average Sherwood number for a droplet system is approximated from equation 3.2 by:

$$\bar{Sh}_d = \frac{\bar{K}_d d}{D} = \frac{4}{\sqrt{\pi \tau}} \tag{3.2}$$

Brunson and Wellek (66) reported that mathematically equation 3.2, describes internally stagnant, non-oscillating droplets reasonably well for $\tau = T_m < 10^{-3}$. Other workers (26, 38, 67, 68) indicated negligible interfacial resistance for absorption of gases into pure water at contact times > 0.01 seconds. Angelo et al (69) extended the Penetration Theory to allow for stretching surfaces. Ruckenstein (70) proposed a modification for mass transfer in the vicinity of a fluid-liquid interface by accounting for the velocity distribution within the eddies during the penetration by the solute. In contrast with the Penetration Theories of Higbie and Angelo et al, Ruckenstein's modification (70) does not neglect the velocity components in the convective diffusion equation. However as discussed in Chapter 4 mechanisms of diffusion to, and from, oscillating drops are considerably more complex than physical gas absorption with a known contact time

3.1.3. Penetration with Random Surface-Renewal Theory

The Penetration Theory was extended by Danckwerts (71) on the basis that in most contacting devices there would be a distribution of contact times. If the elements are replaced in random fashion, an experimental distribution of ages or contact times results, and the average transfer rate is given by:

$$N_A = \sqrt{D_A S}\ (C_{A1} - C_{A2}) \tag{3.3}$$

where S is the fractional rate of surface renewal. This type of distribution was supported by the work of Shulman et al (72) who showed that the static hold-up within a packed bed is replaced infrequently and that it contributes a smaller fraction of the total mass transfer for physical absorption than for vaporisation or for absorption followed by irreversible chemical reaction. Recently Satoru et al (73) proposed a correlation for mass transfer coefficient between two liquid phases;

$$Sh_1 = 0.0119\, S_{c1}^{0.33}\ Ca_1^{0.46}\ [\phi^4 Re_1{}^3 + \overline{Re}_2{}^{2.67}]^{0.25} \qquad (3.4)$$

where:

Ca = Capillary number = $gd^2\rho/\delta$

ϕ = Correction factor = 1 when $\mu_2/\mu_1 \leq 7.00$ or $\phi = (\mu_2/\mu_1)^{-0.2}$ when $\mu_2/\mu_1 > 7.0$

$\overline{Re}_2$ = Modified second-phase Reynolds number = $\dfrac{d^2N_2\rho}{\mu}$

N = agitation speed
1 = First phase
2 = Second phase

This correlation is useful in estimating the role of mass transfer in extraction with chemical reaction, and also provides important information about the transport phenomenon involved in turbulent mass transfer across a liquid-liquid interface.

3.1.4. Film Penetration Theory

This theory, developed by Toor et al (74) is a combination of three earlier theories reviewed above. The entire resistance to mass transfer is considered to lie in a laminar surface layer of a certain thickness. Surface renewal occurs by eddies which penetrate the surface from the bulk of the phase. Thus transfer through young elements of the surface obeys the Penetration Theory ($K \alpha \sqrt{D}$), transfer through older elements follows the Film Theory ($K \alpha D$), and transfer through elements of intermediate age is by a combination of both mechanisms.

3.1.5. Mass-Flow or Convective-Transfer Theory

In contrast with the theories described above, Kishinevskii and co-workers (75, 76, 77, 78) proposed a surface-renewal mechanism, which postulates that transfer into an eddy at the interface occurs predominantly by convective mass flow and not by molecular diffusion They did not agree that the probability of replacement of a surface element is independent of its age. King (79) proposed another model for turbulent liquid phase mass transfer to and from a gas-liquid interface. The model requires the evaluation of three parameters and involves concepts of surface renewal in which surface tension exerts a damping effect upon the smaller eddies. Allowance is made for a continuous eddy diffusivity profile near the free interface, which avoids the postulation of a film, or discontinuity in transport properties, as required by film-penetration theory.

3.2 AMPLITUDE OF OSCILLATION

Rose and Kinter (80) measured the amplitude of oscillation of drops of fifteen individual organic liquids flowing countercurrent to water. The amplitude of oscillation was measured frame by frame from cine film and the length of the major and minor axes were measured from the films at maximum and minimum distortion of the drops. The equation proposed for amplitude of droplet oscillation was;

$$a_p = \frac{X_{max}}{2} - X_o \qquad (3.5)$$

A considerable scatter of the data existed, and therefore an average drop axis length at maximum and minimum distortion was obtained. Angelo et al (69) proposed an alternative equation for more accurate estimation of amplitude of oscillation,

$$\varepsilon = \frac{A_{max}}{A_o} - 1 \qquad (3.6)$$

Schroeder and Kintner (30) modified Lamb's correlation for frequency of oscillation, equation (2.8), by the addition of an empirical amplitude coefficient (b) estimated by:

$$b = \frac{de^{0.225}}{1.242} \qquad (3.7)$$

Haberman et al (67) reported that the factor (b) in equation (3.7) should approach unity for small oscillations. They agreed that the amplitude data are very scattered, and that equation (3.7) should not be used to predict the amplitude but only the frequency of oscillation. A comparison of the observed data by Haberman et al with that predicted by Lamb (the Rayleigh-Webb derivation equation 2.9) shows an average error in prediction of frequency of oscillation of 16.33%. The average error in prediction of (b) was 9.01%.

Recently Al-Hassan (1) reported that the amplitude can be measured more accurately by measuring the change in the area of the droplet during oscillation, since area is the factor affecting the mass transfer rate. The correlation proposed for amplitude, with an absolute deviation of 13% was:

$$\varepsilon = 0.434 \ Sr_c^{-0.46} \ We_c^{-0.53} \ \sigma_r^{0.11} \qquad (3.8)$$

Al-Hassan also proposed a correlation for amplitude, including the viscosity ratio instead of the interfacial tension ratio, with similar accuracy:

$$\varepsilon = 0.477 \ Sr_c^{-0.48} \ We_c^{-0.64} \ \mu_R^{-0.05} \qquad (3.9)$$

The first correlation was preferred to the second one because of the small power on μ_R in equation 3.9 which shows that it is largely superfluous.

3.3 INTERFACIAL CONVECTION (MARANGONI EFFECT)

Movements in the plane of the interface result from local variations of interfacial tension during the course of mass transfer. These variations may be produced by any significant local variations which affect the interfacial tension. Interfacial motions have been related to variations in interfacial concentration, temperature, and electrical properties. In partially miscible binary systems, interfacial temperature variations are the major factor causing interfacial motion.

At the interface between the fluids, interfacial motions may take the form of ripples (81) or of ordered cells (82). Slowly growing cells may exist for long periods of time (82) or the cells may oscillate and drift over the surface. When the phases are in relative motion, interfacial distrubances usually take the form of localized eruptions, termed "interfacial turbulence".

The shape of a drop moving under the influence of gravity may be affected by interfacial motions; the drop may also wobble and move sideways. Interfacial convection tends to increase the rate of mass transfer above that which would occur in the absence of interfacial motion. The interaction between mass transfer and interfacial convection has been studied by Sawistowski (83).

3.3.1. Interfacial Turbulence

The various kinds of small flows generated at the interface and in the layers immediately adjacent to it are grouped together as interfacial turbulence. Interfacial turbulence induces a substantial increase in the rate of mass transfer between two phases. Thus transfer rates may be much higher than predicted from a proper combination of single-phase rate coefficients on the assumption of a quiescent interface.

Interfacial phenomena can affect the rate of mass transfer in many ways ie:

i) By changing the mass transfer coefficient.

ii) By changing the interfacial area.

iii) By retarding internal circulation of the droplet and hence increasing the drag.

In some cases interfacial phenomena effects are strong with mass transfer in one direction but completely absent when the solute diffuses in both directions (84). Sherwood and Weir (85) showed that the most pronounced interfacial turbulence is observed when a chemical reaction occurs simultaneously with mass transfer eg. in the extraction of acetic acid from benzene droplets by water containing ammonia.

Interfacial turbulence covers many aspects of interfacial films, eg. interfacial gradient (Marangoni effect), or density gradient (Rayleigh effect) and cellular convection currents in the vicinity of the interface (82). The influence of the interfacial tension gradient has been studied most frequently. Thomson (86) was the first to observe the existence of spontaneous interfacial convection. Marangoni (87) subsequently observed that liquids of lower surface tension will spread on liquids of higher surface tension. This phenomenon was observed with miscible liquids as well as with immiscible and partially-miscible liquid pairs and is referred to as the Marangoni effect.

In many cases the effect of natural convection currents is, in general, greater than the Marangoni effect in terms of the effect of interfacial turbulence on the mass transfer (88). However the Marangoni effect increases with an increasing rate of solute transfer, as a result of the increase in local interfacial tension (89). The theoretical aspects of interfacial turbulence have been widely studied (80, 88, 89, 90), but there have been no experimental investigations because of the difficulties of quantifying turbulence, the incomplete state of data on interfacial tension in contrast to mass transfer rate data, and the dependence of interfacial turbulence on conditions of flow within the bulk phase in the apparatus.

Sawistowski et al (90) reported from their work on drop formation, that in the turbulent regime, the mass transfer coefficients increased almost linearly with local decrease in the interfacial tension. This increase was claimed to be due to the surface being renewed more rapidly than would be the case for drop formation alone. They concluded that surface renewal due to interfacial turbulence may control the mass transfer rate in this regime.

Theoretical studies of the Marangoni effect were presented by Pearson (91) and by Sternling and Scriven (84). The latter workers (84) employed a simplified two-dimensional roll-cell model based on the following assumptions to develop a quantitative theory for the onset of instability:

1) The two semi-immiscible liquid phases are in contact along a plane interface. The phases are considered to be in thermal equilibrium.
2) The concentration of solute is low enough for the fluid properties to be considered constant and the interfacial tension large enough so that the interface remains mobile
3) The concentration gradients in the two phases are taken to be linear, thus implying a steady transfer of solute.

The stability of a system with the above conditions was then examined by introducing a two-dimensional infinitesimal disturbance. If the disturbances decay, the system is said to be stable, if it grows the system is unstable. Sterling and Scriven's analysis suggests that interfacial turbulence is usually promoted by:

1) Solute transfer out of the phase of higher viscosity;
2) Solute transfer out of the phase in which its diffusivity is lower;
3) Large differences in kinematic viscosity and solute diffusivities between the two phases;
4) Steep concentration gradients near the interfaces;
5) Interfacial tension that is highly sensitive to solute concentration;
6) Low viscosities and diffusivities in both phases;
7) Absence of surface-active agents;
8) An increase in interfacial area eg. associated with an increase in mobility of the interface.

Sawistowski (90), Davies (33, 92, 93) and Levich (57) presented excellent reviews of research on interfacial phenomena.

Recently Brian et al (94, 95, 96) suggested that the Gibbs adsorption layer, of molecular dimensions, has a profound stabilising influence on Marangoni convection. This analysis incorporated the effect of the Gibbs adsorption hydrodynamic stability theory and is more in line with experimental observations (97). It is evident, however, that a great deal needs to be done before the effects of interfacial turbulence can be quantified for use in extraction process design.

3.3.2. Cellular Interfacial Motions

Sternling et al (171) investigated the factors determining the appearance of ordered cell-like motions, and considered the two dimensional stability of a plane interface separating two immiscible, semi-infinite, fluid phases with mass transfer occuring between the phases. This system was shown to be unstable for mass transfer in one direction. For an interfacial tension-lowering solute, instability was predicted for transfer out of the phase with lower diffusivity or out of the phase with high kinematic viscosity.

Cellular interfacial motions are generally observed in quiescent systems when the mass transfer driving forces and interfacial tension gradients are small, and when natural or buoyancy-driven convection is suppressed. The presence of these cell-like motions enhances the rate of mass transfer (98), since fresh fluid is brought to the interface.

3.4. INTERFACIAL BARRIERS TO MASS TRANSFER DUE TO AN ADSORBED TRACE SUBSTANCE

Trace amounts of surface-active substances of unknown structure and concentration are frequently present in commercial liquid-liquid extraction processes. This leads to difficulties in interpreting extraction performance in terms of experimental and theoretical studies on drops.

These surface-active materials may be surfactants, impurities, plasticiser from tubing used in the equipment, or metallic colloids from pipes and fittings. The presence of these materials has important effects on the rate of mass transfer through the surface. It reduces, and often eliminates, the Marangoni effect and also introduces a surface resistance to diffusion across the interface. The reduction in interfacial tension therefore becomes less dependent on solute concentration and the interface compressibility will also decrease, thus adversely affecting surface renewal (83). In addition surface viscosity will increase and slow down any movements in the interface.

There have been numerous theoretical and experimental studies of the effects of surface-active agents on mass transfer between a single drop and a continuous phase (55, 56, 99). However the formulation of a generalised expression to account for these effects is prevented by their specific dependence upon the structure and concentration of the surface-active substances. Several forms have been suggested:

1. Retardation of internal circulation: The coefficient of mass transfer inside a droplet depends on the velocity of circulation of the liquid within it. Frumkin and Levich (56) suggested that the adsorbed surface film reduces the internal circulation by being swept back towards the rear of the moving drop (ie. the cap), where it is concentrated until the force tending to spread it forwards is just balanced by the hydrodynamic stress at the interface, Figure 3.1. This surface tension gradient opposes further flow in the plane of the surface, which is hence immobilised so that drop circulation ceases in this region. The terminal velocity of a drop depends largely on the properties of the rear portion, while much of the mass transfer occurs into the newly-formed interface at the front of the drop. Thus the terminal velocity would be expected to be reduced almost to V_{Stokes} (equation 2.6).

2. Surface rigidity: It has been demonstrated that surface-active materials tend to render droplets more rigid so that the mass transfer rates approach those of stagnant droplets (100, 101, 41. 102, 90). Thus, Garner and Hale (102) showed that the addition of small quantities of Teepol (0.015% by volume) to water reduced the rate of extraction of diethylamine from a single toluene drop to 45% of its original value. Similarly a 68% reduction was reported by Lindland and Terjesen (100) who studied the effect of sodium olelyl -p-anisidine sulphonate on the extraction of iodine from an aqueous phase to a single falling drop of carbon tetrachloride.

3. Blocking of the interface: Certain materials eg. ethyl alcohol, when spread as a monomolecular film upon water, reduce the rate of evaporation. This has been attributed to a reduction of the area through which the water molecules must pass (7, 103) ie. a barrier effect.

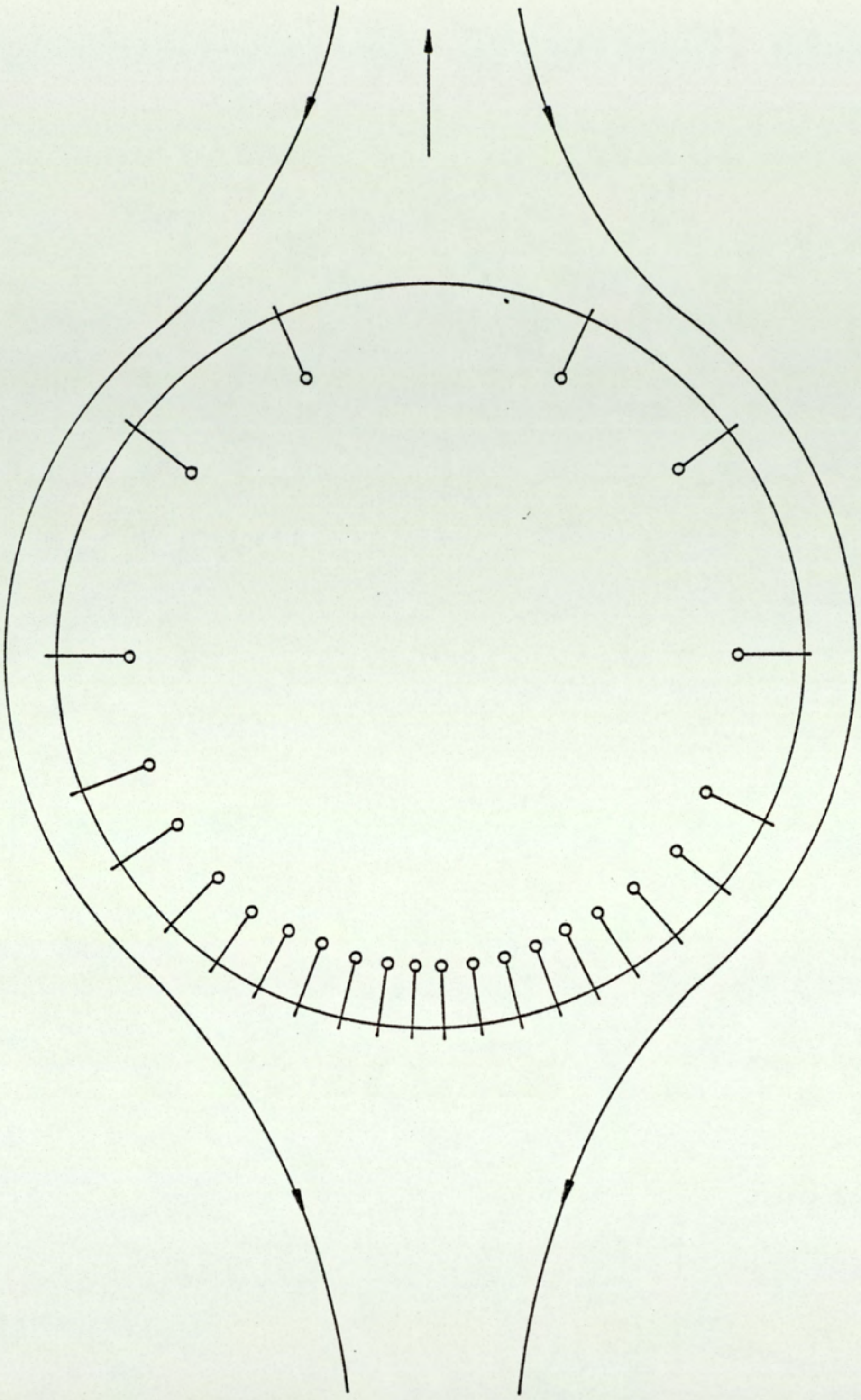

Figure 3·1 Influence of Surface Active Agent on the Internal Circulation within a Rising Droplet (33)
[Tending to inhibit circulation and to concentrate at surface near rear cap.]

The effect of different surfactants upon mass transfer coefficients during drop formation (90), for the transfer of acetic acid into water from a 0.98m solution in benzene were studied by Sawistowski and James (103). Their values of experimental overall mass transfer coefficients are plotted against the concentration of surfactant in Figure 3.2. In the case of Teepol, Lissapol, dodecylamine chloride and sodium lauryl sulphate, the addition of a small quantity of the surfactant reduced the mass transfer to a value equal to that obtained in the diffusional regime (ie. corresponding to stagnant drop behaviour) in the absence of surfactant (88, 104, 69). The action of these surfactants was entirely hydrodynamic in nature ie. they suppressed interfacial convection.

Polar oils are much less susceptible than non-polar oils to the effect of small amounts of surface-active material. Apart from other considerations therefore more polar oils are preferable in extraction processes because of the maintenance of drop circulation, and hence high mass transfer rates (33, 105).

Kintner (43) reported a reduction of about 20% in the terminal velocity of oscillating drops of chlorobenzone fallng through water when surface active materials were added, but Thorsen et al (39) reported a reduction of only 12%. The mass transfer rate to, or from, oscillating drops is also affected by traces of surface-active material. This may be due to surface tension gradients and the rigidity of the surface inhibiting surface movement of the drop as it oscillates (43, 33).

Unfortunately, there are insufficient experimental data from which to predict how much a surface active agent will affect the mass transfer data for oscillating droplets. Any such data are likely to be system-specific.

3.5 EFFECT OF DROP COALESCENCE AND REDISPERSION ON MASS TRANSFER RATE

Johnson and Bliss (106) found that drop sizes in spray towers were considerably larger when solute was diffusing from the drop phase to the continuous phase than for the reverse direction. A reduction in column efficiency is associated with this, ie. an increased coalescence rate,because the total interfacial area is reduced. Other

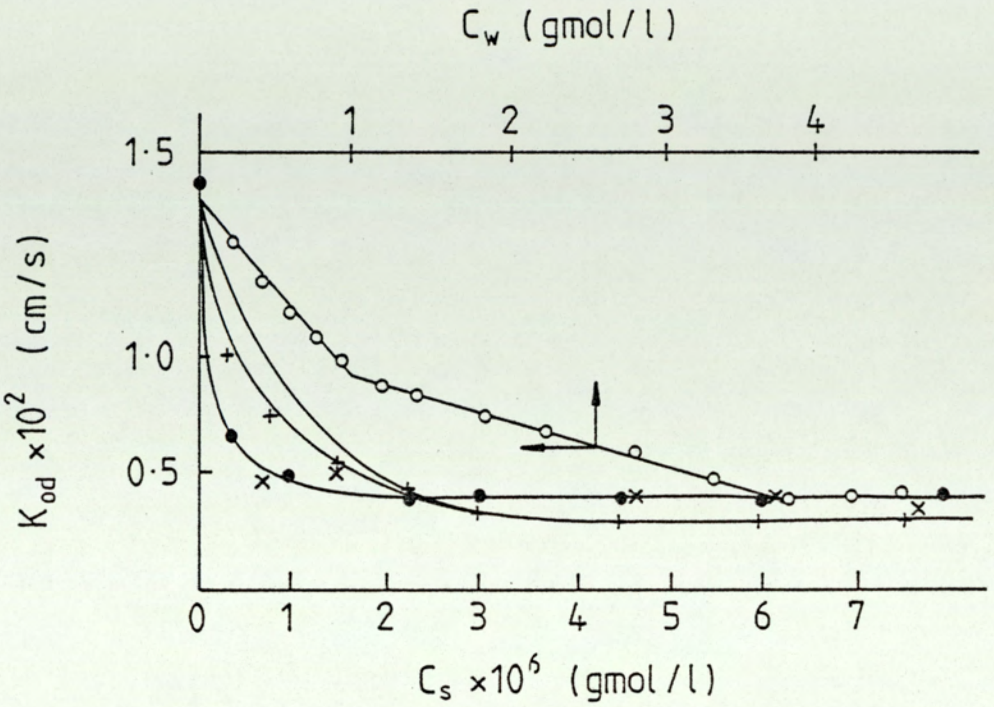

Figure 3·2 Effect of Surfactants on Mass Transfer Coefficients. Transfer of Acetic Acid from 0·98M Solution in Benzene Drops to Solute - Free Water.

C_s	Concentration of Surfactant
C_w	Concentration of Acetic Acid in Water
○	No Surfactant
●	Dodecylamine Hydrochloride
+	Manoxol
×	Sodium Lauryl Sulphate

workers (107) observed similar effects in Rotating Disk Contactors.

Groothuis and Zuiderweg (108) explained this phenomenon by demonstrating the effect of mass transfer on the coalescence of pairs of drops. By pushing two drops together whilst attached to nozzles, they observed that in every case coalescence was promoted if solute transfer was from the drop phase.

This promotion of coalescence was attributed to interfacial tension gradients developed in the region of the approaching drops. With pairs of immiscible liquids the addition of a third component soluble in each phase generally, but not always, lowers the interfacial tension. Thus when mass transfer takes place from the drop the concentration of solute in the contact zone between the two approaching drops rapidly reaches equilibrium with the drop. This results in a decrease in interfacial tension locally which causes the interface in the contact zone to dilate drawing with it part of the intervening film which promotes coalescence. When solute is transferred into the drop the situation is reversed and material from the bulk continuous phase is drawn towards the contact area, which retards film drainage and hence stabilizes the drops. This effect also occurs in binary systems, when the phases are not in equilibrium. Jeffreys and Lawson (109) measured coalescence times in the ternary system benzene-acteone-water and their results confirmed the findings of Groothuis and Zuiderweg.

CHAPTER FOUR

MASS TRANSFER COEFFICIENTS - THEORY AND CORRELATION

In any liquid-liquid extraction process the rate of mass transfer depends upon three factors: the area of contact, the effective driving force, and the mass transfer coefficient. However, these three factors cannot be easily evaluated eg. even for the spray column there is no simple relation for the contact area as a function of design variables such as phase throughputs and geometries of the distributor and contactor. The average contact area depends on the drop size distribution and the rate of rise of the drops relative to the continuous phase. These factors are determined by fluid-mechanics processes too complicated for theoretical evaluation. Furthermore a very large number of experiments would be necessary for an empirical evaluation. In any event the interfacial area, the driving force, and the mass transfer coefficient are best considered separately for the three distinct stages in the life of each drop, ie. formation, travel and coalescence at the bulk interface.

4.1. MASS TRANSFER DURING DROP FORMATION

Numerous correlations have been published for mass transfer rates or coefficients during drop formation, the most important of which are summarised in Table 4.1. Other data on drop formation in the absence of mass transfer is of limited value for design purposes since uncertainty exists regarding the influence of concentration, density, viscosity and, especially, interfacial tension.

Humphrey et al (110) studied the effect of enhancement of internal circulation on mass transfer rate in forming drops. Drop formation, circulation and tangential convection were found to depend upon the ratio of the drop height from the nozzle exit to drop apex at time (t). Circulation also depended upon the momentum of fluid entering

Table 4.1 Correlations of Mass Transfer During Drop Formation

Author and Reference	Correlation	Remarks
Licht and Pensing (111)	$K_{df} = \frac{6}{7} \left(\frac{D_d}{\pi t_f}\right)^{0.5}$	The whole area ages according to penetration theory. Only area variation with time is considered.
Heertjes et al (53)	$K_{df} = \frac{24}{7} \left(\frac{D_d}{\pi t_f}\right)^{0.5}$	Velocity of diffusion is small compared with velocity of drop growth.
Groothuis et al (112)	$K_{df} = \frac{4}{3} \left(\frac{D_d}{\pi t_f}\right)^{0.5}$	With drop diameter between 0.035-0.085cm the rate of absorption increases at Re > 750.
Coulson et al (113)	$K_{df} = 2\sqrt{(3/5)} \left(\frac{D_d}{\pi t_f}\right)^{0.5}$	Average time of exposure and average exposed surface elements of different age.
Heertjes and de Nie (114)	$K_{df} = 2\left[\frac{r_o}{a_d} + \frac{2}{3}\right] \left(\frac{D_d}{\pi t_f}\right)^{0.5}$	At slow formation rates, the fresh surface model was very successful.

Table 4.1 continued

Author and Reference	Correlation	Remarks
Ilokovic (115)	$K_{df} = 1.31 \ (\frac{D_d}{\pi t_f})^{0.5}$	Based on surface stretch mechanism, proved by many workers and used successfully.
Angelo et al (69)	$K_{df} = \frac{2}{\sqrt{\tau}} \ (\frac{D_d}{\pi t_f})^{0.5}$	For the more restricted situation of Ilkovic (115)
Sawistowski (83)	$K_{df} = \frac{40}{7} \ (\frac{D_d}{\pi t_f})^{0.5}$	For a sphere, whose volume is linearly related to time.
Johnson et al (23)	$E_m = \frac{C_1 - C_2}{C_1 - C^*}$ $= \frac{20.6}{de} \ (\frac{D_d t_f}{\pi})^{0.5}$	Most practical because, "the end effect criteria" still exist.

the drop relative to its size (110). However Lochiel (58) reported extremely high values for mass transfer rate during drop formation caused by instabilities resulting from large concentration differences rather than the mechanism of drop formation (92).

Hayworth and Treybal (116) developed a semi-empirical equation for drop volume in the absence of mass transfer based on a force balance by expressing the various contributing forces acting on the drop as fractions of the total drop volume. This procedure is not entirely justified since neither the exact instant at which the forces act, nor their quantitative contribution to the total volume are known. Null and Johnson (117) based their model for prediction of drop volume without mass transfer on the geometry of the drop during the formation process. They neglected the effect of viscosity of the continuous phase, which was found to be important by Hayworth and Treybal. Null and Johnson found maximum average errors of 20% and 87% when comparing their experimental data on drop volume with predictions from their model and that of Hayworth and Treybal respectively.

Izard (118) claims a method to predict the drop volume which reduced empiricism, but this was derived for conditions of no mass transfer. In a similar study Halligan et al (119) determined the shape of a growing drop by means of a pressure balance for a static drop but with an additional term to account for the pressure on the interface due to internal fluid motion. Their data was for mutually-saturated fluids so that the interfacial tension could be considered constant during the entire period of growth.

A widely-used correlation is that of Scheele and Meister (105) for calculating the drop volume at low velocities of dispersed phase into a stationary continuous phase. Drop diameter is correlated as a function of injection velocity and nozzle diameter using the Harkins and Brown (120) correction factor. This correlation was tested using mutually-saturated phases and low solute concentrations. The experimental results deviated by an average of 11.0% when the percentage error was calculated by dividing the deviation from the experimental volume by the smaller of the two diameters. Using the same method the percentage error for Hayworth-Treybal and Null-Johnson (116,

112) predictions had deviations of 83.3 and 139.5% respectively.

Several investigators (121, 122, 123) reported that mass transfer during drop formation accounted for between 10% to 50% of the total solute transferred. Unfortunately however much of the published experimental work lacked an appropriate technique for direct measurements of the extent of mass transfer.

Other investigators (53, 54, 83, 104) have estimated the amount of mass transfer to be approximately 10%. However, Sherwood (123) observed that 40% of the overall transfer occurred during the drop formation period. Recently Brounshtein et al (124) reported that good prediction of mass transfer rate during formation could be obtained by sampling close to the nozzle whichever phase the limiting resistance is in.

Numerous mathematical expressions have been proposed to predict the dispersed phase mass transfer coefficient during drop formation. Licht and Pensing (111) reported that the amount of solute extracted during drop formation was sufficiently small that experimental results did not exhibit any variation with drop formation time. Their results were correlated by;

$$K_{df} = \frac{6}{7}\left[\frac{D_d}{\pi t_f}\right]^{0.5} \tag{4.1}$$

Heertjes et al (53) found that the rates of mass transfer for water into isobutanol drops and vice versa were two to five times the value predicted by their model Equation 4.2, with formation times <1.5 sec. They attempted to calculate the order of magnitude of the mass transfer during formation under the assumptions that only molecular diffusion takes place, the velocity of diffusion is small compared with the velocity of drop growth, the drop is formed by introducing a constant amount of liquid of constant concentration into the centre of the drop, and the drop is spherical with a constant boundary concentration. Their correlation is:

$$K_{df} = \frac{24}{7}\left[\frac{D_d}{\pi t_f}\right]^{0.5} \tag{4.2}$$

Groothuis et al (112) proposed a model using the Penetration Theory to explain their experimental results of the amount of SO_2 gas absorbed by water and for its transfer between hydrocarbon drops and water. The rates were measured during droplet formation in times of 1 to 40 seconds.

Their model is:

$$K_{df} = \frac{4}{3} \left[\frac{D_d}{\pi t_f} \right]^{0.5} \tag{4.3}$$

They concluded that at long formation times however the rate of absorption is increased somewhat by free convection currents, whereas with short times of formation a considerable increase in absorption rate may be found as a consequence of the mixing produced by jetting of liquid leaving the capillary.

Coulson and Skinner (113) used a different method to measure the rate of mass transfer to a drop during formation. They used an apparatus in which the drop was ejected automatically and analysed its contents immediately after formation. They correlated the overall mass transfer coefficient by:

$$K_{df} = 2\sqrt{3/5} \left[\frac{D_d}{\pi t_f} \right]^{0.5} \tag{4.4}$$

and concluded that the transfer rate during drop formation is almost independent of the time of formation, within the range of 0.5-1.0 sec. The overall transfer coefficient K, based on the average area exposed during formation of the drop, decreases with increased time of formation but is practically independent of the drop size. They also concluded that the mass transfer rate during formation was very small (ie. <10%) compared with the results of other workers. Heertjes and de Nie (114) studied the rate of mass transfer of water to isobutanol drops during formation. They proposed a model for the behaviour of different portions of the drop during formation and release at slow rates; ie. they accounted for the residue of the drop retained at the capillary after drop release.

$$K_{df} = 2\left(\frac{r_o}{a_d} + \frac{2}{3}\right)\left[\frac{D_d}{\pi t_f}\right]^{0.5} \tag{4.5}$$

For the binary system studied, the mass transfer to a drop was considered to be described by assuming that drop growth occurs by the formation of fresh elements, rather than by stretching of the surface.

Angelo et al (69) developed a generalized penetration theory for the surface stretch model;

$$K_{df} = \frac{2}{\tau}\sqrt{\tau}\left[\frac{D_d}{\pi t_f}\right]^{0.5} \tag{4.6}$$

This includes the special case of the more restricted situation considered by Ilkovic (115), who proposed an equation for the estimation of diffusion controlled current in a dropping mercury cathode;

$$K_{df} = 1.31\left[\frac{D_d}{\pi t_f}\right]^{0.5} \tag{4.7}$$

Sawistowski (90) has shown that it is difficult to present precise extraction rates during drop formation because of the rapid changes in interfacial tension, and interfacial area, which occur during this period. His experimental data were best correlated by:

$$K_{df} = \frac{40}{7}\left[\frac{D_d}{\pi t_f}\right]^{0.5} \tag{4.8}$$

Skelland and Minhans (125) concluded that the above models are unrealistic since they do not allow for the effect of internal circulation, interfacial turbulence and disturbances caused by detachment. A modified expression was proposed for the mass transfer coefficient,

$$\frac{K_{df}\, t_f}{d} = 0.0432 \left[\frac{V^2 n}{dg}\right]^{0.089} \left[\frac{d^2}{t_f D_d}\right]^{-0.334} \left[\frac{\mu_d}{\rho_d\, d_\sigma}\right]^{-0.601} \qquad (4.9)$$

This correlation is for the total mass transfer occurring during formation, which includes mass transfer during drop growth, during detachment, and the contribution from the portion of the drop left after detachment. There was approximately 26% deviation between the predicted and experimental values. The predicted values were also higher than those predicted by the models of Heertjes et al (114) and Ilkovic (115).

Mass transfer studies in connection with different rates of formation have, to date, been limited. The only significant work is due to Popovich et al (126) who, on the basis of a fresh surface model and the associated diffusion mechanism of transport, proposed the following expression for the prediction of mass transfer rate.

$$N_A = \frac{4n}{2n+1} \int_o^1 [(1-y^2)^{n-1}\, d_y\, (C^* - C_o) \left(\frac{D_n}{\pi}\right)^{0.5} B_p t^{(2n+1)/2}] \qquad (4.10)$$

n and B_p are defined by the surface area $A = B_p t^n$ and $y = (1 - t/t_1)^{0.5}$, t is the time at which a fresh surface element is formed, and t_1 is the time of formation with mass transfer taking place. It is assumed that only a moderate rate of formation is applicable given by:

$$1.28 \times 10^4 < \left(\frac{d^2}{t_f D_N}\right) < 12.31 \times 10^4$$

Vrentas et al (127) studied mass transfer during drop formation when there was a significant change of solute concentration in the drop. An analytical perturbation solution and finite difference solutions were derived for this situation and efficiencies determined as,

$$E = - \sum_{n=1}^{\alpha} (-1)^n An\, y^{n/2} \tag{4.11}$$

$$A_1 = 2$$

where An is the series coefficient defined by;

$$A_{n+1} = \frac{\pi^{0.5} \gamma (n/14 + 1) A_n}{\gamma (n/14 + 3/2)} \qquad n \geq 1$$

It was concluded that at high solute concentration it is better to consider extraction efficiency than mass transfer coefficients (127).

Heertjes et al (128) reported that at high drop formation rates ie. $Re > 40$ large contributions to mass transfer are caused by strong circulation in the drop. However, no theory or experimental data have been presented for situations involving high rates of drop formation. The best fit of the experimental data was provided by a correlation proposed by Johnson and Hamielec (23) giving a 67% deviation between the experimental and calculated overall mass transfer coefficients. The correlation is:

$$E_m = \frac{C_1 - C_2}{C_1 - C^*} = \frac{20.6}{d_e} \left[\frac{D_d\, t_f}{\pi} \right]^{0.5} \tag{4.12}$$

Obviously equations 4.1-4.12 are all similar with merely a different value of the constant.

Mass transfer at low rates of formation has not been studied extensively. The only information available suggests that mass transfer in these circumstances is comparable to that with drops formed at moderate speed with an added contribution from free convection (128).

4.2. MASS TRANSFER DURING DROP TRAVEL THROUGH THE CONTINUOUS PHASE

Mass transfer during drop travel through the continuous phase is significantly influenced by the hydrodynamic state of the drop, ie. whether it is stagnant, circulating or oscillating. Rigid or stagnant drops in which there is no internal mixing, possess a low mass transfer rate, whereas circulation or oscillation induces vigorous mixing inside the drops resulting in higher mass transfer rates to, or from, the drops. It is concluded in most of the literature that the rate of mass transfer is five or more times higher for oscillating drops. The overall mass transfer rate is also affected by the presence of a wake behind the moving drop (129, 130, 131). All the above droplet hydrodynamic states will be discussed, considering the effects on the dispersed and continuous phases separately.

4.2.1. The Continuous Phase Mass Transfer Coefficient

The continuous phase mass transfer coefficient may be evaluated in terms of the resistance in the film surrounding the drop through which the transfer takes place by molecular diffusion

$$K_c = \frac{D_c}{X_c} \tag{4.13}$$

where X_c is the thickness of the continuous phase film. Numerous correlations for the continuous phase mass transfer coefficient have been published in the literature but, since it is impracticable to present all these correlations, only the most well-known will be discussed. Summaries of theoretical predictions and experimental correlations can be found in the work of Linton et al (132), Sideman et al (133) and Griffith et al (134). An assumption for the interfacial area is implicit in all expressions and the usual choice for a deformed droplet is to consider a sphere of an equivalent volume. The size of the drop and the internal solute hydrodynamic state (ie. droplet Reynolds number and droplet shape), lead to enormous changes in droplet characteristics, as it either remains stagnant, or exhibits internal circulation, or deforms and oscillates.

4.2.1.1. Stagnant Droplets

For the case of a rigid drop theoretical analysis by Garner and Suckling (135) and Garner and Jenson (136) based on the boundary layer theory, has shown that the rate of mass transfer from, or to, a solid sphere can be correlated by the general equation;

$$Sh_c = A + C\,Re^m\,S_c{}^n \tag{4.14}$$

where A, C, m and n are constants. Examples of values of these constants are given in Table 4.2.

Linton et al (132) proposed a model for mass transfer coefficients of stagnant drops of benzoic acid measured in uniform flow in a water tunnel at $490 < Re < 7580$. The overall transfer coefficient was correlated by;

$$Sh_c = 5.82 \times 10^{-2}\,Re^{0.5}\,S_c{}^{0.33} \tag{4.15}$$

The transfer rate from the front of the drop was in fair agreement with theory and the results of other workers, while the absolute local values at the front stagnation point were about 40% lower than expected (132). The discrepancies may be due in part to a gradual transition from viscous flow to potential flow outside the boundary layer as Re increased from 1 to 10^5. Whilst equation 4.14 has been recommended and used by Griffiths (134) a review of published data by Rowe et al (137) covering heat and mass transfer in the range of $10 < Re < 10^4$ shows that there is insufficient evidence to establish the relationship between transfer coefficient and Reynolds number. The correlation proposed by Rowe et al (137) is;

$$Sh_c = 2 + 7.6 \times 10^{-1}\,Re^{0.5}\,S_c{}^{0.33} \tag{4.16}$$

Equations 4.15 and 4.16 make no allowance for the effect of the wake on mass transfer coefficient. Therefore, Kinard et al (131) proposed a correlation which includes the wake effect,

$$Sh_c = 2 + (Sh_c)_n + 4.5 \times 10^{-1} Re^{0.5} S_c^{0.33} \qquad (4.17)$$

Garner and Tayeban (21), proposed a modified correlation for mass transfer from stagnant, non-circulating spherical drops,

$$Sh_c = 2 + 0.55 \, Re^{0.5} S_c^{0.5} \qquad (4.18)$$

which applied to solid spheres. Correlations for stagnant drop mass transfer coefficient were found through Sherwood number and are summarised in Table 4.2.

4.2.1.2. Circulating Droplets

Many studies (21, 23, 138, 16) have indicated that the continuous phase mass transfer coefficient is increased when circulation occurs inside a droplet and this is explained by the reduction in the boundary layer thickness.

Hadamard (6) postulated that the drag on the surface of a fluid droplet moving in a fluid medium caused internal circulation; thus a droplet should fall more quickly than an equivalent solid sphere in the same fluid medium since there is less drag. Boussinesq modified Hadamard's theory, in that two surface layers are present on the drop. The surface viscosities cause a resistance to motion of the surface and the velocity of internal circulation is also reduced. Both theories indicated circulation in fluid droplets in all circumstances.

Boussinesq (15) and Ruckenstein (70) using the velocity distribution for potential flow, found the average Sherwood number to be given by

$$Sh_c = 1.13 \, (Re)^{0.5} (S_c)^{0.5} \qquad (4.19)$$

which assumes that there is no boundary layer separation. The proportionality constant may be lower than 1.13 due to the presence of a wake under practical conditions. A correction factor (fc) depends upon dispersed phase properties (for instance, the value of fc is 0.31 for benzene drops and 0.68 for methyl isobutyl ketone). This factor has been introduced by West et al (121),

$$Sh_c = 1.13 \, fc \, (Re)^{0.5} (S_c)^{0.5} \qquad (4.20)$$

Their results (121) differ by as much as five fold from those previously obtained in similar experimentation. Garner and Skelland (16) concluded that, for droplets containing 40% butyl alcohol falling in water, internal circulation only occurred when the local Reynolds number of the droplet was > 70. The rate of diffusion was investigated as a function of the Reynolds number, and it was found that the time taken for mass transfer was much longer below the Reynolds number of 70, at which circulation commences.

As the viscosity of the dispersed phase increases, high Reynolds numbers are required to obtain internal circulation (16, 139). The transition Reynolds number at which internal circulation occurs is proportional to the log of the absolute viscosity. The lower the interfacial tension between the phases, the lower is the Reynolds number required to give internal circulation. Garner and Tayeban (21) developed a correlation for their experimental data taking into account the influence of the wake

$$Sh_c = 0.6\,(Re)^{0.5}\,(S_c)^{0.5} \qquad (4.21)$$

Heertjes et al (53) suggested that a function h is necessary instead of the constant in equation 4.21.

$$Sh_c = h\,(Re)^{0.5}\,(S_c)^{0.5} \qquad (4.22)$$

where h is a function of $(\mu_c/(\mu_c + \mu_d)$ and varies from 0.1 to 0.95 while $(\mu_c/(\mu_c + \mu_d)$ varies from zero to ten.

In another study Garner et al (140) using partially-miscible, binary liquid-liquid systems of low interfacial tension, observed that the exponent of the Schmidt group in equation 4.14 is 0.5 for fully-circulating potential flow, and 0.33 for stagnant drops. They concluded that the exponent of Schmidt number for a circulating drop should be between 0.5 and 0.33. They proposed the correlation,

$$Sh_c = -126 + 1.8\,(Re)^{0.5}\,(S_c)^{0.42} \qquad (4.23)$$

In a recent study by Mekasut et al (41) of the transfer of iodine from an aqueous continuous phase to carbon tetrachloride drops the resistance to mass transfer was assumed to be solely in the continuous phase. Sherwood number was correlated to

Galileo number for drops < 0.26cm diameter by

$$Sh_c = 1.04\, Ga^{0.4} \tag{4.24}$$

At droplet Reynolds number > 4 (10, 40) a boundary layer separation occurs giving rise to a wake which travels behind the droplet. Initially an unsteady build-up of solute in the wake occurs due to the transfer from the rear of the droplet and from the boundary layer surrounding the outside of the wake. Eventually, a steady-state condition is attained and solute transfer occurs from the wake to the boundary layer surrounding the wake and then into the continuous phase. The high initial rates of mass transfer were attributed to the presence of the wake. Elzinga and Banchero (141) working with heat rather than mass transfer correlated data for circulating drops by;

$$Sh_c = 5.52 \left[\frac{\mu_c + \mu_d}{2\mu_c + 3\mu_d}\right]^{3.47} \left[\frac{d\,\sigma\,\rho_c}{\mu_c{}^2}\right]^{0.056} Pe_c{}^{0.5} \tag{4.25}$$

but found that oscillation produced values of Sherwood number up to 45% greater. Treybal (156) reported that drop oscillation and interfacial turbulence produced higher coefficients than for stagnant and circulating drops.

Thorsen et al (142) presented a correlation claimed to be applicable to both circulating and non-circulating drops. This indicates that internal circulation does not affect the specific mechanisms of mass transfer in pure liquid-liquid systems;

$$Sh_c = 178 + 3.62\, Re^{0.5}\, S_c{}^{0.33} \tag{4.26}$$

The rapid increase in the continuous phase mass transfer coefficient with increasing Reynolds number was attributed to the combined effect of an increased disturbance intensity around the separation point.

4.2.1.3. Oscillating Droplets

In the majority of correlations for continuous phase mass transfer coefficient a sphere, or equivalent sphere, is used to characterise the liquid circulating drop. In the calculation of mass transfer the significance of distortion is primarily that the surface area increases rapidly with any increase in distortion.

Skelland and Cornish (143) have summarised possible criteria for estimating the characteristic length for droplet phenomena correlation. These are the diameter of a sphere of identical volume to the particle, the diameter of sphere of identical surface area to the particle, the length of the minor axis of the particle, the average of the axis length parallel and at right angles to the flow, or the sphericity multiplied by the diameter of a sphere of the same volume as the particle.

Many investigators (23, 144, 145) have used correlations to estimate mass transfer rates for oscillating droplets with turbulent internal circulation, but the effect of oscillation causes higher rates of mass transfer than circulation (21, 80). Garner and Tayeban (21) proposed the most acceptable, correlation to predict the mass transfer coefficient in a continuous phase surrounding an oscillating droplet.

$$Sh_c = 50 + 8.5 \times 10^{-3}(Re)\,(S_c)^{0.7} \qquad (4.27)$$

They reported a Schmidt number exponent >0.5, since for oscillating drops there is less dependence on diffusivity.

Yamaguchi et al (146) proposed a correlation for continuous phase mass transfer coefficient based upon a modified Reynolds number for oscillating drops,

$$\bar{Re} = \frac{\rho_c\,\omega\,de^2}{\mu_c} \qquad (4.28)$$

The correlation,

$$Sh_c = 1.4\,(Re)^{0.5}\,(S_c)^{0.5} \qquad (4.29)$$

hence neglects the effect of drop velocity. The maximum deviation of the experimental data from that predicted was approximately ± 20%.

Angelo et al (69) presented a model developed from the Penetration Theory depending on surface stretch for oscillating droplets. The theory was assumed to apply with the same characteristic lifetime for both phases, ie. the time for one cycle of oscillation.

A new approach was used by Mekasut et al (41) who correlated the Sherwood number with the Galileo number to predict the mass transfer coefficient of the continuous phase for oscillating drops between 0.2-0.4cm in equivalent spherical diameter,

$$Sh_c = 6.74\,(Ga)^{0.34} \tag{4.30}$$

However the experimental data were limited and the effect of the frequency of oscillation of the drop was neglected.

Brunson et al (66) showed that a correlation of the mass transfer coefficient developed using low interfacial tension systems gave large deviations when applied to high interfacial systems. They recommended the use of equation 4.27 for oscillating drops. Later Lochiel et al (148) suggested that the use of theoretical equations developed to describe mass transfer around rapidly oscillating drops between oblate and prolate forms, the proposed equation is,

$$Sh_c = 1.13\,Pe^{0.5} \tag{4.31}$$

Table 4.2 summarises the most useful correlations for prediction of mass transfer within the continuous phase and their limitations.

4.2.2. The Dispersed Phase Mass Transfer Coefficient

The mass transfer coefficient inside the droplet depends on the degree of internal circulation and oscillation. Both circulation and oscillation rates are known to increase with the droplet diameter and with the ratio of the viscosity of the continuous phase to that of the dispersed phase. Thus Hadmard (6) showed that the liquid inside the droplet would circulate at droplet's Reynolds number ($de\,\rho c\,V/\mu_c$) >1.0 and Levich (57) postulated that circulation would occur between Reynolds numbers of 1.0 and 1500. Levich (57) and Garner and Skelland (16) considered that the surface tension of the dispersed phase would affect the circulation rate. When the resistance to mass transfer is in the dispersed phase, the overall transfer rate will be controlled by the transfer

Table 4.2 Continuous phase mass transfer correlations during drop travel.

Author and Reference	Correlation	State of Drops	Remarks
Linton et al (132)	$Sh_c = 0.0582 (Re)^{0.5} (Sc)^{0.33}$	Stagnant	Ignores diffusion and wake effects
Rowe et al (137)	$Sh_c = 2 + 0.76 (Re)^{0.5} (Sc)^{0.33}$	Stagnant	Accounts for diffusion process
Kinard et al (131)	$Sh_c = 2 + (Sh_c)_n + 0.45 (Re)^{0.5} (S_c)^{0.33}$	Stagnant	Includes diffusion process and wake effects
Boussinesq et al (15)	$Sh_c = 1.13 (Re)^{0.5} (Sc)^{0.5}$	Circulating	Assumes no boundary layer separation
Garner and Tayeban (21)	$Sh_c = 0.6 (Re)^{0.5} (S_c)^{0.5}$	Circulatiing	Not valid for Re > 450
Garner et al (140)	$Sh_c = -126 + 1.8 (Re)^{0.5} (S_c)^{0.42}$	Circulating	For partially miscible binary systems of low
Mekasut et al (41)	$Sh_c = 1.04 (Ga)^{0.49}$	Circulating	$Ga = de^3 \rho c^2 g/\mu^2 c$
Garner and Tayeban (21)	$Sh_c = 50 + 8.5 \times 10^{-3} (Re) (S_c)^{0.7}$	Oscillating	Successfully used by other workers (137)
Yamaguchi et al (146)	$Sh_c = 1.4 (Re')^{0.5} (S_c)^{0.5}$	Oscillating	$Re' = \rho_c \omega d^2/\mu_c$
Mekasut et al (41)	$Sh_c = 6.74 (Ga)^{0.34}$	Oscillating	Ignores the effect of frequency of oscillation

mechanism inside the drop which is influenced by the hydrodynamics of the system. In many cases the experimental mass transfer rate has been greater than predicted by the model (21, 23, 138, 145). The models have been presented in the form of an extraction efficiency (E_m) or an internal mass transfer coefficient (k_d) and the common assumptions are that the droplet is spherical and of constant volume and that the solute concentration is sufficiently dilute for the physical properties to be considered constant. The fluids are also assumed to be Newtonian and incompressible.

4.2.2.1. Stagnant Droplets

Usually for very small droplets, <1mm in diameter, with no internal circulation, mass transfer by molecular diffusion is considered to be the dominant mechanism. For the case of no resistance to mass transfer in the continuous phase. Newman (149) developed a correlation for the drying of porous solids with negligible resistance to transfer in the continuous phase,

$$E_m = 1 - \frac{6}{\pi^2} \sum_{n=1}^{\alpha} \frac{1}{n^2} \exp\left[\frac{-n^2 \pi^2 D_d t_f}{r^2}\right] \tag{4.32}$$

For n=1, equation 4.32 can be closely approximated by an empirical expression by taking the first term only and neglecting the ratio ($6/\pi^2$) (150) yielding:

$$E_m = 1 - \exp\left[\frac{-\pi^2 D_d t_f}{r^2}\right]^{0.5} \tag{4.33}$$

which for values of E_m <0.5 reduces by a series expansion neglecting higher order terms to:

$$E_m = \pi \left[\frac{D_d t_f}{r^2}\right]^{0.5} \tag{4.34}$$

Grober (151) considered the effect of a finite continuous phase resistance for the rigid sphere in the expression:

$$k_d = \frac{d}{6t} \ln [6 \sum_{n=1}^{\alpha} A_n \exp (-\lambda^2{}_n \frac{4 D_d t}{d^2})] \tag{4.35}$$

Treybal (156) proposed a correlation for mass transfer coefficient based on a linear concentration-difference driving force:

$$k_d = \frac{2 \pi^2 D_d}{3d} \tag{4.36}$$

which has been considered theoretically for several circumstances, and it is useful to compare the results with those for rigid spheres (156).

4.2.2.2. Circulating Droplets

At a given drop size and Reynolds number the solute inside a drop commences to circulate. Experimental studies indicate that due to the mobility of the interface of the circulating drop, the rate of mass transfer is greater when circulation occurs in comparison with rigid spheres. As a result of circulation the fluid inside the drops is completely mixed by either laminar or turbulent circulation.

a. Laminar Circulation

Internal circulation is laminar for Re <1.0. Calderbank et al (44) proposed a correlation for the efficiency of mass transfer of droplets experiencing laminar internal circulation of the solute. Assuming a constant effective diffusivity (R) equal to 2.25 times the molecular diffusivity in equation 4.33, they obtained;

$$E_m = 1 - \exp \ -\pi^2 \left[\frac{R D_d t_f}{r^2}\right]^{0.5} \tag{4.37}$$

For $E_m < 0.5$ equation 4.37 reduces to:

$$E_m = \pi \left[\frac{R\, D_d\, t_f}{r^2} \right]^{0.5} \tag{4.38}$$

The best-known correlation for this type of circulation is due to Kronig and Brink (138). The basic assumptions are that the time of circulation is small compared to the time of solute diffusion, the solute diffusion is in a direction perpendicular to the internal streamlines, and that the continuous phase resistance is negligible. They obtained the expression:

$$E_m = 1 - \frac{3}{8} \sum_{n=1}^{\alpha} A_n^2 \exp \left[-\lambda_n \frac{16\, D_d t_f}{r^2} \right] \tag{4.39}$$

A_n and λ_n values have been presented by Heertjes et al (48). However, Johnson and Hamielec (23) found that in some cases equation 4.39 can be used for higher values of Reynolds number <200 and that when circulation is completely developed the mass transfer increases to about five times that for a rigid sphere. Elzinga and Banchero (147) presented an extension of Kronig and Brink's solution to the case including a finite continuous phase resistance. This final expression is of similar form to equation 4.39 except that A_n and λ_n are fractions of the continuous phase resistance. Values of the constants for n=1, 2 and 3 are given (141).

b. Turbulent Circulation

Circulation is generally present, so that the interior of the drop may be considered perfectly mixed at any time. At low Reynolds number the drop shape is normally spherical and, therefore, the circulation is laminar. With increased Reynolds number random mixing commences inside the drop; after this stage the drop starts to change in shape and oscillate.

Handlos and Baron (152) proposed a mass transfer mechanism within spherical droplets, which predicts rates much greater than either Newman's (149) stagnant drop model, or the Kronig and Brink (138) laminar circulation model. Their model (152) is clearly described by Wellek et al (153) who reported that Handlos and Baron's model (152) describes the unsteady state mass transfer mechanism for droplets possessing a special type of turbulent internal circulation. The propcsed model is:

$$Sh_d = \frac{3.75 \times 10^{-3} Pe_d}{(1 + (\mu_d/\mu_c))} \tag{4.40}$$

or

$$k_d = \frac{3.75 \times 10^{-3} V}{(1 + (\mu_d/\mu_c))} \tag{4.41}$$

Handlos and Baron recommended that when resistance to mass transfer exists in the continuous phase, the Higbie (65) relation should be assumed for k_c.

$$k_c = \sqrt{\frac{4}{\pi}\frac{D_c}{t_f}} \tag{4.42}$$

k_c is combined with k_d to obtain an overall mass transfer coefficient by means of two film resistance theory:

$$\frac{1}{K_d} = \frac{m}{(k_c)_{HG}} + \frac{1}{(k_d)_{HB}} \tag{4.43}$$

The discrepancies between their experimental (152) and calculated overall mass transfer coefficients (equation 4.43) reach 20% due, in part, to the significant interfacial tension effects or because the concentration gradient is not the true driving force as the correlation assumed.

Skelland and Wellek (145) studied the resistance to mass transfer inside droplets for organic water systems using Colburn and Welsh's technique (68). They also concluded that mass transfer rates for circulating drops falling in a stationary continuous phase were somewhat greater than those predicted by Kronig and Brink's model for non-oscillating circulating droplets. The data were correlated with an average absolute deviation of 34%. The Kronig and Brink and Newman correlations fitted the experimental results for non-oscillating drops with average absolute deviations of 46% and 56% respectively. The experimental results for the oscillating drops were correlated by two relationships with an average absolute deviation of 10.5%. The Handlos and Baron model fitted the experimental results for oscillating drops with 38% absolute deviation. They presented their results in a dimensionless correlation for the dispersed phase Sherwood number (145),

$$Sh_d = 31.4T_m^{-0.338}\ Sc_d^{-0.125}\ We_c^{0.371} \tag{4.44}$$

Johnson et al (23) have modified the expression of Handlos and Baron, equation 4.40, by introducing a ratio "R" between the mass transfer rate into a circulating drop and the rate into a stagnant drop of equal volume. Thus, at low Reynolds number ie. <1.0 the value of "R" is about 3, but for drops with turbulent circulation "R" is much greater. They found that,

$$R = \frac{Pe_d}{(2048\ (\mu_d/\mu_c))} \tag{4.45}$$

at high Re <200 the value of "R" increases, because drop diameter and velocity are included in the definition of Pe.

Davies (33) reported that Handlos and Baron's model does not apply when the drop oscillates and there is a third component transferring into or out of the drop, that the observed values of R (from 29 to 52) fall somewhat below those calculated by equation 4.45 which increase with increasing Re, and that at the onset of visible droplet oscillations R increases sharply by a factor of two.

Olander (154) suggested a modification to the Handlos and Baron model for short contact times, the actual k_d being related to the k_{HB} of Handlos and Baron by;

$$k_d = 0.792\, k_{HB} + 0.075 \frac{d}{t} \qquad (4.46)$$

Patel and Wellek (155) presented a numerical solution for the general case where there is a continuous phase resistance, to be used in conjunction with the Handlos and Baron model.

4.2.2.3. Oscillating Droplets

Several single oscillating drop models and correlations have been presented depending upon different concepts of droplet physical phenomena. Hydrodynamic factors affecting any one of the three variables on the right hand side of equation 1.1 will be reflected in the transfer rate. Thus the area of the drop may be in a state of dynamic renewal, the concentration gradient ($\Delta C/\Delta x$) may vary enormously over short time increments, or the value of K may be affected by temperature, since field viscosity, diffusivity, and density are temperature-dependent. All these factors have been considered in the following single oscillating drop models.

a. Rose and Kintner's Model

Rose and Kintner (80) proposed a model to calculate the mass transfer coefficient through the modification of the film theory expression, by regarding the film (or interfacial resistance zone) to vary with time due to droplet oscillation. Every droplet which exhibited oscillation ($Re > 200$) showed deformed, or completely damped, circulation. This work covered five mutually-saturated, organic-water systems with the continuous phase stationary and they observed that droplet oscillations were from a spherical shape to an oblate one, or from oblate to more-oblate, rather the stylized oblate-prolate cycle.

Rose and Kintner's model was based on the following assumptions:

1. Resistance to mass transfer for the continuous and dispersed phases lie only in thin films near the interface. Further, during each oscillation, the interface must be expanded locally in certain regions, thereby thinning the surface region across which

there is a concentration gradient. This thinning is particularly significant at the poles of the flattened drop, leading to faster mass transfer in these regions. The zone thickness at the ends of the major axis is the original thickness X_o and is thinned to a maximum value at the end of the minor axis.

2. Volumes of the zone of transfer resistance and the drop are constant.

3. The drop oscillates from a spherical shape to an oblate ellipsoid and back to the spherical shape in one period of oscillation (Figure 4.3). This kind of oscillation occurs for droplets of small sizes, ie. in transition from non-oscillation to oscillation, while for vigorous oscillation the drops have many different shapes (Figures 4.1 and 4.2). It is further assumed that the interface is renewed during each drop oscillation and the drop shape is symmetrical at the major axis. So there are two criteria for the interface, that the film theory applies as well as surface renewal.

4. The oscillation is of sinusoidal type so that the amplitude is related to the major axis by,

$$a = a_o + a_p \ / \ \mathrm{Sin}\ \bar{\omega}\, t / \tag{4.47}$$

where $\bar{\omega}$ is one half the frequency predicted from equation 2.9.

5. The core of the drop is assumed to be well-mixed. This permits internal concentration to be represented by a single value as shown in Figure 4.3.

The basic equation for unidirectional mass transfer across a stagnant interface is:

$$\frac{d N_A}{dt} = D A \frac{\Delta C}{\Delta X} \tag{4.48}$$

If the thickness of the zone of transfer resistance ΔX is decreased and the drop area is increased, the rate of mass transfer should markedly increase. Oscillatory motion, resulting in an alternate deviation from, and a return to, a spherical shape, causes such an interfacial area stretch and an accompanying variation in the term ($\Delta C / \Delta X$). The resulting increase in the rate of mass transfer can be very large ie. more

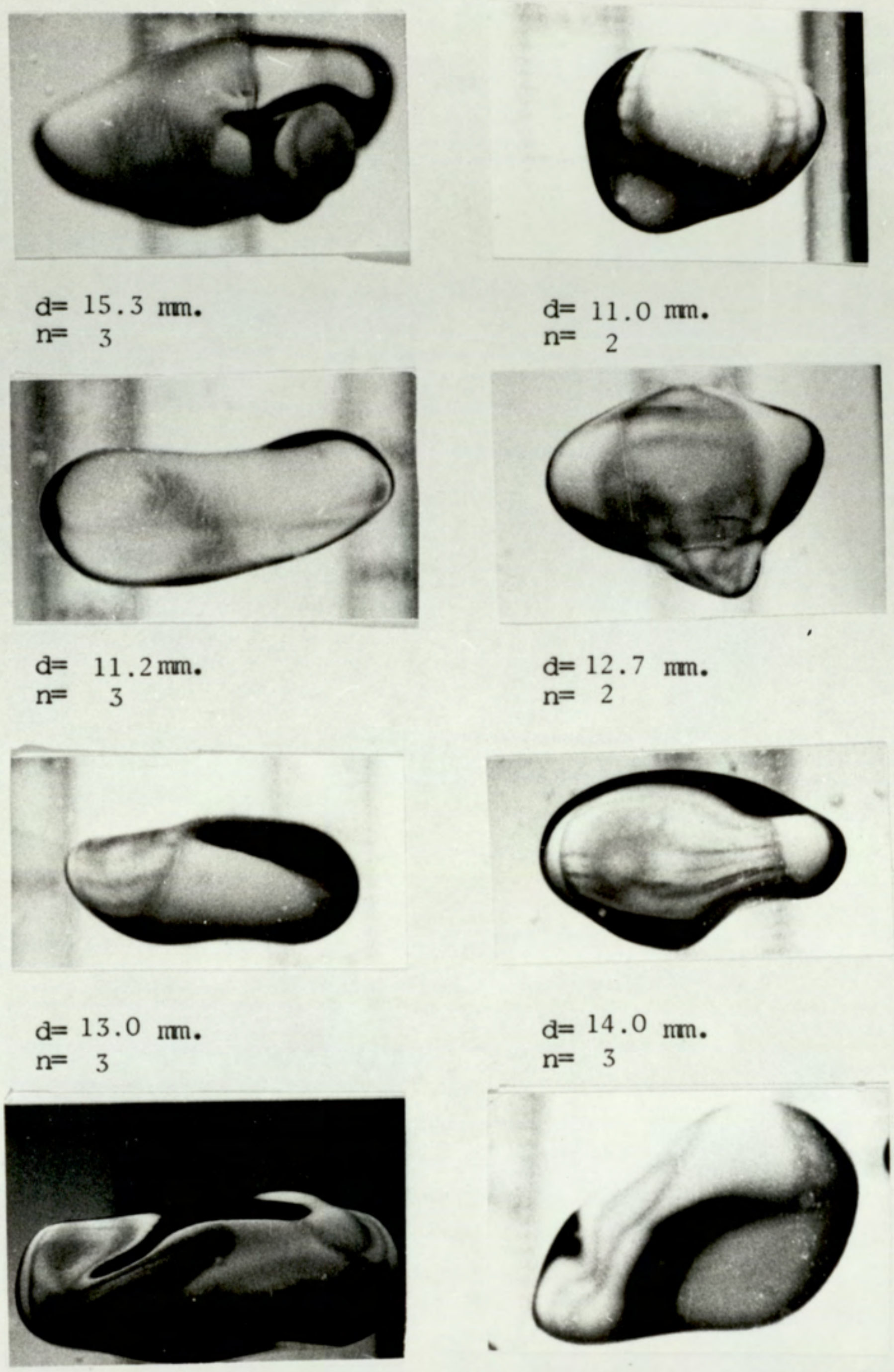

d= 15.3 mm.
n= 3

d= 11.0 mm.
n= 2

d= 11.2 mm.
n= 3

d= 12.7 mm.
n= 2

d= 13.0 mm.
n= 3

d= 14.0 mm.
n= 3

d= 17.7 mm.
n= 3

d= 13.3 mm.
n= 3

Figure 4.1 Illustration of the relation between the shape of the single drop and the value of (n).

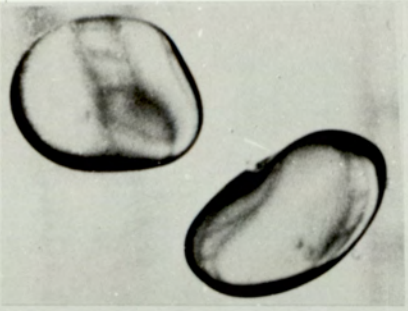

d1= 9.0 mm.
d2= 8.3 mm.
n= 3

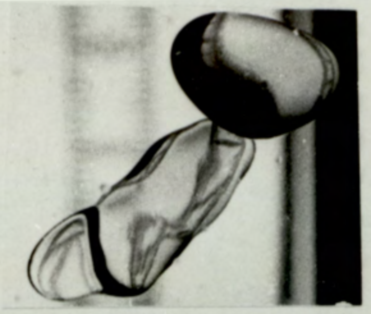

d1= 6.3 mm.
d2= 7.5 mm.
n= 3

d1= 7.4 mm.
d2= 10.7 mm.
n= 3

d1=11.0 mm.
d2= 7.7 mm.
n= 3

d1= 7.6 mm.
d2= 10.0 mm.
n= 2

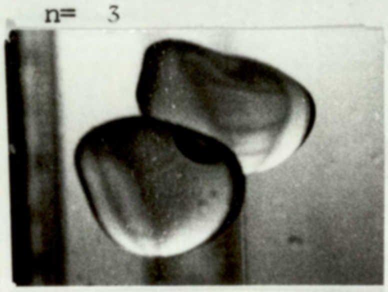

d1= 8.0 mm.
d2= 8.3 mm.
n= 2

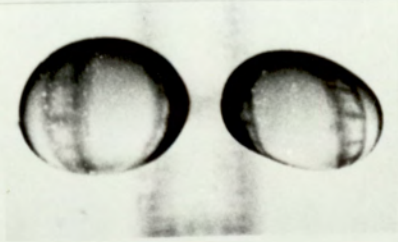

d1= 8.0 mm.
d2= 7.6 mm.
n= 2

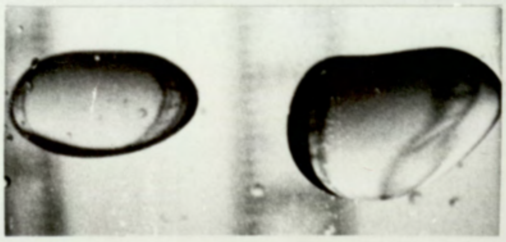

d1= 8.6 mm.
d2= 10.0 mm.
n= 3

Figure 4.2 Illustration of the relation between the shape of the drops pair and the value of (n).

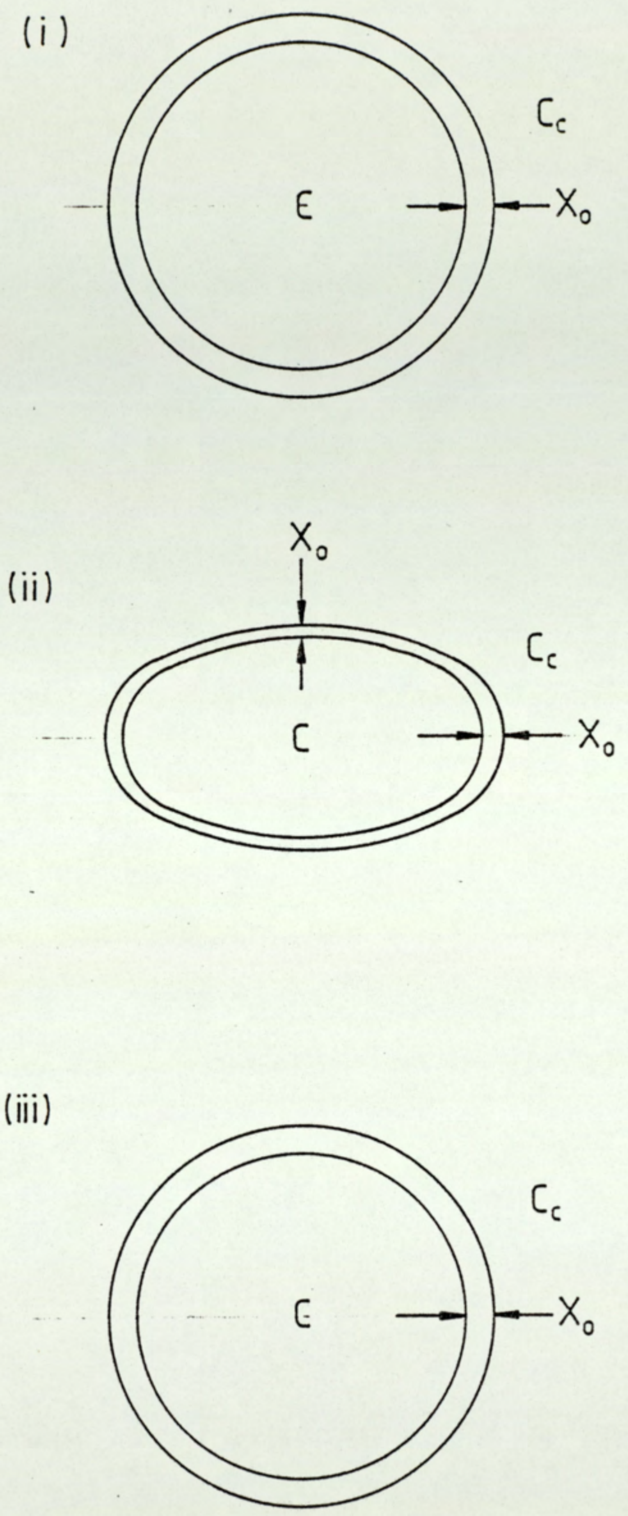

Figure 4·3 Drop Profiles during One Period; Oscillating Spheroid Mass Transfer Model (80) than 5 times.

The instantaneous value of X, as the drop oscillates will vary between X_o and X as shown in the following equation:

$$X = \frac{[a_o^2 b_o - (a_o - X_o)^2 (b_o - X_o)] - 2abX_o + bX_o^2}{a^2 - 2aX_o + X_o^2} = f_1(t) \quad (4.49)$$

The value of the major axis (a) was estimated from photographs, but the value of (b) the minor axis was not in agreement with the assumption of a symmetrical oblate drop. However the value of b can be found since the drop is of constant volume:

$$b = \frac{3v}{4 \pi a^2} \quad (4.50)$$

Garner et al's (21) correlation was used to evaluate k_c for a circulating droplet:

$$\frac{k_c d}{D_d} = 0.6 \left[\frac{\mu}{\rho D} \quad \frac{d V \rho}{\mu} \right]^{0.5} \quad (4.51)$$

Rose and Kintner (80), also proposed a correlation to calculate the dispersed phase mass transfer coefficient of an oscillating droplet:

$$k_d = C \quad (D_d \omega)^{0.5} \quad (4.52)$$

The overall dispersed mass transfer coefficient was then calculated by applying equation 1.2.

To evaluate the fractional extraction rates, the assumption was made of a constant volume drop,

$$- v \frac{d_c}{dt} = \frac{D_E}{X} A (C - C^*) \quad (4.53)$$

where D_E = (fraction of resistance in dispersed phase) D_d + (fraction of resistance in continuous phase) D_C (4.54)

Considering equation 4.53 above with the boundary equation:

$$C = C_o \quad \text{at} \quad t = t_o$$
$$C = C_f \quad \text{at} \quad t = t_f \qquad (4.55)$$

which results in,

$$E_m = 1 - \exp \frac{2\pi D_E}{v} \int_{t_o}^{t_f} \frac{1}{f_1(t)} \left[\left(\frac{3v}{4\pi W} \right)^2 + \frac{1}{2\alpha} \ln \left(\frac{1+\alpha}{1-\alpha} \right) + W \right] dt \qquad (4.56)$$

where:

$$\alpha = \frac{W - (3v/4\pi W)^2}{W} \qquad (4.57)$$

and,

$$W = (a_o + a_p / \mathrm{Sin}\, \bar{\omega}\, t/)^2 \qquad (4.58)$$

The fractional extraction rates calculated by equation 4.56 gave higher predictions than the experimental values, but it was more accurate when the resistance lay in the continuous phase only (80).

b. Angelo, Lightfoot and Howard's Model

Angelo et al (69) extended the Penetration Theory of heat and mass transfer to a system in which the surface area is a function of time. Their model is based on surface stretch and internal mixing of the drop. They expressed the periodic change of the surface area for an oscillating droplet as:

$$A = A_o\, (1 + \varepsilon \sin^2 \omega t) \qquad (4.59)$$

where

$$\varepsilon = \frac{A_{max}}{A_o} - 1 \qquad (4.60)$$

Equation 4.59 allows an analytical integration of the resulting mass transfer relations and yields the following relation for the mass transfer coefficient:

$$k_d = \left[\frac{4 D_d \omega (1 + \varepsilon_o)}{\pi} \right]^{0.5} \tag{4.61}$$

where

$$\varepsilon_o = \varepsilon + \frac{3}{8} \varepsilon^2 \tag{4.62}$$

The corresponding overall coefficient, based on the dispersed phase is given by:

$$K_d = k_d \left[\frac{1}{1 + m \sqrt{\frac{D_d}{D_c}}} \right] \tag{4.63}$$

Equations 4.61 and 4.63 are only correct for an integral number of complete oscillations.

Jeffreys et al (166) reported that some of the mass transfer coefficients predicted using equations 4.61 and 4.63 were somewhat greater than those predicted by the Rose and Kintner (80) model. In both models the change in the area of the drop is not accurately described since the drop shape is much more complex than the restricted specific geometrical shape.

c. The Ellis Model

Ellis (168) considered an oscillating droplet divided into different regions of mass transfer according to assumed flow regions in the droplet (Figure 4.4). The toroidal section (T) was assumed to be in laminar flow even during droplet oscillation. The remainder of the droplet (the cylindrical core [C], outside layer [L] and polar end sections [E]) was assumed to be in various forms of turbulent flow. However this division of the droplet is not in agreement with the physical phenomena involved in drop oscillation and the drop shape is not spherical during oscillation.

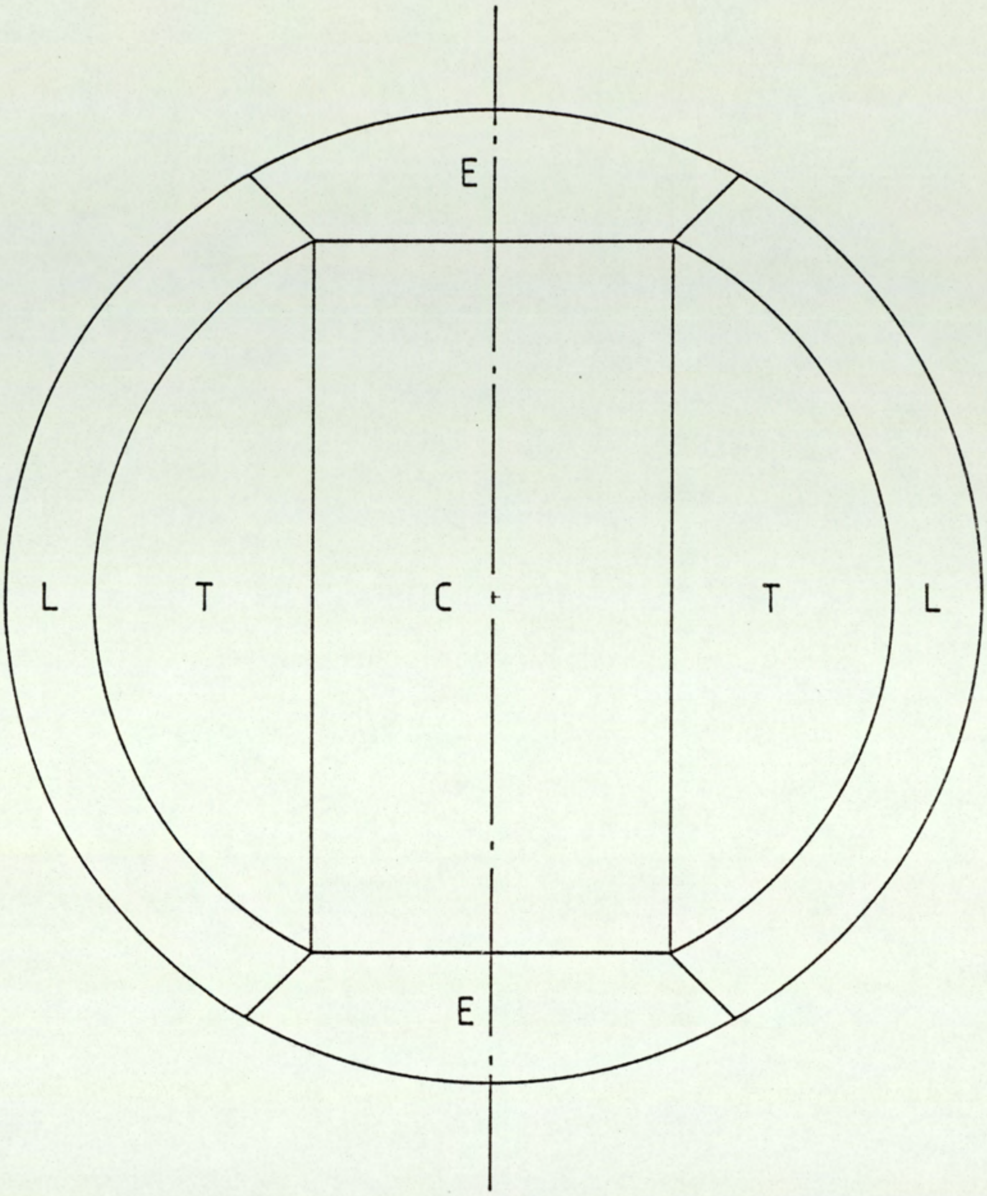

Figure 4·4 Geometrical Description of Layer-Core Model of Ellis (168).

The numerical solution presented considered each of these droplet regions in order to obtain the mass transfer coefficient at the droplet interface, and the effective Sherwood numbers:

$$Sh_d = \frac{2615}{(0.995 + 0.03x)} (Re - \Delta Re)^{0.789} Sc_d^{0.692} G^{-6.03} \qquad (4.64)$$

where: $x = \mu_d/\mu_c$

$$G = We_d \left(3 + 2 \frac{\rho_c}{\rho_d}\right)^{0.5} \qquad (4.65)$$

and

$$\Delta Re = \frac{(x + 2)\,(0.1105 + 0.02325 \exp(-(x - 2.09)^2))}{(0.000018 \times 0.00216)} \qquad (4.66)$$

The above correlation was recommended for use in the range $(4 < G < 6)$ and the effective Sherwood number average error was 20% in this range.

d. Brunson and Wellek Techniques

Brunson et al (66) developed a correlation to fit these experimental results, and concluded that the correlation developed earlier by Skelland et al (145) gave the best prediction of the mass transfer coefficient during fall, or rise, of an oscillating droplet.

They followed the assumption of Rose and Kintner that the characteristic time in equation:

$$\overline{Sh}_d = \frac{k_d\, d}{D} = \frac{4}{\sqrt{\pi \tau}} \qquad (4.67)$$

may be approximated for the time of one oscillation:

$$t = \frac{2\pi}{\omega} \qquad (4.68)$$

Substitution of this into equation 4.67 yielded:

$$\bar{Sh}_d = \frac{2}{\pi}\sqrt{\frac{d^2\,\omega}{2\,D}} \qquad (4.69)$$

However this equation (4.64) did not give a good prediction of mass transfer coefficient. They (66) also assumed that the entire oscillating droplet interfacial area ages according to the unsteady state Higbie theory (65). In other words, all the surface is assumed to have the same age. Taking this into account for the area variation with time as in equation 4.59 resulted in a modified Sherwood number:

$$\bar{Sh}_d = \frac{2}{\pi}\sqrt{\frac{d^2\,\omega}{2\,D}}\,(1 + 0.378\,\varepsilon) \qquad (4.70)$$

This equation gave a 32% absolute deviation from Brunson et al's (66) experimental results. Finally, they used Beek and Kramer's (169) concept, which assumes that an expanding surface is not stretched at all, but that an additional interface is formed in the course of time which is completely fresh, and that there is no transfer of solute between surface elements of different age. A contracting surface is a surface parts of which are disappearing in the course of time. Brunson et al (66) also assumed that the first part of the time-variable, surface to form would be the last to disappear in the course of time. This required the flux to be averaged over the surface and also with respect to time.

e. Empirical Correlations

Numerous correlations have been developed for the mass transfer, inside or outside droplets, as follows:

Skelland et al (145) studied the resistance to mass transfer inside droplets of four organic water system using Colburn and Welsh's (68) technique. This study concentrated on the mass transfer rates of circulating drops and limited results were presented on oscillating drop mass transfer rate for two systems. Nevertheless two empirical correlations were presented for the dispersed phase Sherwood number.

$$Sh_d = 0.320\,T_m^{-0.141}\;Re^{0.683}\;\rho^{0.10} \qquad (4.71)$$

and $$Sh_d = 0.142\, T_m^{-0.141}\, We^{0.769}\, p^{0.285} \tag{4.72}$$

where (p) is the physical property group used by Hu and Kintner (34) in correlating droplet fall velocity. The drop Reynolds numbers ranged from 360-600. Brunson et al (66) reported that equation 4.71 predicted the mass transfer coefficients better than other models for oscillating droplets.

Yamaguchi et al (144) presented a correlation for mass transfer rates for oscillating droplets using a modified Reynolds number which included the frequency of oscillation (equation 4.28). The experimental Sherwood number was assumed to be proportional to the 0.5 power of Schmidt number, and they obtained by the method of least squares:

$$Sh_d = 1.14\, (\bar{R}e)^{0.5}\, (Sh_d)^{0.5} \tag{4.73}$$

Recently Al-Hassan (1) reported experimental overall dispersed phase mass transfer coefficients calculated by assuming that the continuous phase mass transfer coefficient developed by Garner and Tayeban (21) was valid. The amplitude and frequency of oscillation, area of droplet and the diffusivity are the main factors affecting the mass transfer coefficient.

The Penetration Theory was found to be the basis for the common approach applied by previous investigators (69, 80, 66, 144) and all make use of equation 4.52 where C is either a constant or a function of one or more of the factors mentioned above. By regression analysis and least square technique, values of C were evaluated by Al-Hassan as:

$$C = 4.3\ \varepsilon^{2.692}\ E_o^{1.672}\ \text{(Toluene-acetone-water)}$$

$$C = 1.65\ \varepsilon^{0.966}\ E_o^{0.623}\ \text{(Heptane-acetone-water)}$$

ie. $$K_d = 4.3\ \varepsilon^{2.692}\ E_o^{1.672}\ (D_d\, \omega)^{0.5} \tag{4.74}$$

$$K_d = 1.65\ \varepsilon^{0.966}\ E_o^{0.623}\ (D_d\, w)^{0.5} \tag{4.75}$$

The above correlations gave an average absolute deviation of 19.5% and 9.0%

respectively. Al-Hassan (1) also found a correlation for the amplitude of oscillation (ε), equations 3.9 and 3.10.

For the present study the correlations of most relevance are:

a. Johnson and Hamielec's (23) equation 4.12, was used to study the overall mass transfer coefficient of the dispersed phase during droplet formation.

b. Newman's (149) correlation equation 4.34, was used to calculate the overall mass transfer coefficient of the dispersed phase, when the drop was stagnant.

c. Calderbank et al's (44) correlation equation 4.38, was used to calculate the overall mass transfer coefficient of the dispersed phase for droplets with laminar circulation.

d. Handlos and Baron's (152) correlation, equation 4.43, was used for droplets with turbulent circulation.

e. Rose and Kinter's (80), Angelo et al's (69) and Al-Hassan's (1) correlations equations 4.52, 4.63 and 4.74 respectively were used to calculate the overall dispersed phase mass transfer coefficient for droplets during oscillation.

The most useful correlations of dispersed phase mass transfer during drop travel are listed in Table 4.3.

Table 4.3 Dispersed phase mass transfer correlations during drop travel

Author and Reference	Correlation	State of Drops	Remarks
Newman (149)	$E_m = \frac{C_1 - C_o}{C_1 - C^*} = \pi \left(\frac{D_d t_f}{r^2}\right)^{0.5}$	Stagnant	For small drop size
Calderbank et al (44)	$E_m = \frac{C_1 - C_o}{C_1 - C^*} = \pi \left(\frac{R D_d t_f}{r^2}\right)^{0.5}$	Laminar Circulation	R is the ratio of effective diffusivity to molecular diffusivity = 2.25
Kronig and Brink (138)	$E_m = 1 - \frac{3}{8} \sum_{n=1}^{\alpha} A_n^2 \left[\frac{-\lambda_n 16 D_d t}{r^2}\right]$	Laminar Circulation	Values of A_n and λ_n for (n) from 1-7 presented by (101)
Handlos and Baron (152)	$Sh_d = 3.75 \times 10^{-3} Pe_d/(1 + (\frac{\mu_d}{\mu_c})$	Turbulent Circulation	Recommended when resistance to mass transfer exists in continuous phase
Skelland and Wellek (145)	$Sh_d = 31.4 T_m^{-1.338} Sc_d^{-0.125} We^{0.371}$	Circulating	Drops falling in a stationary continuous phase
Rose and Kintner (80)	$K_d = 0.45 (D_d \omega)^{0.5}$	Oscillating	For symmetrical spheroid droplet, widely accepted
Angelo et al (69)	$k_d = \left[\frac{4 D_d \omega (1 - \varepsilon + \frac{3}{8}\varepsilon^2)}{\pi}\right]^{0.5}$	Oscillating	For integral number of completed oscillations

Table 4.3 continued

Author and Reference	Correlation	State of Drops	Remarks
Brunson et al (66)	$Sh_d = \frac{2}{\pi}\left[\frac{d^2\,\omega}{2D}\,(1 + 0.687\,\varepsilon^2)\right]^{0.5}$	Oscillating	With 26% absolute deviation
Yamaguchi et al (144)	$Sh_d = 1.14\ (Re')^{0.56}\ (Sc_d)^{0.5}$	Oscillating	For transfer of low solute concentration from aqueous drop to organic continuous phase
Al-Hassan (1)	$K_d = 4.3\,\varepsilon^{2.69}\ E_o^{1.62}\ (D_d w)^{0.5}$	Oscillating	

CHAPTER FIVE

EXPERIMENTAL INVESTIGATION

This experimental investigation constituted a study of mass transfer rates and hydrodynamic characteristics of oscillating droplets, during unimpeded, gravity flow in a countercurrent spray column for either:

a. The case of single droplets, or

b. Pairs of drops released simultaneously from adjacent nozzles to promote mutual interactions.

The system studied was toluene-acetone-distilled water; the toluene comprised the dispersed phase and the initial solute (acetone) concentration was varied up to 25% w/w.

This system was selected because all the constituents were to the required high purity and physical property data were known for comparison with experimentally-determined values. Furthermore the interfacial tension range (26.1 to 11.0 dyne.cm^{-1}) and density difference had previously been shown to give observable, oscillating droplets (1, 90).

The nozzles employed were of internal diameters 0.2cm to 0.6cm and yielded drops with mean diameters of 0.5cm to 1.0cm, dependent on the flow rates. The basic hypothesis was that a droplet in a practical, non-agitated gravity extraction column is surrounded by a swarm of other droplets. Assuming a mono-dispersion and constant hold-up, the idealised situation is of equi-sized drops all equally spaced and travelling at identical velocities. At low hold-up these participate in the mass transfer process as single droplets. However, above a certain finite hold-up, they also come under the influence of adjacent drops. With drops which are stagnant or circulating this influence would be expected to be limited because of the non-oscillating behaviour (other than any effects due to concentration, or depletion, of solute in the regions between the drops). With oscillating drops however, the mutual effects may be significant with the interference of the oscillation being transmitted through the continuous phase by thinning of the boundary layer.

Strictly the situation would arise in a spray column or in the individual stages of a sieve plate column, ie. between dispersion at one sieve plate and flocculation at the next plate.

The essential operating requirements were:

1. That observations could be made of the effect of pairs of oscillating drops on mass transfer rate and coefficients, when the two drops travelled in parallel separated by a certain distance; or when they collided, bounced, and moved apart again without coalescence; or when they collided and coalesced.
2. That a range of significant operating parameters could be studied ie. drop size, nozzle diameter, solute concentration, flow rates and temperatures.
3. That the drops' behaviour could be followed by photographic techniques and samples of dispersed phase could be withdrawn reproducibly from different positions within the column.

5.1 DESCRIPTION OF EQUIPMENT

A flow diagram of the equipment is given in Figure 5.1 and a general arrangement in Figure 5.2. The process lines and the feed and effluent tanks were arranged for counter-current contact of the two phases in a column of 5.0cm diameter and 100cm long. All valves were within easy reach and a drain point was incorporated at the lowest point in the system.

The apparatus incorporated some improvements to that designed by Al-Hassan (1) to enable a uniform stream of drops to be formed in parallel, with a specific distance between them so that they would not coalesce between formation and discharge from the column. A novel collecting device was developed to facilitate measurements of the concentration of the solute in a drop as it was detached from the nozzle and also as the drops travelled through the continuous phase. All process lines

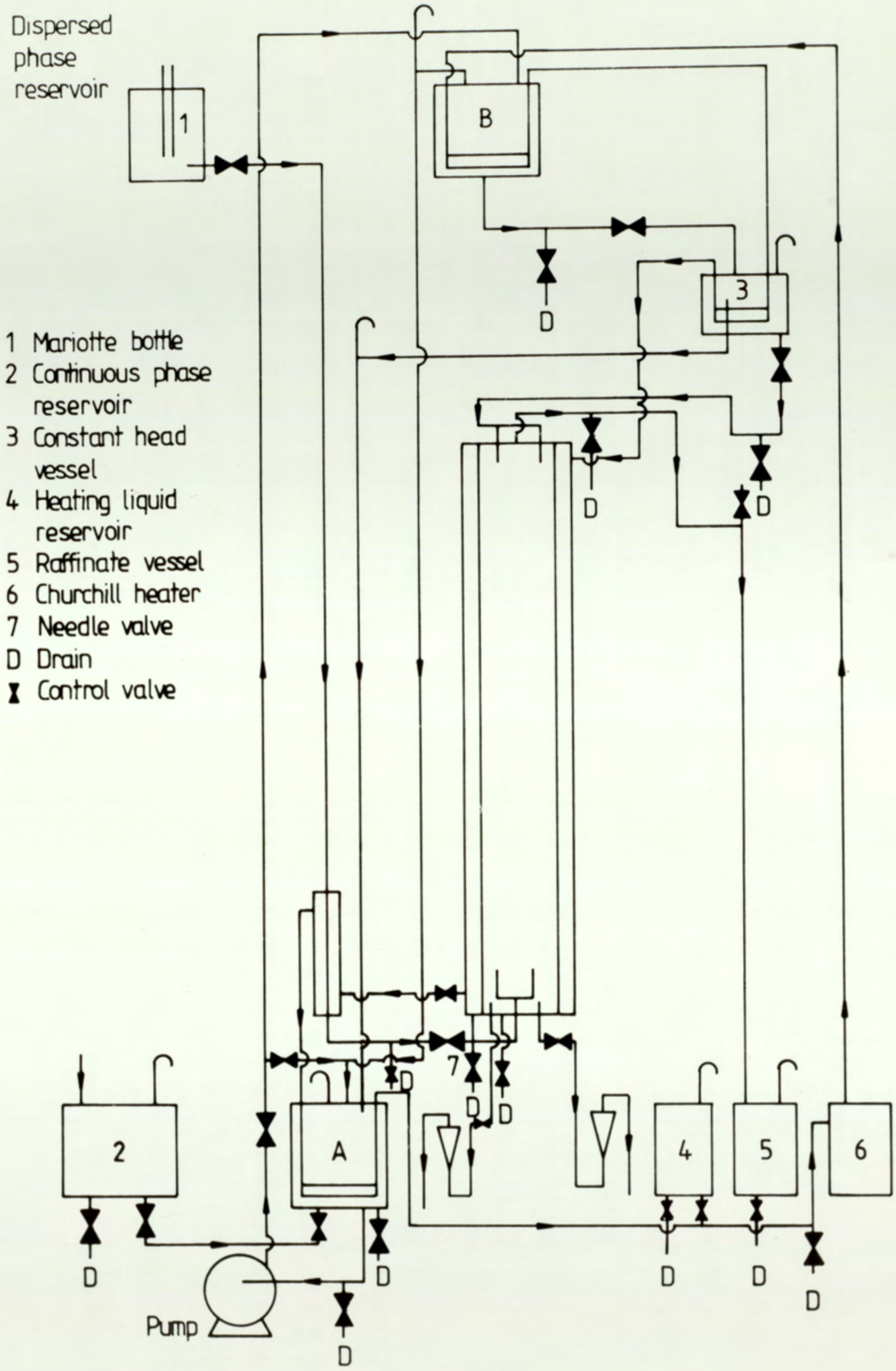

Figure 5.1 Diagram of Experimental Apparatus

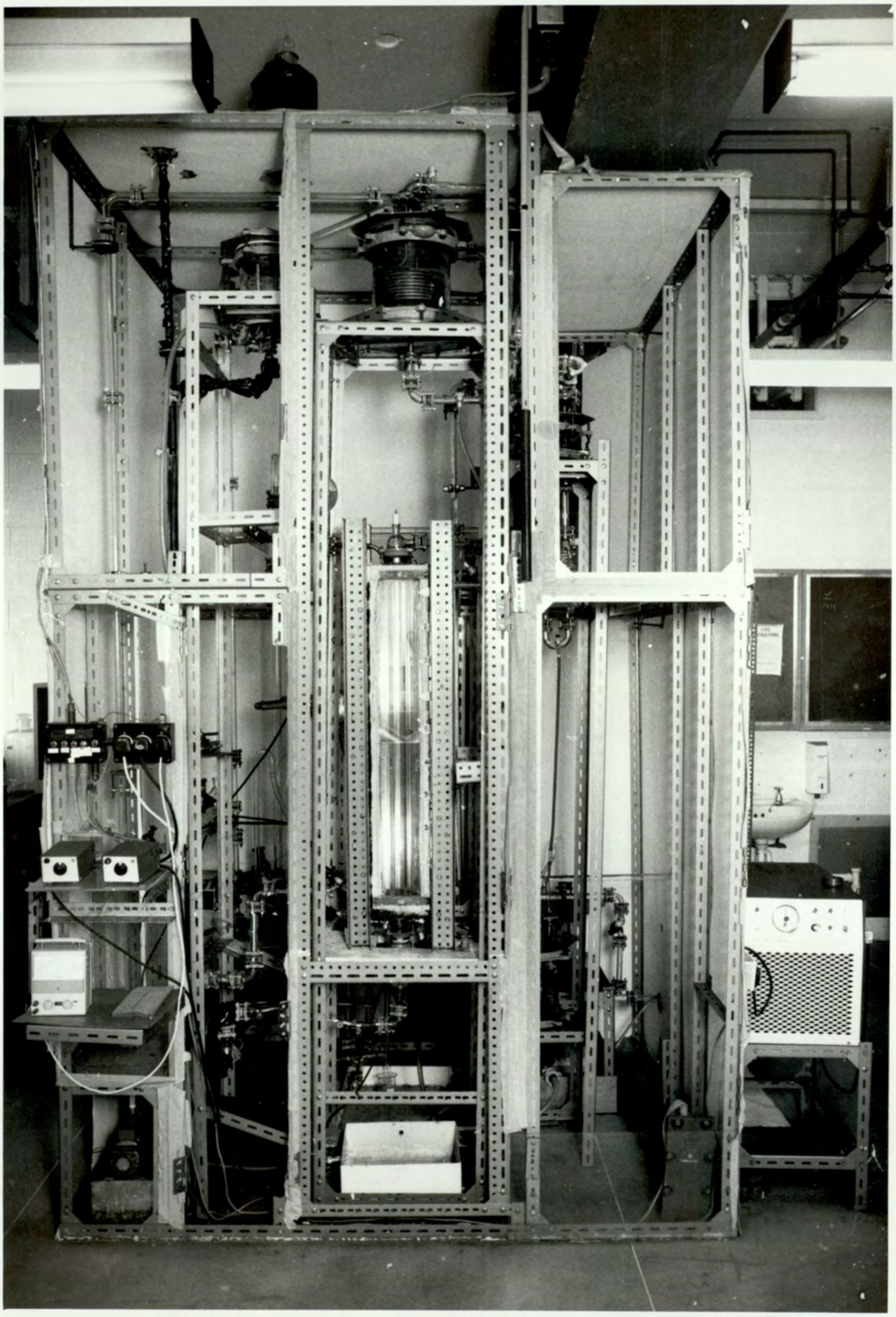

Figure 5.2 General Arrangement of Experimental Apparatus

and valves were redesigned to eliminate bottle-necks and increase the flexibility of the operation.

A Stuart-Turner stainless steel centrifugal pump, type number 12, was used to transfer the continuous phase from reservoir (A) to the top vessel (B), or to saturate the continuous phase with the toluene by recirculating the liquid. The continuous phase reservoir was made up of two vessels of 60 litres capacity together with an intermediate vessel of 10 litres capacity located immediately before the test section to provide a constant delivery head.

A normal glass wool filter 6.0cm thick was pressed to 2.0cm thickness and placed before the test section in the continuous phase line to separate any micro droplets that might be present. The dispersed phase, toluene, was gravity fed from a 5.0 litre vessel to the test section. The flow of the continuous phase was supplied from the constant head vessel and regulated by a p.t.f.e. valve (1.75mm, QVF). The continuous phase flow rate was controlled by a small rotameter (type metric 7F with rubber float) and was kept constant during the experiment. The precise flow rate was measured by collecting the output (extract) over a fixed time period. The dispersed phase flow rate was determined by measuring the volume of the output (raffinate) over a fixed time period.

The temperature of both phases was controlled by circulating water through an external electric heater. The heating liquid reservoir was a 20L vessel made from 300mm QVF pipe with stainless steel backing flanges. The test section temperature was controlled by passing the heating liquid (distilled water) through the jacket. The temperature for all the experiments was set at 22°C. This was just above the highest temperature reached in the room. A Churchill chiller Thermocirculator "05CTC/V" with the following operating parameters was chosen to cover all the temperatures; working temperature range -15° to 60°C, pump circulating rate 680 1/hr with zero head, maximum pump head for no restriction 4.75m, heater rating 1.5kW; nominal HP of refrigeration 0.5. The heater was fitted with an overall temperature safety cutout device. The thermocirculator was chosen for its fine control within ± 0.05°C, simplicity of operation, and safety. The control was achieved by setting the required temperature on the controller dial.

Chilling was necessary since the lighting required to photograph the droplets tended to heat the liquids. Comark thermocouples K76P (Ni Cr/Ni Al, p.t.f.e. 0.19mm diameter wire) were used to measure the temperature at different points in the test section and in the transfer lines: the probes were inserted in carefully selected positions so as not to disturb the flow. The temperatures were indicated on a Comark electronic thermometer (type 1601) which incorporated a Comark themocouple selector unit (type 169 HF). Stainless steel coils, as shown in Figures 5.1 and 5.2, maintained the temperature of the continuous phase in the storage vessels.

A glass shell and tube heat exchanger was fitted in the dispersed phase feed lines immediately before the test section. In addition an electric heater (air convector of 1kw capacity) was fitted inside the cabinet enclosing the equipment to control its temperature.

5.1.1 Design of Test Section

The test section consisted of a 5.0cm internal diameter by 100.0cm long QVF glass column, as shown in Figure 5.3, enclosed in a square jacket. The opposite sides were constructed from 6mm thick glass sheet and the other two sides of 6mm thick polypropylene backed by mild steel sheets 9mm thick. This arrangement allowed droplets to be photographed without any appreciable distortion when the square section was filled with the continuous phase. The top end of the jacket was constructed of polypropylene (6mm thick) supported by stainless steel sheet of 6mm thick. The seal of the four walls of the jacket was obtained by securing them to the base and bottom, and with steel straps as shown in Figure 5.3. Thus the glass sheets were placed in grooves of the polypropylene, and p.t.f.e. sealant was inserted inside the grooves. In addition Dow Corning Silastic (733RTV) was used as a seal on the outside of the column and inside the jacket, and Silastic (733RTV) and Silastic (732 RTV) were used on the outside

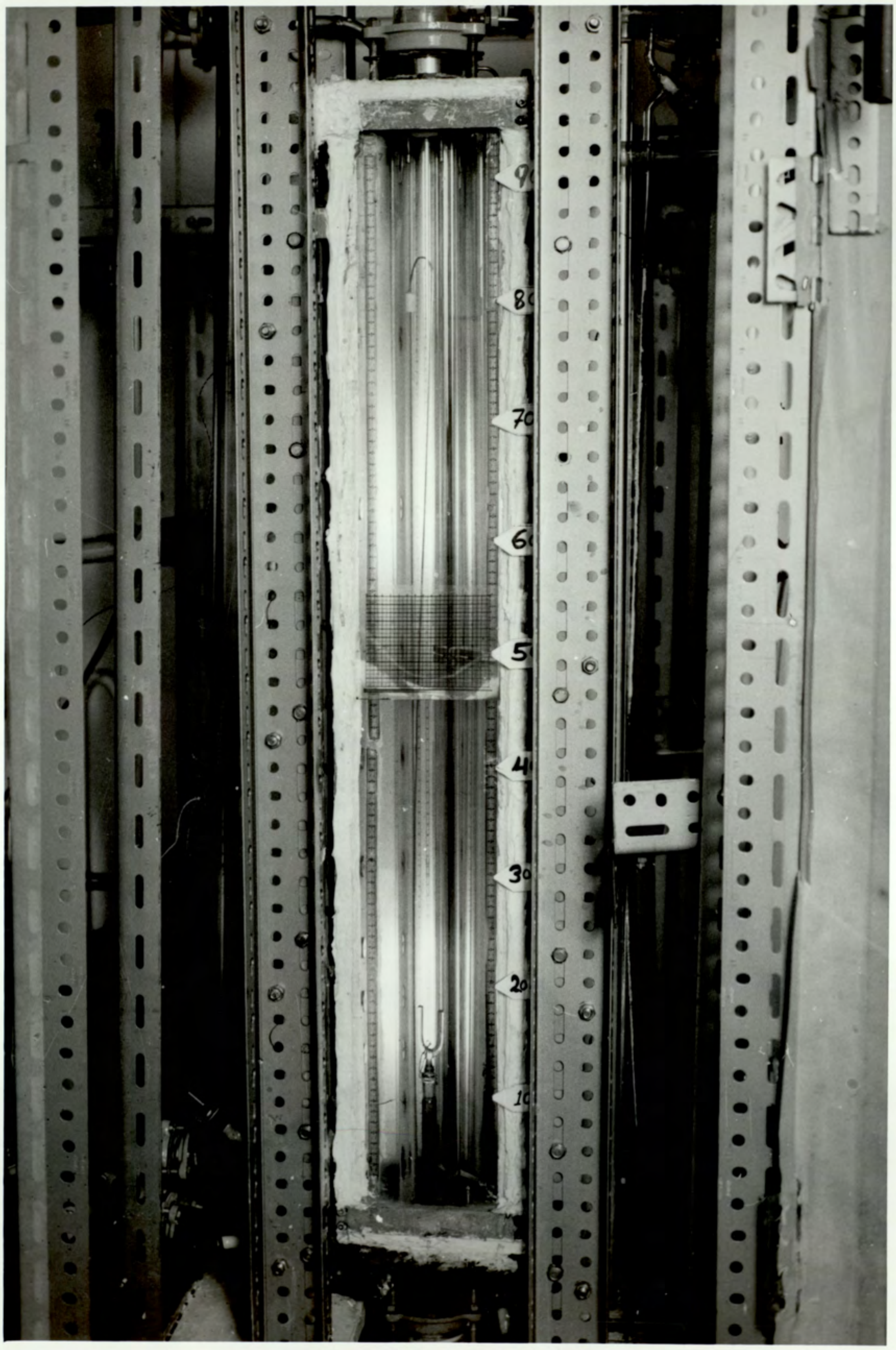

Figure 5.3 Test Section

of the jacket. The lower end of the column was constructed from glass as shown in Figure 5.4 with provision for inserting and holding the nozzles to provide single or parallel streams of drops of dispersed phase. The heavy phase (continuous phase) was introduced into the column via two stainless steel distributors, which were connected to the column by a p.t.f.e. insert, p.t.f.e. paste and a Viton gasket.

Seven dispersed phase sampling points were built in to the column to allow the drops to be withdrawn , immediately after detachment from the nozzles or at 10, 20, 30, 40, 50 and 60cm respectively from the top of the nozzles by means of hypodermic needles. This followed the technique developed by Jeffreys and Bonnet (157). The sampling probe incorporated a drop filter, a small hollow cylinder made from materials wetted by the dispersed phase, which accommodated successive layers of dispersed phase wetted, micromesh cloth. The materials used were p.t.f.e. and nylon micromesh (1μ width of opening). One end of the cylinder was welded to a 22 gauge hypodermic needle with its open tip protruding into the cylinder chamber, as in Figure 5.5 and Figure 5.6.

Nine continuous phase sampling points were installed on the left side, each using a stainless steel compression fitting with a Viton gasket and 6mm diameter p.t.f.e. cap. Sampling lines were extended through the jacket by inserting stainless steel compression fittings and Viton gaskets. A hypodermic needle (17 gauge) was used for sampling through the Viton gasket, and at the other end a three-way polypropylene stopcock (type K-75a) containing a luer fitting enabled a glass syringe to be used to withdraw the continuous phase sample. Additional sampling points were provided at the respective phase inlets and outlets.

Mirrors were installed in the jacket in order to measure the third dimension of any drop. These mirrors were supported on a stainless steel shaft on the right side of the column as shown in Figure 5.3. They were secured in a vertical plane by a shaft that could be rotated. These mirrors were adjusted to enable the shape of a drop to be photographed from the side.

a. Glass Nozzles G_1 - G_5 (left to right)

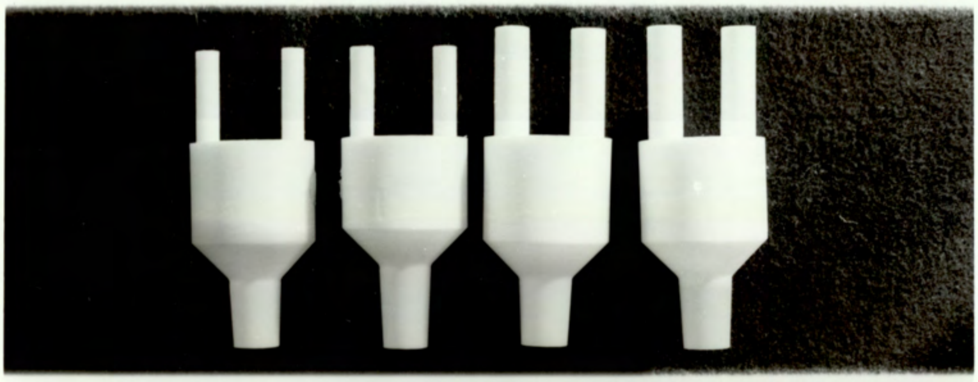

b. pfte Nozzles PT1-PT4 (left to right)

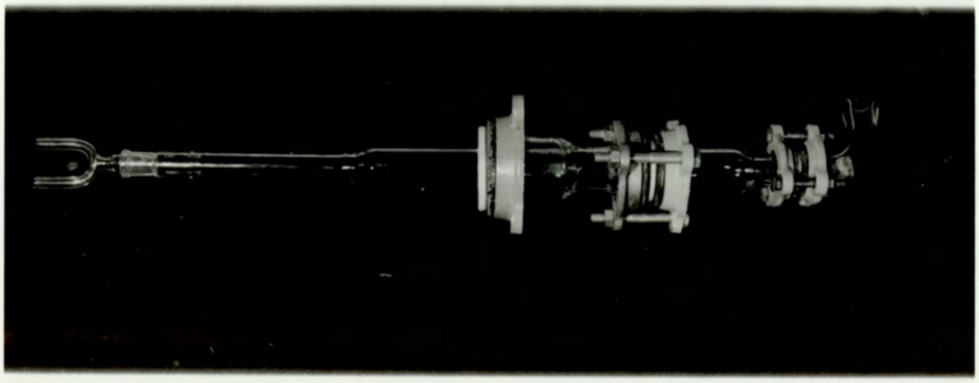

c. Nozzle Holder

Figure 5.4 Range of Nozzles (See Table 5.1)

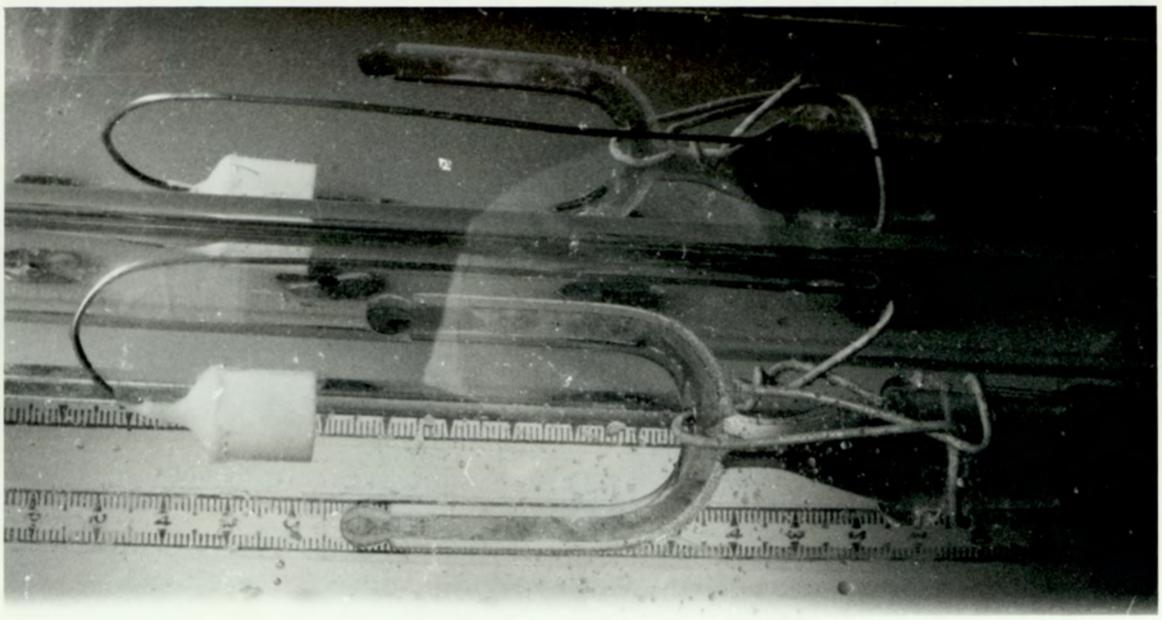

a. Assembled Sampling Head Inside Column.

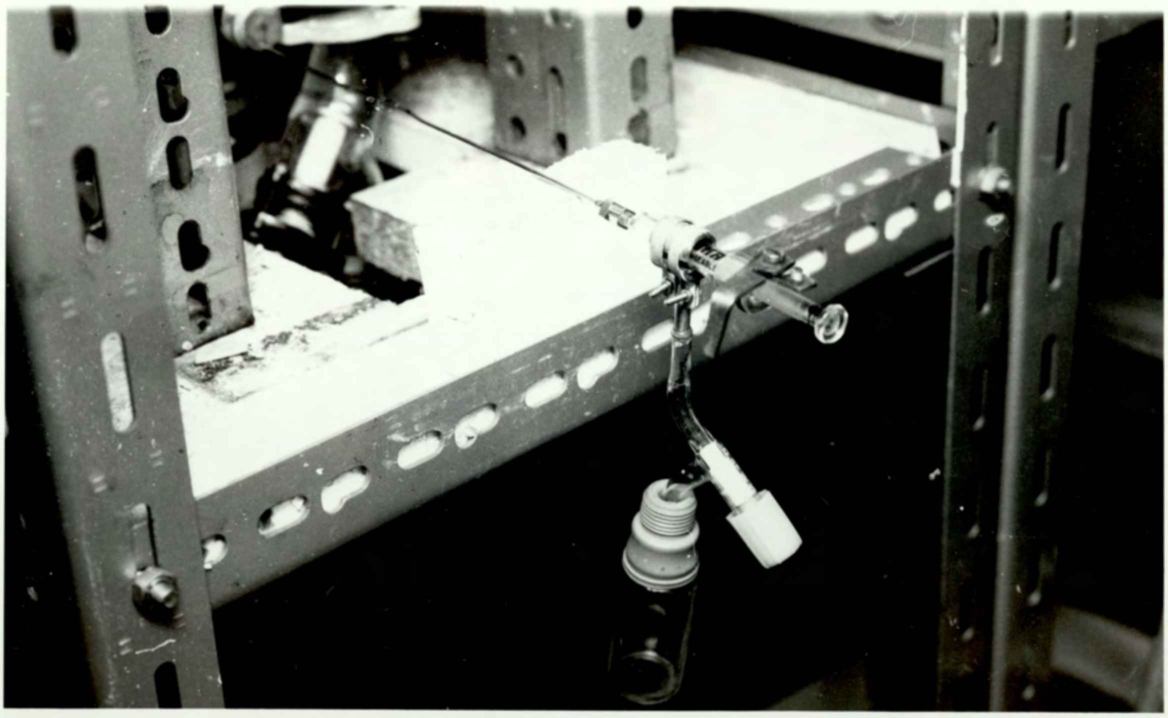

b. Sample Bottle and Syringe Assembly.

Figure 5.5 Dispersed Phase Sampling Assembly

5.1.2 Nozzles

Glass nozzles of 0.2cm to 0.6cm internal diameter were used in the study as shown in Table 5.1 and Figure 5.4. The top of each nozzle was ground so that the plane of the tip was at right angles to the axis of the nozzle.

P.t.f.e. nozzles were found to be necessary to overcome the wetting phenomena observed when studying high solute concentrations of the dispersed phase. Above a certain solute concentration, depending on the nozzle size, the aqueous continuous phase tended to creep down the inside wall of the nozzle, as shown in Figure 5.7. This prevented the formation of equal size droplets. Hence to avoid it p.t.f.e. nozzles, which are hydrophobic, were used in these situations. These nozzles had internal diameters of between 0.5cm to 0.8 cm as illustrated in Figure 5.4, and their tips were tapered to prevent the dispersed phase wetting the tips from the outside.

5.2 SELECTION OF LIQUID-LIQUID SYSTEM

The physical properties eg. viscosity, density, surface and interfacial tension of the organic solvent would be expected to strongly influence droplet behaviour. Therefore great care was taken with purity. The system toluene-acetone-distilled water was chosen for the investigation for the following considerations:

1. The system was selected in order to make a comparison with previous work.
2. The solubility data was available for the system (158, 159) as shown in Figures A1, Appendix A.
3. The concentration of solute (acetone) has a significant effect on interfacial tension of the system, ie. interfacial tension increases as acetone concentration decreases inside the drop as in Table 5.3, which tends to increase the rate of interdrop coalescence.
4. The solvent could be easily recovered and purified.
5. The acetone solution could be expected to reach equilibrium at all points along the interface very rapidly (90).

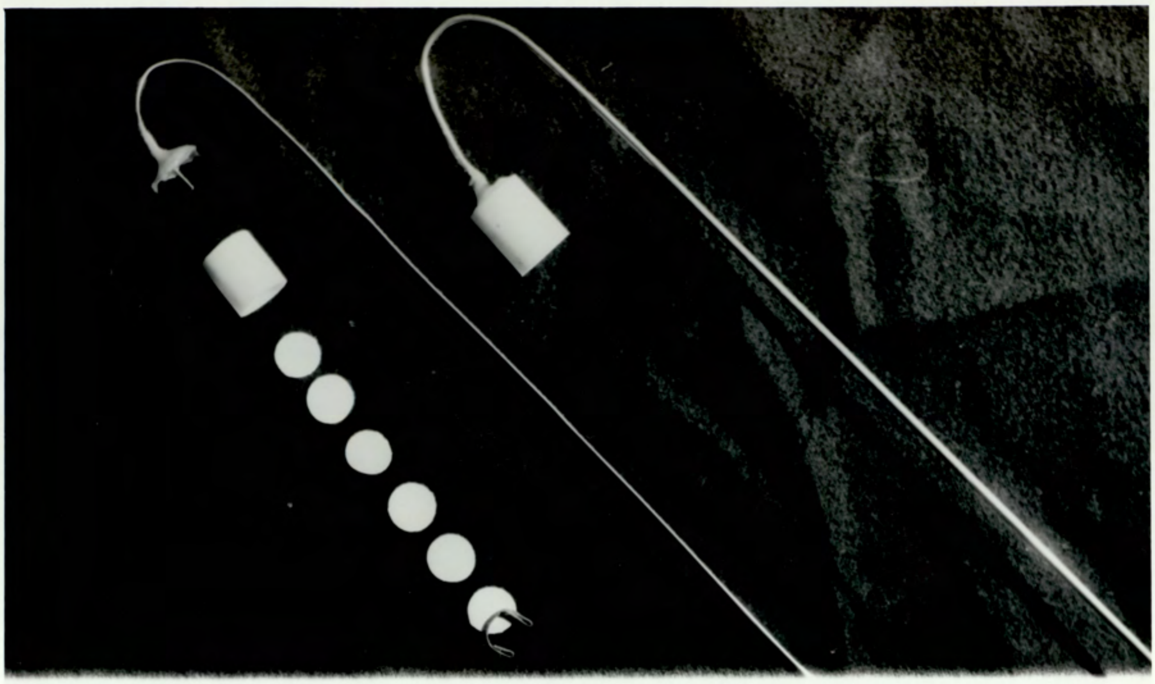

Figure 5.6 The Sampling Head - Dismantled for Illustration Purposes

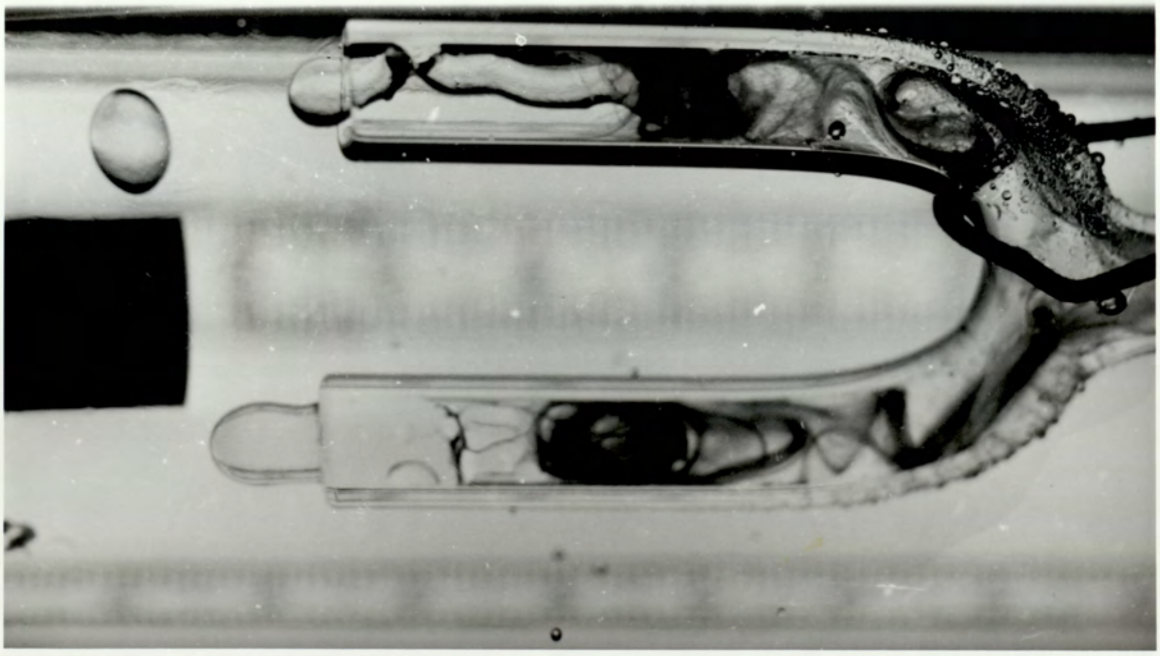

Figure 5.7 Continuous Phase Filming Down the Inside of the Nozzle at High Solute Concentration (Ac. Conc. > 20% w/w).

5.2.1 Materials Used

Toluene and acetone of Analar grade were used without further purification. The specifications of these materials are given in Appendix A. Toluene solutions used in the extraction study were treated with excess of sodium thiosulphate to remove the iodine used as a dye as described in Chapter 6 , then washed thoroughly with distilled water. The washing was accomplished by mixing distilled water with the solution in a 10 litre vessel using a Gallenkamp Handilab Stirrer (SS425), and this was repeated many times. Toluene was distilled by producing an azeotropic point with water at 85°C.

Surface and interfacial tensions were checked repeatedly after each experiment. The raffinate, and any unused feed, were treated prior to recycle (to remove iodine) using solium thiosulphate solution. The solution was then mixed with charcoal powder and shaken vigorously; the charcoal was filtered and the surface and interfacial tensions were measured. Whenever a significant discrepancy (more than 5%) was observed in the values of these properties, the liquid was discarded.

5.3 EXPERIMENTAL TECHNIQUES

5.3.1 Cleaning Procedures

In single and double droplets experimentation, meticulous attention must be given to system purity (156, 55-62, 101, 102) and the cleanliness of the apparatus, in order to obtain reproducible results. Therefore in this work a 1% to 2% aqueous solution of Decon-90 decontaminant was used to clean the column, tanks and the process lines. The column was filled with this solution which was circulated through the system for one hour, at about 40°C and then left overnight. Next morning it was pumped through all parts of the equipment again and then discharged to drain. Following this, hot filtered water was pumped through the system for half an hour and then drained via different drain ports. The equipment was next filled with distilled water heated to 60°C and kept at this temperature whilst recirculating for one hour. The contents were drained and, finally, the apparatus was rinsed with distilled water.

Great attention was paid to cleaning which was repeated during each series of experiments, and repeated whenever it was thought necessary. Between the tests the continuous phase side of the equipment was rinsed with distilled water, while the dispersed phase side was rinsed with pure solvent.

Special care was taken in cleaning the nozzles, ie. glass nozzles were cleaned with chromic acid and then washed thoroughly with distilled water. The p.t.f.e. nozzles were soaked for 48 hours in a high concentration of acetone solution to remove any plasticiser prior to use and then washed with Decon-90 solution, and finally rinsed with distilled water.

5.3.2 System Purity Checks

The system purity was checked at regular intervals during the experimentation by measuring the relevant surface and interfacial tension of the system. If a significant discrepancy (more than 5%) was observed in the values of these properties, presumably due to a build-up of surfactant materials or other impurities, the apparatus was cleaned and the liquid system replaced.

5.4 PHYSICAL PROPERTIES

The physical properties of the system used (toluene-acetone-distilled water) viz density, viscosity, interfacial and surface tension and diffusivity were determined. It was found necessary to determine these at different acetone concentrations to estimate the variation in these properties due to the presence of solute and to use the exact value of any property at any given solute concentration in the mass transfer calculations.

5.4.1. Densities

Water density at 20.5°C was quoted from the Handbook of Chemistry and Physics (158). The densities of solutions were measured using a specific gravity bottle at 20.5± 0.1°C, allowing the absorbed air to be released. These were corrected to the density of water quoted, relative to that of distilled water used. The results are shown in

Figure A.2 Appendix A.

5.4.2 Viscosities

Viscosities were determined by timing the passage of the fluid through a capillary viscometer immersed in a constant temperature bath (20.5 ± 0.1°C). A Cannon-Fenske Viscometer (type 35/IP/CF) was always used. The measurements were corrected to that of water at 22°C and the results are shown in Figure A.3, Appendix A.

5.4.3. Interfacial and Surface Tensions

Interfacial and surface tensions were measured with a ring tensiometer (torsion balance) at 20.5 ± 0.1°C. The measurements of the interfacial tension were made with water saturated with the solvent (toluene), and the recorded measurement was that taken within 60 seconds of the contact of the two phases. The results are shown in Figure A.4 Appendix A.

5.4.4 Diffusivities

The diffusivities were predicted using the Wilke and Chang correlation (160) for acetone diffusion in both phases at 21.0°C, as follows:

$$D = 7.4 \times 10^{-8} \frac{(xM)^{0.5}T}{\mu V^{0.6}} \tag{5.1}$$

Where:-

x = Association parameter, usually (1.0) for non-polar solvent and (2.6) for water.

M = Molecular weight gm.

T = Temperature, °K.

μ = Viscosity of solvent in centipoise.

V = Molal volume of solute at normal boiling point, cc./gm. mole.

The properties of the toluene-acetone-distilled water studied are summarized in Table 5.2.

Table 5.1 Nozzle Diameter

Glass Nozzles		p.t.f.e. Nozzles	
Nozzle	Diameter mm	Nozzle	Diameter mm
G1	2.768	PT1	4.397
G2	2.901	PT2	4.979
G3	4.005	PT3	5.617
G4	4.995	PT4	7.525
G5	5.995		

Table 5.2 Physical Properties of the System (Toluene-Acetone-Water)

Exp No	Acetone Conc^n *	Acetone Conc^n %w/w	Density **	Viscosity μ cP	Interfacial tension dyne cm^{-1}	Diffusivity D m^2 x 10^{-4}.s^{-1}	Distribution coefficient m
1	0.00	0.00	0.8636	0.618	26.1	-	-
2	0.45	3.06	0.8621	0.595	23.8	2.674	0.70
3	0.51	3.46	0.8619	0.595	21.8	2.691	0.72
4	1.11	7.47	0.8610	0.572	19.1	2.780	0.76
5	1.50	10.21	0.8587	0.567	17.4	2.840	0.80
6	2.05	14.00	0.8542	0.545	15.3	2.920	0.85
7	3.01	20.67	0.8499	0.521	12.9	3.030	0.95
8	3.19	21.90	0.8490	0.519	12.7	3.067	0.96
9	3.50	24.11	0.8476	0.511	12.2	3.101	1.00
10	3.75	25.87	0.8451	0.505	11.0	3.118	1.00
11	3.92	27.07	0.8438	0.499	10.8	3.176	1.04

* = kg. x 10^{-3}.mol/L

** = kg x 10^{-3}/m^3 x 10^{-6}

CHAPTER SIX

MEASUREMENT TECHNIQUES AND EXPERIMENTAL PROCEDURES

6.1 MEASUREMENT TECHNIQUES

The study of mass transfer involving oscillating drops necessitated the measurement of two parameters.

1. The concentration of the solute in both phases from which to evaluate the mass transfer rate;

and,

2. The frequency of change of the interfacial area of the droplet, which could only be studied photographically.

6.1.1 Concentration Determination

Acetone concentrations were determined by measurement of the relative absorbance of ultra-violet radiation. Calibration charts of relative absorbance against concentration were prepared by measuring the relative absorbance of solutions of known acetone concentration in the organic (toluene phase) and aqueous (water phase), Figures (A.5) and (A.6) Appendix A.

A Pye Unicam Ultra-Violet Spetrophotometer (SP 1800) was used for the measurement of relative absorbance of the sample placed in 10mm path-length cells. The apparatus was first zeroed by inserting a liquid blank in both cells. The wave length (λ) at which maximum absorption of acetone occurred was found to be 286mm for the toluene phase solutions and 276mm for the aqueous solutions. The cells and the samples were maintained at a constant temperature of 20.5 ± 0.1°C in a thermostat ically-controlled water bath for about one hour before the readings were taken. The above method was in fact selected from three methods of analysis previously used to estimate acetone concentration in aqueous and organic solutions (161, 162, 1). The other two methods were via measurement of refractive index and the Messinger idoform method (163).

The initial experiments involving the measurement of refractive index did not give reproducible results. Indeed it was observed that one sample gave a range of readings between 19.0 to 19.50° when checked over a period of time. This could have been due firstly to manual errors during the test procedure, and secondly the thin layer of sample used introduced the possibility of solute evaporation from the refractometer cell. By comparison the larger sample used in the ultra-violet spectrophotometer eliminated this kind of error.

The Messinger idoform method, which involved a reaction between an alkaline solution of acetone with an excess of iodine to form iodoform (163), did not yield satisfactory results. This was probably due to the sensitivity of the chemicals involved, ie. iodine and sodium thiosulphate, to light, temperature and time. The reaction proceeds according to the equation:

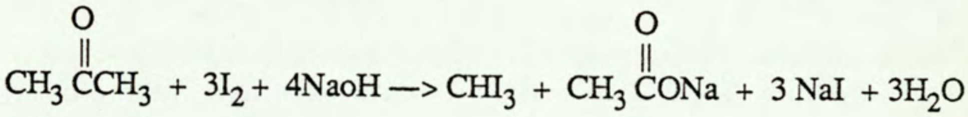

$$CH_3\overset{O}{\overset{\|}{C}}CH_3 + 3I_2 + 4NaoH \longrightarrow CHI_3 + CH_3\overset{O}{\overset{\|}{C}}ONa + 3\,NaI + 3H_2O$$

The above reaction is very slow and the sample should be allowed to stand for at least one hour in the dark in an ice-water bath. The excess concentration of iodine can then be measured by titration with a standard solution of sodium thiosulphate; hence the acetone concentration can be calculated by molar equivalence. The method of relative absorbance was found to be very convenient and gave more accurate, reproducible results than the other methods described.

6.1.2 Determination of Equilibrium Distribution Diagrams

Equilibrium concentrations were determined by making-up mixtures on a weight basis to represent points below the mutual solubility curve (159). Each mixture was contained in a stoppered flask and brought to equilibrium by repeated shaking and standing for several hours in a thermostat bath at 20.0°C. The layers were then separated using a separating funnel and the samples analysed using the relative absorbance method. The equilibrium diagrams for the ternary system used, viz Toluene-Acetone-Water, are given in Appendix A, Figure A1.

6.1.3. Photography and Associated Techniques

A novel photographic technique was used to follow the drop behaviour during its travel in the test section. A National Panasonic WV3030E colour video camera with a 12.5 - 75mm zoom lens with maximum aperture of f1.4 was subsequently used at a distance of 1.6m to reduce parralax errors, with a frame rate of 25f/sec. The data required from the film were:

1. Size and velocities of a rising droplet.
2. Droplet interfacial area and volume changes.
3. Droplet residence time in the test section.

Because of the small difference in densities and refractive indices between liquid drops and the continuous phase it was difficult to use the photographic technique (17, 21, 40, 45, 69, 80, 117, 125). Therefore a dye was used to improve the contrast, especially for high speed photography. Iodine was found (1) the most suitable. Measurements showed that it had no effect on the interfacial tension, and surface tension and other physical properties in the range of concentrations necessary (20 to 30 ppm). However, acetone reacts with an excess of iodine and in a strong basic medium it also tends to change colour from violet-brown to brown and then to yellow depending on the concentrations of each substance. In neutral or slightly acidic solutions, PH 6-7, and at low concentrations of both substances, the above reaction and colour change is very slow. Therefore the iodine was added prior to the start of an experiment.

Preliminary tests with a Gossen Lunasix 3 CdS light meter showed that a greater intensity of light was emitted from the column than from the mirrors, due to the positioning of the mirrors. Therefore a neutral density filter in the form of an acetate sheet was positioned on the bright side of the column to reduce the light intensity to that from the mirrors.

A Beaulieu R16 cine camera was first used to photograph the droplet with an aperture setting of f5.5 at a distance of approximately 5 ft from the front glass face of the column. A 125 ASA black and white, 16mm film was used. The camera was operated at 64 fps. A Hadland high speed cine camera was also used to photograph the initial changes in the drop shapes. This was operated at 1000 fps with a 75mm lens, using Ilford HP5 400 ASA black and white film. The lighting was provided by four Jupiter, 650 watt quartz iodine, sealed beam flood lights, with an R R Beard 1000 watt quartz iodine flood light as "fill in", as in Figure 6.1.

Four transparent plastic millimetre scales were fixed at the rear of the square jacket over its full length; another two scales were fixed on the front of the jacket, one either side. In each run several drop pairs were followed from their formation at the nozzle's tip to the top of the column by panning the motion picture camera on the tripod or the video camera as explained earlier, as the droplet ascended. In this way a complete record was made of droplet behaviour during its entire ascent. Projection of the movie film on to a screen or a video cassette on a television screen enabled the data to be analysed

The drop velocity was calculated using the vertical distance travelled in the measured time increment. The surface areas and volumes of drops during travel were calculated on the basis that the (x) and (y) axes were the horizontal and vertical axes of the droplet in the column and (z) was the horizontal axis read from the reflection in the mirror as shown in Figure 6.2.

6.2 PREPARATION OF PHASES

The two phases were prepared 24 hours prior to the experiment. A 10 litre QVF aspirator was used to prepare a quantity of dispersed phase sufficient for four experiments. The toluene was first saturated with water by mixing with a Gallenkamp stirrer (SS 530) for two hours; the two phases were then separated. The calculated

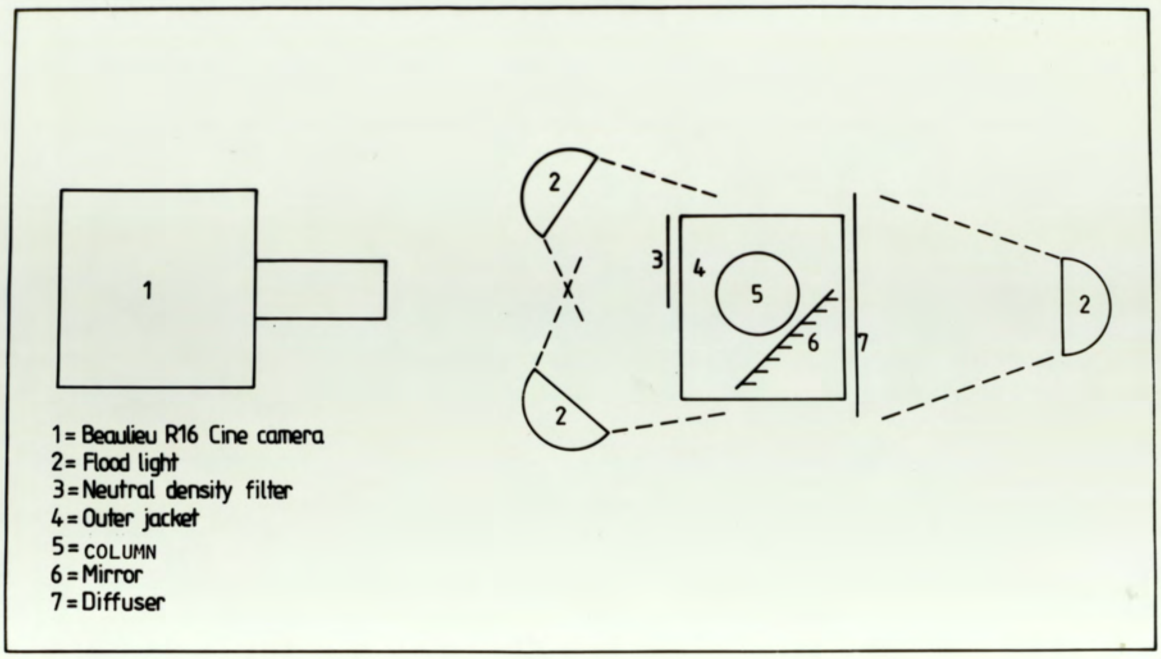

Figure 6.1 Arrangement for Droplet Photography

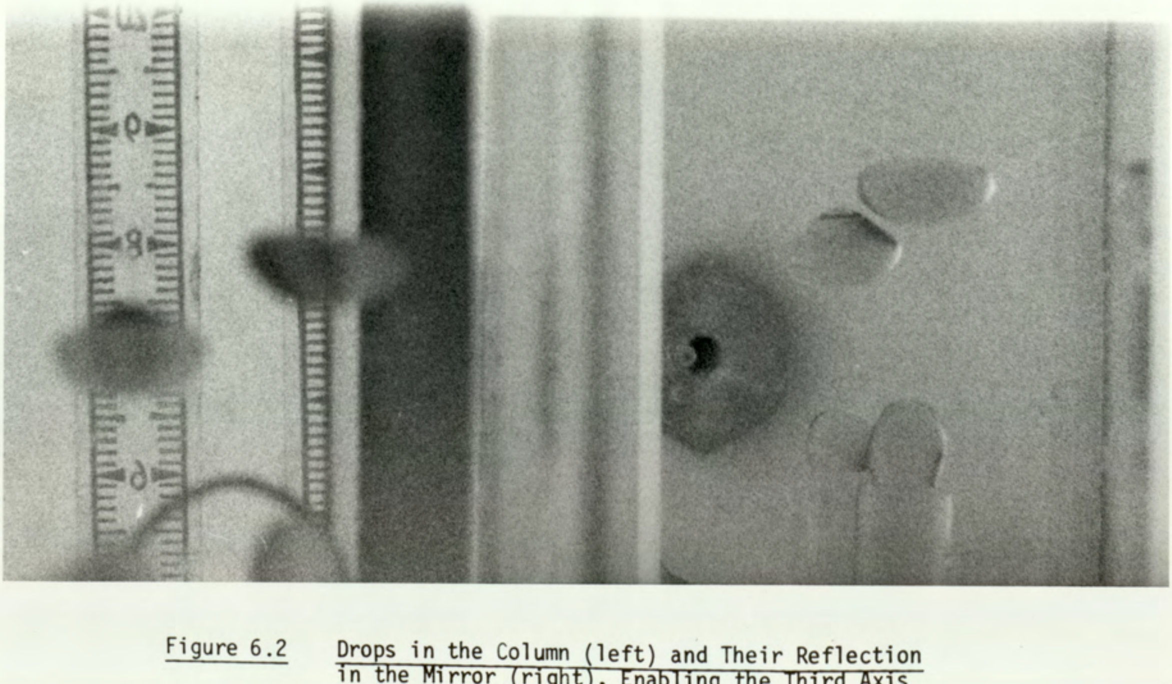

Figure 6.2 Drops in the Column (left) and Their Reflection in the Mirror (right), Enabling the Third Axis to be Measured.

d = 7.00 m.m
Ac. Conc = 0.511 gm.mol/L
U = 0.359 $cm^3.sec^{-1}$
Vel = 11.76 $cm.sec^{-1}$

volume of solute for the required concentration (159) was then added, the solution remixed for one hour, and then left overnight. The exact concentration obtained was determined just prior to an experiment by ultra-violet spectrophotometry.

The continuous phase was mixed with an excess of toluene (20-25 ml) by circulation of the liquids through the apparatus using a Stuart Turner centrifugal pump. The liquids were circulated for an hour to ensure complete saturation and then separated.

6.3 EXPERIMENTAL PROCEDURE

6.3.1 Non Mass Transfer Studies

Studies in the absence of solute transfer were performed in support of the main study to provide a good understanding of the effect of solute mass transfer on drop oscillation through dispersed phase hold-up, drop size and drop velocity. The experiments also indicated the distance required between the two nozzles to facilitate the formation of a pair of drops which would travel closely in parallel without coalescence prior to the end of the column, Figure 6.3 and Table 6.1 illustrate the idea.

6.3.2 Mass Transfer Studies

Extraction efficiency and drop hydrodynamics under mass transfer conditions were studied for different acetone concentrations in the dispersed phase, ie. with mass transfer from the dispersed to the continuous phase. The effect of solute concentration on droplet characteristics and upon the tendency to bounce and rebound, or to coalesce, during travel, was observed.

Subsequently an investigation was made of droplet shapes, size, velocity and interfacial area and how these parameters were affected by dispersed phase hold-up and the physical properties of the system. A graticule scale, Figure 6.4, was used to measure the dimensions of small drops (<40mm in diameter) at high acetone concentrations (>20% w/w).

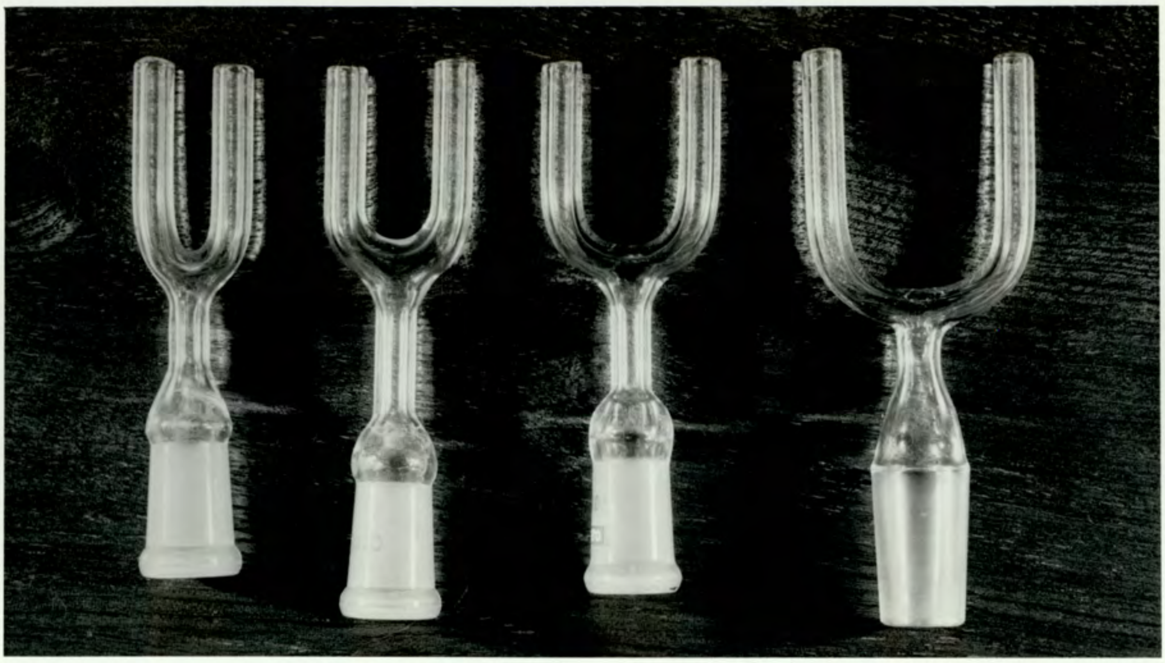

Figure 6.3 Glass Nozzles - Showing the Pitch Centre Diameter (PCD) (See Table 6.1)

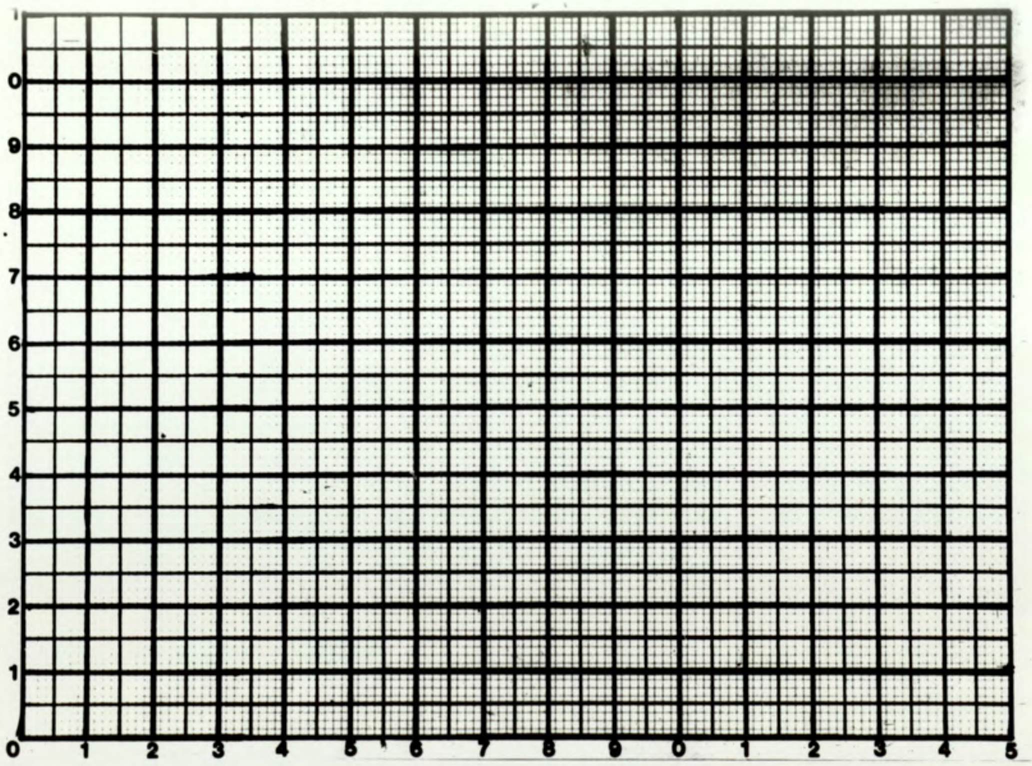

Figure 6.4 Graticule Scale to Facilitate the Interpretation of the 16 mm, and Video, Films.

6.3.3 Mass Transfer Experiments

Experiments were conducted involving the transfer of acetone from the dispersed phase to the continuous phase. Acetone concentration in the dispersed phase was in the range of (3-25% w/w). In all cases of solute transfer from the dispersed to the continuous phase the initial acetone concentration in the continuous phase was always zero. The dispersed phase outlet stream was collected with the unused dispersed phase and reused after purification, for another run.

The cabin heater, was turned on an hour before the start of an experiment. The valves on the heating liquid circulation line were opened and the Churchill heater turned on with a setting of 22°C. Following this the required volume of the dispersed phase was transferred to the reservoir and mixed with iodine. Then the input line to the test section was filled with dispersed phase to the tip of the nozzles, to avoid any continuous phase creeping into the line

The test section was filled with continuous phase, and the desired flow rate was set via the constant head line and control valve, to maintain a constant level of liquid at the top of the column, and such that no continuous phase flowed via the raffinate outlet. Thus, when the droplet reached the top of the column, it flowed sideways and was separated from the continuous phase, as shown in Figure 6.5.

To avoid any effects of coalescence the continuous phase was introduced 15cm lower than the coalescence phase. At this stage the flow of dispersed phase was turned on and set by adjusting the needle valve; this marked the start of the experiment. The flow rate of dispersed phase was controlled by regular adjustments, by measuring the time required for 10 drops discharged from the nozzle using a stop watch with a ± 0.2 second accuracy. The flow rate could be adjusted to within $\pm 1.0 \times 10^6$ m^3/s of the required value. The continuous phase flow rate was measured with an accuracy of ± 2 ml per minute, by collecting the output flowing to drain in a measuring cylinder for one minute.

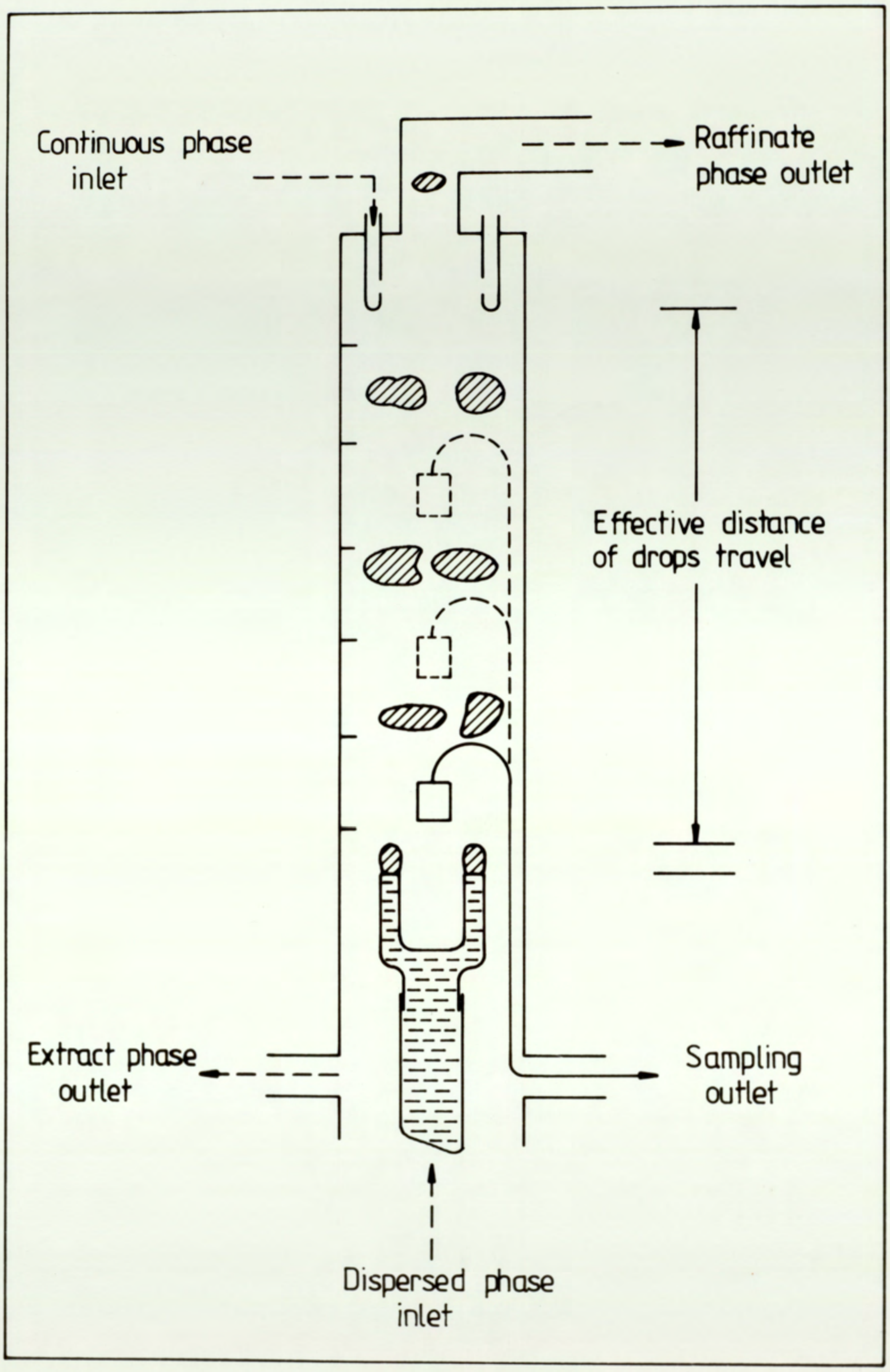

Figure 6.5 Diagrammatic Representation of Droplet Travel and Coalescence.

Table 6.1 The Distance Between the Two Nozzles ie. the Pitch Centre Diameter (PCD)

NOZZLES USED	PCD Cm
G1	1.22
G2	1.65
G3	2.18
G4	2.85

Initial runs were carried out to determine the time taken for the column to reach steady state conditions. This was done by taking samples from the outlet streams at 3 minute intervals until identical acetone concentrations were obtained for consecutive time intervals. This was found to require about 20 minutes. In subsequent experiments after steady state conditions had been reached, 5 ml samples were withdrawn from the dispersed phase sample ports after drop formation and along the column at distances of 10, 20, 30, 40, 50 and 60cm from the top of the nozzles, as mentioned in Chapter 5 and shown in Figure 6.5. In addition samples were withdrawn from the continuous phase along the column at distances of 0.0, 10, 20, 30, 40, 50 and 60cm from the top of the nozzles at intervals of 3 minutes. Due to the laminar flow of the continuous phase, the positioning of the needle to withdraw continuous phase samples was hence critical to give reproducibility (since the concentration of the acetone in continuous phase decreased as the column wall was approached, because of the laminar flow of the continuous phase). The dispersed and continuous phase samples were analysed by ultra-violet spectrophotometry as discussed earlier.

Results of mass transfer runs were evaluated and the mass transfer coefficient calculated as discussed in the Chapter 7.

CHAPTER SEVEN

TREATMENT OF RESULTS

The application of the different theoretical single droplet models and empirical correlations discussed in Chapters 3 and 4, for prediction of oscillation frequencies, amplitude, efficiencies of mass transfer and overall mass transfer coefficients for the range of drop sizes studies experimentally are presented in this Chapter.

The overall mass transfer coefficients during formation were predicted and compared with the experimental data. The dispersed phase mass transfer coefficients for large oscillating single drops and drop pairs of the relevant sizes during travel were also calculated using three correlations:

i) Rose and Kintner's model (80)

ii) Angelo et al's model (69)

iii) Al-Hassan's correlation (1)

The continuous phase mass transfer coefficients during drop travel were also calculated, using the correlation proposed by Garner et al (21), and the overall mass transfer coefficients were predicted using equation 1.3.

Improved models are proposed to predict the overall mass transfer coefficients during formation, and the dispersed phase mass transfer coefficients including a modified correlation for oscillation frequency of large oscillating drops.

7.1. DATA COLLECTION

The video cassettes and cine films provide a permanent record of the experimentally-observed droplet oscillation frequencies and velocities. These have been deposited in the Chemical Engineering Department. The data collected from these films, are presented in Appendix B.

Measurement of the three axes of each droplet and their change with frame number was obtained from a TV screen or by projection of the cine film. This also provided the time in which the droplets had ascended a fixed vertical distance and enabled the velocities and oscillation frequencies to be calculated. Some of the hydrodynamic and mass transfer data for drop pairs are presented in Tables 7.1A and B. The remaining data are presented in Appendix D.1.

Runs 10, 11 (A - E) for single drops

Runs 12, 13 (A - D) for single drops

Runs 14-23 (A - D) for drop pairs

Runs 24-28 (A, B) for drop pairs

Figures 4.1 and 4.2 illustrate some of the observed drop profiles.

7.2 TREATMENT OF DATA

A number of computer programs written in Fortran 4 and 77 using Aston University subroutines, were used to evaluate the results. A BBC micro computer was also used with certain programs eg. Basic programs, (Apple II). The programs, outputs and a sample calculation are presented in Appendices C, D and E respectively.

7.2.1. Frequency of Droplet Oscillation

Existing correlations to determine the frequency of oscillation are, as summarised in Chapter 2, for single droplets only. All necessitate first estimating the variation of the characteristic parameters with time. The parameters are:

1) The eccentricity

$$E = d_h/d_v \qquad (7.1)$$

2) The ratio of the area of an ellipsoid to that of a sphere of equal volume.

This utilises the equation proposed by Angelo et al (69) for a single droplet:

$$A = Ao\,(1 + \varepsilon \sin^2 \omega' t) \qquad (7.2)$$

Table 7.1A Data from hydrodynamic experiments with droplet pairs

Run No	Nozzle Used (Fig 5.4)	t_f s	d_e m x 10^{-2}	Average Area m^2x10^{-4}	Terminal Velocity m x $10^{-2}.s^{-1}$	f_d $m^3x10^{-6}.s^{-1}$	f_c $m^3x10^{-6}.s^{-1}$
1	G1	1.51	0.80	2.01	11.24	0.18	1.50
2	G2	1.03	0.77	1.86	10.65	0.23	1.45
3	G3	3.15	0.90	2.54	9.71	0.12	1.47
4	G4	1.21	0.87	2.27	10.86	0.29	1.60
5	G5	4.05	2.08	3.66	9.11	0.16	1.63
6	PT1	1.01	0.74	1.72	10.15	0.21	1.83
7	PT2	3.03	0.90	2.54	9.76	0.13	1.75
8	PT3	0.81	0.85	2.27	10.30	0.40	1.63
9	PT4	2.51	1.26	4.99	9.08	0.69	1.92

where

$$\omega' = 1/2\ \omega$$

3) Deformation ratio, the ratio [(X - Y)/(X + Y)]; (165)

A study of three dimensions of each drop enabled an accurate prediction to be made of the change in surface area during a cycle of oscillation. Thus, the lateral area of an ellipsoid with semi-axes X, Y, Z (164) is:

$$A = 2\pi Z^2 + \frac{2\pi Y}{\sqrt{X^2 - Z^2}} \left[Z^2\, \mathrm{FI}(I, \phi) + (X^2 - Z^2)\, \mathrm{EI}(I, \phi)\right] \qquad (7.3)$$

where

$$I = \frac{X}{Y}\sqrt{\frac{Y^2 - Z^2}{X^2 - Z^2}} \qquad \phi = \arccos \frac{Z}{X}$$

and FI (I, ϕ) and EI (I, ϕ) are elliptic integrals of the first and second kinds (164) for $0 < I < 1.0$.

The program presented in Appendix C.3 was used to calculate the changes in the lateral area of the droplet with time, the volume, and the velocity with time. The following parameters were also estimated: E from equation 7.1, XY/Y, Y/X, Y/Z, (X - Y)/(X + Y) and the ratio of the area of the droplet to the area of a sphere of equal volume.

The statistical characteristics ie. the mean and the variance of the above parameters, were also evaluated and a straight line fit was obtained to show the general trend of these parameters with time, Appendix D.3. Typical results are presented graphically in Figures 7.1-7.4; the remainder are presented in Appendix D.4. A typical output listing of the area velocity program is given in Appendix D.3.

7.2.2. Droplet Amplitude

Three different correlations, described in Chapter 3 section (3.2) were used to calculate the amplitude of drop oscillation, namely,

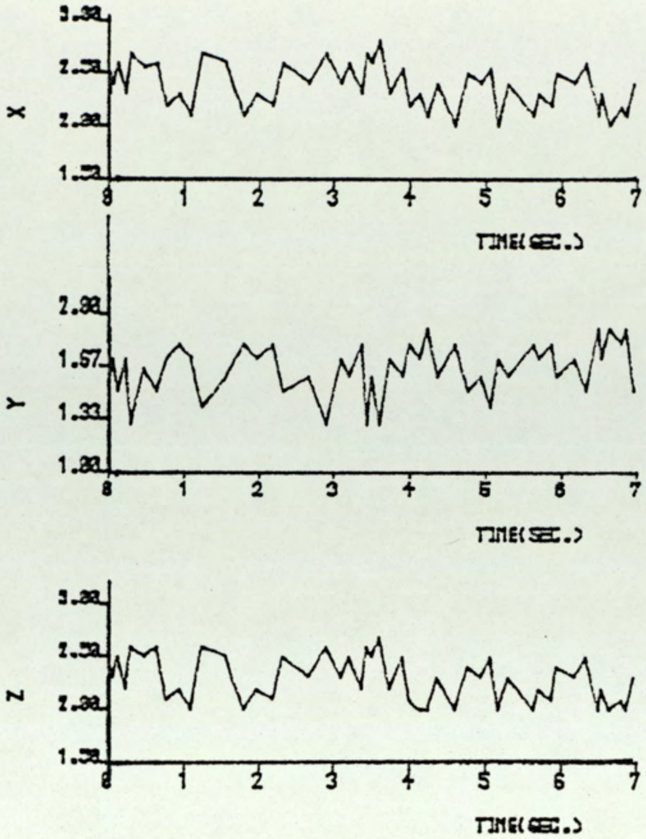

RUN(10A)

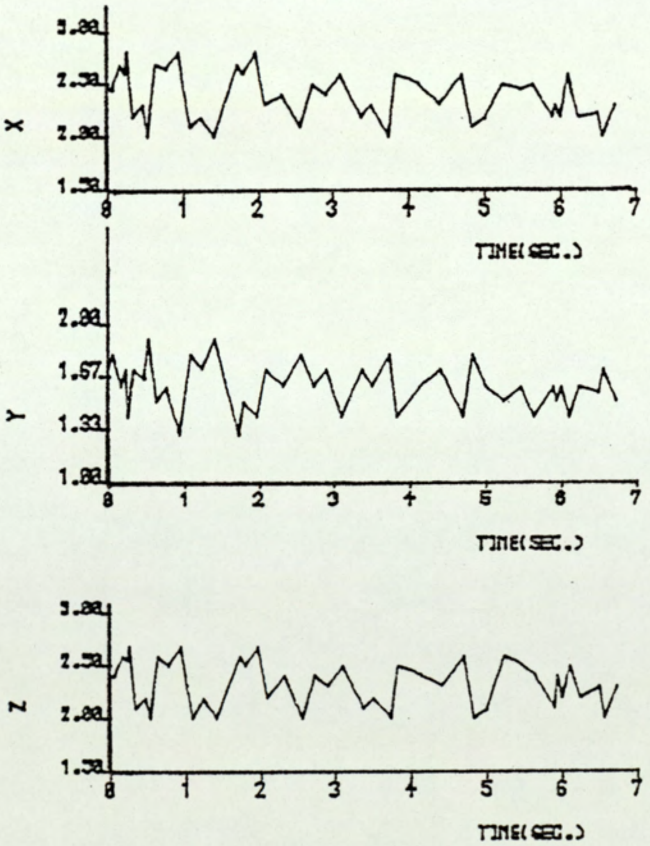

RUN(10E)

FIG.7.1 Fluctuation of drop dimensions with time of Single Drop.

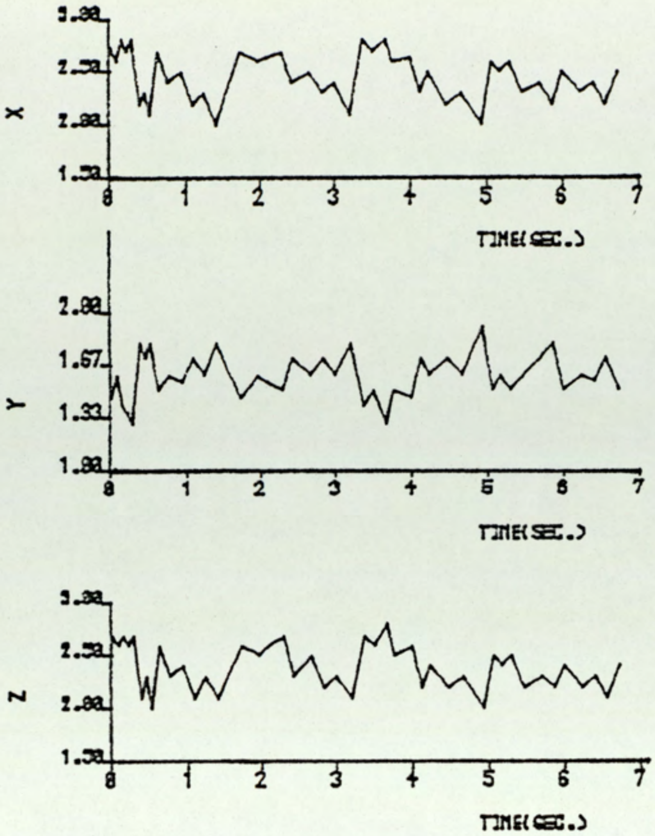

RUN(11D)

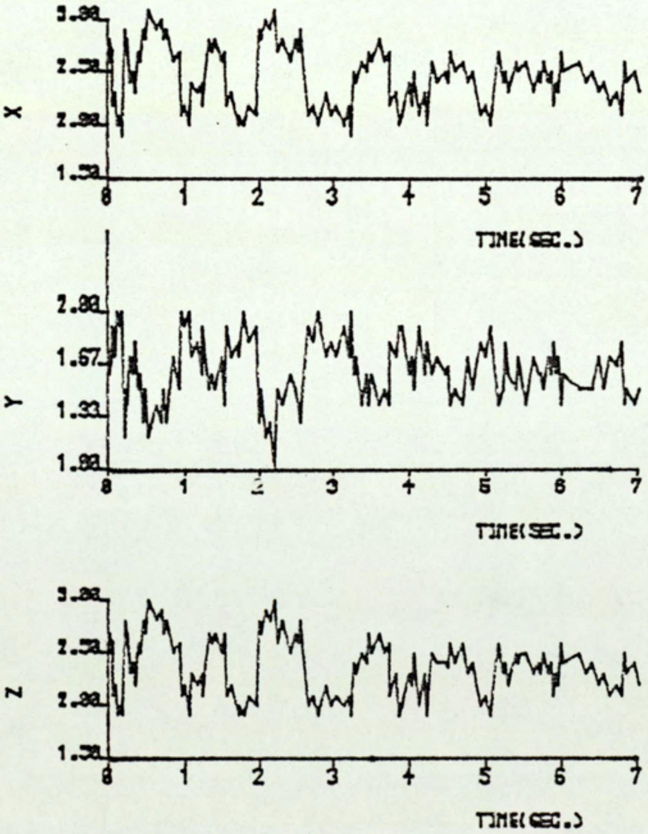

RUN(11E)

FIG.7.2 Fluctuation of drop dimensions with time of Single Drop.

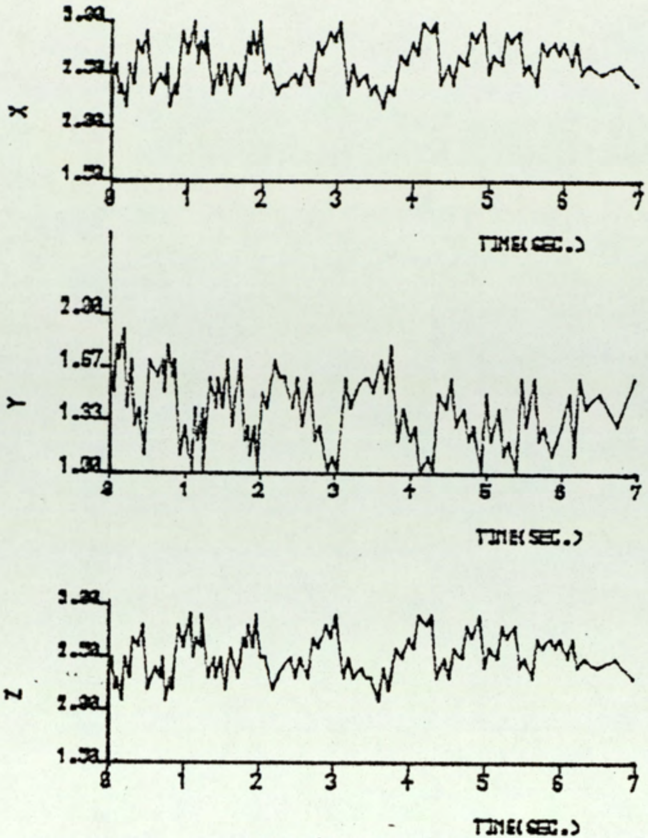

RUN(17C2)

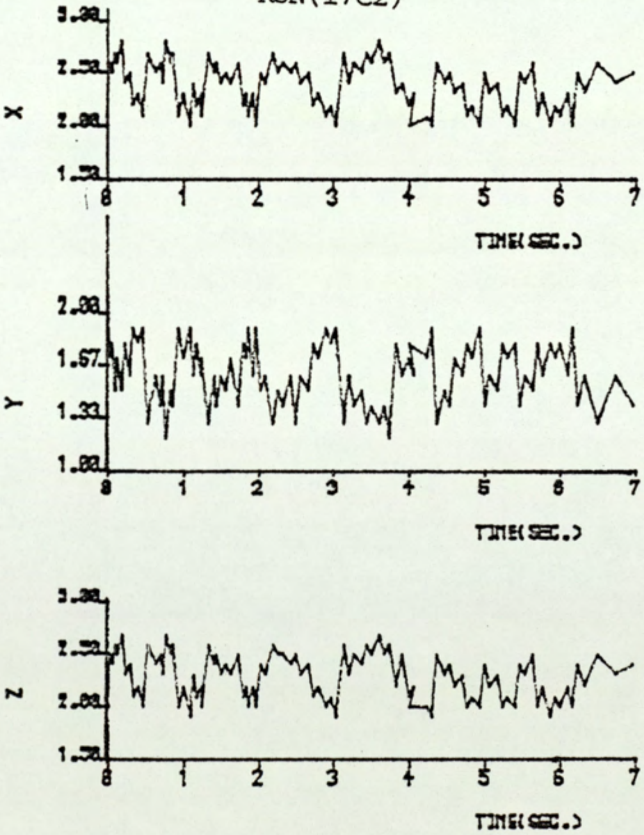

RUN(17C1)

FIG.7.3 Fluctuation of drop dimensions with time of Drop Pairs.

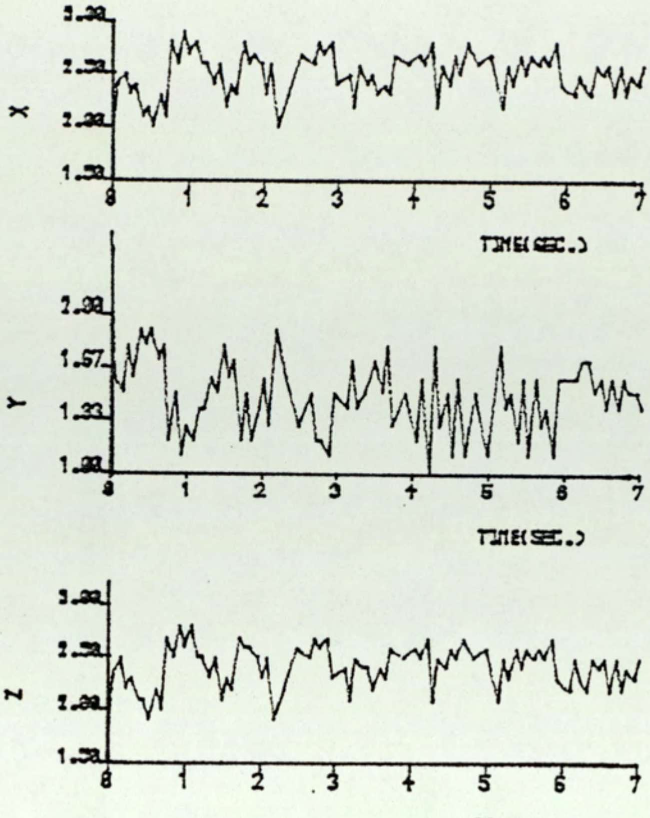

RUN(21C2)

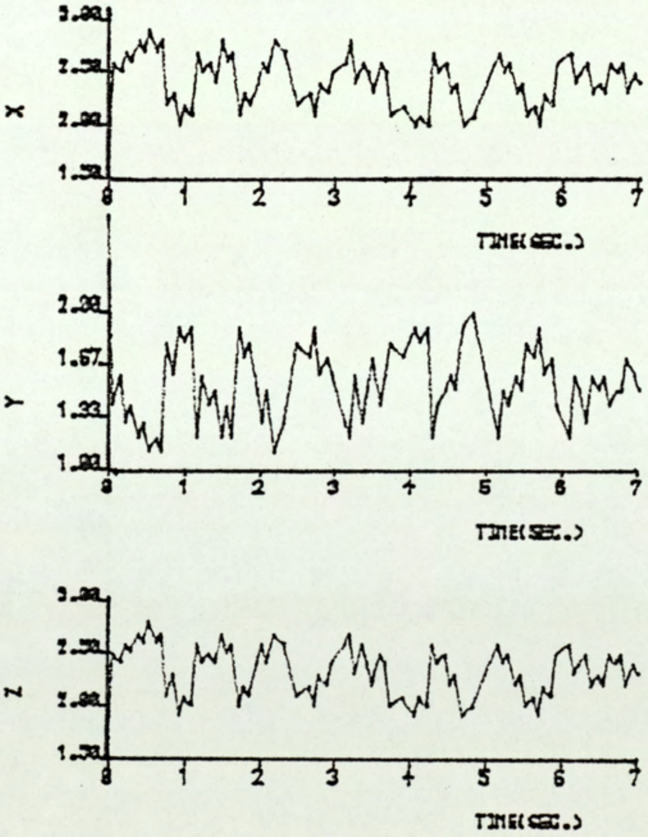

RUN(21C1)

FIG.7.4 Fluctuation of drop dimensions with time of Drop Pairs.

$$a_p = \frac{Xmax}{2} - X_o \quad (3.5)$$

$$\varepsilon = \frac{Amax}{Ao} - 1 \quad (3.6)$$

$$\varepsilon = 0.434\, S_r^{-0.46}\, We^{-0.53}\, \sigma_r^{0.11} \quad (3.8)$$

The observed and calculated ε values are presented in Table 7.2

7.2.3. Droplet Velocity and Drag Coefficient

The point velocities of the drops were determined and the results are listed in Appendix D.3.

The terminal velocity of each drop was measured by estimating the time taken for it to travel 20cm after it had already travelled a distance of 50cm above the nozzle. The results are in good agreement with the literature (156) showing that the drops had attained their terminal velocities. The average value was taken from three consecutive single drops or single drop pairs and the results are presented in Table 7.1B.

The drag coefficient was calculated using the equation:

$$v\Delta\rho g = C_D \bar{A} \left[\frac{V^2 \rho_c}{2} \right] \quad (7.4)$$

from which

$$C_D = \frac{2\, v\Delta\rho g}{\bar{A}\, V^2 \rho_c} \quad (7.5)$$

7.3 MASS TRANSFER RATE CALCULATION

The experimental values of mass transfer efficiency, transfer rate and overall mass transfer coefficients during:

Table 7.1B Mass transfer data of single drops and drop pairs

	Acetone Concentration		Nozzles	t_f	d_e	Average Area	Terminal Velocity	C_2	C_R	f_d	f_c	C_E	Mass Transfer Rate	
RUN NO	*	% w/w	Used	Sec	m $\times 10^{-2}$	$m^2 \times 10^{-4}$	**	*	* $\times 10^{-2}$	***	***	* $\times 10^{-2}$	Out of Drop	Into Cont. Phase
10 C	0.51	3.46	G1	1.00	0.69	1.50	8.38	0.44	5.80	0.17	1.23	4.84	89	68
11 C	1.01	6.85	G1	1.00	0.68	1.45	9.81	0.76	5.50	0.16	2.27	4.79	95	97
12 C	2.04	13.93	G1	1.00	0.66	1.37	11.11	1.65	3.87	0.13	4.17	5.41	98	80
13 C	3.01	20.67	G1	1.00	0.62	1.21	10.83	2.34	3.72	0.11	3.67	6.71	99	92
14 B	0.51	3.46	G1	1.00	0.70	1.54	10.10	0.38	5.16	0.36	3.00	4.28	89	70
15 B	1.01	6.85	G1	1.00	0.69	1.50	10.11	0.73	5.18	0.34	3.00	7.89	95	68
16 C	2.11	14.41	G1	1.00	0.67	1.41	11.28	1.42	3.87	0.31	3.80	13.10	98	75
17 C	0.51	3.46	G2	1.00	0.75	1.77	10.25	0.40	5.00	0.44	2.87	7.20	90	91
21 C	0.51	3.46	G3	1.00	0.80	2.01	9.43	0.37	4.60	0.54	3.17	8.00	91	92
25 B	2.11	14.41	G4	1.05	0.75	1.77	10.36	1.52	2.75	0.42	3.33	18.79	99	71
26 A	3.50	24.11	PT1	1.00	0.71	1.58	10.28	2.34	2.28	0.37	5.33	17.01	99	69
28 A	3.36	23.15	PT3	1.10	0.76	1.81	9.28	2.21	1.65	0.42	4.83	21.61	99	74

* = kg $\times 10^{-3}$.mol/L ** m $\times 10^{-2}$.sec^{-1} *** = $m^3 \times 10^{-6}$.sec^{-1}

Table 7.2 The observed and calculated amplitude of oscillation together with the drag coefficient

a. Single Drop

Run No.	Acetone Conc$^{\underline{n}}$ kg x 10^{-3}.mol/L	d_o m x 10^{-2}	d_{max} m x 10^{-2}	ε_{obs}	C_D x 10^{-2}	We	Sr	ε_{cal}
10C	0.51	0.65	0.72	0.23	3.43	1.92	3.74	0.23
11C	0.01	0.64	0.70	0.20	2.50	2.28	3.10	0.23
12C	2.04	0.61	0.68	0.24	2.00	4.52	2.52	0.17
13C	3.01	0.59	0.65	0.21	2.04	4.04	2.44	0.18

b. Drop Pairs

Run No.	Acetone Conc$^{\underline{n}}$ kg x 10^{-3}.mol/L	d_o m x 10^{-2}	d_{max} m x 10^{-2}	ε_{obs}	C_D x 10^{-2}	We	Sr	ε_{cal}
14B	0.51	0.67	0.70	0.09	2.44	2.82	2.91	0.22
15B	1.01	0.66	0.68	0.06	2.39	2.99	2.87	0.20
16C	2.04	0.64	0.67	0.10	1.98	4.74	2.32	0.19
17C	0.51	0.72	0.76	0.11	2.53	3.13	2.96	0.21
21C	0.51	0.76	0.80	0.10	3.18	2.81	3.14	0.20
25B	2.11	0.61	0.75	0.11	2.63	4.48	2.48	0.13
26A	3.50	0.68	0.71	0.09	2.60	5.21	2.26	0.16
28A	3.36	0.72	0.76	0.11	3.45	4.33	2.20	0.18

i) Droplet formation,

ii) Droplet ascent

where calculated by measuring the acetone concentration in droplets after detachment, or after detachment and travel for a given distance countercurrent to the continuous phase.

7.3.1. Mass Transfer During Drop Formation

The overall mass transfer coefficient during droplet formation was estimated from experimental data and predicted in the following ways

a) Based on Experimental Data

The fundamental equation to calculate the mass transfer coefficient of a dispersed phase droplet during formation from experimental data is,

$$N_f = K_{df} A_{mf} (C_1 - C^*) \tag{1.1}$$

The value of C* in the above equation was taken as zero because the volumetric flow rate of the continuous phase was in all cases approximately 50 times greater than that of the dispersed phase. A sample calculation is presented in Appendix E. Some of the results are listed in Table 7.3 and the complete set of results is listed in Appendix D.2A.

b) Predicted by Johnson and Hamielec's Equation

The theoretical overall mass transfer coefficient of a dispersed phase droplet during formation was calculated using the equation developed by Johnson and Hamielec (23) discussed in Chapter 4 to calculate the efficiency of extraction (Equation 4.12) from which the value of C_2 could be calculated theoretically and then, through Equation 1.1, the mass transfer coefficient was calculated.

$$E_m = \frac{C_1 - C_2}{C_1 - C^*} = \frac{20.6}{d_e} \left[\frac{D_d t_f}{\pi} \right]^{0.5} \tag{4.12}$$

Table 7.3 Experimental Overall Mass Transfer Coefficient during formation of single drops and drop pairs.

a. Single Drop

Run No	t_f s	d $m \times 10^{-2}$	A $m^2 \times 10^{-4}$	C_1	C_2 $kg \times 10^{-3}$.mol/L	$N_f \times 10^{-2}$ $kg \times 10^{-3}$.mol/s	$k_{df\,exp} \times 10^{-2}$ $m \times 10^{-2} s^{-1}$
10 C	1.00	0.69	1.50	0.51	0.44	1.22	1.60
11 C	1.00	0.68	1.45	1.01	0.83	2.96	2.02
12 C	1.00	0.66	1.37	2.04	1.65	5.87	2.23
13 C	1.00	0.62	1.21	3.01	2.34	8.36	2.30

b. Drop Pairs

Run No	t_f s	d $m \times 10^{-2}$	A $m^2 \times 10^{-4}$	C_1	C_2 $kg \times 10^{-3}$.mol/L	$N_f \times 10^{-2}$ $kg \times 10^{-3}$.mol/s	$k_{df\,exp} \times 10^{-2}$ $m \times 10^{-2} sec^{-1}$
14 B	1.00	0.70	1.54	0.51	0.38	4.67	5.98
15 B	1.00	0.69	1.50	1.01	0.73	9.63	6.36
16 C	1.00	0.67	1.41	2.11	1.42	21.72	7.30
17 C	1.00	0.75	1.77	0.51	0.40	4.86	5.42
21 C	1.00	0.80	2.01	0.51	0.37	7.50	7.36
25 B	1.05	0.75	1.77	2.11	1.52	24.82	6.65
26 A	1.00	0.71	1.58	3.50	2.34	43.48	7.86
28 A	1.10	0.76	1.81	3.36	2.21	48.3	7.90

The diffusion coefficient (D_d) was estimated using the Wilke and Chang correlation (160) Equation 5.1. A sample calculation of these theoretical values is presented in Appendix E. Some of the results are listed in Table 7.4 and the complete set of results is listed in Appendix D.2B. Figure 7.5 presents experimental and calculated values of the overall mass transfer coefficient of a dispersed phase droplet pair, against acetone concentration. Figures 7.6 and 7.7 present the observed and calculated values of overall mass transfer coefficient during formation of single drops and drop pairs.

7.3.2. Surface Area Calculation During Drop Formation by Using Least Squares Technique

It is generally agreed that the enhanced mass transfer rate during drop formation results from creation of new interfacial area of the droplet, Figure 7.8, in comparison with the other stages in the column. Therefore it was appropriate to study such phenomena in more detail and to compare the results with mass transfer during other stages.

A series of experiments were performed to study the creation of the droplet surface area during formation as a function of time. From Equation 1.1,

$$N_A = K\,A\,\Delta C$$

$$= K\ \left[\int_o^t f(a)\,dt\right] \Delta C$$

where

$$A = \int_o^t f(a)\,dt \tag{7.6}$$

Regression analysis by least squares method was applied to fit the experimental data. The change of the surface area of a single droplet with time was found to be fitted by a polynomial equation of the form:

$$Y = C + a_1\,x + a_2\,x^2 + \ \ldots\ldots\ a_n\,x^n \tag{7.7}$$

Table 7.4 Theoretical Overall Mass Transfer Coefficient during formation of single drops and drop pairs.

a. Single Drops

Run No	t_f s	d_e m x 10^{-2}	C_1 kg x 10^{-3}.mol/L	E_m x 10^{-2}	C_2 kg x 10^{-3}.mol/L	A m^2 x 10^{-4}	N_f x 10^{-3} kg x 10^{-3}.mol/s	$K_{df\,theo}$ x 10^{-3} m x 10^{-2}. s^{-1}
10 C	1.00	0.69	0.51	8.74	0.46	1.49	7.4	9.76
11 C	1.00	0.68	1.01	8.98	0.92	1.45	12.7	8.72
12 C	1.00	0.66	2.04	9.48	1.84	1.37	24.4	8.74
13 C	1.00	0.62	3.01	10.32	2.69	1.21	32.8	9.02

b. Drop Pairs

Run No	t_f s	d_e m x 10^{-2}	C_1 kg x 10^{-3}.mol/L	E_m x 10^{-2}	C_2 kg x 10^{-3}.mol/L	A m^2 x 10^{-4}	N_f x 10^{-3} kg x 10^{-3}.mol/s	$K_{df\,theo}$ x 10^{-3} m x 10^{-2}. s^{-1}
14 B	1.00	0.70	0.51	8.61	0.46	1.47	7.7	9.86
15 B	1.00	0.69	1.01	8.85	0.92	1.42	13.3	8.86
16 C	1.00	0.67	2.11	9.34	1.91	1.34	26.8	9.01
17 C	1.00	0.75	0.51	8.04	0.47	1.68	0.76	8.44
21 C	1.00	0.80	0.51	7.53	0.47	1.91	0.92	9.02
25B	1.05	0.75	2.11	8.58	1.92	1.68	3.57	9.57
26 A	1.00	0.71	3.50	9.11	3.18	1.51	5.08	9.19
28 A	1.10	0.76	3.35	8.93	3.05	1.73	5.85	9.45

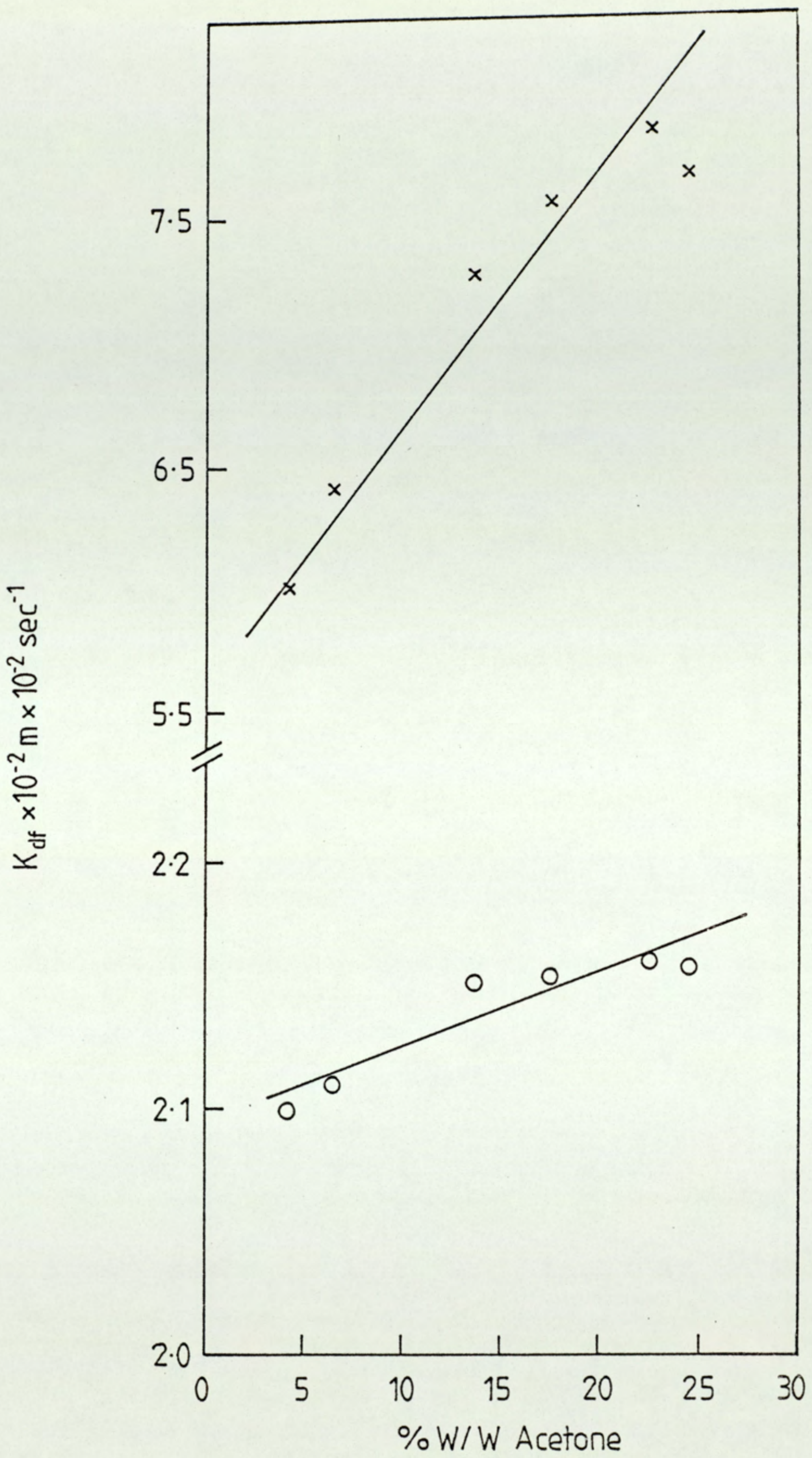

Figure 7·5 Overall mass transfer coefficient of dispersed phase droplet during formation of drop pairs vs. Acetone concentration.
× Observed, ○ Calculated by Single drop model

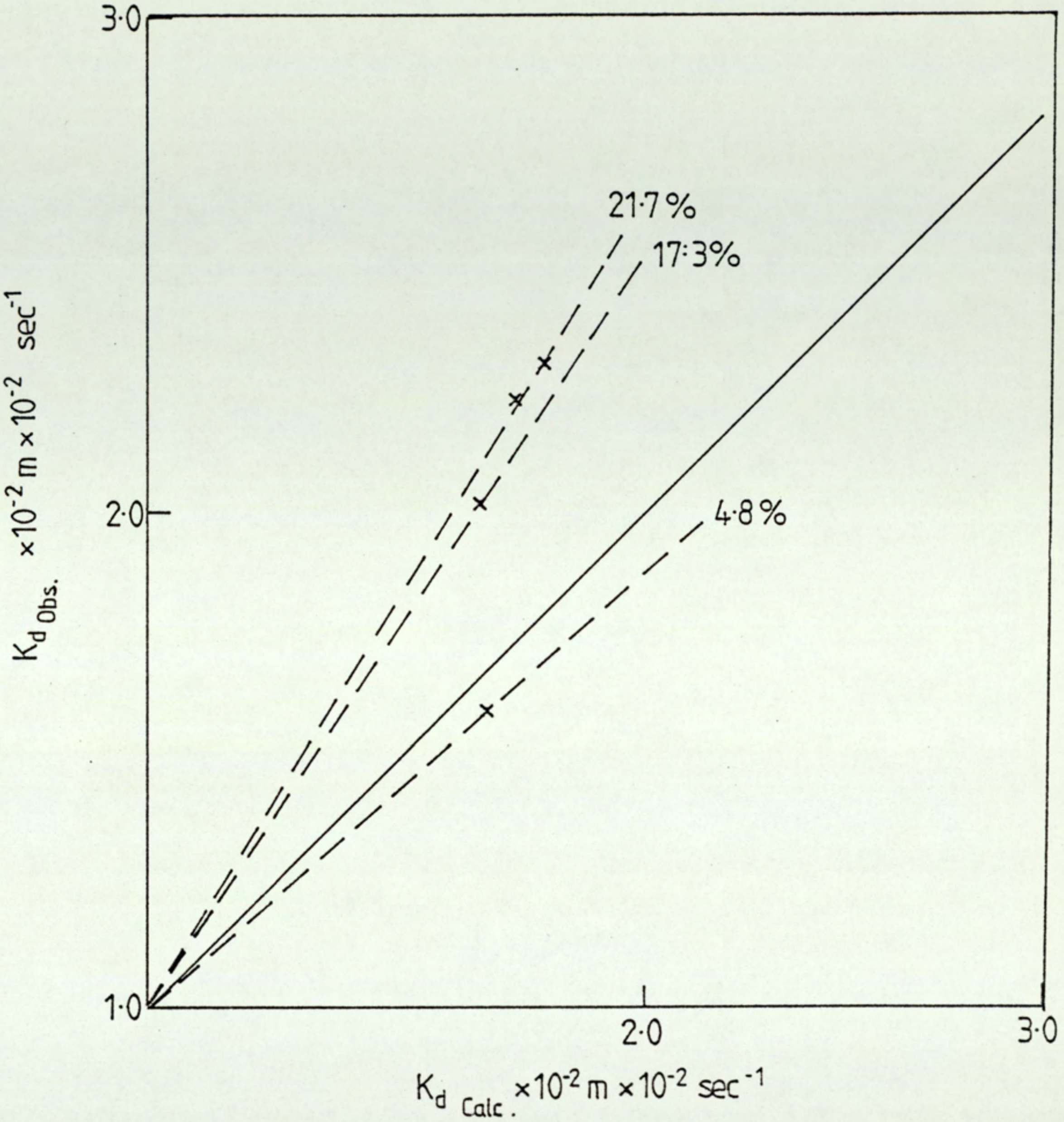

Figure 7·6 Observed and Calculated $K_{df's}$ of Single Drop using equation (4·12)

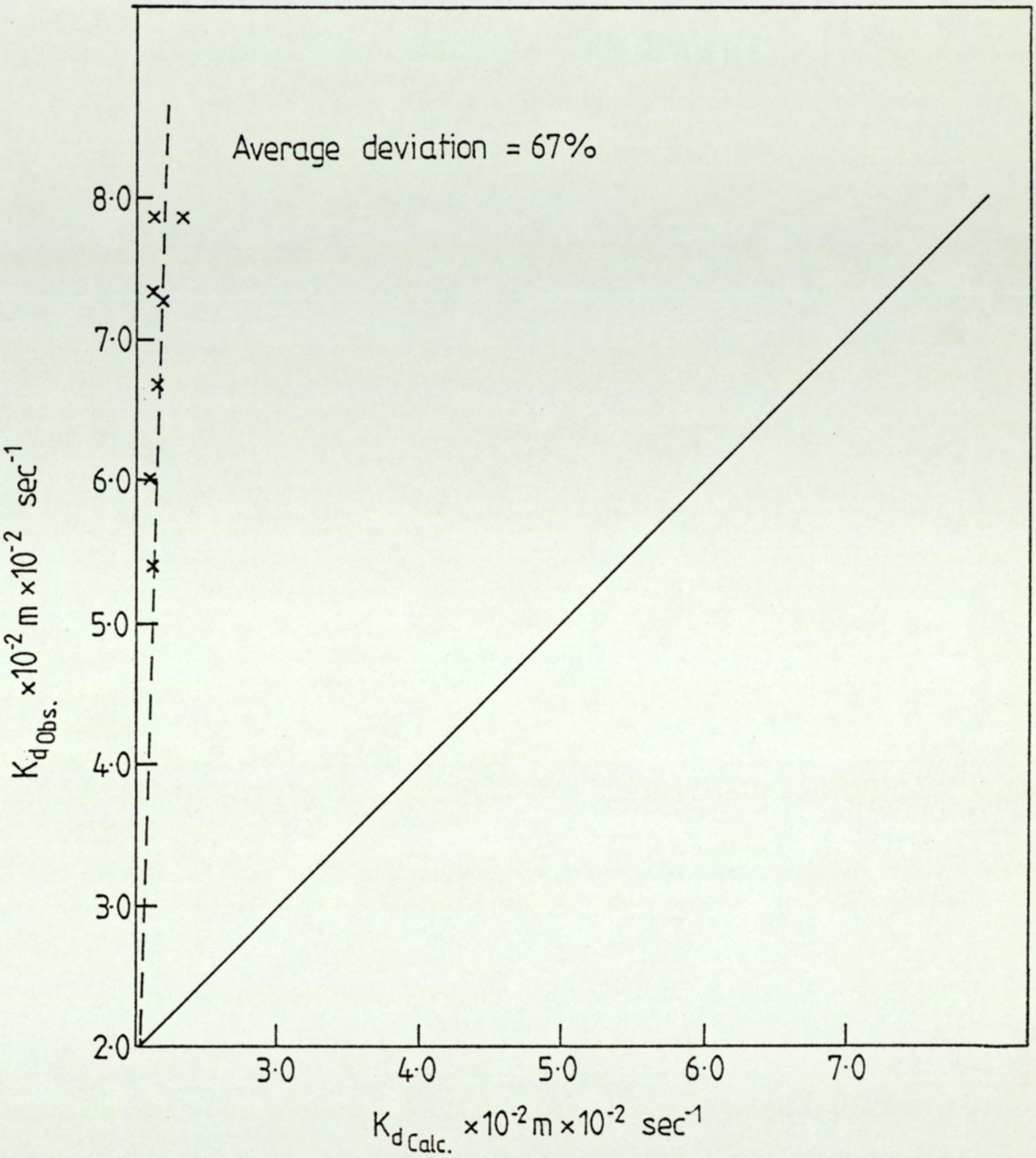

Figure 7·7 Observed and Calculated $K_{df's}$ of Drop pairs using equation (4·12)

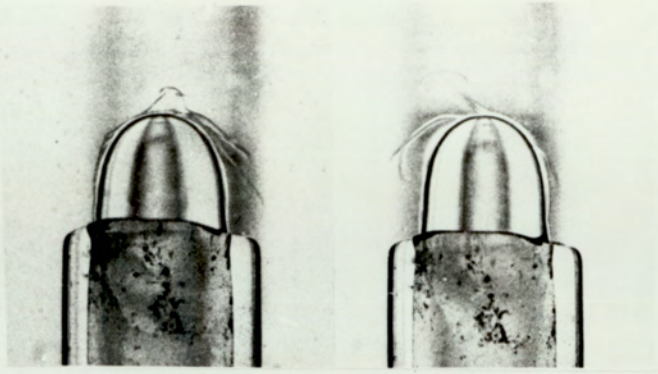

Figure 7.8a Illustration of Mass Transfer During Formation

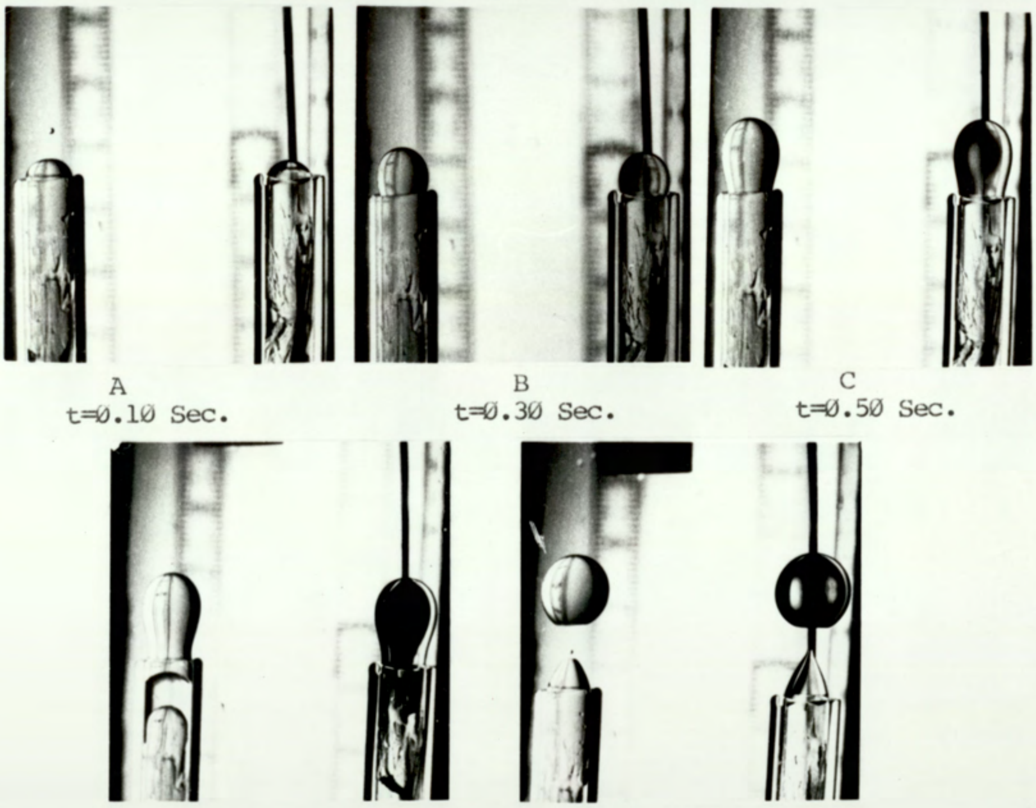

A
t=0.10 Sec.

B
t=0.30 Sec.

C
t=0.50 Sec.

D
t=0.70 Sec.

E
t=1.00 Sec.

Figure 7.8 Extract from cine film showing droplet formation

Ac.Conc. = 0.51 gm.mol/l
f_d = 0.35 m^3/Sec.
Nozzle Diameter= 3.99 mm.

where (Y) is the dependent variable ie. the area of the drop, (C) is a constant, a_1, a_2 and a_n are coefficients of independent variables x, x^2 and x^n, which represent the time in seconds of the drop formation determined frame by frame from the cine film. However, equation 7.7 can be represented by

$$A = \int_o^t (C + a_1 x + a_2 x^2)\, dt \tag{7.8}$$

Substitution of equation 7.8 in equation 1.1 yields,

$$N_A = K\, [\int_o^t (C + a_1\, x + a_2\, x^2)\, dt]\, \Delta C \tag{7.9}$$

Using the computer program given in Appendix C the equation coefficients, coefficient of determination, coefficient of correlation, and standard error of estimate are printed, by providing values for x and Y coordinates for known data points. Once the equation has been computed, values of Y for a given value of x may be predicted. A complete listing of the program (Appendix C.6), using the BBC micro computer, the results, graphs, and correlations of the drop area during formation found by experiment and predicted by the model are listed in Appendix D.6. Table 7.5 presents the results of the computer program (Appendix C.6) to evaluate the area (A) from equation 7.7 for run A. Figure 7.9 shows the typical variation of the droplet areas with time, and Figure 7.10 the results of the regression analysis illustrating the maximum and the minimum deviation between the observed and calculated areas.

A comparison between the overall mass transfer coefficients found by experiment, and those calculated from single drop models, and from the new correlation are listed in Table 7.6 and Figure 7.11. A complete set of data together with the results and graphs are listed in Appendix D.7.

Table 7.5 The Results of Program C.6 for Run (A)

Run No (A)

Nth-order Regression

By least square

Degree of Equation = 2

Number of known points = 10

Point	x	Y
1	1.0	0.75
2	1.1	0.95
3	1.2	1.29
4	1.3	1.54
5	1.4	1.63
6	1.5	1.63
7	1.6	1.63
8	1.7	1.63
9	1.8	1.58
10	1.9	1.48

Constant = -5.22
1. Degree of Coefficient = 8.68
2. Degree of Coefficient = -2.73
Coefficient of Determination (R^2) = 0.97
Coefficient of Correlation = 0.98
Standard Error or Estimate = 5.54

Interpretation (0 to end diagram)

Value of	x	Y
	1.0	0.73
	1.1	1.02
	1.2	1.27
	1.3	1.45
	1.4	1.58
	1.5	1.66
	1.6	1.68
	1.7	1.65
	1.8	1.56
	1.9	1.42

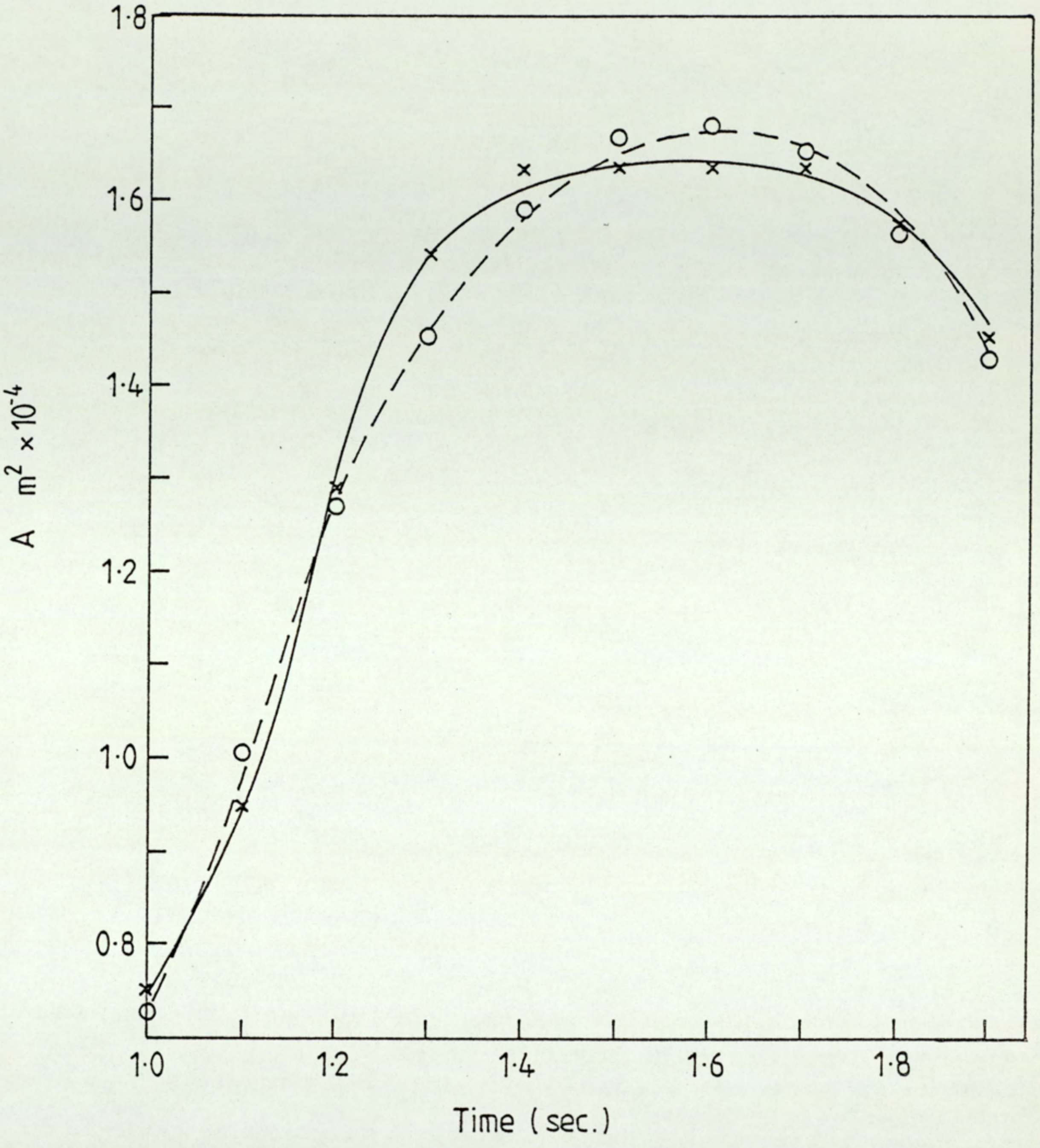

Figure 7·9 Droplet area during formation vs. Time (Run A)
(× Observed, ○ Calculated by equation (7·8)

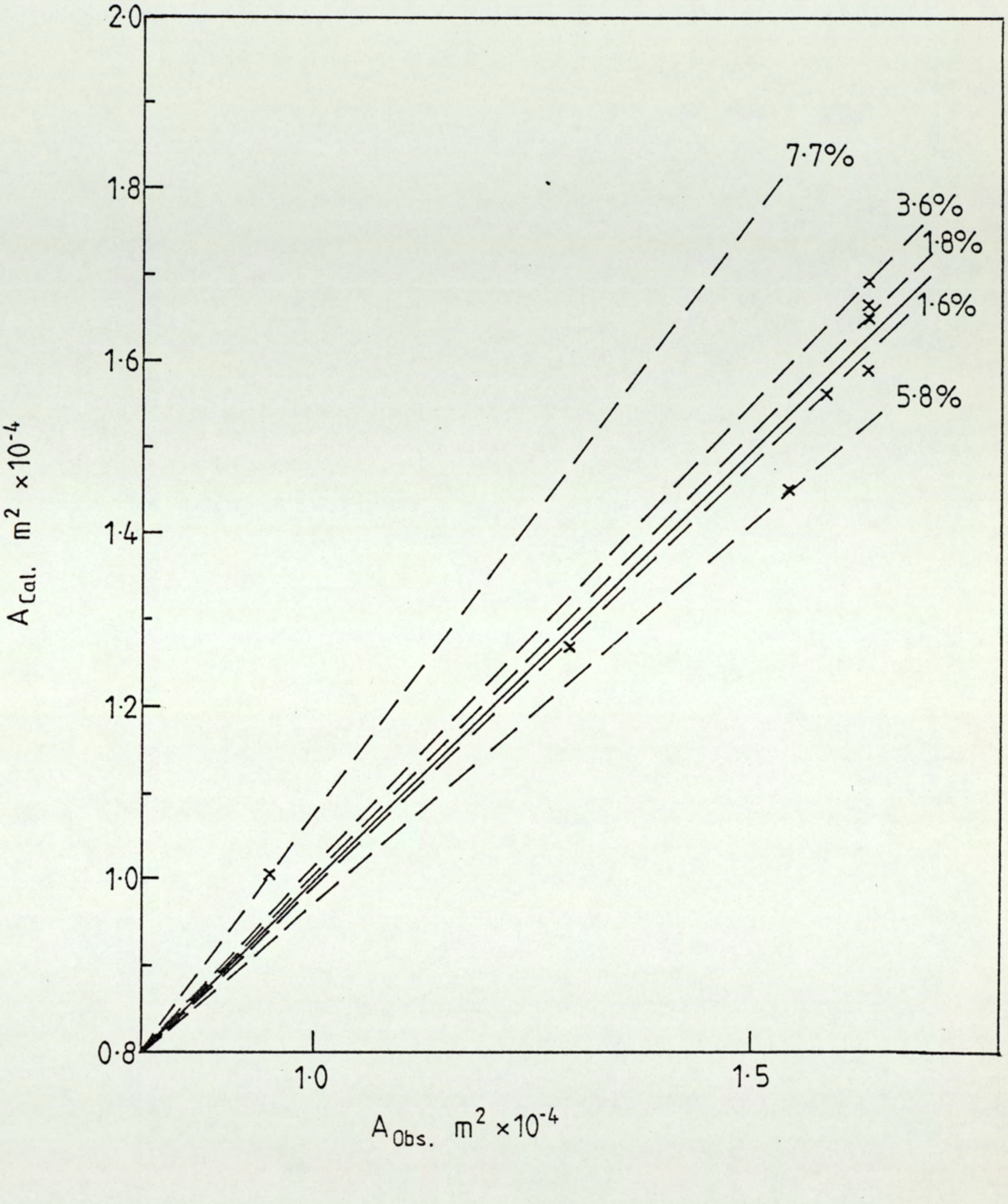

Figure 7·10 Comparison of the observed interfacial area during formation with those predicted by equation (7·8) (Run A)

Table 7.6 Comparison between overall mass transfer coefficient of dispersed phase during formation of drop pairs, Experimental, Theoretical by single drop model, and Predicted by new correlation

Run No	Nozzle Used	Acetone Conc$^{\underline{n}}$	d	C_{2exp}	E_m	C_2 theor.	f_d	#	##	A_{obs}	A_{theor}	A_{model}	###	####	#####
		*	$m \times 10^{-2}$	*	$\times 10^{-2}$	*	**	***	***	$m^2 \times 10^{-2}$	$m^2 \times 10^{-2}$	$m^2 \times 10^{-2}$	$m \times 10^{-2}.sec^{-1}$		
A	G1	0.50	0.73	0.38	8.26	0.459	0.14	4.88	1.68	1.67	1.01	1.68	5.85	3.30	5.78
B	G2	0.50	0.76	0.36	7.93	0.460	0.46	6.44	1.82	1.81	1.09	1.77	7.11	3.34	7.27
C	G3	0.50	0.79	0.33	7.63	0.462	0.52	8.83	1.98	1.96	1.18	1.91	9.01	3.36	9.18
D	G4	0.50	0.84	0.31	7.18	0.464	0.62	11.79	2.23	2.22	1.33	2.06	10.62	3.36	11.44
E	G5	0.50	0.92	0.28	6.55	0.467	0.82	18.07	2.71	2.65	1.60	2.52	13.64	3.38	14.34
F	G3	0.35	0.86	0.28	7.01	0.325	0.67	4.66	1.67	2.32	1.39	2.24	5.74	3.43	5.94
G	G4	0.85	0.80	0.62	7.53	0.786	0.54	12.33	3.43	2.01	1.21	1.94	7.28	3.33	7.47
H	PT1	0.50	0.71	0.35	8.49	0.457	0.37	5.62	1.61	1.58	0.95	1.72	7.11	3.41	1.87
J	PT2	0.50	0.94	0.32	6.41	0.468	0.87	15.65	2.78	2.77	1.66	2.52	11.30	3.34	12.42
K	PT3	1.00	0.81	0.68	7.44	0.925	0.56	17.81	4.17	2.06	1.24	2.12	8.65	3.36	8.40

* = $kg \times 10^{-3}.mol/L$

** = $m^3 \times 10^{-6}.sec^{-1}$

*** = $kg \times 10^{-3}.mol/s$

\# = $N_{fobs.} \times 10^{-2}$

\## = $N_{ftheor.} \times 10^{-2}$

\### = $K_{dfobs.} \times 10^{-2}$

\#### = $K_{dftheo} \times 10^{-2}$

\##### = $K_{dfmodel} \times 10^{-2}$

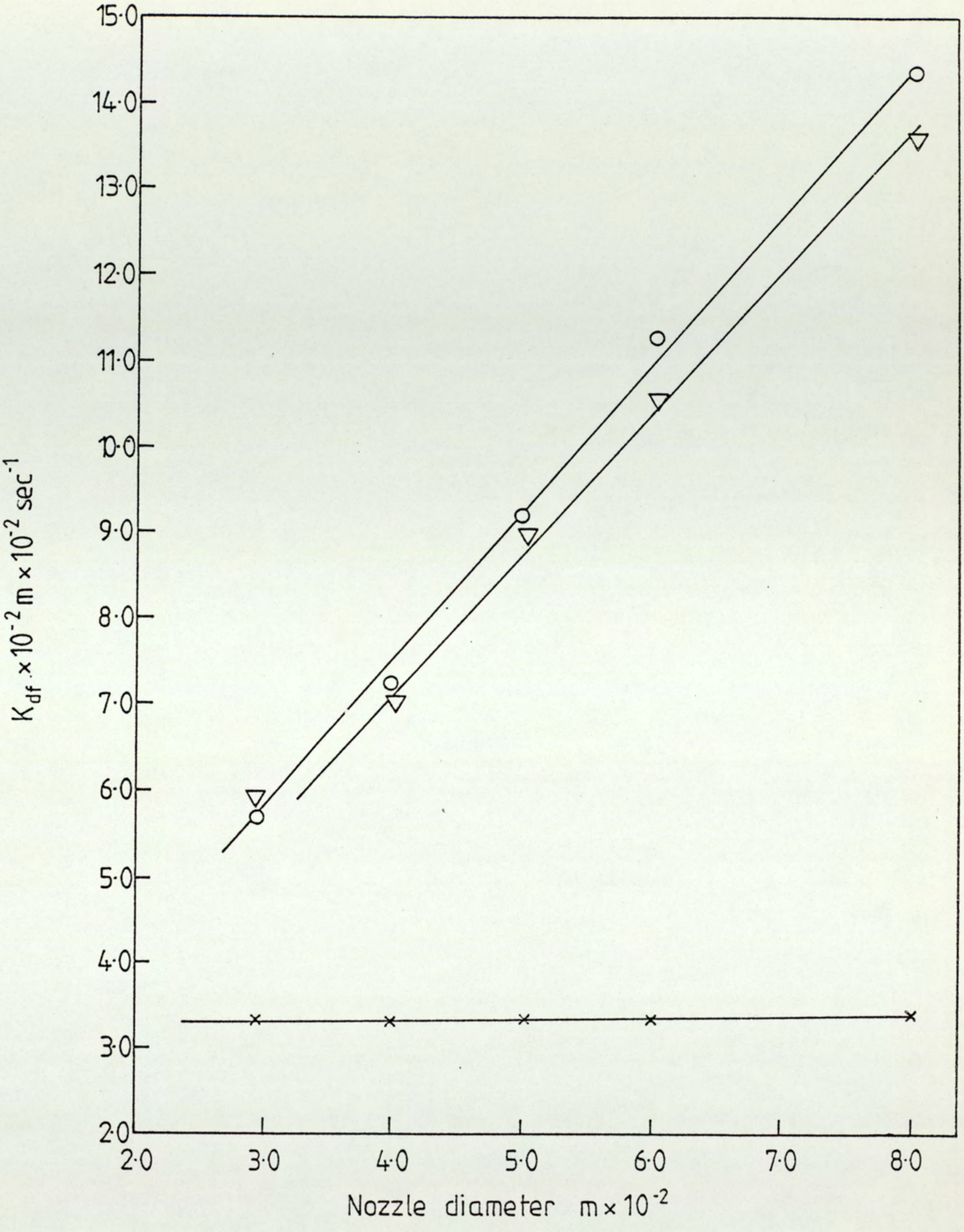

Figure 7·11 Comparison between overall mass transfer coefficient during drop formation using three equations.

× Existing model, equation)4.12)

▽ Observed value

○ New correlation, equation (7.9)

7.3.2.1. Drop HydrodynamicsDuring Formation

It is of interest to compare the experimentally determined overall mass transfer coefficient Table 7.3 and Appendix D.2A with those predicted for different droplet hydrodynamics ie assuming circulation, surface stretch or oscillation behaviour.

Therefore overall coefficients were calculated for 8 typical runs on the basis of:

a) Surface-Stretch Model

Angelo et al (69) proposed a model for an oscillating drop based upon surface stretch and internal mixing of the drop as discussed earlier, equation 4.63. The results of applying this equation to the drop formation data are shown in Table 7.6a.

A typical calculation for run 10E is shown below:

1) Determination of the velocity of the drop during formation

volume of pandent drop

$$= \frac{4}{3} \pi \, (x^2 y)$$

$$= \frac{4}{3} \pi \, (0.325^2 \times 0.36)$$

$$= 0.16 \text{ m}^3 \times 10^{-6}$$

$$\text{Volumetric flow rate (fd)} = \frac{0.16}{0.58} = 0.27 \text{ m}^3 \times 10^{-6}.\text{s}^{-1}$$

$$\text{Cross section area of the nozzle (Ao)} = \frac{\pi}{4} d_o^2$$

$$= \frac{\pi}{4} (0.2701)^2$$

$$= 0.06 \text{ m}^2 \times 10^{-4}$$

$$\text{Velocity of the dispersed phase} = \frac{0.27}{0.06} = 4.50 \text{ m} \times 10^{-2}.\text{s}^{-1}$$

2. Determination of the corrected droplet area during formation

$$A_{max} = \pi \ (X^2 \times Y^2 + Z^2)$$

$$= \pi \ (2X^2 + Y^2)$$

$$= \pi \ (2 \times 0.65^2 + 0.72^2)$$

$$= 4.28 \ m^2 \times 10^{-4}$$

From the eccentricity relation proposed by Wellek et al (52) for estimation of the interfacial area of drop distortion from the spherical shape, the above A_{max} can be corrected to get

$$E = 1 + 0.093 \ \left(\frac{dV^2\rho}{\sigma}\right)^{0.98}$$

$$= 1 + 0.093 \left(\frac{0.69 \times 4.5^2 \times 0.86}{21.8}\right)^{0.98}$$

$$= 1.05$$

Therefore A_{max} (corrected) $= 4.28 \times 1.05 = 4.49 \ m^2 \times 10^{-4}$

3. Determination of the amplitude (ε)

It may be calculated from equation 3.8 for large oscillation drops.

$$\varepsilon = 0.434 \ \left(\frac{\omega d}{V}\right)^{-0.46} \left(\frac{dV^2 \rho_d}{\sigma}\right)^{-0.53} \qquad \text{as } \sigma_r^{0.11} \cong 1.0$$

$$= 0.434 \ \left(\frac{42.16 \times 0.69}{4.67}\right)^{-0.46} \left(\frac{0.69 \times 4.67^2 \times 0.86}{21.8}\right)^{-0.53}$$

$$= 0.25$$

$$\varepsilon_o = \varepsilon + \frac{3}{8} \ (\varepsilon)^2$$

Table 7.6a Comparison between the experimental overall mass transfer coefficients during formation and theoretical values calculated by surface-stretch model of oscillating drops equation 4.63

Run No	t_f s	X max *	Y max *	Z max *	d mean *	f_d **	A_o ***	Velocity $m \times 10^{-2}.s^{-1}$	E	A_{max} Corr-ected ***	ε	ε_o	ω s^{-1}	$K_{dftheo} \times 10^{-2}$ $m \times 10^{-2}.s^{-1}$	$K_{dfexp} \times 10^{-2}$ $m \times 10^{-2}.s^{-1}$	Ratio of K_{dfexp}/K_{dftheo}
10 B	1.50	0.74	0.82	0.80	0.79	0.15	0.06	2.50	1.01	5.60	0.36	0.41	34.94	2.05	1.63	0.80
C	1.00	0.69	0.74	0.73	0.72	0.18	0.06	3.00	1.02	4.80	0.33	0.37	39.74	2.16	1.59	0.74
D	0.76	0.68	0.77	0.76	0.74	0.24	0.06	4.00	1.03	4.91	0.28	0.31	38.26	2.07	1.48	0.71
E	0.58	0.65	0.72	0.70	0.69	0.27	0.06	4.50	1.04	4.45	0.27	0.30	42.15	2.17	1.50	0.69
14 A	1.50	0.76	0.84	0.82	0.77	0.17	0.07	2.43	1.01	5.90	0.37	0.42	36.20	2.10	5.01	2.39
B	1.00	0.70	0.78	0.78	0.76	0.20	0.07	2.86	1.02	5.09	0.34	0.38	36.87	2.09	5.98	2.86
C	0.78	0.71	0.80	0.79	0.77	0.27	0.07	4.50	1.05	5.44	0.25	0.27	36.20	1.98	6.60	3.33
D	0.55	0.68	0.74	0.72	0.71	0.33	0.07	4.70	1.05	4.86	0.26	0.29	40.52	2.12	9.69	4.57

* $m \times 10^{-2}$ ** $m^3 \times 10^{-6}/s$ *** $m^2 \times 10^{-4}$

$$= 0.25 + \frac{3}{8}(0.25)^2 = 0.27$$

Thus the overall mass transfer coefficient of dispersed phase (equation 4.63)

$$K_d = \left(\frac{4 \times 2.69 \times 10^{-5} \times 42.15 \times 1.27}{\pi}\right)^{0.5} \times 0.5$$

$$= 2.14 \times 10^{-2} \text{ m} \times 10^{-2}.\text{s}^{-1}$$

b) Circulating Model

Kronig and Brink (138) proposed a model for dispersed phase mass transfer coefficient of a circulating drop, equation 7.9a,

$$k_d = \frac{17.9\, D_D}{d} \qquad (7.9a)$$

and k_c may be found from Garner et al's correlation (140) (equation 4.23). Thus the overall mass transfer coefficient can be calculated. The results are listed in Table 7.6b and a typical calculation for Run 10E is:

$$k_d = \frac{17.9 \times 2.69 \times 10^{-5}}{0.69} = 7.00 \times 10^{-4} \text{ m} \times 10^{-2}.\text{s}^{-1}$$

$$\frac{k_c d}{D} = -126 + 1.8 \left(\frac{0.69 \times 4.5 \times 0.86}{0.006}\right)^{0.5} \left(\frac{0.006}{1.0 \times 2.69 \times 10^{-5}}\right)^{0.42}$$

$$= 241.96 \quad \text{m} \times 10^{-2}.\text{s}^{-1}$$

$$k_c = \frac{241.96 \times 2.69 \times 10^{-5}}{0.69} = 9.43 \times 10^{-3}$$

Table 7.6b Comparison between experimental overall mass transfer coefficients during drop formation and theoretical values calculated by the circulation model eq (7.9a)

Run No.	$k_c \times 10^{-3}$ $m \times 10^{-2}.s^{-1}$	$k_d \times 10^{-4}$ $m \times 10^{-2}.s^{-1}$	$K_{df\ theo} \times 10^{-4}$ $m \times 10^{-2}.s^{-1}$	$K_{df\ exp} \times 10^{-2}$ $m \times 10^{-2}.s^{-1}$	Ratio of $K_{df\ exp}/K_{df\ theo}$
10 B	5.71	6.12	7.40	1.63	22.03
C	6.79	6.71	8.19	1.59	19.41
D	8.50	6.53	8.20	1.48	18.05
E	9.70	7.00	8.82	1.50	17.01
14 A	5.58	6.28	7.54	5.01	66.45
B	6.44	6.36	7.77	5.98	76.96
C	9.19	6.28	7.97	6.60	82.81
D	9.69	6.81	8.62	9.69	112.41

$$\frac{1}{K_d} = \frac{1}{7.0 \times 10^{-4}} + \frac{0.72}{9.4 \times 10^{-3}}$$

$$K_d = 8.82 \times 10^{-4}\ m \times 10^{-2}.s^{-1}$$

X, Y, Z, d_{mean} and velocity are from Table 7.6a, acetone concentration was 0.51gmol/L, physical properties are in Table 5.2.

It may be concluded from Tables 7.6a and 7.6b that during drop formation the surface of the drop stretches in a normal manner, but the contents are not violently mixed as in the case of an oscillating drop. Therefore it is reasonable to assume that the mass transfer mechanism will comprise a combination of surface stretching and dispersed phase circulation. Therefore the value of the mass transfer coefficient would be expected to lie somewhere between K_d of Angelo et al (69) and Kronig and Brink (138).

The maximum deviation between the average of K_ds calculated by both models and experimental K_d at formation of single drop is 24.7%.

$$\frac{2.14 \times 10^{-2} + 8.82 \times 10^{-4}}{2} = 1.13 \times 10^{-2}$$

$$\frac{1.5 \times 10^{-2} - 1.13 \times 10^{-2}}{1.5 \times 10^{-2}} \times 100 = 24.7\%$$

Alternatively a constant numerical value of (0.7) may be applied to the values from the surface-stretch model to fit the drop formation experimental data with the present system, (see the last column in Table 7.6a).

$$K_d = 1.4 \left[\frac{D_d \, \omega \, (1 + \varepsilon o)}{\pi} \right]^{0.5} \left[\frac{1}{1 + m \sqrt{\frac{D_d}{D_c}}} \right] \tag{7.9b}$$

In the formation of pairs of drops (Figure 7.8) the continuous phase between the drops is shared thereby inducing considerable turbulence. Furthermore because of the Bernoulli effect the drops will tend to be attracted to one another, which will induce oscillation thereby enhancing the rate of mass transfer considerably above that of the surface stretch model. This is difficult to predict at the present time and further work is required to identify the turbulent condition inside and around the drops.

7.3.3. Mass Transfer During Droplet Ascent

The overall mass transfer coefficient during droplet ascent may be estimated experimentally and theoretically:

7.3.3.1. Based on Experimental Data

From the fundamental equation the overall mass transfer coefficient during ascent may be estimated;

$$N_t = K_{dexp}\,\bar{A}\,(C_2 - C^*) \qquad 1.1$$

where $\bar{A}$ is the mean area of droplet during ascent.

A study by Angelo et al (69) to find the area and amplitude of a single liquid drop during oscillation yielded,

$$\bar{A} = \left(\frac{\varepsilon}{2} + 1\right) Ao$$

where Ao is the initial area of the droplet after formation which is always regarded as sphere in this stage and ε is the amplitude of droplet oscillation, which is discussed in section 7.2.2. A selection of the results are listed in Table 7.7 and the remainder in Appendix D.2C.

7.3.3.2. Predictions from Theory

In assessing the theoretical overall mass transfer coefficient during ascent with Reynolds numbers well below 200, it is necessary to consider that the drop may exhibit three different kinds of phenomena. It may be stagnant, or complete circulation of the solute inside might be laminar or turbulent, depending upon the Reynolds number and the physical properties of the phases;

a. Stagnant Droplets by Newman's Correlation

Newman's correlation gave promising results when applied to droplets with Reynolds number <1.0. The value of K_d may be evaluated from,

Table 7.7 Experimental Overall Mass Transfer Coefficient of single drops and drop pairs during ascent at n = 2

a. Single Drops

Run No	ω rad.s^{-1}	ε	d_o* m x 10^{-2}	A_o m^2 x 10^{-4}	$\bar{A}$ m^2 x 10^{-4}	N_f x 10^{-2} kg x 10^{-3}.mol/s	$K_{d\,exp}$ x 10^{-2} m x 10^{-2}s^{-1}
10 C	45.50	0.23	0.72	1.63	1.82	6.57	8.20
11 C	44.71	0.21	0.70	1.54	1.70	10.13	7.84
12 C	42.46	0.17	0.63	1.25	1.36	22.13	9.86
13 C	42.56	0.16	0.58	1.06	1.45	26.06	7.68

b. Drop Pairs

Run No	ω rad.s^{-1}	ε m x 10^{-2}	d_o*	A_o m^2 x 10^{-4}	$\bar{A}$ m^2 x 10^{-4}	N_f x 10^{-2} kg x 10^{-3}.mol/s	$K_{d\,exp}$ x 10^{-2} m x 10^{-2}s^{-1}
14 B	44.50	0.21	0.75	1.77	1.96	11.82	15.87
15 B	43.81	0.20	0.72	1.63	1.79	23.33	17.85
16 C	44.31	0.16	0.70	1.54	1.66	43.48	18.45
17 C	40.43	0.20	0.78	1.91	2.04	15.46	18.49
21 C	36.97	0.21	0.83	2.16	2.37	17.37	19.81
25 B	34.07	0.17	0.78	1.91	2.06	62.78	20.05
26 A	32.79	0.16	0.75	1.77	1.96	86.86	19.54
28 A	29.30	0.17	0.80	2.01	2.17	91.65	19.11

*d_o The drop diameter at half volume during formation.

$$E_m = \frac{C_2 - C_3}{C_2 - C^*} = \pi \left[\frac{D_d t_f}{r^2} \right]^{0.5} \tag{4.34}$$

by substitution of the values of E_m and C_3 as already described.

Typical results are listed in Table 7.8 and a complete set of results is listed in Appendix D.2D.

b. Laminar Circulation in Droplet by Kronig and Brink's Correlation

For laminar circulation use was made of the correlation developed by Kronig and Brink (138), for the range 1.0 < Re < 10.0. The limiting assumptions are that the time of circulation is small compared with the time of solute transfer or diffusion, that the solute transfer is in a direction perpendicular to the internal stream lines, and that the continuous phase resistance is negligible. The equation is,

$$E_m = \frac{C_2 - C_3}{C_2 - C^*} = \pi \cdot \left[\frac{R\, D_d t_f}{r^2} \right]^{0.5} \tag{4.38}$$

where R (the effective diffusivity) = 2.25. Typical results are listed in Table 7.9 and a complete set of results is listed in Appendix D.2E.

c. Turbulent Circulation in Droplet by Handlos and Baron's Correlation

The overall mass transfer coefficient of a dispersed phase droplet undergoing turbulent circulation of the solute inside was predicted using Handlos and Baron's (152) correlation, since the Reynolds number was still below 200.

$$\frac{1}{K_d} = \frac{m}{(k_c)_{HG}} + \frac{1}{(k_d)_{HB}} \tag{4.43}$$

where k_c and k_d can be found through Higbie's theory and Handlos and Baron's correlation respectively

Table 7.8 Theoretical Overall Mass Transfer Coefficient of stagnant single drops and drop pairs during ascent.

a. Single Drops

Run No	r m x 10^{-2}	$\bar{A}$ m^2 x 10^{-4}	C_2 kg. x 10^{-3}.mol/L	E_m x 10^{-2}	C_3 kg.x 10^{-3}.mol/L	N_f x 10^{-3} kg x 10^{-3}.mol/s	$K_{d\ theo}$ x 10^{-3} m x 10^{-2}. s^{-1}
10 C	0.345	1.82	0.44	4.72	0.42	2.97	3.71
11 C	0.340	1.69	0.83	4.79	0.79	5.66	4.10
12 C	0.330	1.36	1.65	5.13	1.57	10.28	4.58
13 C	0.310	1.45	2.34	5.58	2.21	13.78	4.06

b. Drop Pairs

Run No	r m x 10^{-2}	$\bar{A}$ m^2 x 10^{-4}	C_2 kg. x 10^{-3}.mol/L	E_m x 10^{-2}	C_3 kg. x 10^{-3}.mol/L	N_f x 10^{-3} kg x 10^{-3}.mol/s	$K_{d\ theo}$ x 10^{-3} m x 10^{-2}. s^{-1}
14 B	0.350	1.94	0.38	4.66	0.36	3.10	6.12
15 B	0.345	1.78	0.73	4.65	0.70	4.44	3.42
16 C	0.335	1.66	1.42	5.02	1.35	9.37	3.98
17 C	0.375	2.09	0.40	4.35	0.38	3.81	4.56
21 C	0.400	2.37	0.37	4.07	0.35	4.62	5.27
25 B	0.375	2.06	1.52	3.98	1.46	11.26	3.60
26 A	0.355	1.90	2.34	4.37	2.24	15.88	3.57
28 A	0.380	2.17	2.21	4.83	2.10	21.46	4.47

Table 7.9 Theoretical Overall Mass Transfer Coefficient of single drops and drop pairs with laminar circulation of solute inside.

a. Single Drops

Run No	r m x 10^{-2}	$\overline{A}$ m^2 x 10^{-4}	C_2 kg x 10^{-3}.mol/L	E_m x 10^{-2}	C_3 kg x 10^{-3}.mol/L	N_f x 10^{-3} kg x 10^{-3}.mol/s	$K_{d\,theo}$ x 10^{-3} m x 10^{-2}. s^{-1}
10 C	0.345	1.82	0.44	7.08	0.41	3.72	4.64
11 C	0.340	1.69	0.83	7.28	0.79	8.50	6.06
12 C	0.33	1.36	1.65	7.75	1.52	16.71	7.45
13 C	0.31	1.45	2.34	8.33	2.15	21.21	6.25

b. Drop Pairs

Run No	r m x 10^{-2}	$\overline{A}$ m^2 x 10^{-4}	C_2 kg x 10^{-3}.mol/L	E_m x 10^{-2}	C_3 kg x 10^{-3}.mol/L	N_f x 10^{-3} kg x 10^{-3}.mol/s	$K_{d\,theo}$ x 10^{-3} m x 10^{-2}. s^{-1}
14 B	0.350	1.94	0.38	6.98	0.35	5.38	9.26
15 B	0.345	1.78	0.73	7.18	0.68	7.40	5.69
16 C	0.335	1.66	1.42	7.64	1.31	14.76	6.26
17 C	0.375	2.09	0.40	6.52	0.37	5.71	6.83
21 C	0.400	2.37	0.37	6.11	0.35	5.46	6.23
25 B	0.440	2.06	1.52	5.82	1.43	18.80	6.00
26 A	0.400	1.90	2.34	7.31	2.17	27.21	6.12
28 A	0.380	2.17	2.21	6.83	2.06	21.26	6.52

$$k_c = \sqrt{\frac{4}{\pi} \; \frac{D_c}{t_f}} \qquad (4.42)$$

and
$$k_d = \frac{\lambda \, V}{768 \, (1 + \mu_d/\mu_c)} \qquad (4.41)$$

where: $\lambda = 2.88$

$D_c = 1.13 \times 10^{-5}$cm.sec^{-2}

Typical results are listed in Table 7.10 and a complete set of results is listed in Appendix D.2F.

Samples of calculations for these three different cases are given in Appendix E.

7.3.4. Mass Transfer During Droplet Oscillation

The overall mass transfer coefficient during droplet oscillation may be estimated from experimental data and theoretically:

7.3.4.1. Based on Experimental Data

Droplet Reynolds numbers in this stage may reach 1000 in a spray column and the mode of oscillation will reach 3 or 4 (Figure 4.1 and 4.2).

The minimum diameter each drop reached during oscillation was recorded for three individual single drops and three individual drop pairs. The recorded value of d_m was the mean of each of the three readings. The calculation then followed the procedure as described in section 7.3.3. Typical results are listed in Table 7.11 and a complete set of results is listed in Appendix D.2G. Comparisons between the experimental overall mass transfer coefficients for single drops and drop pairs during the three regimes (stagnant, circulating and oscillating) are illustrated in Table 7.12 and Figure 7.12.

Table 7.10 Theoretical Overall Mass Transfer Coefficient of single drop and drop pairs during ascent with turbulent internal circulation of solute.

a. Single Drops

Run	t_f s	Velocity m x 10^{-2} s^{-1}	C_1 kg x 10^{-3}.mol/L	K_d x 10^{-33} m x 10^{-2} s^{-1}	K_d x 10^{-2} m x 10^{-2} s^{-1}	K_d x 10^{-2} m x 10^{-2} s^{-1}
10 C	1.00	8.38	0.51	5.85	1.92	1.57
11 C	1.00	9.81	1.01	5.93	2.33	1.76
12 C	1.00	10.43	2.04	6.03	2.53	1.86
13 C	1.00	10.83	3.01	6.21	2.67	1.82

b. Drop Pairs

Run	t_f s	Velocity m x 10^{-2} s^{-1}	C_1 kg x 10^{-3}.mol/L	K_d x 10^{-33} m x 10^{-2} s^{-1}	K_d x 10^{-2} m x 10^{-2} s^{-1}	K_d x 10^{-2} m x 10^{-2} s^{-1}
14 B	1.00	11.76	0.51	5.85	2.22	2.03
15 B	1.00	10.11	1.01	5.93	2.41	1.80
16 C	1.00	11.28	2.04	6.13	2.76	1.93
23 C	1.00	10.87	2.42	3.76	2.66	1.57
26 A	1.00	10.28	3.50	6.28	2.55	1.76

Table 7.11 Experimental Overall Mass Transfer Coefficient of single drops and drop pairs during oscillation at n = 4

a. Single Drops

Run No	ω rad.s^{-1}	ε	d_{min}* m x 10^{-2}	A_o m^2 x 10^{-4}	$\bar{A}$ m^2 x 10^{-4}	N_f x 10^{-2} kg x 10^{-3}.mol/s	$K_{d\,exp}$ x 10^{-2} m x 10^{-2}.s^{-1}
10 C	130.62	0.14	0.53	0.88	0.94	6.57	15.86
11 C	128.64	0.15	0.15	0.51	0.81	10.13	15.32
12 C	117.03	0.01	0.48	0.72	0.76	22.13	17.65
13 C	116.83	0.10	0.40	0.50	0.53	26.06	21.01

b. Drop Pairs

Run No	ω rad.s^{-1}	ε	d_{min}* m x 10^{-2}	A_o m^2 x 10^{-4}	$\bar{A}$ m^2 x 10^{-4}	N_f x 10^{-2} kg x 10^{-3}.mol/s	$K_{d\,exp}$ x 10^{-2} m x 10^{-2}.s^{-1}
14 B	128.04	0.12	0.50	0.78	0.83	11.81	37.44
15B	126.06	0.12	0.45	0.64	0.68	23.33	47.00
16 C	114.61	0.11	0.40	0.55	0.58	43.49	52.80
17 C	116.35	0.12	0.53	0.88	0.93	15.46	41.56
21 C	106.38	0.10	0.58	1.06	1.11	17.37	42.29
25 B	98.01	0.11	0.56	0.98	1.03	62.78	40.10
26 A	94.32	0.09	0.38	0.45	0.47	86.86	78.98
28 A	85.83	0.10	0.41	0.53	0.56	91.65	74.05

*d_{min} = The minimum diameter of droplet during oscillation.

Table 7.12 Experimental Overall Mass Transfer Coefficient of single drops and drop pairs during three stages.

a. Single Drops

Run No.	t_f s	Acetone conc$^{\underline{n}}$ kg x 10^{-3}.mol/L	$K_{df} \times 10^{-2}$ m x $10^{-2}.s^{-1}$	$K_{dc} \times 10^{-2}$ m x $10^{-2}.s^{-1}$	$K_{ds} \times 10^{-2}$ m x $10^{-2}.s^{-1}$
10 C	1.0	0.51	1.60	8.20	15.86
11 C	1.0	1.01	2.02	7.84	15.32
12 C	1.0	2.04	2.23	9.86	17.65
13 C	1.0	3.01	2.30	7.68	21.01

b. Drop Pairs

Run No.	t_f s	Acetone conc$^{\underline{n}}$ kg x 10^{-3}.mol/L	$K_{df} \times 10^{-2}$ m x $10^{-2}.s^{-1}$	$K_{dc} \times 10^{-2}$ m x $10^{-2}.s^{-1}$	$K_{ds} \times 10^{-2}$ m x $10^{-2}.s^{-1}$
14 B	1.0	0.51	5.98	16.52	37.44
15 B	1.0	1.01	6.36	17.85	47.00
16 C	1.0	2.04	7.30	18.45	52.80
17 C	1.0	0.51	5.42	18.49	41.56
21 C	1.0	0.51	7.36	19.89	42.29
25 B	1.05	2.11	6.65	20.05	40.10
26 A	1.00	3.50	7.86	19.54	78.98
28 A	1.10	3.36	7.90	19.11	74.05

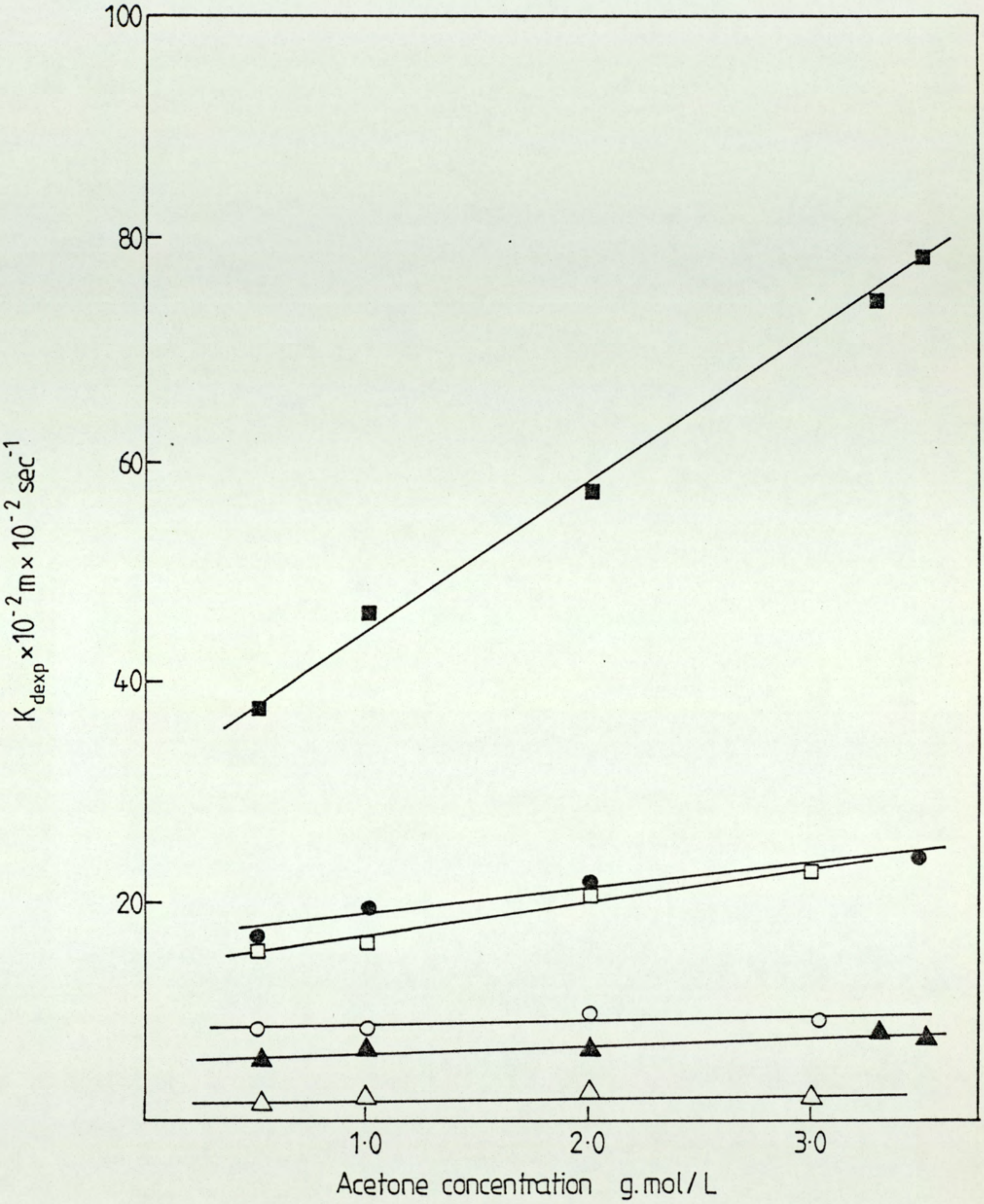

Figure 7·12 Comparison between overall mass transfer coefficient of dispersed phase (single and drop pairs) for three stages. Shaded symbols for Drop pairs.

△, ▲ Drop formation
○, ● Drop circulation
□, ■ Drop oscillation

7.3.4.2. Predictions from Theory

The theoretical overall dispersed phase mass transfer coefficient was calculated using different correlations, as discussed earlier:

1) By Rose and Kintner's Model

The dispersed phase mass transfer coefficient was given by

$$k_d = 0.45\,(D_d\omega)^{0.5} \tag{4.52}$$

The continuous phase mass transfer coefficient was given by Garner et al (21)

$$\frac{k_{cd}}{D_d} = 50 + 8.5 \times 10^{-3}\,(Re)\,(Sc)^{0.7} \tag{4.27}$$

Finally the overall dispersed phase mass transfer coefficient was calculated by applying:

$$\frac{1}{K_d} = \frac{1}{k_d} + \frac{m}{k_c} \tag{1.2}$$

2. By Angelo, Lightfoot and Howard's Model

The equation for the dispersed phase coefficient is:

$$k_d = \sqrt{\frac{4D_d\,\omega\,(1 + \varepsilon + \frac{3}{8}\varepsilon^2)}{\pi}} \tag{4.61}$$

and the overall mass transfer coefficient is given by the following equation:

$$K_d = k_d\left[\frac{1}{1 + m\sqrt{\frac{D_d}{D_c}}}\right] \tag{4.63}$$

3) By Al-Hassan's Correlation

Al-Hassan extended Rose and Kintner's model by correlating a new value for the constant (C) in equation 4.52 to give,

$$k_d = 4.3\, \varepsilon^{2.692}\, E_o^{\,1.672}\, (D_d\, \omega)^{0.5} \qquad (4.74)$$

The simplest and best estimation of the amplitude 'ε' was obtained by correlating Strouhal, Weber numbers and interfacial tension ratio to the powers, given in equation 3.8.

In the present work a computer program (Appendix C.7) was written and used to calculate the overall mass transfer coefficients for droplets by the above three correlations. Typical results are listed in Table 7.13 (in comparison with the experimental values) and a complete set of results is listed in Appendix D.5 with n = 2 and ε calculated from Table 7.7 and Appendix D.2C.

7.4 EMPIRICAL CORRELATIONS

The observed disagreement between experimental and predicted overall mass transfer coefficients for droplet pairs, for most of the single oscillating drops models necessitates development of a new correlation to fit the observed data more closely.

7.4.1. Correlation of the Frequency of Oscillation

The frequency of oscillation equation given by Lamb (28), is:

$$\omega^2 = \frac{n\, \sigma\, b}{r^3_d} \left[\frac{(n+1)\,(n-1)\,(n+2)}{(n+1)\,\rho_d + n\rho_c} \right] \qquad (2.9)$$

This equation does not take into account the effect of adjacent drops on the drop under study, or even the effect upon the oscillation of both drops of any collisions involving rebound.

Table 7.13 Comparison between Experimental and Calculated $K_{d,s}$ of oscillating single drops and drop pairs, by three different correlations for two values of (n)

a. Single Drops

Run No	$K_{d\,exp} \times 10^{-2}$	$K_{d\,theo} \times 10^{-2}$			$K_{d\,theo} \times 10^{-3}$		
		n = 2			n = 4		
	*	K_{dRO} *	K_{dAO} *	K_{dTO} *	K_{dRO} *	K_{dAO} *	K_{dTO} *
10C	15.86	7.99	30.06	2.30	10.09	51.00	7.51
11C	15.32	8.46	29.54	1.68	10.85	50.11	6.31
12C	17.65	8.05	26.15	1.58	10.24	44.36	5.90
13C	21.01	7.69	24.03	1.58	9.65	40.75	5.75

b. Drop Pairs

Run No	$K_{d\,exp} \times 10^{-2}$	$K_{d\,theo} \times 10^{-2}$			$K_{d\,theo} \times 10^{-3}$		
		n = 2			n = 4		
	*	K_{dRO} *	K_{dAO} *	K_{dTO} *	K_{dRO} *	K_{dAO} *	K_{dTO} *
14B	37.44	9.17	29.77	1.19	12.09	50.49	5.07
15B	47.00	8.53	29.24	1.61	10.98	49.61	6.17
16C	52.80	8.35	25.62	1.32	10.80	43.45	5.29
17C	41.56	13.69	28.37	1.84	10.83	48.13	6.81
21C	42.29	8.19	27.13	1.92	10.73	46.02	7.06
25B	40.10	8.43	23.93	1.17	11.15	40.60	4.93
26A	78.98	7.27	19.77	1.78	9.18	33.53	6.14
28A	74.05	7.51	18.86	1.50	9.70	31.98	5.68

* = $m \times 10^{-2} . Sec^{-1}$.

The observed frequency of oscillation was in fact much higher than that predicted, especially before and after bouncing between drops, ie:

Frequency of oscillation before bouncing > 1.0

Frequency of oscillation during bouncing < 1.0

Frequency of oscillation after bouncing >> 1.0

Hence there is apparently a factor affecting the frequency of oscillation, caused by the presence of neighbouring drops eg.interaction between both drop wakes, which results in a change in the drop characteristics.

The frequency of oscillation is as a function of the wake interaction (S):

$$\omega^2_{corr} = f\,S \qquad (7.10)$$

from equation 7.10

$$\omega^2_{corr} = Q\,S \qquad (7.11)$$

where;

$$Q = \frac{n\,\sigma\,b}{r^3}\left[\frac{(n+1)\,(n-1)\,(n+2)}{(n+1)\ \rho_d + n\rho_c}\right] \qquad (7.12)$$

and

$$S = \frac{\omega_{obs}}{\omega_{cal}} \qquad (7.13)$$

ω_{obs} is the value of frequency of oscillation observed from frame by frame analysis of high speed cine film, and depends mainly upon the value of the mode of oscillation (n) and drop diameter (d). The values of interfacial tension, viscosity and density were considered constant from drop formation until coalescence, since in this study the changes were very small compared with the starting values. ω_{cal} is the value of frequency of oscillation calculated from the displaced volume of dispersed phase, using Lamb's equation (28);

For example,

$$\text{at} \quad n = 2$$

$$\sigma = 21.8 \text{ dyne. cm}^{-1}$$

$$\text{drop diameter } d = 0.70\text{cm}$$

therefore $$b = \frac{0.70^{0.225}}{1.242}$$

$$= 0.74$$

therefore $$\omega^2_{cal} = \frac{2 \times 21.8 \times 0.74}{(0.35)^3} \left[\frac{(2+1)\ (2-1)\ (2+2)}{(2+1)\, 0.8619 + 2 \times 0.9968} \right]$$

$$= 44.50 \text{ rad.sec}^{-1}$$

ω_{obs} values were different from frame to frame depending upon the degree of distortion and the shape of the drop, ie. the values of (n) and (d) in each frame. Figures 8.4 and 8.5 present the observed and calculated ω of single drop and drop pairs.

The disagreement between the observed and calculated frequency of oscillation, necessitated examining the requirements for evaluating the term "S" in equation 7.13. The factors considered to be important in the evaluation of "S" are:

1. Drop Weber number
2. Weber number of continuous phase
3. Drop Reynolds number
4. Reynolds number of continuous phase
5. Viscosity ratio of continuous to dispersed phases
6. Concentration driving force which can be represented by interfacial tension
7. Strouhal number

$$S = K(V^a \; d^b \; \sigma^c \; \rho_d{}^d \; \rho_c{}^e \; \mu_d{}^f \; \mu_c{}^g) \qquad (7.14)$$

A multiple linear regression program Appendix C.8 was applied to determine the significance of these parameters. Weber number was found to be most significant and the following correlation was obtained for the toluene-acetone-water system with a maximum deviation of 30% (Figure 7.13).

$$S = 2.8 \, (We)^{0.40} \qquad (7.15)$$

therefore $\omega^2_{corr} = 2.8 \, (We)^{0.40} \, Q$ (7.16)

with a maximum deviation of 19% from the observed value (Figure 8.6).

7.4.2. Correlation of the Dispersed Phase Mass Transfer Coefficient

The dispersed phase mass transfer coefficient was calculated experimentally by regarding the continuous phase mass transfer coefficient correlation developed by Garner and Tayeban (2) as valid. The frequency of oscillation, area of droplet, the diffusivity and the amplitude are the main factors affecting the mass transfer coefficient.

The penetration theory was found to be the basis for the common approach applied by previous investigators (1, 69, 80) and all are an embellishment of the equation:

$$k_d = C \, (\omega \, D_d)^{0.5} \qquad (4.52)$$

where C is a constant or a function of one or more of the factors mentioned above. The experimental dispersed phase mass transfer coefficients estimated in this investigation were in all cases higher than those predicted by different models and correlations (1, 69, 80), as will be seen in Appendix D.2. This necessitated examining the requirements for evaluating the term "C" in equation 4.52.

The factors which have been considered to be important in the evaluation of "C" are:

1. The drop Weber number $\left[\dfrac{d \, V^2 \rho_d}{\sigma}\right]$

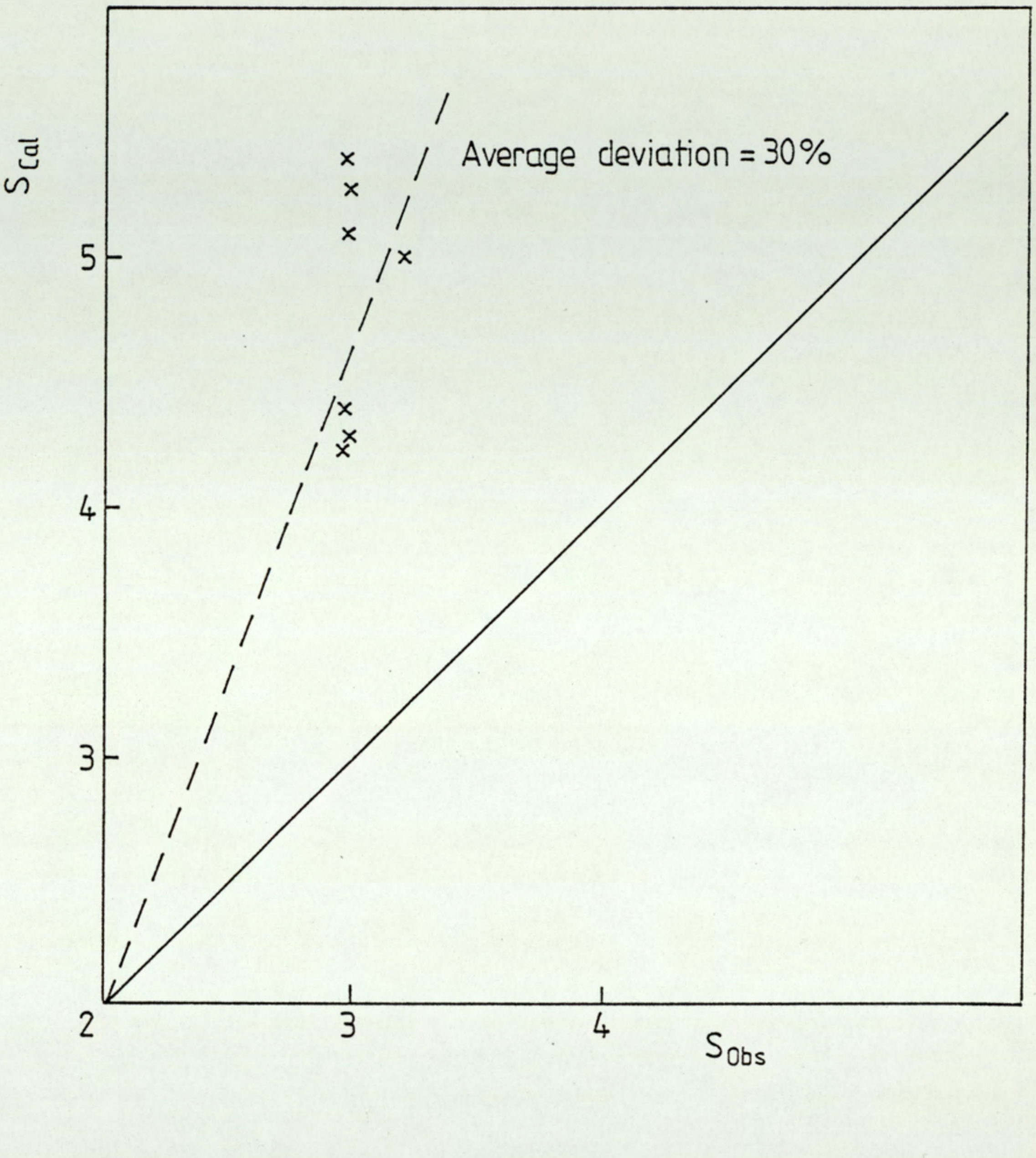

Figure 7·13 Observed and Calculated (S) for Drop pairs according to equation (7·15)

2. Droplet Reynolds number $\dfrac{d\,V\,\rho_d}{\mu_d}$

3. Continuous phase Weber number $\dfrac{d_e\,V^2\,\rho_c}{\sigma}$

4. Continous phase Reynolds number $\dfrac{d\,V\,\rho_c}{\mu_c}$

5. Surface tension group $\dfrac{Re^2{}_d}{We_d}$

6. Schmidt number $\dfrac{\mu_d}{\rho_d\,D_d}$

7. Nozzle Reynolds number $\dfrac{d\,V\,\rho_d}{\mu_d}$

8. Nozzle velocity $\dfrac{d}{T}$

The above groups were considered to be a function of "C" of the form:

$$C = k \quad d^a \left[\frac{d}{T}\right]^b \rho_d{}^c \ \rho_c{}^d \ \mu_d{}^e \ \mu_c{}^f \ \sigma^g \tag{7.17}$$

and a multiple linear regression program Appendix C.8 was applied to determine the significance of these parameters. The Weber and Reynolds numbers were most significant and the following correlation was obtained:

$$C = K\,(\mathrm{We})^{-e}\,(\mathrm{Re})^{-f}$$

$$= 1.32\,(\mathrm{We})^{0.177}\,(\mathrm{Re})^{0.190} \qquad (7.18)$$

However the dispersed phase mass transfer coefficient of a droplet, equation 4.52, is a function of frequency of oscillation. It is vital to include the modified frequency of oscillation equation 7.16 for drop pairs:

$$K_{dcorr} = 1.32\,(\mathrm{We})^{0.177}\,(\mathrm{Re})^{0.190}\,(\omega_{corr}\,D_d)^{0.5} \qquad (7.19)$$

The above correlation gave an average absolute deviation of 9.0% as in Figure 8.7. The significance of these results will be discussed in Chapter 8.

CHAPTER EIGHT

DISCUSSION OF RESULTS

Mass transfer to, or from, an oscillating droplet in a spray tower is affected by changes in the interfacial area during operation including the changes during formation. An accurate assessment of the interfacial area of a droplet as a function of time during formation will assist in the prediction of overall mass transfer coefficients in practical columns. A new correlation for this purpose is given in Chapter 7, Appendix D.4, and is discussed in this chapter.

With regard to droplet hydrodynamics during travel, most investigators (1, 28, 29) of the prediction of the frequency and or amplitude of oscillation of a fluid drop at rest in a stagnant continuous fluid have assumed that the drop oscillation is of small amplitude. There are at present no models to account for the effect of the presence of an adjacent drop on the behaviour of the drop under study, in respect of the frequency of oscillation, whilst mass transfer of solute is taking place. The present investigation was undertaken to study the parameters controlling solute transfer under steady-state conditions from a pair of large oscillating drops taking into account the collision and rebound of these drops, and how this phenomena affected frequency of oscillation of both drops and consequently the overall mass transfer coefficients from these drops to the counterflowing continuous phase.

The dispersed phase mass transfer coefficient for oscillating drop pairs was found to depend on the frequency of oscillation of both drops and the continuous phase Weber number.

8.1. IMPROVED EXPERIMENTAL TECHNIQUES

The results of previous studies on the mass transfer rate from droplets demonstrated that, during the coalescence stage, a drop has the lowest mass transfer rate and coefficient in comparison with the other stages during passage through the column.

In order to study the hydrodynamic characteristics of two or more adjacent drops in a countercurrent process using a spray or perforated plate tower, with mass transfer taking place, the coalescence between drops must be prevented. Several experiments were undertaken with nozzles of either glass or ptfe plastic to minimise the extent of coalescence between a pair of drops travelling along the length of the column.

The dependence of coalescence upon the distance between two drops of the same size and the flow rate was studied and the average space to avoid coalescence was recorded. A distance of 2.85cm between the centre of the drops approximated to the minimum practical distance. Different pairs of glass nozzles with different distances between them are shown in Figure 6.3.

In order to minimise the error in the measurements of the droplets' characteristics, the three droplet dimensions were measured, photographing the drops with a video and cine cameras and using a mirror image to estimate the Z-dimension. The graticule scale shown on Figure 6.4 was used to facilitate the interpretation of the video and cine films.

An improved sampling technique developed by Jeffreys and Bonnet (157) was used to withdraw the dispersed phase droplet after formation or from different positions within the column.

8.2. MASS TRANSFER DURING DROP FORMATION

In the present investigation, the drop formation time was found to be between 0.5-3.15 seconds. The transfer of solute occurred faster with short or moderate formation times, eg. between 0.5-1.5 seconds, than at long formation times eg. 1.6-3.15 seconds. The overall coefficient of mass transfer during drop formation was evaluated using Johnson and Hamielec's correlation to calculate the efficiency of solute transfer.

$$E_m = \frac{C_1 - C_2}{C_1 - C^*} = \frac{20.6}{d_e} \left[\frac{D_d t_f}{\pi} \right]^{0.5} \qquad (4.12)$$

from which the theoretical value of (C_2) was calculated. The overall dispersed phase mass transfer coefficient during formation was then evaluated by equation 1.1.

At solute concentrations > 20% w/w the continuous phase started creeping down inside the nozzle, due to the low value of the interfacial tension (ie. about 10 dyne/cm) which caused drops to decrease in size. At the same time the glass nozzle was wettable by the continuous phase, which encouraged this phenomenon as shown in Figure 5.7. Therefore the glass nozzles were replaced by ptfe nozzles which were wettable by the organic solvent only.

The experimental overall mass transfer coefficient during drop formation was found as a function of solute concentration (Figure 7.5).

Several mathematical models for evaluating the mass transfer coefficient of the dispersed phase during drop formation are summarised in Table 4.1. Of those equation 4.12 gave the best fit to the experimental results with 12% and 67% deviation from the experimental values of single and drop pairs respectively (Figures 7.6 and 7.7). Therefore a new correlation was derived for the overall mass transfer coefficient during drop formation, based upon the accurate measurement of the surface area during drop formation between t_1 and t_2 seconds. This is given in equation 7.9 which gave values deviating by only 5% from the experimental overall mass transfer coefficient for drop pairs. This is shown in Figure 7.11.

8.3 THE HYDRODYNAMICS OF OSCILLATING DROPS

Small liquid drops of diameter between 1.0 to 3.0mm with a Reynolds number of approximately 1.0 tend to behave like solid spheres which obey Stokes Law of motion. However any change in the boundary conditions on the surface of the drop leads to a significant change in the velocity of the drop. Liquid drops have a mobile surface due to the movement of the liquid inside the drop, which increases the droplet velocity above that of a solid sphere. When the drop increases in size to a diameter > 3.0mm, the Reynolds number will generally become $10 \leq Re \leq 200$ and circulation patterns develop which exert a pressure from inside to the outside of the liquid drop. Above $Re = 200$ drop deformation from the spherical shape occurs. When such a drop starts to oscillate the velocity decreases as shown in Figure 2.3.

In the present study two drops ascended together from the forming device in the surrounding fluid media. With small non-oscillating drops moving in parallel, the velocity of the continuous phase between them is greater than that of the rest of the continuous phase due to the "Bernoulli effect" and this increases the surface renewal between the drops and a thinning of the boundary layer in comparison with the other two poles of the drops.

When the drops commence to oscillate with diameter ≥ 3.0mm and $Re \geq 200$, they may collide and coalesce forming a very large droplet with low velocity and lower interfacial area per unit volume, or collide and rebound forming newly-shaped drops, together with an increase in interfacial area.

8.4. AMPLITUDE OF DROPLET OSCILLATION

The amplitude was calculated using the area of the drop, hence taking into account the three axes, rather than depending on one axis only. Large size droplets deviated significantly from a symmetrical spherical shape as shown in Figures 4.1 and 4.2, and confirmed from cine and video films. Only small drops < 6.0mm in diameter could be assumed to be symmetrical spheroids.

It was observed that the eccentricity "ε" was greater for high interfacial tension systems and was also higher with a system with a low solute concentration compared with a high concentration. In a hydrodynamic experiment the droplet always exhibited a larger amplitude of oscillation than under corresponding conditions when mass transfer was taking place. The high concentration of solute ie. (20-25% w/w),

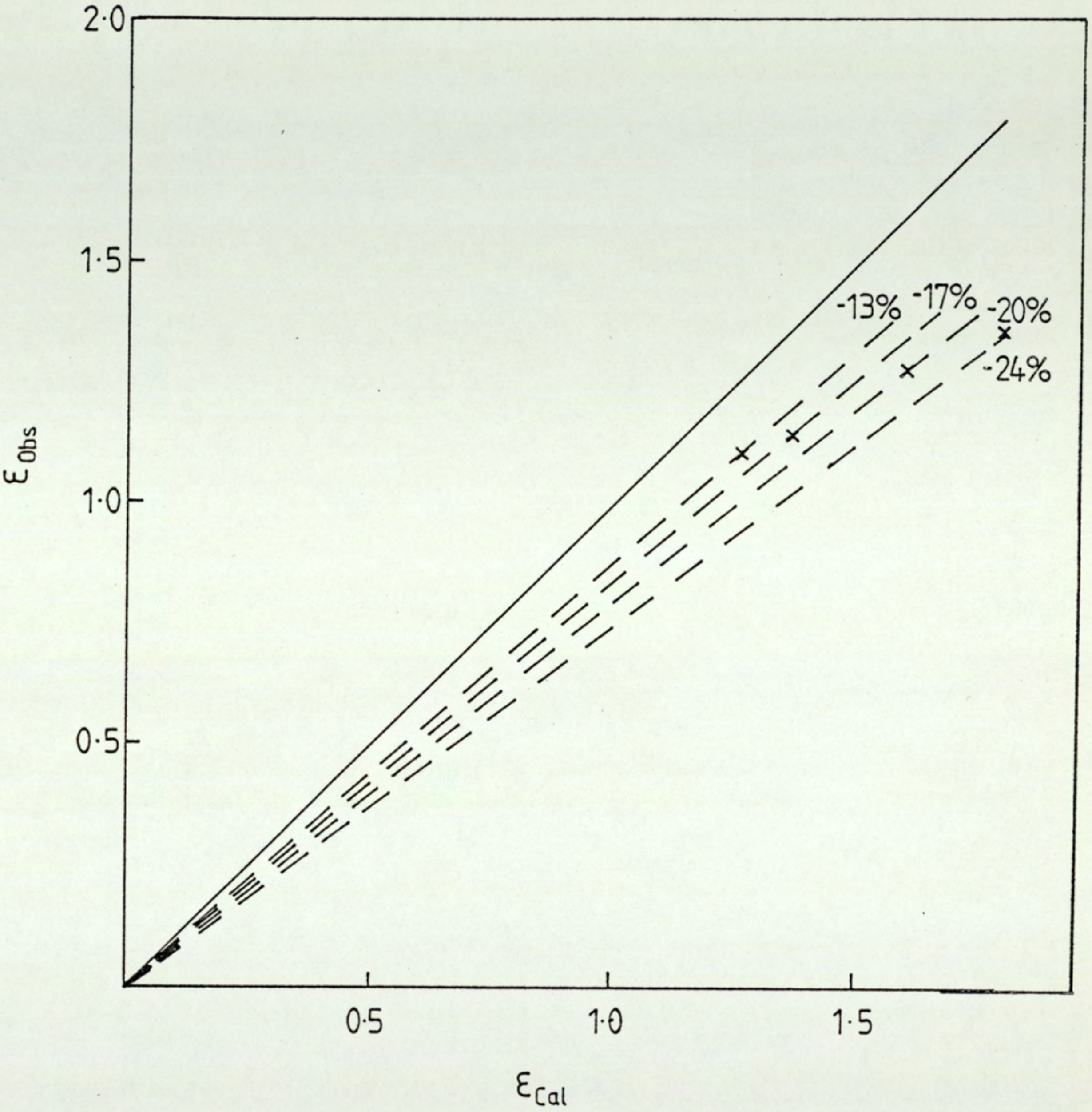

Figure 8·1 Observed and Calculated ε's of Single drops.

which results in a lowering of the interfacial tension, might cause amplitude damping.

In the present study it was found that the amplitude of a single large oscillating droplet was always greater than for corresponding drop pairs. This was possibly due to the collision of the drop with the adjacent drop causing depression of the amplitude of oscillation which increased the frequency of oscillation.

The observed amplitude was found by measuring the initial area after formation and the maximum area the drop reached during its travel through the continuous phase and then applying equation 3.6.

Calculated amplitudes for single drops and drop pairs were estimated by Al-Hassan's correlation for eccentricity, equation 3.8. Figures 8.1 and 8.2 represent the observed and calculated eccentricities and demonstrate a deviation of 18% for single drops and 46% for drop pairs. The fluctuation of single and drop pair dimensions with time under similar conditions of drop size, dispersed phase flow rate, solute concentration and temperature, is shown in Figure 8.3. This figure shows how the eccentricity of single drops and drop pairs varied with time. All previously reported studies on amplitude are only for single drops with, or without, mass transfer.

8.5. FREQUENCY OF DROPLET OSCILLATION

In the present investigation the drop started to oscillate immediately after detachment from the nozzle. It is well-known that the frequency of oscillation is a function of drop diameter, interfacial tension and the mode of oscillation (28). The oscillation frequency of a small droplet is known to be higher than that of large drops when the other variables are kept constant. The frequency of oscillation was damped during droplet ascent as shown in Figure 8.3 and also with increasing solute concentration due to a decrease in drop size.

The frequency of oscillation during mass transfer from drop pairs of size > 6.0mm was more complicated than can be predicted by Lamb's hydrodynamic equation (28). Hence there were deviations of 13% and 68% respectively between the observed frequency of oscillation of single and drop pairs and those calculated by

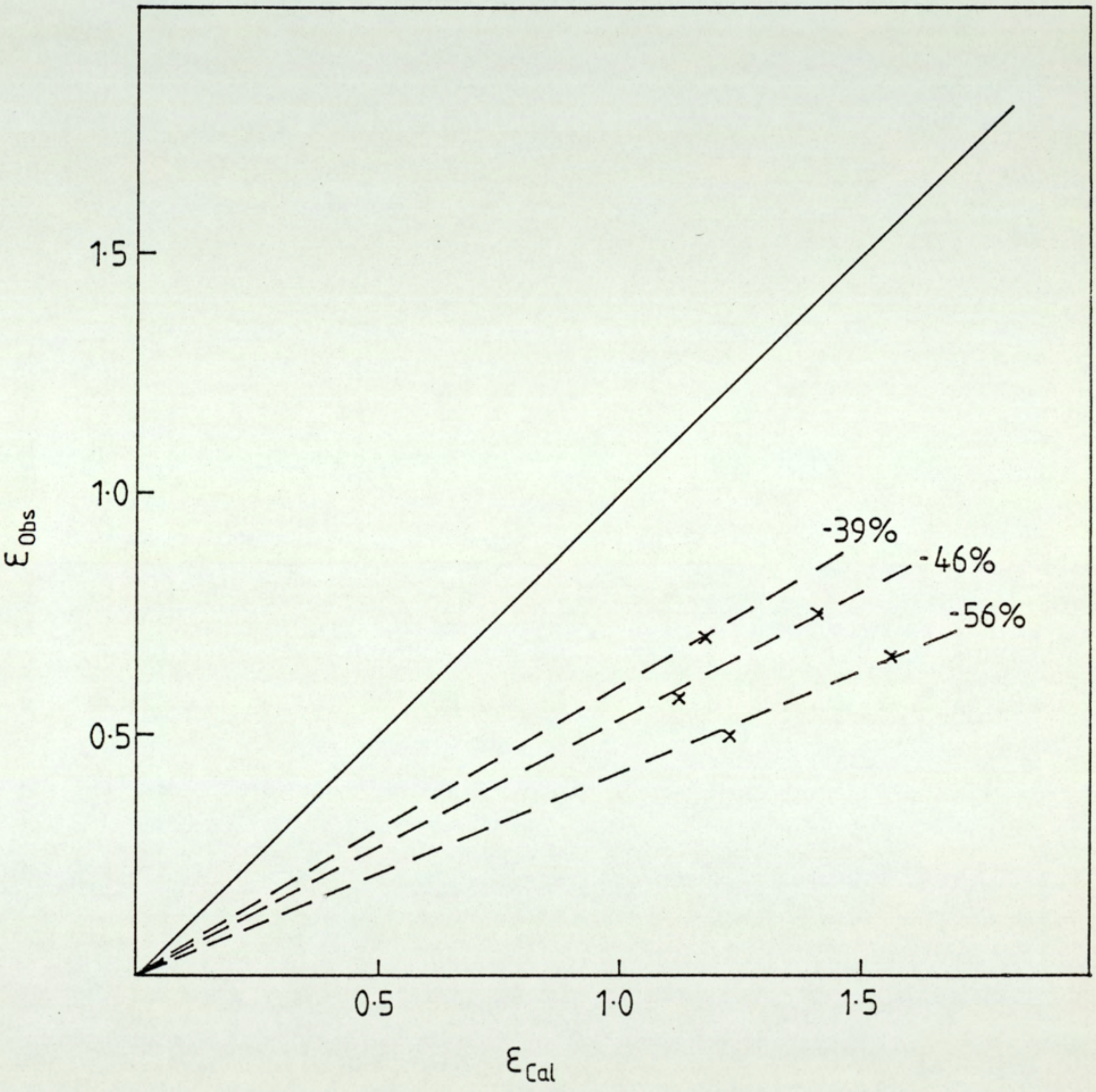

Figure 8·2 Observed and Calculated ε's of Drop pairs.

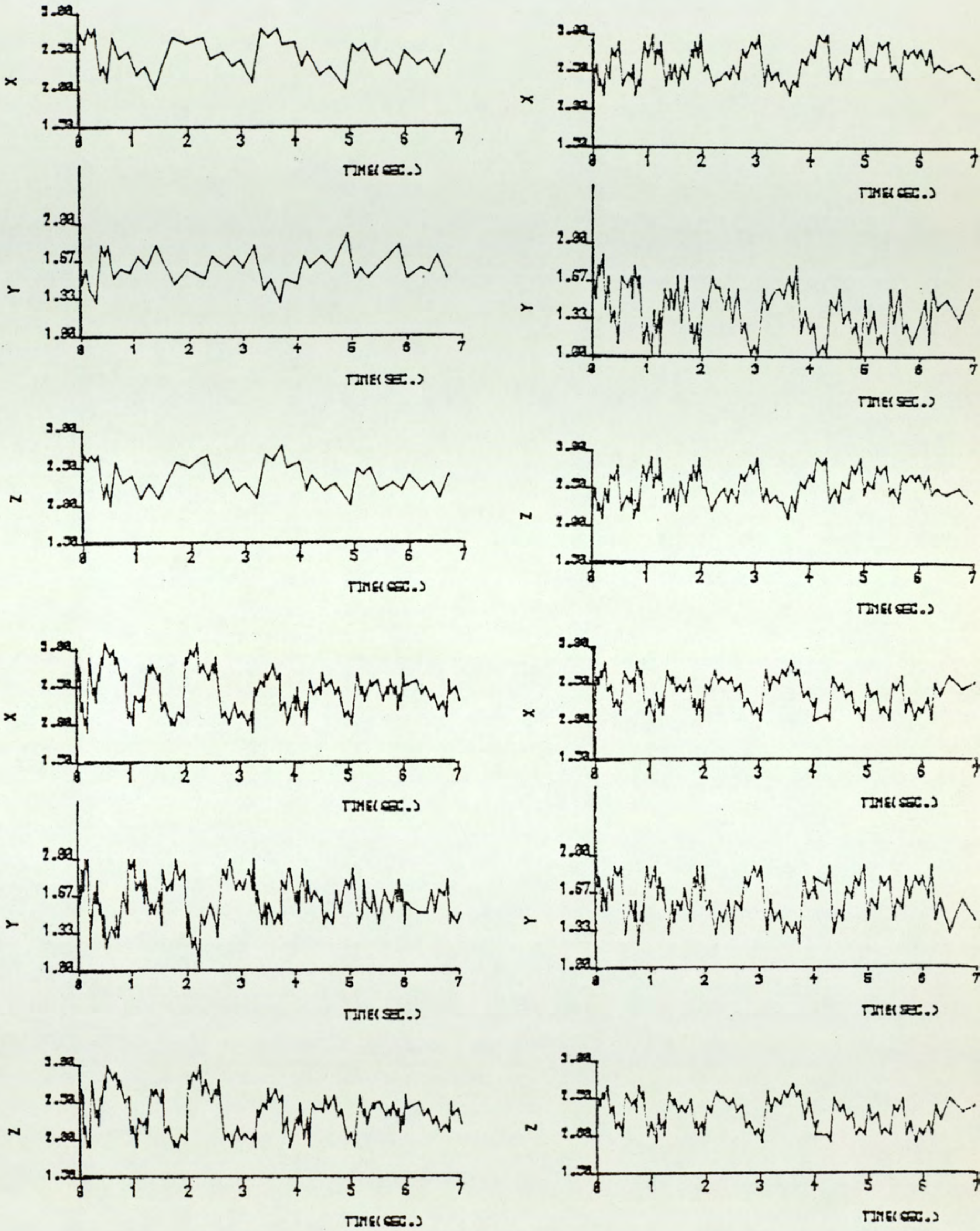

(a) Single drop

(b) Equi-sized drop pair

Figure 8.3 Fluctuations in single and drop pair dimensions (x, y and z - axes) with time

Lamb's equation as shown in Figures 8.4 and 8.5. Therefore a new correlation has been proposed taking into account the effect of the adjacent drop on the drop under study. This correlation, equation 7.16 gave good agreement with previous studies on the significance of the Weber number of the continuous phase in the analysis of large oscillating single drops. Equation 7.16 gave a 19% deviation from the observed frequency of oscillation of drop pairs, Figure 8.6 demonstrates much better agreement than previously obtained using single drop correlations.

8.6. MASS TRANSFER COEFFICIENT FROM OSCILLATING DROPS

The overall mass transfer coefficients of single drops and drop pairs for the system toluene-acetone-water were studied with different solute concentrations, dispersed phase flow rates and nozzle diameters. The observed overall mass transfer coefficients of single drops and drop pairs were compared with known single drop correlations and the results, and the deviations, recorded in Chapter 7 and will now be discussed.

8.6.1. Single Drops

The observed overall mass transfer coefficients for single dispersed phase droplets during oscillation were compared with those predicted by the correlations of Rose and Kintner, Angelo et al and Al-Hassan (80, 69, 1) and in general the experimental values were always higher than the predicted values. The observed overall mass transfer coefficients of the dispersed phase are given in Table 7.11 and Appendix D.2G and the calculated values in Table 7.13 and Appendix D.5. A comparison between the observed and calculated values is presented in Table 7.13. Generally the deviation was considerable eg. in the case of drop pairs the average deviation was found to be as much as 90%.

The predictions from the models and empirical correlations, together with their deviations from the experimental mass transfer coefficients of single droplets, will be

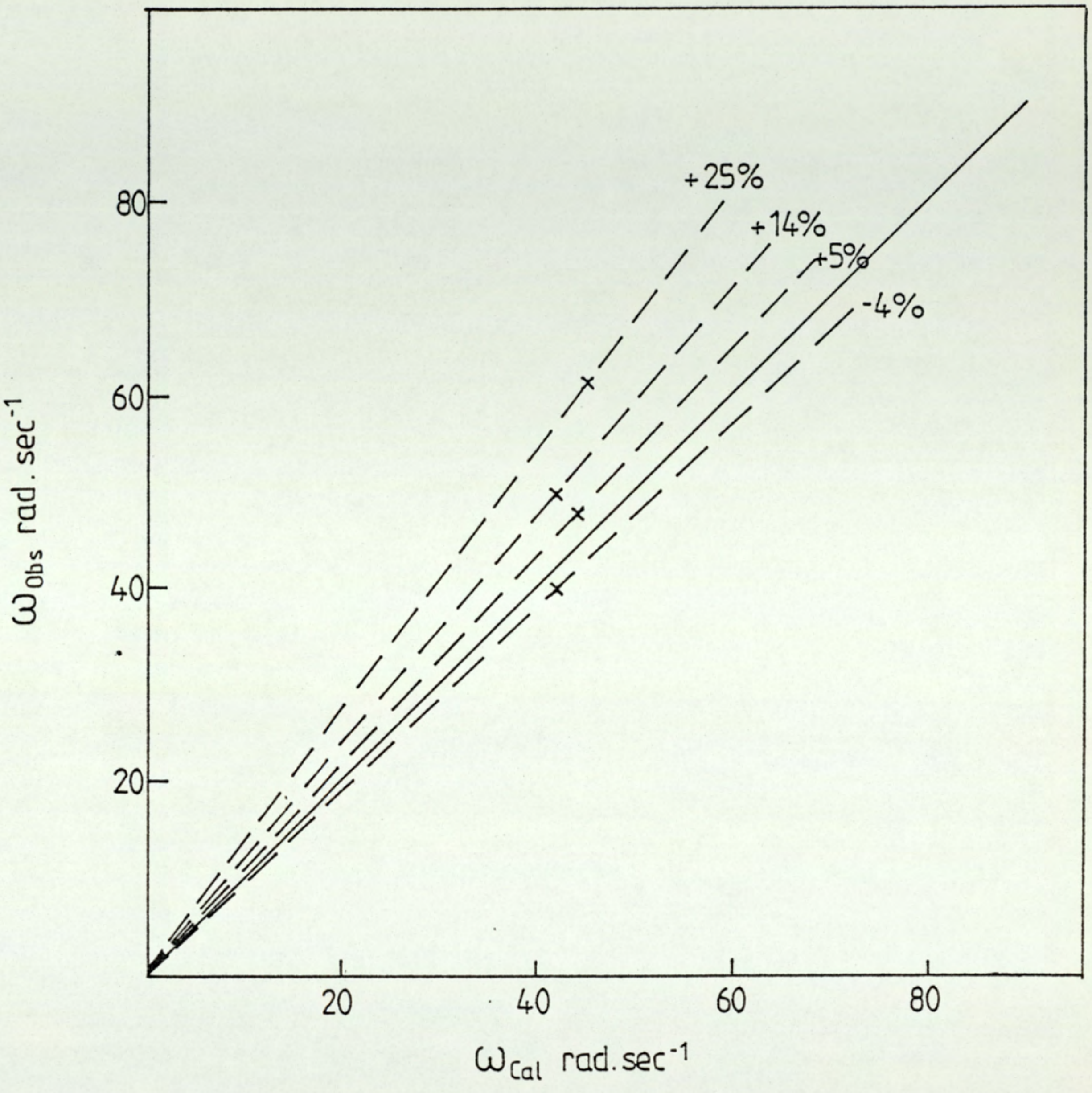

Figure 8·4 Observed and Calculated ω of single drops using equation (2·9), n = 2.

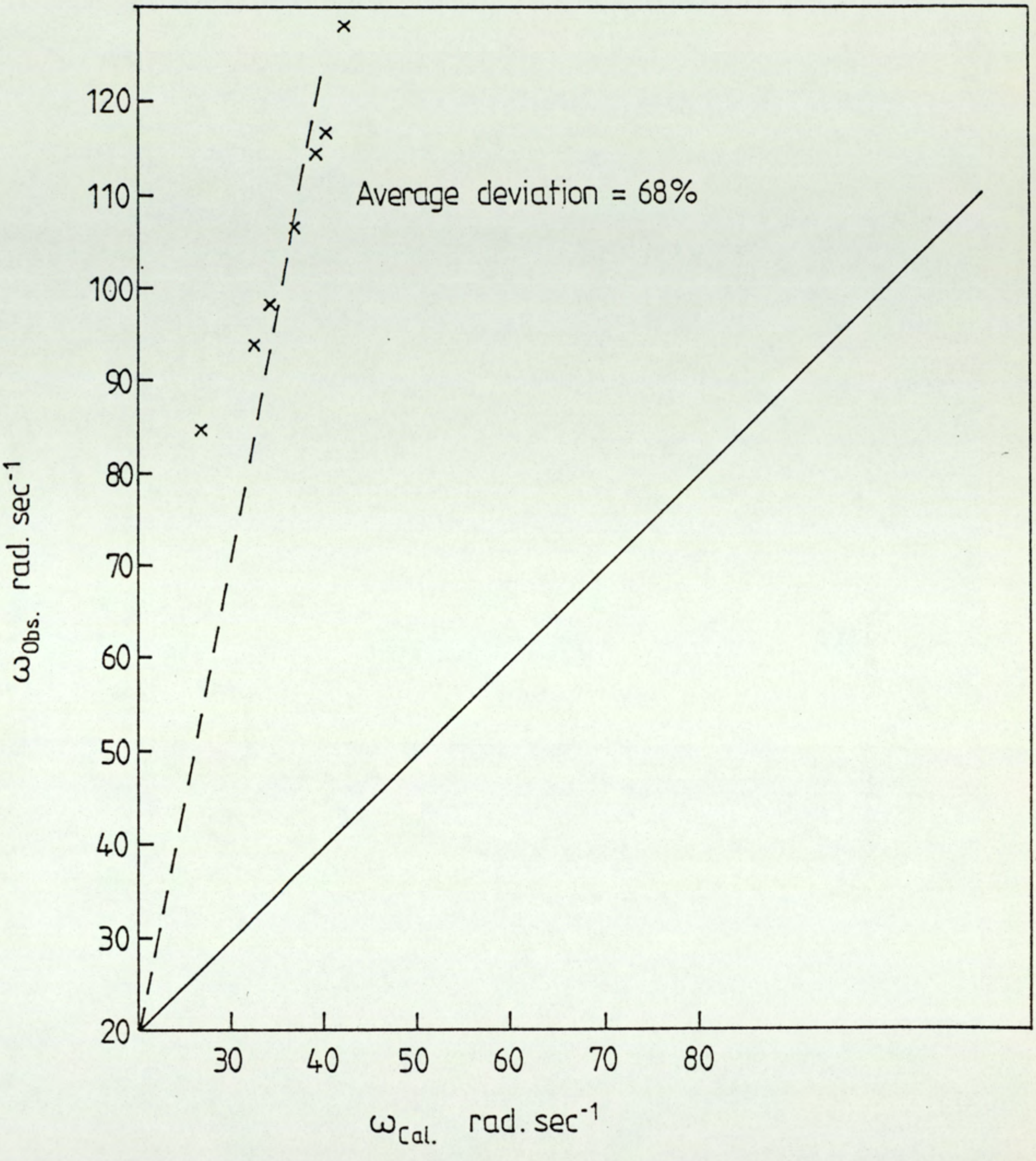

Figure 8·5 Observed and Calculated ω of drop pairs using equation (2·9). n = 4

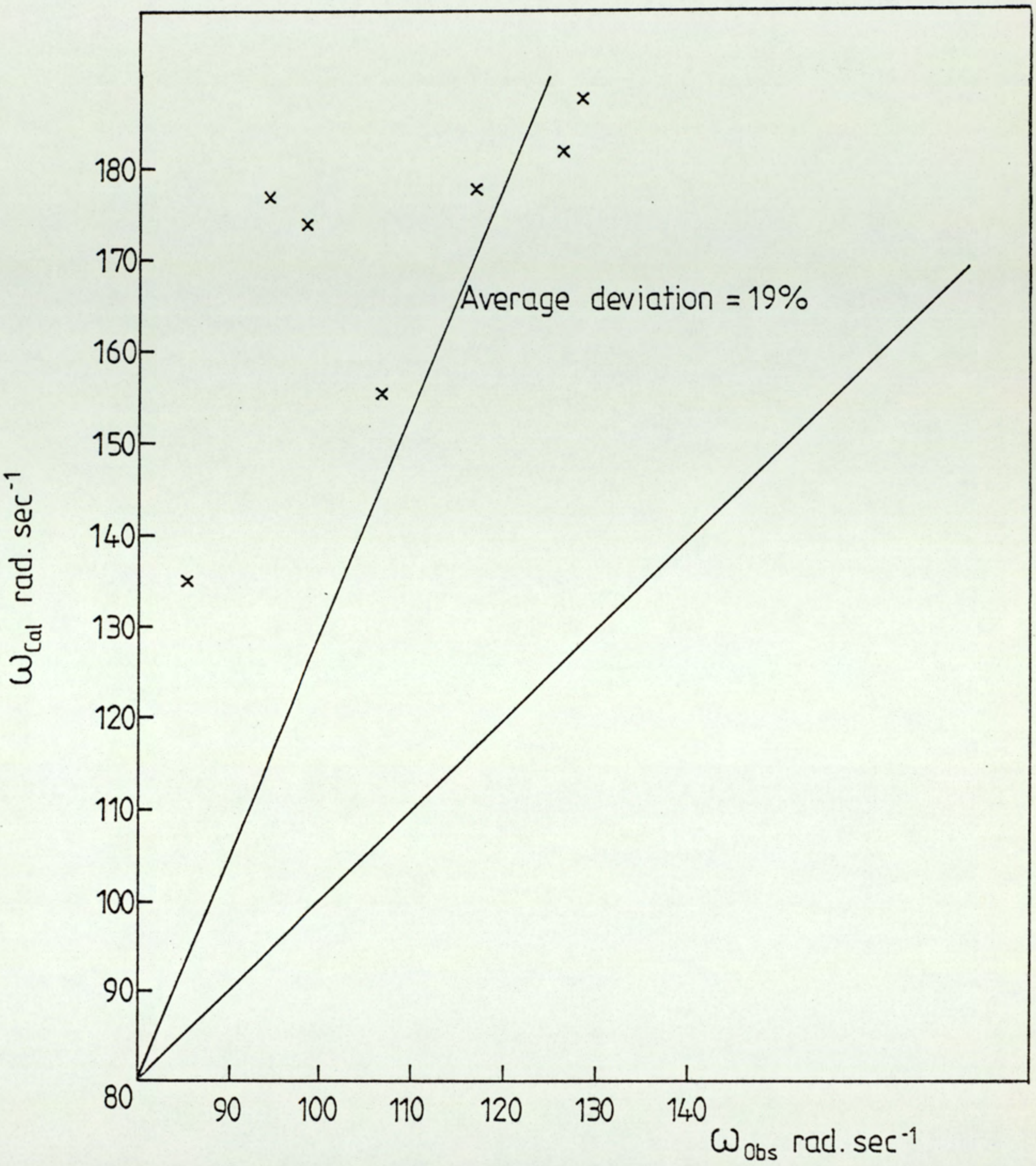

Figure 8·6 Observed and Calculated ω of Drop pairs using equation (7·16) discussed separately.

8.6.1.1. Rose and Kintner's Model (80)

The deviations between the observed and calculated $K_{d.s}$ based on Rose and Kintner's model were large for single oscillating drops and drop pairs at n = 4, ie. 86% for single drops and 94% for drop pairs. This was attributable to:

a. The model depended upon the amplitude of oscillation calculated by measuring only one axis of the drop neglecting the change in the other two dimensions.

b. The assumption in the model that a symmetrical spheroid shape is applicable for large oscillating liquid drops.

8.6.1.2. Angelo, Lightfoot and Howard's Model (69)

The deviations between the observed and calculated $K_{d.s}$ based on Angelo et al's model were also large at n = 4. It was found to be 65% and 85% for single drops and drop pairs respectively. This was attributable to,

a. The area changes being more complex than described by the equation:

$$A = Ao\,(1 + \varepsilon \sin^2 \omega t) \qquad (4.59)$$

b. The model neglecting the effects of the wake and hence assuming that the mechanisms of solute transfer at the front and rear of the drop are similar.

8.6.1.3. Al-Hassan's Model (1)

The deviations between the observed and calculated $K_{d.s}$ based on Al-Hassan's model were also large at n = 4, reaching 99% deviation in the case of drop pairs, and approximately 68% for single drops. This was attributable to,

a. An existing 13% deviation in the eccentricity model (section 3.2) being inserted into the mass transfer coefficient model.

b. This model depends upon the correlation of the penetration theory equation constant, equation 3.2 which has a 19.5% deviation, and may therefore require consideration of other variables eg. modified Sr.

From the above discussion of the three single drop models it may be concluded that Angelo et al's (69) provides the best fit for the observed single drop results. However none of the above models considered the presence of adjacent drops and this may partly explain the large deviations when they are applied to drop pairs.

8.6.2. Drop Pairs

There have been no previous attempts to correlate the overall mass transfer coefficient of a droplet within a swarm. Hence in extractor design reliance has been placed on single drop predictions which, even if proper allowance is made for the size distribution (166) is inherently inaccurate.

Drops in any column exhibit a range of physico-chemical hydrodynamic phenomena. They may travel at such a distance apart that there is no effect of one drop on the others, especially at low hold-ups, or they may travel at a distance apart such that some hydrodynamic effect is transmitted through the continuous phase between them. In the latter case they may rise in parallel without collision, or collide and rebound, or collide and coalesce.

8.6.2.1. Drop Pairs without Collision

Drops can rise in a spray column at a distance between them such as to guarantee that there are no collisions from formation to coalescence at the end of the column. This phenomenon increases with decreasing drop size and decreasing hold-up. In this case, for any given drop size and solute concentration, the factor affecting the mass transfer coefficients of both drops is the magnitude of the velocity profile between them, which may increase the process of thinning the surfaces of both drops and increase surface renewal by fresh continuous phase fluid. This factor helps to increase the overall mass transfer coefficient.

8.6.2.2. Drop Pairs with Collision

When drops approach within a certain distance of each other collision may occur. This has a large effect on the mass transfer coefficient from a dispersed phase droplet to the continuous phase and can increase the rate as much as 88 times that for a single oscillating drop due to the continuous changes in the shape of the drop which increase the interfacial area and also increase the turbulent mixing inside the drop.

The correlation presented for the prediction of the dispersed phase mass transfer coefficients equation 7.19, includes the correlation presented for the frequency of oscillation for drop pairs (equation 7.16) and gave results that agreed better than the correlations proposed earlier. This correlation takes account of the characteristics of the phenomenon of mass transfer from a large oscillating drop in the presence of an adjacent drop. The average absolute deviation between the observed and calculated mass transfer coefficient was 9.0% as shown in Figure 8.7.

8.7. APPLICATION TO PRACTICAL COLUMNS

The results reported for drop pairs represent the simplest case of a "swarm" of drops in a practical column. The operating hold-up in this work was of the order of 2.5×10^{-3}, while the hold-up corresponding to flooding in a spray column is 5.0×10^{-1}. Thus, even allowing for operation at eg. 70% of the flooding condition, there is far more potential for inter-drop effects in a practical column.

In an ideal system the arrangement of the drops will be geometrically equispaced. The effect of drops which travel in parallel was discussed above. Other drops, to the front and rear of the one considered, will tend to exert different effects, such as the interactions of their wakes on the drop, which will greatly affect the rate of mass transfer.

Whilst, the drops as large as 0.5 to 0.95cm in diameter may be uncommon in modern columns, eg. involving packings or agitation, study of the characteristics of each individual drop (eg. photographically such that the circulation path and the circulation break down by turbulent mixing and the initiation of oscillation can be observed) assists

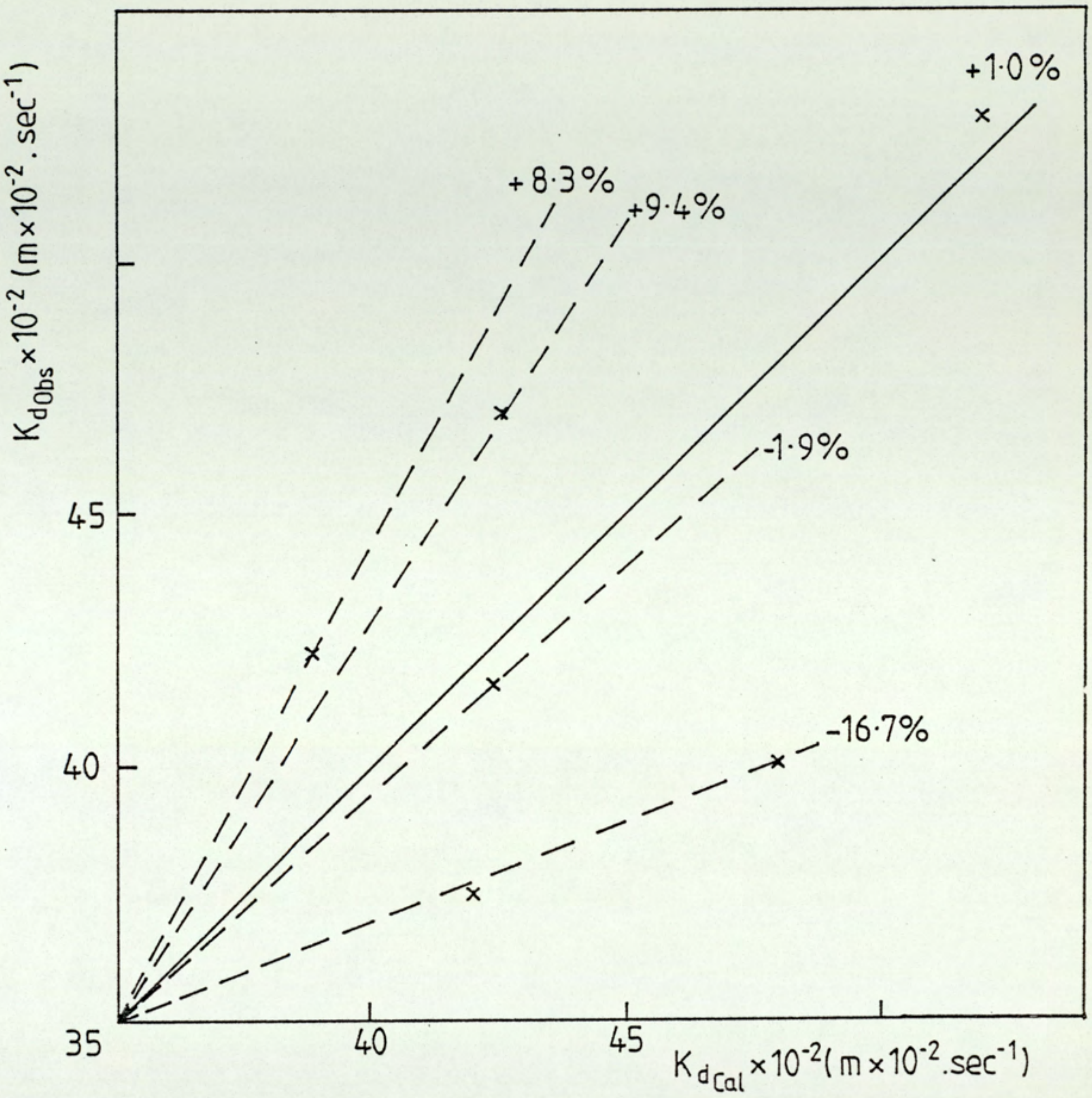

Figure 8 · 7 Observed and Calculated $K_{d's}$ of Drop Pairs according to modified correlation equation (7·19) in understanding practical columns. In other words the extent of the hydrodynamic behaviour of the drop can be studied.

When mechanical agitation is applied smaller drops oscillate (2, 3) because Re > 200 when local $V > V_s$ in most practical columns. Therefore it is of interest to know the mutual effects between adjacent drops on their hydrodynamic behaviour and on the behaviour of the continuous phase between them.

However the difficulty accompanying the derivation of a mathematical correlation for a system with a swarm of oscillating drops will make it extremely complicated to apply single large oscillating drop models.

CHAPTER 9

CONCLUSIONS AND RECOMMENDATIONS FOR FURTHER WORK

Mass transfer rate and mass transfer coefficients were studied for large oscillating single drops, or drop pairs, under steady-state conditions in a spray column with countercurrent flow. Toluene was the dispersed phase and water was the continuous phase. These phases were mutually-saturated and acetone, initially present in the toluene up to 25% w/w, constituted the solute.

A technique was developed to sample the dispersed phase from different positions in the column. Ultra-violet spectrophotometry was used to analyse the acetone in both phases. This technique ensured more accurate results than the sampling techniques used previously. The oscillatory, and associated mass transfer, behaviour of drop pairs were found to differ significantly from those of single drops, depending on whether drops in a pair travelled in parallel, collided or coalesced.

9.1. CONCLUSIONS

The following major conclusions arise from this work.

1. The range of shapes of large oscillating single drops (ie. d > 6mm) and drop pairs are far from definite geometrical shapes. The mode of oscillation may take the value of 2, 3 or may be 4 depending upon the difference in physical properties of the system used, and is not restricted to the geometries previously described in the literature eg. spheroids, oblate, prolate and spherical cap.

2. The amplitude and frequency of oscillation of droplet pairs were always less than those for corresponding single droplets (Tables 7.2 and 7.7) by approximately 2 and 1.5 times respectively. The amplitude of oscillation of single drops and drop pairs decreased with decrease in drop diameter or increase in solute concentration (Table 7.2).

The frequency of oscillation of both single drops and drop pairs increased with decrease in drop diameter, as described in Appendices D.2C, D.2G and D.5.

3. The frequency of oscillation of drop pairs could be correlated with the Weber number of the continuous phase, (equation 7.16).

$$\omega^2 = 2.8\,(\mathrm{We})^{0.40}\,Q \tag{7.16}$$

The effect of Weber number increased with increase in the quantity of solute diffused from the drop, as a result of increase in the frequency of oscillation due to the decrease in interfacial tension which always accompanied increase in solute diffusion.

4. The correlation proposed for frequency of oscillation for droplet pairs (Equation 7.16) gave improved accuracy compared with that presented by Lamb (28) and modified by Schroeder and Kintner (30) for single drops (Equation 2.9). The former gave a 19% absolute deviation from the experimental values compared with 68% for the latter.

5. Since the dispersed phase overall mass transfer coefficient increased with collision and rebound of large oscillating droplet pairs, it was concluded that there was increased intensity of turbulent mixing inside both drops resulting from an increase in the frequency of oscillation. As well as decreasing the interfacial area, collision followed by coalescence resulted in a decrease in the frequency of oscillation. These factors affected mass transfer rates - Appendix D.2C - in a similar way to mass transfer coefficients.

6. All the previous models and correlations for mass transfer coefficient during droplet formation from nozzles predicted values lower than those determined experimentally. This was due to:

   a. The different behaviour of the interface between drops of d > 6.0mm (ie. the different shapes, the effect of distortion and Marangoni effects) and the continuous phase, especially in the case of drop pairs, as discussed in Section 3.3.

   b. These models take no account of interfacial area generation with time during formation.

c. The accuracy of measuring the rate of mass transfer and droplet diameter during formation was not precise in previous studies.

The proposed correlation:

$$N_A = K \left[\int_0^t (C + a_1 x + a_2 x^2)\, dt \right] \Delta C \qquad (7.9)$$

predicted the overall mass transfer coefficient during formation with a deviation of 5% from the observed values, Figure 7.11.

The mass transfer coefficient for a single drop correlated with an average between circulatory and surface-stretch behaviour, but this was not applicable to drop pairs because of the Bernouli effect.

7. No correlations have previously been published for mass transfer coefficients of large oscillating droplet pairs during ascent. The proposed correlation:

$$K_{dcorr.} = 1.32\, (We)^{0.177}\ (Re)^{0.190}\ (\omega_{corr} D_d)^{0.5} \qquad (7.19)$$

depends upon the hydrodynamic conditions of the continuous phase between the parallel drops, Weber number and Reynolds number of the continuous phase. Equation 7.19 gave a 9% absolute deviation from the experimental results, Figure 8.7.

It is believed that application of these findings can be extended to cases in which numerous oscillating drops are present in practical extraction columns eg. agitated or packed columns to explain the enhanced mass transfer performance in swarms.

Minor conclusions arising from this work are,

8. Improved contrast for photography can be achieved with liquid-liquid systems of the type studied here by using an iodine dye. In the range of concentration used (20 to 30 ppm) this had no effect on the physical properties of the specific system .

9. With the system investigated, at solute concentrations >20% w/w the continuous phase began to creep down inside the glass nozzles used for drop formation, because at such high concentration of solute the interfacial tension of the system decreased from 26.0 to 11.0 dyne/cm. This reduced the droplet size and also changed the shape during formation allowing the continuous phase to creep inside the glass

nozzle. This was overcome by the use of p.t.f.e. nozzles which were preferentially wetted by the organic solvent alone.

10. Provision of a mirror inside the column to enable the third dimensions of individual drops to be measured, improved the accuracy of the area and volume measurements of the drops.

9.2. RECOMMENDATIONS FOR FURTHER WORK

1. This study could be extended to a liquid-liquid system of low interfacial tension eg. MIBK (Methyl-iso butyl ketone) - water system for which $\sigma < 10.0$ dyne/cm, or any glycol and water systems for which $\sigma < 5.0$ dyne/cm. Comparison of the results following interaction between drops of these systems with those given earlier would provide a general correlation for liquid-liquid systems of different physical properties.

2. In view of the known effect of surfactants, it would be interesting to repeat some of the present experimentation with traces of Teepol or Decon-90, to study the effect on drop hydrodynamics and upon mass transfer rates. This could be studied with surfactant concentrations from eg. 10 ppm upwards.

3. Accurate detection of the amplitude of oscillation could be obtained by inserting a number of capacitor plates (eg. a platinum plate with 1.0cm^2 area). The difference in capacity (C) from the equation:

$$C = \frac{k\,\varepsilon_0 A}{d} \tag{9.1}$$

would indicate the difference in droplet volume, which is as a function of the amplitude of oscillation. It could be assumed that such a capacitor plates would not disturb the flow pattern in the column. A full description of this technique is given in Appendix F.

4. Consideration could be given to reconstruction of the apparatus to facilitate photography by replacing the left side of the water jacket by glass. The intensity of the light reflected from the column would then be even.

5. It would be of practical interest to test the correlation for mass transfer coefficient of a large oscillating drop in the presence of an adjacent drop, equation 7.19, in a situation involving an increased number of adjacent drops, and ultimately a swarm. A complex nozzle arrangement would be necessary to provide equal, reproducible drop spacing geometries.

APPENDIX A

A.1 SPECIFICATION OF MATERIALS USED

A.1.1. Toluene "Analar"

ex. supplied from BDH Chemicals

wt. per ml at 20°C	0.863 - 0.866g
Refractive Index at 20°C	1.494 - 1.497

Not less than 92% distils within 0.4°C in the range 110.0-111.0°C.

Impurities	Maximum Limit Percent
Acidity	0.012
Alkalinity	0.012
Non-Volatile Matter	0.002
Benzene	0.5
Organic Impurities	Passes Acid-Wash Test
Sulphur Compounds	0.0003
Thiophen Homologues	0.0002
Water	0.03

A.1.2. Acetone "Analar"

ex. supplied from BDH Chemicals

wt. per ml at 20°C	0.789 - 0.791g
Boiling Range (95%)	56.0 - 56.5°C
Refractive Index	1.3580 - 1.3600

Impurities	Maximum Limit Percent
Water	0.2
Acidity (CH_3COOH)	0.02
Alkalinity	0.03 ml N/L
Non-Volatile Matter	0.0005
Aldehyde (HCHO)	0.002
Methanol (CH_3OH)	0.05

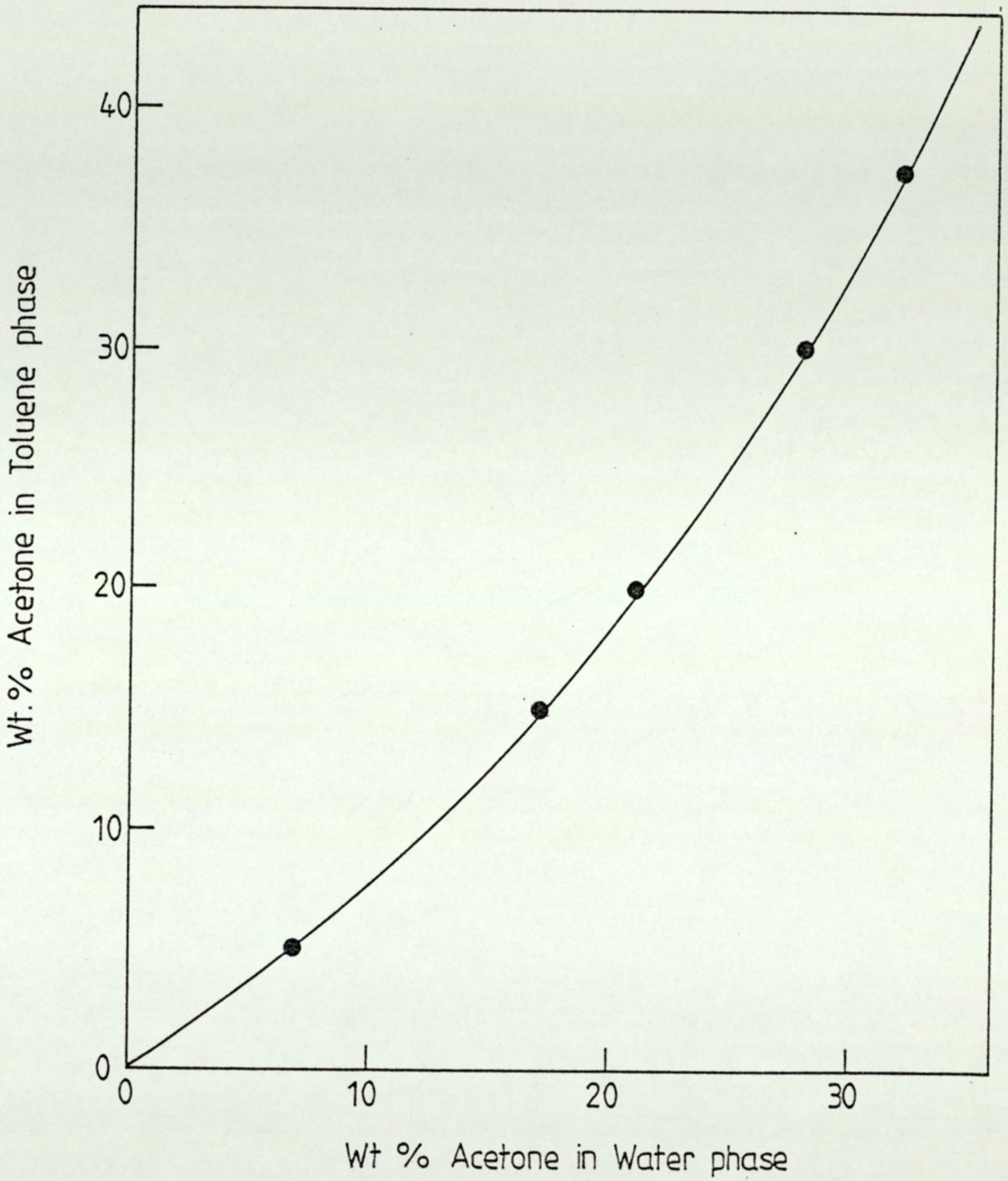

Figure A1. Distribution of Acetone between Water and Toluene at 25-26°C

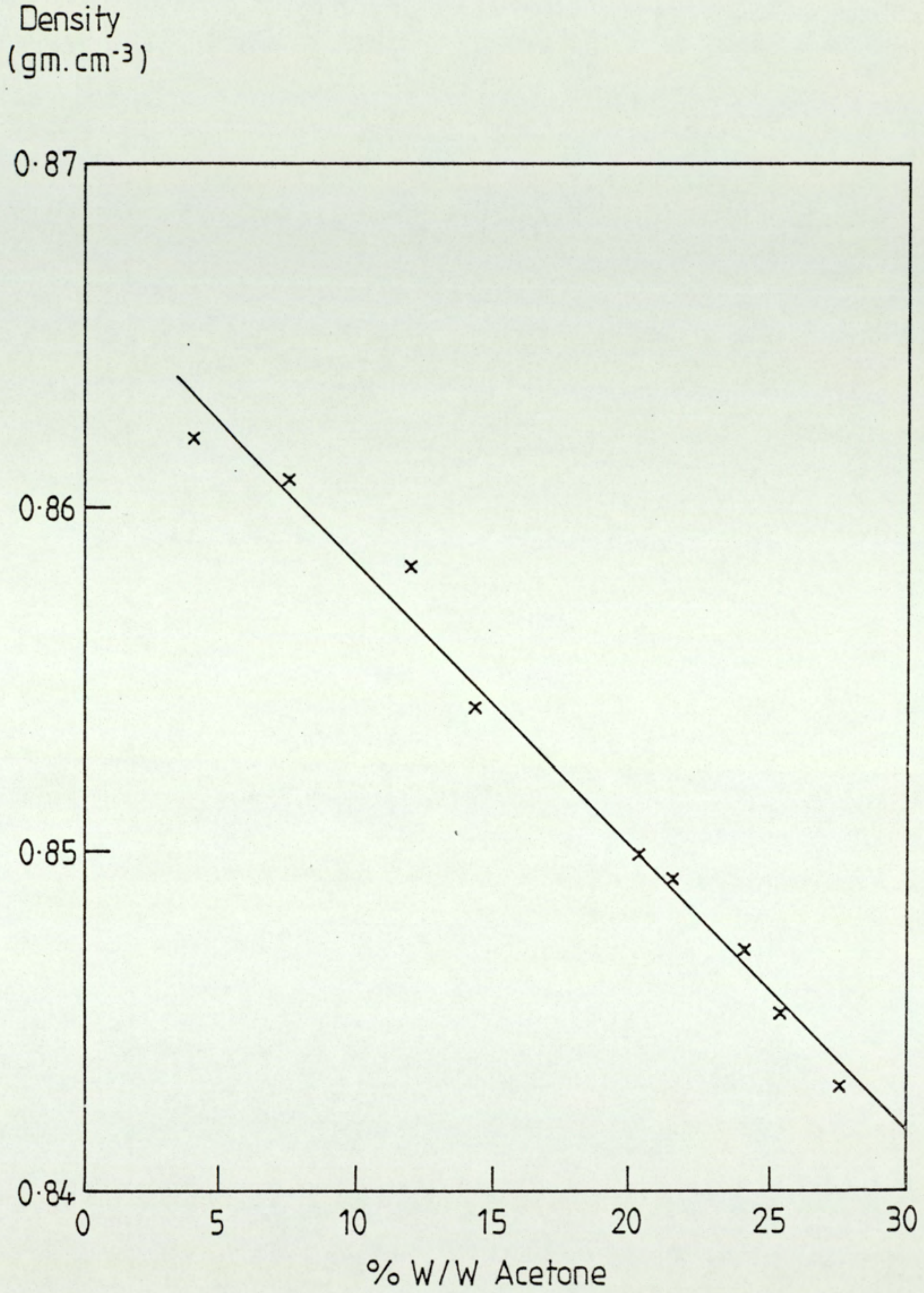

Figure A.2 Density vs. Acetone concentration in Dispersed phase

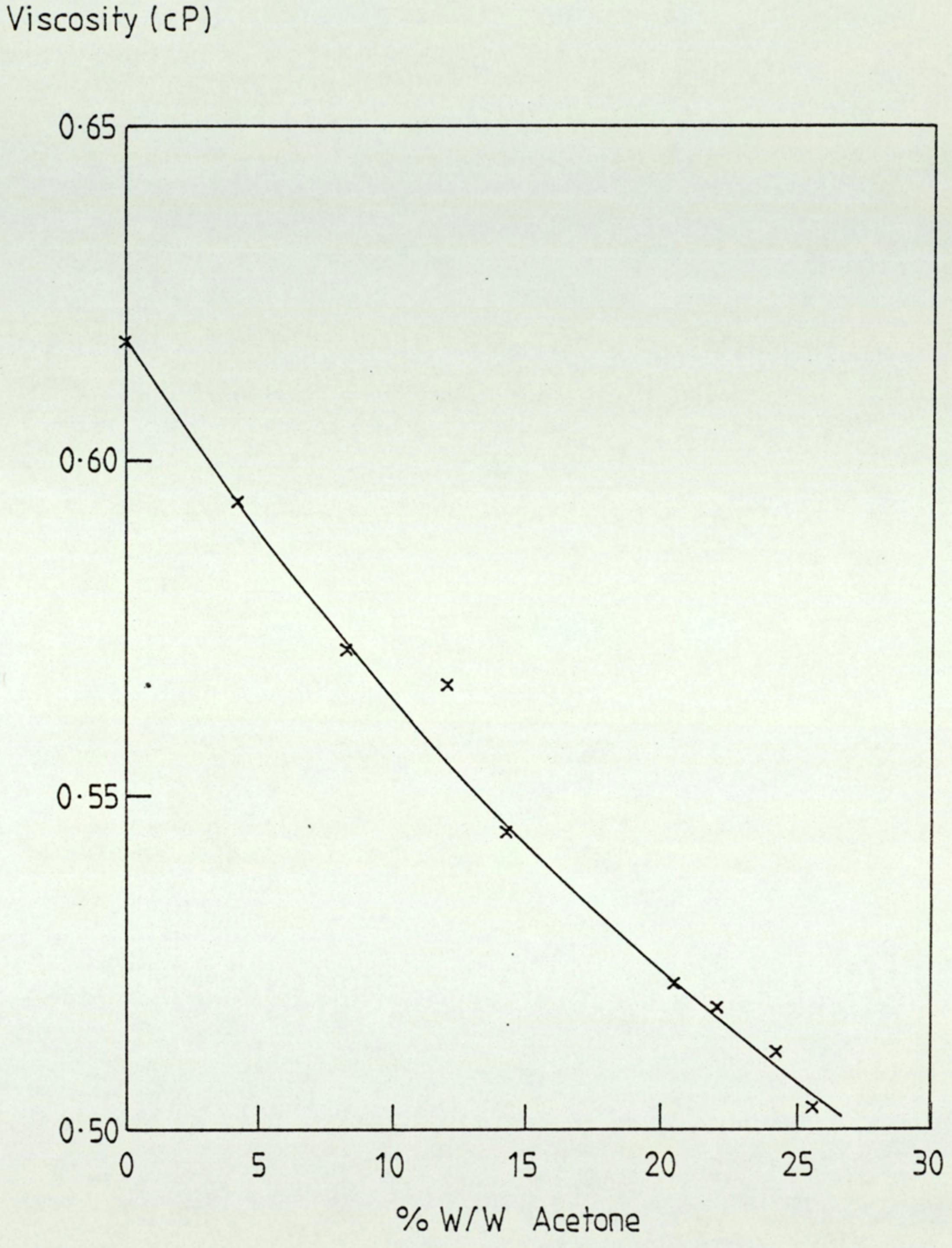

Figure A.3 Viscosity vs. Acetone concentration in Dispersed phase

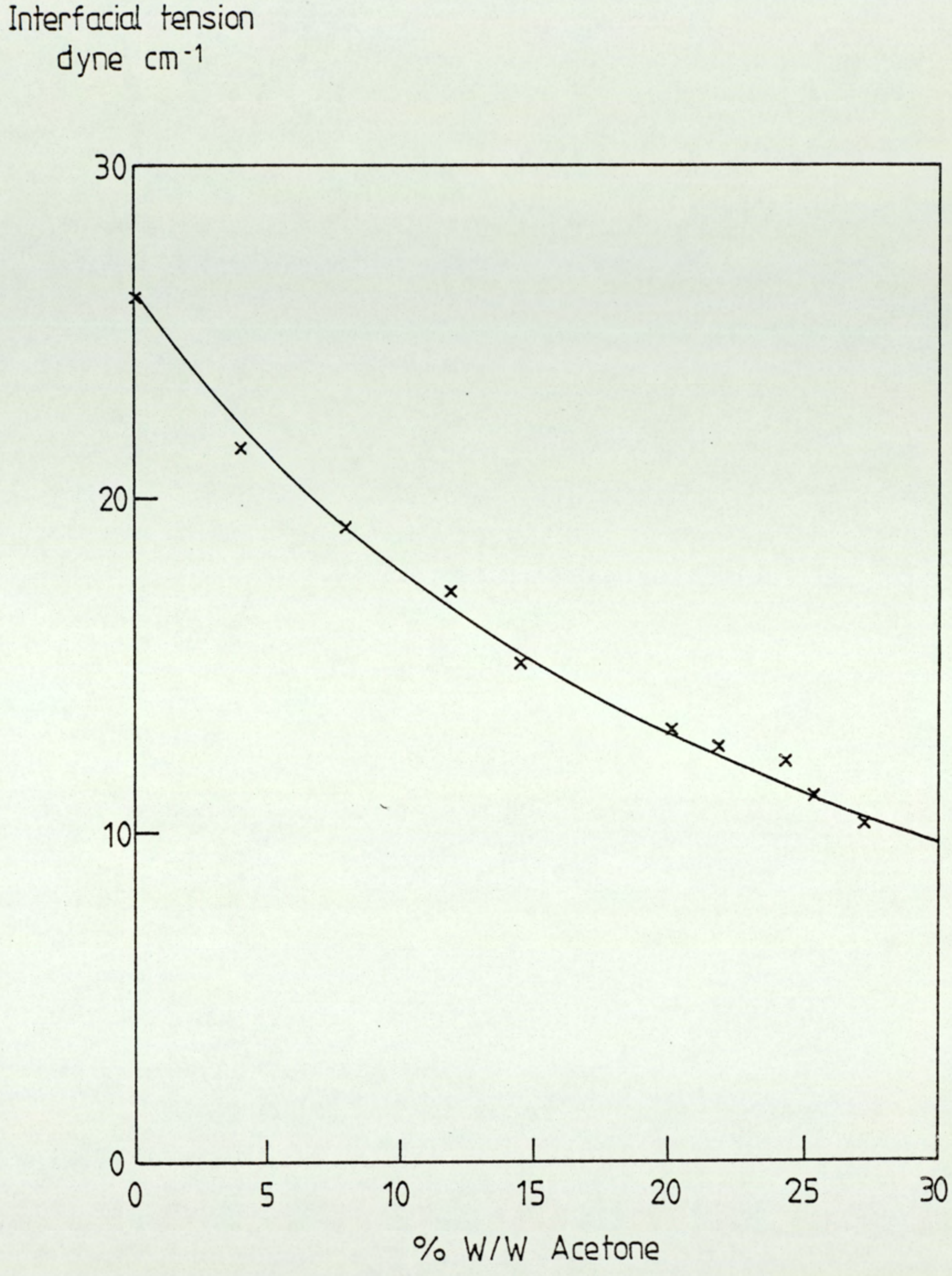

Figure A.4 Interfacial tension vs. Acetone concentration in Dispersed phase.

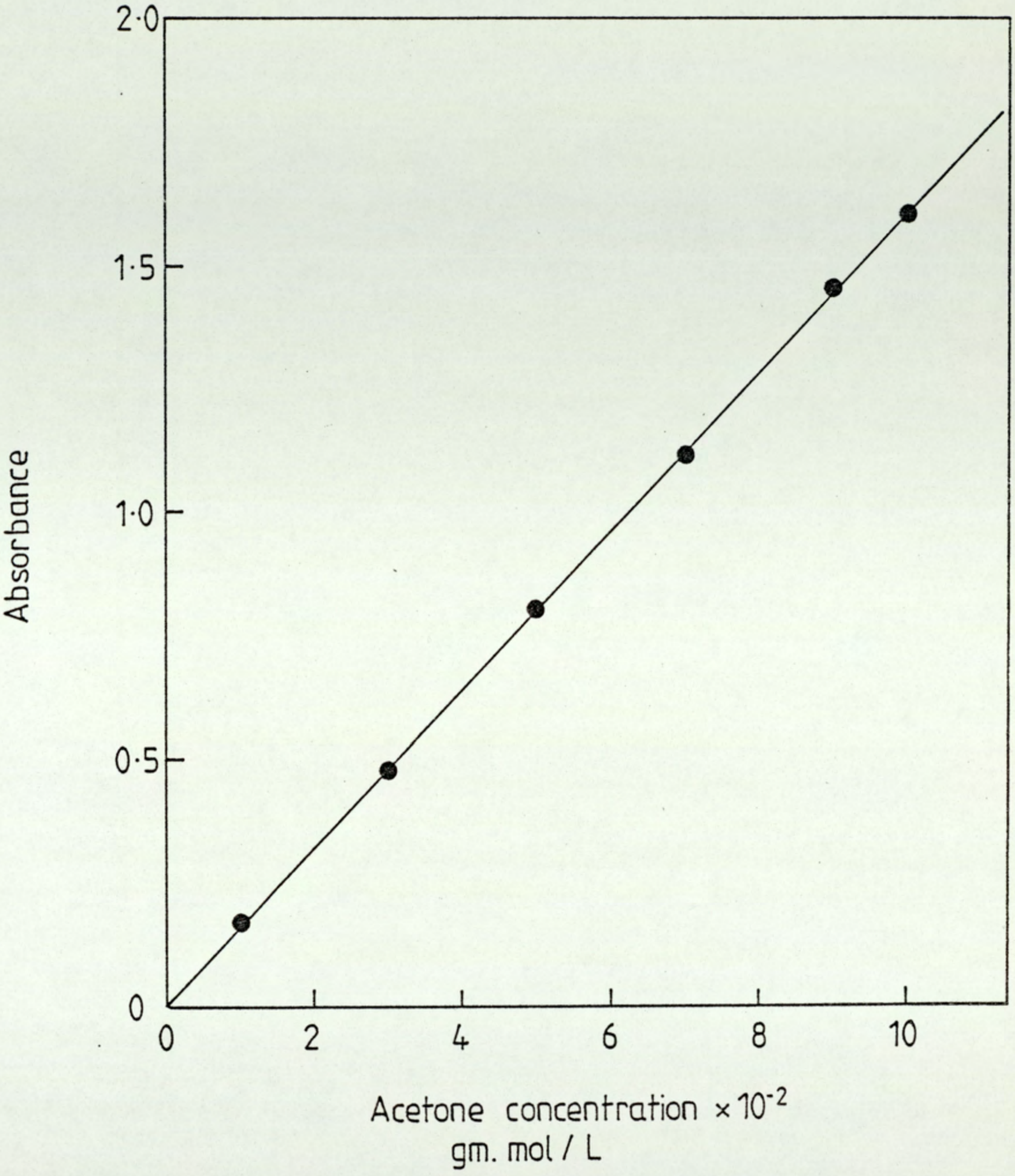

Figure A5. Ultra-violet spectrophotometry calibration chart for Toluene layer at max. λ = 286 nm with 10 mm cell.

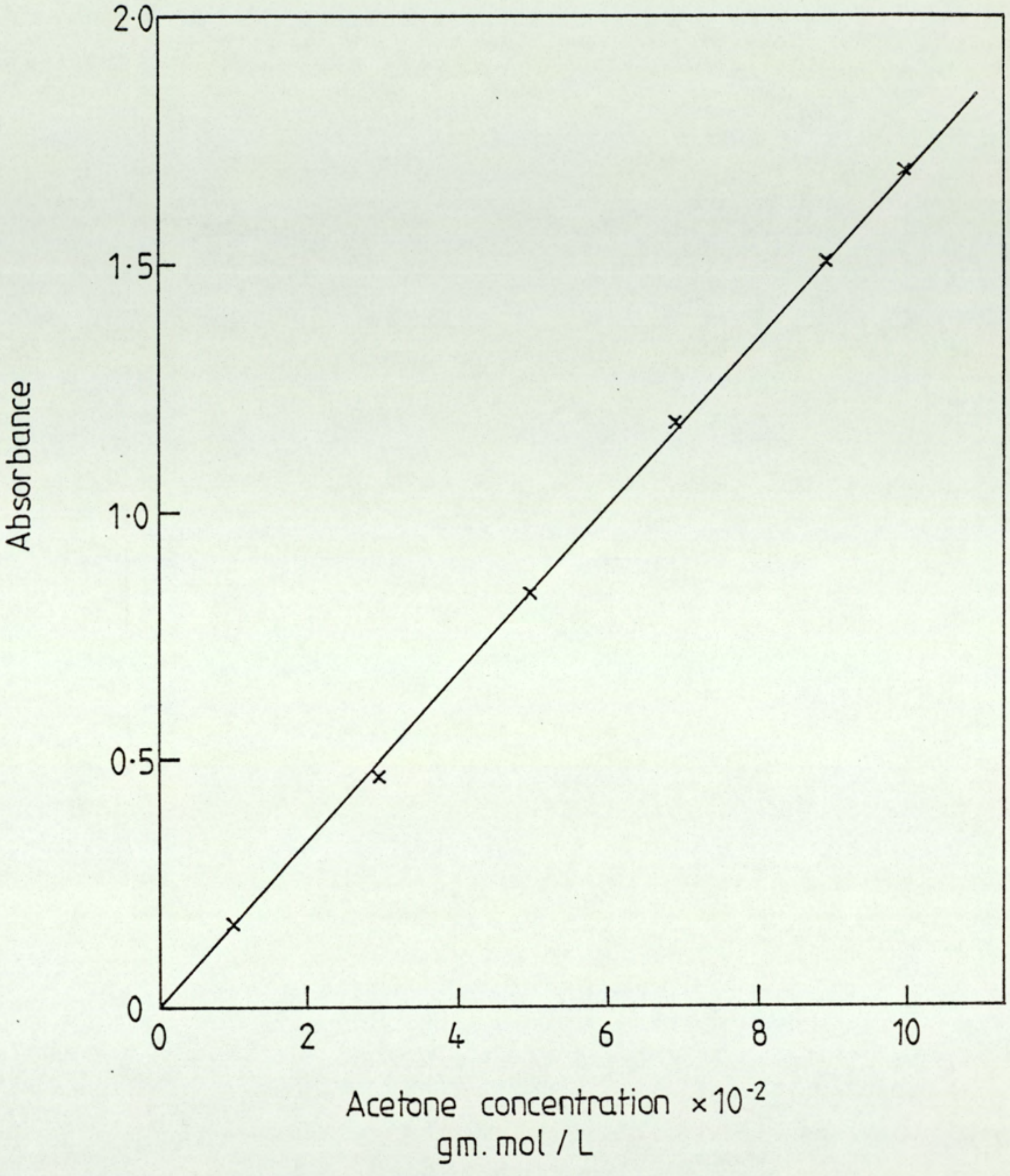

Figure A6. Ultra-violet spectrophotometry calibration curve for Water layer max. $\lambda = 276$ nm with 10 mm cell

APPENDIX B

DATA READ FROM CINE AND VIDEO FILMS FOR SINGLE DROPS AND DROP PAIRS

APPENDIX B
****

DATA READ FROM CINE AND VIDEO FILMS
RUN (10A-13D) FOR SINGLE DROPS
RUN (14A-28B) FOR DROP PAIRS

APPENDIX B.3 DATA READ FROM THE CINE FILM FOR RUN 10C RATE 64 FRAME/SEC.M.F.=(10/27):

FRAME NO.	DISTANCE (CM.)	X	Y	Z
0.00	0.00	1.70	2.60	1.60
4.00	0.25	2.50	1.80	2.60
9.00	0.41	2.70	1.40	2.70
13.00	1.15	2.40	1.80	2.50
18.00	2.56	2.20	1.70	2.10
21.00	5.36	2.15	1.70	2.10
26.00	7.81	2.50	1.70	2.60
38.00	9.98	2.60	1.70	2.60
50.00	11.25	2.70	1.50	2.60
61.00	15.01	2.20	1.50	2.60
75.00	16.26	2.30	1.60	2.20
81.00	18.29	2.45	1.75	2.45
98.00	21.61	2.60	1.80	2.50
110.00	22.23	2.50	1.70	2.60
140.00	25.61	2.40	1.80	2.50
165.00	25.61	2.30	1.90	2.30
182.00	32.25	2.75	1.85	2.65
191.00	38.29	2.80	1.70	3.10
205.00	40.05	2.90	1.80	3.00
221.00	42.11	2.80	1.70	3.10
238.00	44.45	2.50	1.80	2.40
255.00	46.78	2.65	1.75	2.85
260.00	49.01	2.40	1.90	2.50
271.00	52.09	2.30	1.70	2.40
281.00	56.18	2.50	1.80	2.50
290.00	57.61	2.35	1.75	2.30
299.00	57.61	2.35	1.75	2.30
315.00	60.09	2.30	1.80	2.20
321.00	62.31	2.20	1.60	2.10
340.00	64.71	2.15	1.55	2.05
348.00	65.01	2.20	1.40	2.10
360.00	65.81	2.00	1.50	1.90
363.00	66.01	2.40	1.60	2.50
371.00	66.19	2.50	1.70	2.60
380.00	66.82	2.30	1.60	2.30
391.00	67.82	2.25	1.55	2.15
398.00	68.11	2.10	1.60	2.00
414.00	68.82	2.00	1.50	2.20
425.00	69.13	2.20	1.60	2.10
431.00	69.82	2.10	1.45	2.05

APPENDIX B.8 DATA READ FROM THE CINE FILM FOR RUN 11C RATE 64 FRAME/SEC.M.F.=(10/29):

FRAME NO.	DISTANCE (CM.)	X	Y	Z
0.00	0.00	1.90	2.60	1.80
1.00	0.15	2.30	1.80	2.20
4.00	0.37	2.40	1.60	2.30
6.00	0.43	2.30	1.70	2.20
10.00	0.98	2.50	1.60	2.40
13.00	1.67	2.10	1.80	2.00
17.00	2.56	2.20	1.70	2.20
20.00	3.61	2.00	1.85	2.00
25.00	4.71	2.60	1.60	2.50
35.00	5.59	2.40	1.70	2.30
40.00	6.91	2.50	1.50	2.50
50.00	7.05	2.20	1.80	2.10
60.00	8.28	2.30	1.70	2.30
73.00	9.98	2.60	1.40	2.50
89.00	12.52	2.50	1.50	2.50
100.00	15.31	2.55	1.60	2.50
120.00	20.21	2.10	1.80	2.10
130.00	25.61	2.20	1.70	2.10
140.00	27.47	2.00	1.80	2.00
150.00	29.21	2.50	1.60	2.50
160.00	31.51	2.40	1.70	2.30
170.00	33.67	2.50	1.40	2.40
180.00	38.29	2.10	1.70	2.00
190.00	40.10	2.20	1.60	2.10
200.00	40.85	2.00	1.80	2.00
215.00	41.63	2.60	1.40	2.50
225.00	42.21	2.50	1.60	2.40
235.00	45.60	2.20	1.70	2.20
245.00	48.21	2.30	1.60	2.20
255.00	49.31	2.10	1.80	2.00
265.00	52.67	2.50	1.60	2.40
270.00	54.18	2.40	1.70	2.30
275.00	56.11	2.00	1.80	2.00
285.00	57.92	2.10	1.55	2.00
299.00	58.31	2.00	1.60	2.00
310.00	58.88	2.30	1.50	2.20
325.00	59.65	2.10	1.60	2.00
335.00	60.29	2.50	1.40	2.50
345.00	61.28	2.00	1.60	2.00
355.00	63.01	2.10	1.50	2.10
365.00	64.28	2.00	1.65	2.10
375.00	65.41	2.40	1.50	2.30
385.00	66.71	2.10	1.55	2.10
399.00	67.31	2.20	1.60	2.00
410.00	68.61	2.00	1.50	2.00
425.00	69.01	2.40	1.55	2.30
435.00	69.38	2.05	1.60	2.00

APPENDIX B.13 DATA READ FROM THE CINE FILM FOR RUN 12C RATE 64 FRAME/SEC.M.F.=(10/32):

FRAME NO.	DISTANCE (CM.)	X	Y	Z
0.00	0.00	1.80	2.40	1.80
1.00	0.13	2.40	1.70	2.40
3.00	0.27	2.50	1.60	2.40
7.00	0.81	2.40	1.65	2.30
10.00	0.98	2.60	1.50	2.50
15.00	1.63	2.40	1.60	2.40
20.00	3.32	2.50	1.70	2.50
26.00	4.17	2.20	1.90	2.10
31.00	5.01	2.60	1.50	2.50
40.00	5.89	2.40	1.70	2.30
51.00	6.71	2.50	1.60	2.40
60.00	7.72	2.10	1.80	2.00
70.00	8.35	2.50	1.60	2.40
80.00	9.21	2.30	1.60	2.30
90.00	10.00	2.40	1.55	2.30
105.00	11.62	2.20	1.70	2.20
125.00	16.26	2.30	1.65	2.30
135.00	19.61	2.00	1.80	2.00
145.00	20.11	2.40	1.50	2.30
160.00	25.68	2.30	1.60	2.20
170.00	28.69	2.10	1.70	2.00
180.00	30.26	2.40	1.50	2.30
199.00	32.21	2.30	1.60	2.20
210.00	34.01	2.35	1.55	2.30
225.00	36.21	2.00	1.70	2.00
235.00	38.55	2.40	1.50	2.30
240.00	40.21	2.30	1.60	2.20
250.00	41.35	2.40	1.45	2.30
260.00	42.29	2.10	1.60	2.00
270.00	43.65	2.20	1.55	2.10
280.00	44.46	2.00	1.70	2.00
290.00	49.28	2.50	1.50	2.40
300.00	51.81	2.30	1.60	2.30
310.00	54.26	2.40	1.50	2.40
320.00	56.01	2.20	1.80	2.10
330.00	58.62	2.60	1.40	2.50
340.00	60.28	2.30	1.60	2.20
350.00	62.81	2.40	1.50	2.30
360.00	64.73	2.10	1.60	2.10
370.00	66.52	2.30	1.50	2.30
380.00	67.11	2.00	1.70	2.00
390.00	67.78	2.40	1.50	2.30
400.00	68.01	2.20	1.60	2.10
410.00	68.69	2.30	1.50	2.20
420.00	69.29	2.20	1.70	2.10
430.00	69.79	2.40	1.45	2.30
440.00	70.05	2.10	1.60	2.00

APPENDIX B.17 DATA READ FROM THE CINE FILM FOR RUN 13C RATE 64 FRAME/SEC.M.F.=(10/36):

FRAME NO.	DISTANCE (CM.)	X	Y	Z
0.00	0.00	1.70	2.20	1.70
1.00	0.15	2.30	1.50	2.30
2.00	0.20	2.20	1.60	2.20
4.00	0.37	2.30	1.50	2.30
5.00	0.45	2.10	1.60	2.00
10.00	0.91	2.40	1.40	2.30
15.00	1.36	2.20	1.50	2.10
20.00	3.29	2.30	1.45	2.20
30.00	4.29	2.30	1.50	2.30
40.00	5.76	2.40	1.40	2.30
50.00	6.21	2.00	1.60	1.90
60.00	7.35	2.20	1.40	2.10
70.00	8.03	2.15	1.45	2.10
80.00	9.11	2.25	1.50	2.20
90.00	10.00	2.20	1.60	2.10
100.00	10.78	2.40	1.40	2.30
110.00	11.21	2.30	1.50	2.20
120.00	15.13	2.20	1.60	2.10
130.00	17.28	2.50	1.40	2.40
140.00	19.89	2.40	1.50	2.40
150.00	24.76	2.10	1.60	2.00
160.00	25.25	2.20	1.70	2.10
170.00	27.91	2.00	1.70	2.00
180.00	29.83	2.50	1.40	2.40
190.00	31.59	2.30	1.50	2.20
200.00	32.11	2.40	1.45	2.30
210.00	33.91	2.20	1.60	2.10
220.00	34.85	2.30	1.55	2.20
230.00	37.64	2.30	1.60	2.20
240.00	39.11	2.40	1.50	2.30
250.00	40.28	2.15	1.65	2.10
260.00	41.16	2.10	1.70	2.00
270.00	42.93	2.40	1.45	2.30
280.00	44.05	2.00	1.60	2.00
290.00	47.91	2.20	1.50	2.00
300.00	50.29	2.10	1.55	2.10
310.00	53.85	2.40	1.40	2.30
320.00	55.96	2.30	1.50	2.20
330.00	58.01	2.35	1.45	2.30
340.00	60.15	2.20	1.60	2.20
350.00	62.11	2.30	1.50	2.30
360.00	64.35	2.50	1.30	2.40
370.00	66.05	2.40	1.40	2.30
380.00	67.19	2.45	1.45	2.40
390.00	67.78	2.30	1.50	2.20
400.00	68.21	2.00	1.60	1.90
410.00	68.79	2.20	1.50	2.10
420.00	69.21	2.10	1.55	2.00

430.00	69.83	2.30	1.40	2.20
445.00	70.00	2.10	1.50	2.00

APPENDIX B.20 DATA READ FROM CINE/VIDEO FILM FOR RUN 14E RATE 25 FRAME/SEC.M.F.=(10/32):

FRAME NO.	DISTANCE (CM.)	X1	Y1	Z1	X2	Y2	Z2
0	0.00	2.10	2.80	2.00	1.90	2.60	1.90
1	0.26	2.60	1.70	2.50	2.40	1.70	2.30
2	0.51	2.50	1.60	2.40	2.70	1.50	2.60
3	0.80	2.60	1.50	2.50	2.40	1.80	2.30
4	1.01	2.30	1.70	2.20	2.80	1.40	2.70
5	1.50	2.70	1.40	2.60	2.30	1.80	2.20
7	2.16	2.60	1.50	2.50	2.40	1.70	2.30
10	3.05	2.80	1.30	2.70	2.20	1.90	2.10
12	4.15	2.70	1.40	2.60	2.30	1.70	2.20
15	5.00	2.80	1.30	2.70	2.10	1.90	2.00
18	5.88	2.30	1.70	2.20	2.70	1.50	2.60
20	7.19	2.50	1.60	2.40	2.40	1.60	2.30
23	8.12	2.40	1.70	2.30	2.60	1.50	2.50
27	9.55	2.60	1.50	2.50	2.50	1.60	2.40
30	10.10	2.20	1.80	2.10	2.80	1.30	2.70
35	11.88	2.30	1.70	2.20	2.70	1.40	2.60
38	12.98	2.10	1.80	2.00	2.80	1.20	2.70
40	14.86	2.40	1.60	2.30	2.60	1.50	2.50
41	15.91	2.30	1.70	2.20	2.70	1.30	2.60
42	17.05	2.60	1.50	2.50	2.40	1.60	2.40
45	18.88	2.50	1.60	2.40	2.60	1.50	2.50
47	20.06	2.70	1.40	2.60	2.30	1.70	2.20
50	21.11	2.60	1.50	2.50	2.40	1.60	2.30
51	22.31	2.40	1.60	2.30	2.60	1.50	2.50
53	23.77	2.50	1.50	2.40	2.50	1.60	2.40
55	25.16	2.20	1.80	2.10	2.80	1.20	2.70
58	26.03	2.30	1.70	2.20	2.70	1.30	2.60
62	26.78	2.10	1.90	2.00	2.80	1.20	2.80
70	30.61	2.40	1.60	2.30	2.60	1.50	2.50
75	32.16	2.30	1.70	2.20	2.70	1.40	2.60
80	34.71	2.70	1.40	2.60	2.30	1.70	2.20
83	36.81	2.50	1.60	2.40	2.60	1.50	2.50
87	38.79	2.60	1.50	2.50	2.40	1.60	2.30
90	41.21	2.20	1.80	2.10	2.70	1.40	2.60
93	43.61	2.30	1.70	2.20	2.60	1.50	2.50
97	46.11	2.40	1.60	2.30	2.70	1.30	2.60
103	48.19	2.50	1.70	2.40	2.60	1.40	2.50
110	49.13	2.10	1.90	2.00	2.80	1.20	2.70
115	50.11	2.40	1.60	2.30	2.60	1.60	2.50
118	51.80	2.30	1.70	2.20	2.70	1.40	2.60
121	52.01	2.60	1.40	2.50	2.30	1.60	2.20
127	53.36	2.40	1.50	2.30	2.60	1.50	2.50
131	53.89	2.50	1.40	2.40	2.40	1.60	2.30
140	54.81	2.40	1.60	2.30	2.70	1.30	2.60

143	55.66	2.60	1.50	2.50	2.50	1.60	2.40
148	56.29	2.30	1.70	2.20	2.60	1.50	2.60
151	58.19	2.50	1.50	2.40	2.50	1.60	2.40
153	59.39	2.40	1.60	2.30	2.60	1.40	2.50
157	60.06	2.60	1.40	2.50	2.30	1.60	2.20
159	60.71	2.20	1.70	2.10	2.70	1.50	2.60
161	62.11	2.30	1.60	2.20	2.60	1.60	2.50
162	64.01	2.10	1.70	2.00	2.80	1.20	2.70
164	65.71	2.20	1.60	2.10	2.70	1.30	2.60
165	66.12	2.00	1.70	2.00	2.80	1.20	2.70
167	66.78	2.50	1.50	2.40	2.40	1.50	2.30
170	67.31	2.30	1.60	2.20	2.60	1.40	2.50
172	67.98	2.40	1.50	2.30	2.50	1.50	2.40
174	68.18	2.30	1.60	2.20	2.60	1.40	2.50
175	69.23	2.50	1.50	2.40	2.40	1.60	2.30

APPENDIX B.24 DATA READ FROM CINE/VIDEO FILM FOR RUN 15B RATE 25 FRAME/SEC.M.F.=(10/32):

FRAME NO.	DISTANCE (CM.)	X1	Y1	Z1	X2	Y2	Z2
0	0.00	1.80	2.30	1.80	2.00	2.30	2.00
1	0.21	2.70	1.40	2.60	2.60	1.50	2.50
2	0.41	2.70	1.30	2.60	2.40	1.60	2.30
3	0.76	2.60	1.60	2.50	2.70	1.30	2.60
5	1.20	2.80	1.30	2.80	2.20	1.90	2.10
7	1.98	2.70	1.40	2.60	2.30	1.80	2.20
10	2.78	3.00	1.10	2.90	2.10	1.90	2.00
15	4.77	2.80	1.30	2.70	2.20	1.80	2.10
20	7.11	2.90	1.20	2.80	2.00	1.90	2.00
23	8.55	2.20	1.80	2.10	2.80	1.30	2.70
25	9.00	2.30	1.70	2.20	2.70	1.40	2.60
27	10.79	2.20	1.80	2.10	2.80	1.30	2.70
30	11.36	2.00	1.90	2.00	3.00	1.10	2.90
35	12.05	3.00	1.20	2.90	2.10	1.90	2.00
40	14.76	2.80	1.20	2.70	2.20	1.90	2.10
42	16.88	2.90	1.10	2.80	2.00	1.90	1.90
45	17.69	2.70	1.30	2.60	2.60	1.50	2.50
47	20.11	2.80	1.30	2.80	2.20	1.80	2.10
50	21.96	2.70	1.40	2.60	2.30	1.70	2.20
51	22.60	2.30	1.70	2.20	2.80	1.40	2.70
53	23.69	2.40	1.60	2.30	2.60	1.50	2.50
55	24.43	2.10	1.80	2.00	2.70	1.30	2.60
60	25.81	2.20	1.80	2.10	2.70	1.30	2.60
62	26.30	2.30	1.60	2.20	2.60	1.60	2.50
65	27.55	2.00	1.70	2.00	2.80	1.20	2.70
70	29.77	2.20	1.70	2.10	2.60	1.50	2.60
72	30.05	2.10	1.80	1.90	2.70	1.20	2.60
75	33.00	2.40	1.60	2.30	2.50	1.60	2.50
80	34.86	2.30	1.70	2.20	2.60	1.50	2.50
85	38.19	2.60	1.50	2.50	2.40	1.60	2.30
90	41.87	2.50	1.40	2.40	2.60	1.50	2.50
95	45.11	2.70	1.20	2.60	2.30	1.60	2.20

100	46.65	2.50	1.60	2.40	2.40	1.60	2.30
105	47.79	2.80	1.20	2.70	2.10	1.80	2.00
110	48.12	2.60	1.40	2.50	2.20	1.70	2.10
115	49.01	2.70	1.20	2.60	2.30	1.60	2.20
120	49.88	2.50	1.50	2.40	2.60	1.40	2.50
125	50.87	2.40	1.60	2.30	2.50	1.60	2.40
130	51.49	2.60	1.50	2.50	2.70	1.20	2.60
135	53.48	2.30	1.60	2.20	2.60	1.50	2.50
140	54.01	2.40	1.50	2.30	2.70	1.30	2.60
145	54.82	2.20	1.70	2.10	2.70	1.60	2.70
150	56.61	2.30	1.60	2.20	2.60	1.50	2.50
155	57.11	2.10	1.70	2.00	2.60	1.40	2.50
160	59.65	2.70	1.20	2.60	2.20	1.70	2.10
165	61.71	2.50	1.40	2.50	2.60	1.40	2.50
170	65.22	2.60	1.50	2.60	2.50	1.50	2.40
175	69.39	2.50	1.40	2.40	2.60	1.60	2.50

APPENDIX B.29 DATA READ FROM CINE/VIDEO FILM FOR RUN 16C RATE 25 FRAME/SEC.M.F.=(10/32):

FRAME NO.	DISTANCE (CM.)	X1	Y1	Z1	X2	Y2	Z2
0	0.00	2.00	2.40	2.00	1.90	2.50	1.95
1	0.20	2.50	1.60	2.40	2.60	1.50	2.50
2	0.41	2.55	1.55	2.50	2.50	1.60	2.50
3	0.68	2.60	1.60	2.50	2.60	1.60	2.60
5	1.21	2.50	1.65	2.50	2.40	1.70	2.30
7	2.04	2.70	1.40	2.65	2.30	1.90	2.20
10	2.78	2.70	1.45	2.60	2.35	1.95	2.30
12	3.69	2.60	1.50	2.50	2.30	1.80	2.20
15	4.71	2.65	1.55	2.60	2.75	1.60	2.70
20	6.77	2.40	1.60	2.30	2.80	1.55	2.75
25	8.61	2.30	1.70	2.20	2.70	1.60	2.65
28	9.78	2.40	1.80	2.30	2.65	1.70	2.60
30	10.01	2.45	1.60	2.40	2.70	1.60	2.65
33	10.89	2.50	1.80	2.40	2.60	1.70	2.50
35	12.49	2.70	1.50	2.60	2.30	1.80	2.20
40	15.11	2.70	1.25	2.60	2.20	1.85	2.15
45	18.88	2.80	1.30	2.70	2.10	1.80	2.00
50	21.11	2.70	1.35	2.70	2.10	1.75	2.10
55	25.01	2.80	1.30	2.35	2.40	1.70	2.30
60	26.21	2.40	1.70	2.35	2.70	1.40	2.60
65	27.97	2.50	1.70	2.40	2.60	1.50	2.55
68	29.66	2.60	1.65	2.50	2.50	1.60	2.50
70	30.11	2.60	1.50	2.60	2.55	1.55	2.60
72	32.00	2.50	1.70	2.40	2.60	1.70	2.50
75	33.31	2.45	1.80	2.40	2.60	1.60	2.55
80	35.00	2.30	1.90	2.20	2.65	1.65	2.60
85	38.79	2.40	1.80	2.30	2.50	1.50	2.50
90	42.01	2.50	1.70	2.40	2.70	1.40	2.60
95	45.56	2.60	1.80	2.50	2.60	1.50	2.50
100	47.22	2.65	1.70	2.55	2.55	1.55	2.45
105	48.01	2.60	1.60	2.60	2.60	1.50	2.60

110	49.00	2.60	1.55	2.50	2.70	1.45	2.65
115	49.12	2.60	1.70	2.50	2.30	1.70	2.25
120	51.78	2.70	1.70	2.60	2.35	1.80	2.30
125	52.78	2.75	1.55	2.70	2.20	1.90	2.20
130	53.66	2.70	1.60	2.60	2.30	1.80	2.20
135	54.76	2.30	1.80	2.30	2.80	1.40	2.70
140	55.01	2.35	1.75	2.30	2.75	1.80	2.70
145	56.68	2.40	1.70	2.40	2.60	1.40	2.50
150	57.63	2.50	1.60	2.40	2.40	1.70	2.30
155	60.11	2.70	1.50	2.60	2.30	1.80	2.20
160	62.03	2.60	1.60	2.50	2.50	1.60	2.40
165	65.78	2.40	1.60	2.40	2.70	1.40	2.65
170	70.31	2.50	1.50	2.40	2.60	1.50	2.50

APPENDIX B.45 DATA READ FROM CINE/VIDEO FILM FOR RUN 20C RATE 64 FRAME/SEC.M.F.=(10/40):

FRAME NO.	DISTANCE (CM.)	X1	Y1	Z1	X2	Y2	Z2
0	0.00	1.80	2.50	1.70	1.90	2.40	1.90
5	0.42	2.50	1.60	2.40	2.40	1.70	2.30
10	1.00	2.70	1.20	2.60	2.30	1.60	2.20
15	1.80	2.60	1.40	2.50	2.40	1.60	2.30
20	2.59	2.70	1.30	2.60	2.20	1.70	2.10
25	3.45	2.20	1.60	2.10	2.60	1.40	2.50
30	3.79	2.30	1.70	2.20	2.50	1.40	2.40
35	4.80	2.10	1.80	2.00	2.60	1.30	2.50
40	5.50	2.60	1.30	2.50	2.30	1.70	2.20
45	6.45	2.40	1.60	2.30	2.60	1.40	2.50
50	6.85	2.50	1.50	2.40	2.30	1.60	2.20
55	7.30	2.30	1.60	2.20	2.60	1.40	2.50
60	8.25	2.40	1.50	2.40	2.50	1.50	2.40
65	9.05	2.10	1.80	2.00	2.60	1.30	2.60
70	9.50	2.20	1.70	2.20	2.40	1.70	2.30
75	11.00	2.00	1.90	1.90	2.70	1.10	2.60
80	12.55	2.30	1.70	2.20	2.50	1.40	2.40
85	13.20	2.10	1.80	2.00	2.60	1.50	2.50
90	14.04	2.70	1.10	2.60	2.10	1.80	2.00
95	14.78	2.50	1.40	2.50	2.30	1.60	2.20
100	16.00	2.60	1.30	2.50	2.20	1.80	2.10
105	17.10	2.40	1.50	2.30	2.50	1.60	2.40
110	18.00	2.50	1.40	2.40	2.30	1.70	2.20
115	18.70	2.30	1.60	2.20	2.60	1.40	2.50
120	19.95	2.40	1.50	2.30	2.50	1.50	2.40
130	21.56	2.20	1.80	2.10	2.70	1.20	2.60
140	23.85	2.30	1.60	2.30	2.60	1.50	2.50
150	25.20	2.00	1.80	2.00	2.70	1.30	2.60
160	27.60	2.60	1.40	2.50	2.50	1.40	2.40
170	28.05	2.40	1.50	2.40	2.60	1.30	2.50
180	30.70	2.70	1.10	2.60	2.30	1.60	2.20
190	31.59	2.50	1.50	2.50	2.40	1.70	2.30
200	23.20	2.60	1.40	2.50	2.20	1.80	2.10
210	35.15	2.30	1.60	2.30	2.60	1.40	2.50

230	38.10	2.50	1.40	2.40	2.40	1.50	2.30
240	40.25	2.40	1.50	2.30	2.50	1.60	2.40
250	41.65	2.60	1.30	2.50	2.30	1.70	2.20
260	42.05	2.30	1.60	2.30	2.60	1.50	2.50
270	43.96	2.50	1.40	2.40	2.40	1.60	2.30
280	44.89	2.20	1.70	2.10	2.70	1.10	2.60
290	47.87	2.40	1.60	2.30	2.50	1.40	2.40
300	50.00	2.30	1.70	2.20	2.60	1.50	2.50
310	52.90	2.70	1.10	2.60	2.10	1.80	2.00
320	55.02	2.50	1.40	2.40	2.40	1.60	2.30
340	57.55	2.60	1.30	2.50	2.30	1.60	2.20
350	57.88	2.20	1.70	2.10	2.60	1.40	2.50
360	58.68	2.30	1.60	2.20	2.50	1.60	2.40
370	61.20	2.00	1.80	2.00	2.70	1.10	2.60
380	63.00	2.30	1.60	2.20	2.60	1.40	2.50
390	64.96	2.20	1.80	2.10	2.70	1.20	2.60
400	66.00	2.50	1.60	2.40	2.40	1.50	2.30
410	68.68	2.40	1.60	2.30	2.60	1.30	2.50
420	69.86	2.60	1.40	2.30	2.30	1.60	2.20
430	71.96	2.30	1.60	2.20	2.50	1.50	2.50

APPENDIX B.60 DATA READ FROM CINE/VIDEO FILM FOR RUN 24B RATE 64 FRAME/SEC.M.F.=(10/34):

FRAME NO.	DISTANCE (CM.)	X1	Y1	Z1	X2	Y2	Z2
0	0.00	1.80	2.60	1.80	1.90	2.50	1.80
5	0.40	2.50	1.60	2.40	2.40	1.60	2.40
10	0.91	2.70	1.20	2.60	2.20	1.80	2.10
15	1.39	2.60	1.40	2.50	2.50	1.40	2.40
20	2.05	2.70	1.30	2.60	2.30	1.70	2.20
25	2.92	2.50	1.50	2.40	2.60	1.40	2.50
30	3.78	2.60	1.40	2.50	2.40	1.60	2.30
35	4.69	2.20	1.70	2.10	2.70	1.20	2.60
40	5.25	2.30	1.60	2.30	2.60	1.40	2.50
45	6.11	2.00	1.90	1.90	2.80	1.10	2.70
50	7.05	2.50	1.40	2.40	2.60	1.50	2.50
60	8.69	2.40	1.60	2.30	2.70	1.10	2.60
70	10.49	2.60	1.40	2.50	2.40	1.60	2.30
80	11.98	2.50	1.50	2.40	2.60	1.40	2.50
90	13.68	2.70	1.20	2.60	2.20	1.70	2.10
100	14.88	2.50	1.40	2.50	2.40	1.60	2.30
110	16.49	2.60	1.50	2.50	2.30	1.70	2.20
120	17.87	2.30	1.60	2.20	2.60	1.40	2.50
130	19.48	2.40	1.50	2.30	2.50	1.60	2.40
140	21.08	2.10	1.80	2.00	2.70	1.30	2.60
150	22.76	2.20	1.70	2.10	2.60	1.60	2.50
160	24.55	2.00	1.90	1.90	2.80	1.10	2.70
170	26.00	2.70	1.20	2.60	2.10	1.80	2.00
180	26.85	2.50	1.50	2.40	2.60	1.40	2.50
190	28.80	2.60	1.40	2.50	2.40	1.60	2.30
200	30.12	2.10	1.70	2.00	2.70	1.20	2.60
210	31.56	2.30	1.60	2.20	2.50	1.60	2.50

220	33.00	2.00	1.90	1.90	2.70	1.20	2.60
230	34.86	2.40	1.60	2.30	2.50	1.50	2.40
240	36.11	2.20	1.70	2.10	2.70	1.10	2.60
250	37.40	2.70	1.10	2.60	2.20	1.70	2.10
260	39.12	2.50	1.60	2.40	2.60	1.40	2.50
270	41.05	2.60	1.40	2.50	2.30	1.70	2.30
280	42.00	2.30	1.70	2.20	2.50	1.60	2.40
290	43.40	2.70	1.10	2.60	2.10	1.90	2.00
300	44.79	2.50	1.40	2.40	2.50	1.60	2.50
310	46.51	2.60	1.60	2.50	2.30	1.50	2.20
320	47.80	2.40	1.50	2.30	2.60	1.40	2.50
330	49.56	2.50	1.40	2.40	2.30	1.70	2.30
340	50.70	2.30	1.60	2.20	2.50	1.60	2.40
350	52.00	2.40	1.50	2.30	2.40	1.60	2.30
360	53.70	2.20	1.60	2.10	2.60	1.40	2.50
370	56.06	2.30	1.50	2.20	2.40	1.60	2.40
380	56.55	2.00	1.70	2.00	2.70	1.10	2.60
390	58.02	2.50	1.40	2.40	2.20	1.60	2.10
405	61.03	2.30	1.60	2.20	2.50	1.40	2.40
410	60.58	2.40	1.50	2.30	2.30	1.70	2.20
420	61.76	2.20	1.70	2.10	2.60	1.40	2.50
430	63.41	2.60	1.40	2.50	2.40	1.60	2.30
440	64.80	2.40	1.60	2.30	2.50	1.40	2.40
450	66.79	2.70	1.10	2.60	2.30	1.60	2.20
460	67.70	2.30	1.60	2.20	2.50	1.40	2.40
470	70.01	2.50	1.40	2.40	2.40	1.50	2.30

APPENDIX B.67 DATA READ FROM CINE/VIDEO FILM FOR RUN 28A RATE 64 FRAME/SEC.M.F.=(10/40):

FRAME NO.	DISTANCE (CM.)	X1	Y1	Z1	X2	Y2	Z2
0	0.00	2.00	2.70	1.90	1.90	2.70	1.90
5	0.37	2.60	1.60	2.50	2.50	1.60	2.40
10	0.81	2.70	1.50	2.60	2.60	1.60	2.50
15	1.46	2.50	1.60	2.40	2.50	1.70	2.40
20	2.10	2.80	1.40	2.70	2.20	1.80	2.20
25	2.70	2.60	1.60	2.55	2.30	1.70	2.20
30	3.41	2.70	1.40	2.60	2.20	1.80	2.10
35	4.05	2.30	1.60	2.20	2.70	1.40	2.60
40	5.00	2.60	1.50	2.50	2.40	1.70	2.30
45	6.15	2.10	1.80	2.00	2.70	1.30	2.60
50	7.00	2.50	1.60	2.40	2.30	1.70	2.25
55	7.60	2.00	1.70	2.00	2.70	1.40	2.60
60	8.21	2.40	1.60	2.30	2.50	1.50	2.50
65	9.00	2.30	1.70	2.20	2.60	1.40	2.50
70	9.61	2.60	1.60	2.50	2.30	1.70	2.20
75	10.00	2.50	1.60	2.50	2.60	1.60	2.50
80	10.55	2.70	1.30	2.60	2.30	1.70	2.20
85	11.88	2.10	1.70	2.00	2.60	1.40	2.50
90	12.69	2.40	1.50	2.40	2.20	1.80	2.20
95	13.55	2.30	1.70	2.30	2.70	1.40	2.60
100	14.08	2.60	1.60	2.50	2.40	1.60	2.30

105	15.35	2.50	1.50	2.40	2.60	1.40	2.50
115	16.99	2.30	1.70	2.20	2.50	1.40	2.40
120	18.11	2.70	1.30	2.60	2.30	1.60	2.20
125	20.00	2.20	2.80	2.10	2.80	1.20	2.70
130	21.11	2.50	1.60	2.40	2.60	1.40	2.50
135	22.32	2.40	1.50	2.30	2.70	1.40	2.60
140	23.55	2.70	1.30	2.60	2.30	1.60	2.20
145	23.88	2.50	1.60	2.40	2.60	1.50	2.50
150	24.55	2.60	1.60	2.50	2.30	1.60	2.20
155	26.00	2.30	1.70	2.20	2.80	1.30	2.70
160	27.11	2.40	1.60	2.30	2.60	1.50	2.50
165	27.88	2.10	1.80	2.10	2.70	1.40	2.60
170	28.44	2.80	1.30	2.70	2.20	1.80	2.10
175	29.01	2.50	1.40	2.50	2.40	1.60	2.30
180	30.33	2.60	1.50	2.55	2.30	1.60	2.20
185	31.76	2.30	1.60	2.20	2.60	1.50	2.50
190	32.11	2.50	1.50	2.40	2.10	1.60	2.00
195	33.00	2.40	1.60	2.30	2.80	1.30	2.70
200	33.78	2.70	1.30	2.60	2.10	1.80	2.00
205	34.55	2.20	1.60	2.20	2.40	1.60	2.40
210	35.55	2.40	1.70	2.30	2.30	1.60	2.30
215	37.00	2.00	1.80	2.00	2.70	1.40	2.60
220	37.42	2.50	1.60	2.40	2.20	1.70	2.10
225	38.77	2.30	1.60	2.20	2.60	1.40	2.50
230	39.05	2.60	1.50	2.50	2.20	1.70	2.10
235	40.21	2.20	1.70	2.10	2.50	1.60	2.40
240	41.19	2.40	1.60	2.30	2.40	1.50	2.40
245	42.00	2.10	1.70	2.30	2.50	1.60	2.40
250	42.88	2.60	1.50	2.50	2.20	1.70	2.10
255	43.22	2.30	1.60	2.20	2.50	1.60	2.40
260	45.00	2.80	1.30	2.70	2.10	1.80	2.00
265	46.55	2.70	1.40	2.60	2.30	1.60	2.20
270	47.78	2.80	1.20	2.70	2.20	1.70	2.10
275	48.57	2.30	1.60	2.20	2.70	1.30	2.60
280	49.11	2.50	1.60	2.40	2.40	1.50	2.40
285	49.88	2.20	1.65	2.10	2.60	1.60	2.50
290	50.00	2.40	1.60	2.30	2.50	1.60	2.50
300	50.88	2.00	1.60	2.00	2.60	1.50	2.50
310	51.00	2.50	1.50	2.50	2.30	1.60	2.20
320	51.20	2.20	1.60	2.10	2.60	1.50	2.50
330	51.55	2.40	1.55	2.40	2.35	1.65	2.30
340	51.98	2.30	1.50	2.30	2.50	1.50	2.50
350	52.12	2.70	1.40	2.60	2.20	1.70	2.10
360	52.54	2.60	1.50	2.50	2.30	1.50	2.25
370	52.98	2.70	1.30	2.60	2.00	1.80	2.00
375	53.52	2.10	1.70	2.00	2.60	1.60	2.50
380	54.00	2.20	1.60	2.10	2.50	1.55	2.50
385	54.88	2.00	1.80	2.00	2.60	1.50	2.50
390	55.00	2.60	1.50	2.50	2.20	1.80	2.10
395	55.11	2.40	1.60	2.30	2.50	1.60	2.40
400	56.00	2.50	1.50	2.40	2.30	1.70	2.20
410	57.01	2.30	1.60	2.20	2.50	1.40	2.40
420	58.11	2.40	1.45	2.30	2.20	1.60	2.10
430	59.61	2.60	1.60	2.50	2.30	1.50	2.30

440	62.00	2.30	1.60	2.20	2.50	1.70	2.40
450	63.87	2.50	1.60	2.40	2.20	1.70	2.10
455	64.45	2.40	1.60	2.30	2.60	1.50	2.50
460	65.00	2.50	1.50	2.40	2.30	1.70	2.30
470	67.00	2.40	1.60	2.30	2.50	1.50	2.40
475	68.10	2.60	1.40	2.50	2.20	1.60	2.10
480	69.00	2.30	1.60	2.20	2.40	1.50	2.40

All the other Data of Single And Drop Pairs are listed in Appendix (B) wich has been deposited in the Department of Chemical Engineering.

APPENDIX C

COMPUTER PROGRAMS

APPENDIX C

****

COMPUTER PROGRAMS

```
 APPENDIX C.1
************ PROGRAM TO PRINT OUT SINGLE DROP DATA
      DIMENSION FN(200),D(200),X(200),Y(200),Z(200)
           PRINT 2
 2    FORMAT(22X,'APPENDIX B    DATA READ FROM THE CINE',
    +' FILM FOR ',/,22X,11('-'),1X,'RUN      RATE 64 FRAME/SEC.',
    +'M.F.=(10/  ):',/)
     READ *,N
     READ *,(FN(I),D(I),X(I),Y(I),Z(I),I=1,N)
     PRINT 100
100   FORMAT(22X,' FRAME   DISTANCE      X        Y        Z')
      PRINT 150
150   FORMAT(22X,'  NO.      (CM.)')
     PRINT 200
200   FORMAT(22X,' -----   -------   ------  ------  ------')
     DO 5 J=1,N
     PRINT 300 ,FN(J),D(J),X(J),Y(J),Z(J)
 300  FORMAT(22X,F6.2,3X,F8.2,5X,F5.2,3X,F5.2,3X,F5.2)
 5   CONTINUE
     STOP
     END
```

```
 APPENDIX C.2
************ PROGRAM TO PRINT OUT DROP PAIRS DATA
     DIMENSION NF(200),D(200),X(200),Y(200),Z(200),X1(200),
    1Y1(200),Z1(200)
           PRINT 2
 2    FORMAT(16X,'APPENDIX B      DATA READ FROM THE CINE/VIDEO',
    +' FILM FOR',/,16X,12('-'),3X,'RUN-    .AT 25 FRAME PER SEC.',
    +'M.F.=(10/  ):',/)
     READ *,N
     READ *,(NF(I),D(I),X(I),Y(I),Z(I),X1(I),Y1(I),Z1(I),I=1,N)
       PRINT 5
  5   FORMAT(12X,' FRAME   DISTANCE  X1      Y1      Z1',
    +'     X2      Y2      Z2')
       PRINT 15
 15    FORMAT(11X,'   NO.      (CM.)')
       PRINT 10
10      FORMAT(11X,'  ----     ----    ----    ----    ----',
    +'   ----    ----    ----')
     DO 20 J=1,N
     PRINT 100 ,NF(J),D(J),X(J),Y(J),Z(J),X1(J),Y1(J),Z1(J)
100   FORMAT(11X,I5,3X,F8.2,3X,F5.2,3X,F5.2,3X,F5.2,3(3X,F5.2))
 20  CONTINUE
     STOP
     END
```

```
C APPENDIX C.3
C ------------ PROGRAM TO SOLVE FOR AREA AND VELOCITY
C MAIN SEGMENT
C ************
C
C TYPE SPECIFICATION STATEMENTS
C
       REAL FRN(200),DIS(200),X(200),Y(200),Z(200),R1(200),SA(200)
       REAL R2(200),R3(200),RAD(200),DA(200), FSPD,PI,AR(200)
       REAL VEL(200),V(200),RXY(200),T(200),XAV,YAV,ZAV,XSIG,YSIG
      REAL ZSIG,SLOPE(3),CINT(3),X1(200),Y1(200),Z1(200)
      READ(11,5)N
      WRITE(12,5) N
   5  FORMAT(I3)
C
C INPUT NUMBER OF DATA SETS
C
C
C CALL SUBROUTINE TO ALL INPUT DATA
C
       CALL DATA (N,FRN,DIS,X,Y,Z,X1,Y1,Z1)
C
C CALCULATE "PI"
C
        PI=2.0*ASIN(1.0)
        FSPD=64.0
C
C CALL SUBROUTINE TO SORT OUT X,Y,Z DATA
C
        CALL SORTM(X,Y,Z,N)
C
C CALL SUBROUTINE TO CARRY OUT CALCULATIONS INVOLVING X,Y,Z ONLY
C
        CALL RATIO(N,X,Y,Z,RAD,R1,R2,R3)
C
C CALL SUBROUTINE TO CARRY OUT AREA CALCULATIONS
C
        CALL AREAS(N,X,Y,Z,RAD,DA,SA,AR,PI)
C
C CALL SUBROUTINE TO CARRY OUT MISCELLANEOUS CALCULATIONS
C
        CALL MISC(N,X,Y,Z,DIS,FRN,FSPD,T,V,VEL,RXY,PI)
C
C CALL SUBROUTINE TO CARRY OUT STATISTICAL CALCULATIONS
C
        CALL STAT(N,X,Y,Z,XAV,YAV,ZAV,XSIG,YSIG,ZSIG)
C
C CALL SUBROUTINE TO PRINT OUT NUMERICAL RESULTS
C
            CALL PRINT(N,FRN,DIS,T,X,Y,Z,R1,R2,R3,DA,SA,AR,
     1      V,VEL,RXY,XAV,YAV,ZAV,XSIG,YSIG,ZSIG)
C
C CALL SUBROUTINE TO CARRY OUT REGRESSION ANALYSIS AND PRINT OUT RESULTS
C
```

```
            CALL REGRES(N,X,Y,Z,T,SLOPE,CINT)
C
C
            STOP
            END
C
C END OF MAIN SEGMENT
C
C ********************
C SUBROUTINE TO INPUT ALL DATA
C
         SUBROUTINE DATA (N,FRN,DIS,X,Y,Z,X1,Y1,Z1)
C
      REAL X(200),Y(200),Z(200),FRN(200),DIS(200),X1(200),
     1Y1(200),Z1(200)
         READ(11,25)N,C
         WRITE(12,25)N,C
   25    FORMAT(I3,F7.4)
         DO 10 I=1,N
         READ (11,15) FRN(I),DIS(I),X1(I),Y1(I),Z1(I)
        DO 111 K=1,N
         X(K)=X1(K)*C
         Y(K)=Y1(K)*C
         Z(K)=Z1(K)*C
 111    CONTINUE
      WRITE(12,15) FRN(I),DIS(I),X(I),Y(I),Z(I)
  15  FORMAT(5F10.5)
C
  10    CONTINUE
         RETURN
         END
C SUBROUTINE TO SORT OUT X,Y,Z DATA
C
         SUBROUTINE SORTM(X,Y,Z,N)
C
         REAL X(200),Y(200),Z(200),A(3),P
        DO 100 I=1,N
         A(1)=X(I)
         A(2)=Y(I)
         A(3)=Z(I)
         P=0.0
         DO 80 J=1,2
         IF (A(J).GT.A(J+1)) GO TO 80
         P=A(J)
         A(J)=A(J+1)
         A(J+1)=P
  80     CONTINUE
         X(I)=A(1)
         Y(I)=A(2)
         Z(I)=A(3)
  100    CONTINUE
C
C
         RETURN
```

```
        END
C SUBROUTINE TO CARRY OUT CALCULATIONS INVOLVING X,Y,Z ONLY
C
          SUBROUTINE RATIO (N,X,Y,Z,RAD,R1,R2,R3)
C
          REAL RAD(200),R1(200),R2(200),R3(200),X(200),Y(200),Z(200)
        DO 10 I=1,N
C
          RAD(I)=((X(I)+Y(I)+Z(I))/6.0)**0.5
          R1(I)=Y(I)/X(I)
          R2(I)=Y(I)/Z(I)
          R3(I)=X(I)*Z(I)/Y(I)
   10   CONTINUE
C
          RETURN
          END
C SUBROUTINE TO CARRY OUT AREA CALCULATIONS
C
           SUBROUTINE AREAS(N,X,Y,Z,RAD,DA,SA,AR,PI)
C
           REAL X(200),Y(200),Z(200),RAD(200),DA(200),SA(200)
           REAL AR(200)
           REAL PI,PHI,AK,AJ0,AJ2,AJ4,E,F
           DO 10 I=1,N
C
           DA(I)=4.0*PI*(RAD(I)**2.0)
C
           PHI=ACOS(Z(I)/X(I))
           AK=(X(I)/Y(I))*((((Y(I)**2.0)-(Z(I)**2.0))/((X(I)**2.0)-
     1     (Z(I)**2.0)))**0.5)
           AJ0=PHI
           AJ2=(0.5*PHI)+(0.25*(SIN(2.0*PHI)))
           AJ4=(0.25*PHI)+(0.25*(SIN(2.0*PHI)))+(0.125*PHI)+
     1     ((1.0/32.0)*(SIN(4.0*PHI)))
           E=AJ0-(0.5*(AK**2.0)*AJ2)-((1.1/2.4)*(AK**4.0)*AJ4)
           F=AJ0+(0.5*(AK**2.0)*AJ2)+((1.3/2.4)*(AK**4.0)*AJ4)
      SA(I) = 2.0*PI*(Z(I)**2.0)+((2.0*PI*Y(I))/(((X(I)**2.0)-
     1(Z(I)**2.0))**0.5))**(((Z(I)**2.0)*F)+((X(I)**2.0)-
     2(Z(I)**2.0))*E)
           AR(I)=SA(I)/DA(I)
   10      CONTINUE
C
           RETURN
           END
C SUBROUTINE TO CARRY OUT MISCELLANEOUS CALCULATIONS
C
         SUBROUTINE MISC(N,X,Y,Z,DIS,FRN,FSPD,T,V,VEL,RXY,PI)
C
         REAL X(200),Y(200),Z(200),DIS(200),FRN(200),FSPD,T(200),V(200)
         REAL VEL(200),RXY(200),PI
           DO 10 I=1,N
C
         T(I)=FRN(I)/FSPD
         VEL(I)=DIS(I)/T(I)
```

```
      V(I)=(4.0/3.0)*PI*X(I)*Y(I)*Z(I)/8.0
      RXY(I)=((X(I)-Y(I))/(X(I)+Y(I)))
  10   CONTINUE
C
      RETURN
      END
C SUBROUTINE TO CARRY OUT STATISTICAL CALCULATIONS
C
      SUBROUTINE STAT(N,X,Y,Z,XAV,YAV,ZAV,XSIG,YSIG,ZSIG)
C
      REAL X(200),Y(200),Z(200),XAV,YAV,ZAV,XSIG,YSIG,ZSIG
      REAL S(3),Q(3)
C
      INTEGER N,I,J
C
      DO 20 J=1,3
      S(J)=0.0
      Q(J)=0.0
 20   CONTINUE
C
      DO 100 I=1,N
      S(1)=S(1)+X(I)
      S(2)=S(2)+Y(I)
      S(3)=S(3)+Z(I)
 100  CONTINUE
C
      XAV=S(1)/FLOAT(200)
      YAV=S(2)/FLOAT(200)
      ZAV=S(3)/FLOAT(200)
C
      DO 200 I=1,N
      Q(1)=Q(1)+((X(I)-XAV)**2.0)
      Q(2)=Q(2)+((Y(I)-YAV)**2.0)
      Q(3)=Q(3)+((Z(I)-ZAV)**2.0)
 200  CONTINUE
C
     XSIG=Q(1)/FLOAT(200)
      YSIG=Q(2)/FLOAT(200)
      ZSIG=Q(3)/FLOAT(200)
C
      RETURN
      END
C SUBROUTINE TO PRINT OUT NUMERICAL RESULTS
C
     SUBROUTINE PRINT(N,FRN,DIS,T,X,Y,Z,R1,R2,R3,DA,SA,
   1 AR,V,VEL,RXY,XAV,YAV,ZAV,XSIG,YSIG,ZSIG)
C
     REAL FRN(200),DIS(200),T(200),X(200),Y(200),Z(200),R1(200)
     REAL DA(200),SA(200),AR(200),V(200),VEL(200)
       REAL R2(200),R3(200),RXY(200),XAV
     REAL YAV,ZAV,XSIG,YSIG,ZSIG
C
     INTEGER N,I
     WRITE(13,14)
```

```
        WRITE(12,14)
  14    FORMAT(11X,'APPENDIX C.    AREA VELOCITY PROGRAM RUN'//)
        WRITE(13,20)
        WRITE (12,20)
  20    FORMAT(11X,4HTIME,3X,3HY/X,4X,3HY/Z,4X,4HXZ/Y,4X,2HDA,
     1  5X,2HSA,5X,2HAR,5X,1HV,6X,3HVEL,4X,3HRXY)
        WRITE(13,25)
        WRITE(12,25)
  25    FORMAT(11X,3HSEC,26X,3HCM.,4X,3HCM.,11X,3HCM.3X,6HCM/SEC)
        WRITE(13,30)
        WRITE(12,30)
  30    FORMAT(10X,5H-----,7(2X,5H-----),2X,6H------,2X,5H-----)
C
        DO 150 I=1,N
        WRITE(13,80) T(I),R1(I),R2(I),R3(I),DA(I),SA(I),
     1  AR(I),V(I),VEL(I),RXY(I)
        WRITE(12,80) T(I),R1(I),R2(I),R3(I),DA(I),SA(I),
     1  AR(I),V(I),VEL(I),RXY(I)
  80    FORMAT(10X,F5.3,7(2X,F5.3),2X,F6.3,2X,F5.3)
  150   CONTINUE
C
        WRITE(12,200)
        WRITE(13,200)
  200   FORMAT(1H,//,37X,1HX,14X,1HY,13X,1HZ,/)
C
        WRITE(12,250) XAV,YAV,ZAV
        WRITE(13,250) XAV,YAV,ZAV
 250    FORMAT(12X,4HMEAN,18X,3(1PE9.3,6X),/)
C
        WRITE(12,300) XSIG,YSIG,ZSIG
        WRITE(13,300) XSIG,YSIG,ZSIG
 300    FORMAT(12X,8HVARIANCE,14X,3(1PE9.3,6X),//)
C
C
        RETURN
        END
C SUBROUTINE TO CARRY OUT REGRESSION ANALYSIS AND PRINT OUT RESULTS
      SUBROUTINE REGRES(N,X,Y,Z,T,SLOPE,CINT)
      REAL X(200),Y(200),Z(200),T(200),SLOPE(3),CINT(3),RES(20),COR(3)
C
        INTEGER N,IFAIL
C
C CALL SUBROUTINE "G02CAF" FROM THE NAG LIBRARY TO CARRY OUT
C LINEAR REGRESSION BETWEEN TIME (T) AND X,Y,Z RESPECTIVELY
        IFAIL=0
C
        CALL G02CAF(N,T,X,RES,IFAIL)
        SLOPE(1)=RES(6)
        CINT(1)=RES(7)
        COR(1)=RES(5)
        IFAIL=0
C
        CALL G02CAF(N,T,Y,RES,IFAIL)
        SLOPE(2)=RES(6)
```

```
        CINT(2)=RES(7)
        COR(2)=RES(5)
        IFAIL=0
C
        CALL G02CAF(N,T,Z,RES,IFAIL)
        SLOPE(3)=RES(6)
        CINT(3)=RES(7)
        COR(3)=RES(5)
C
        WRITE(12,50)
        WRITE (13,50)
   50   FORMAT(//,35X,5HSLOPE,7X,9HINTERCEPT,7X,
     1  10HCORR.COFF.,5X/)
         WRITE(12,100)SLOPE(1),CINT(1),COR(1)
         WRITE(13,100) SLOPE(1),CINT(1),COR(1)
  100    FORMAT(12X,6HX-VS-T,9X,2(4X,F10.5),6X,F10.5)
         WRITE(12,150) SLOPE(2),CINT(2),COR(2)
         WRITE(13,150)SLOPE(2),CINT(2),COR(2)
  150    FORMAT(12X,6HY-VS-T,9X,2(4X,F10.5),6X,F10.5)
         WRITE(12,200) SLOPE(3),CINT(3),COR(3)
         WRITE(13,200) SLOPE(3),CINT(3),COR(3)
  200    FORMAT(12X,6HZ-VS-T,9X,2(4X,F10.5),6X,F10.5)
         RETURN
         END
C END OF PROGRAM
C **************
```

```
C APPENDIX C.4
C ************ PROGRAM TO PLOT X,Y,Z AXES VS. TIME
       DIMENSION FN(300),D(300),T(600),X(300),Y(300),Z(300)
       READ *,N
       READ *,(FN(L),D(L),X(L),Y(L),Z(L),L=1,N)
       DO 7 I=1,N
       T(I) =FN(I)/64.0
    7  CONTINUE
       PRINT *,(T(I),I=1,N)
      CALL GINO
      CALL UNITS (10.0)
      CALL CHASWI (1)
      CALL SCALE2(0.7,0.7)
      CALL CHASIZ (0.2,0.25)
      CALL SHIFT2 (4.0,3.0)
      CALL AXIPOS (1,1.0,0.0,10.0,1)
      CALL AXIPOS (1,1.0,0.0,3.0,2)
      CALL AXISCA (3,7,0.0,7.0,1)
      CALL AXISCA (3,3,1.5,3.0,2)
      CALL AXIDRA (1,1,1)
      CALL AXIDRA (-1,-1,2)
      CALL MOVTO2 (8.0,-1.3)
      CALL CHAHOL (12HTIME(SEC.)*.)
      CALL MOVTO2 (-0.6,1.2)
      CALL CHAANG (90.0)
      CALL CHAHOL (3HZ*.)
      CALL CHAANG (0.0)
      CALL GRAPOL(T,Z,N)
      CALL MOVTO2 (2.0,-2.6)
      CALL CHAHOL (33HFIG.     X,Y,Z VS. TIME RUN-   *.)
      CALL SHIFT2 (0.0,5.5)
      CALL AXIPOS (1,1.0,0.0,10.0,1)
      CALL AXIPOS (1,1.0,0.0,3.0,2)
      CALL AXISCA (3,7,0.0,7.0,1)
      CALL AXISCA (3,3,1.0,2.0,2)
      CALL AXIDRA (1,1,1)
      CALL AXIDRA (-1,-1,2)
      CALL MOVTO2 (8.0,-1.3)
      CALL CHAHOL (12HTIME(SEC.)*.)
      CALL MOVTO2 (-0.6,1.2)
      CALL CHAANG (90.0)
      CALL CHAHOL (3HY*.)
      CALL CHAANG (0.0)
      CALL GRAPOL (T,Y,N)
      CALL SHIFT2 (0.0,5.5)
      CALL AXIPOS (1,1.0,0.0,10.0,1)
      CALL AXIPOS (1,1.0,0.0,3.0,2)
      CALL AXISCA (3,7,0.0,7.0,1)
      CALL AXISCA (3,3,1.5,3.0,2)
      CALL AXIDRA (1,1,1)
      CALL AXIDRA (-1,-1,2)
      CALL MOVTO2 (8.0,-1.3)
      CALL CHAHOL (12HTIME(SEC.)*.)
      CALL MOVTO2 (-0.6,1.2)
```

```
      CALL CHAANG (90.0)
      CALL CHAHOL (3HX*.)
      CALL CHAANG (0.0)
      CALL GRAPOL (T,X,N)
      CALL DEVEND
      STOP
      END


C APPENDIX C.5
C ************ PROGRAM TO SOLVE FOR ECCENTRICITY USING
C       ALHASSAN CORRELATION FOR SINGLE DROP
        REAL M
        PRINT*,'                                 INPUT DATA'
        PRINT 100,R,ST,VEL,DENC,DEND,VISC,M,DD,DC
 100    FORMAT(//15X,'RADIUS OF DROP IN CM=',F7.4/15X,'SURFACE',
     *         'TENSION IN DYNE/CM =',F7.3/15X,'VELOCITY OF DROP',
     *         'IN CM/SEC =',F7.4/15X,'DENSITY OF CONTINEOUS',
     *         'PHASE IN G/CM3 =',F7.4/15X,'DENSITY OF DISPERESED',
     *         'PHASE IN G/CM3 =',F7.4/15X,'VISCOSITY OF',
     *         'CONTINUEOUS PHASE IN CP =',F7.4/15X,'(M) VALUE IN',
     *         'CORRELATIONS =',F7.3/15X,'DIFFUSIVITY OF DISPERESED',
     *         'PHASE IN (1/CM) =',E10.3/15X,'DIFFUSIVITY OF',
     *         'CONTINUEOUS PHASE IN (1/CM) =',E10.3///)
        READ*,R,ST,VEL,DENC,DEND,VISC,M,DD,DC
 20     DE=R*2
        N=2
        DO
          B=((DE)**0.225)/1.242
     W=(N*ST*B/R**3*(N+1)*(N-1)*(N+2)/((N+1)*DEND+N*DENC))**0.5
          SR=W*DE/VEL
          WEC=DE*(VEL**2)*DENC/ST
          E=0.868*(SR**0.395)*(WEC**-0.229)*(ST**0.144)
          PYE=3.1416
          A1=4.0*PYE*R**2.0
          A2=(E/2.0+1.0)*A1
         PRINT 300,N,W,E,A1,A2
 300     FORMAT(('*'),I4,('*'),F10.3,('*'),5(F9.5,('*'))/66('*'))
         PRINT 400
 400     FORMAT(66('*')///)
         N=N+1
        UNTIL(N.GT.4)
        PRINT*,'        INPUT NEW VALUES OF RADIUS , VELOCITY'
        READ *, R,VEL
        GOTO 20
        STOP
        END
```

APPENDIX C.6

************ TO SOLVE FOR FORMATION MODEL

```
10 PRINT "N-TH ORDER REGRESSION"
15 PRINT "BY LEAST SQUARES"
30 INPUT "DEGREE OF EQUATION: ";D
39 REM DIMENSION A(*),R(*,*),T(*) ACCORDING TO DEGREE OF EQUATION
40 DIM A(2 * D + 1),R(D + 1,D + 2),T(D + 2)
60 INPUT "NUMBER OF KNOWN POINTS:";N
80 A(1) = N
89 REM ENTER COORDINATES OF DATA POINTS
90 FOR I = 1 TO N
100 PRINT "X,Y  OF POINT ";I;
110 INPUT " :";X,Y
119 REM LINES 120-200 POPULATE MATRICES WITH A SYSTEM OF EQUATION
120 FOR J = 2 TO 2 * D + 1
130 A(J) = A(J) + X ^ (J - 1)
140 NEXT J
150 FOR K = 1 TO D + 1
160 R (K,D + 2) = T(K) + Y * X ^ (K - 1)
170 T(K) = T(K) + Y * X ^ (K - 1)
180 NEXT K
190 T(D + 2) = T(D + 2) = T(D + 2) + Y ^ 2
200 NEXT I
209 REM LINES 210-480 SOLVE THE SYSTEM OF EQUATION IN THE MATRICES
210 FOR J = 1 TO D + 1
220 FOR K = 1 TO D + 1
230 R(J,K) = A(J + K - 1)
240 NEXT K
250 NEXT J
260 FOR J = 1 TO D + 1
270 K = J
280 IF R(K,J) < 0 OR R(K,J) > 0 THEN 320
290 K = K + 1
295 IF K < D + 1 THEN 280
300 PRINT CHR£ (7);"NO UNIQUE SOLUTION"
310 GO TO 790
320 FOR I = 1 TO D + 2
330 S = R(J,I)
340 R(J,I) = R(K,I)
350 R(K,I) = S
360 NEXT I
370 Z = 1 / R(J,J)
380 FOR I = 1 TO D + 2
390 R(J,I) = Z * R(J,I)
400 NEXT I
410 FOR K = 1 TO D + 1
420 IF K = J THEN 470
430 Z = - R(K,J)
440 FOR I = 1 TO D + 2
450 R(K,I) = R(K,I) + Z * R(J,I)
460 NEXT I
470 NEXT K
480 NEXT J
490 HOME
```

```
495 PRINT TAB(13) "CONSTANT = ";R(1,D + 2)
499 REM PRINT EQUATION COEFFICIENTS
500 FOR J = 1 TO D
510 PRINT J;" DEGREE COEFFICIENT = ";R(J + 1,D + 2)
520 NEXT J
530 PRINT
539 REM COMPUTE REGRESSION ANALYSIS
540 P = 0
550 FOR J = 2 TO D + 1
560 P = P + R(J,D + 2) * (T(J) - A(J) * T(1) / N)
570 NEXT J
580 Q = T(D + 2) - T(1) ^ 2 / N
590 Z = Q - P
600 I = N - D - 1
620 PRINT
630 J = P / Q
640 PRINT "COEFFICIENT OF"; PRINT "DETERMINATION (R^2) = ";J
650 PRINT "COEFFICIENT OF"; PRINT "CORRELATION = ";SQR (J)
660 PRINT STANDARD ERROR OF ESTIMATE = "; SQR (Z / I)
670 PRINT
679 REM COMPUTE Y-COORDINATE FROM ENTERED X-COORDINATE
680 PRINT "INTERPOLATION (0 TO END PROGRAM)"
690 P = R(1,D + 2)
700 INPUT VALUE OF X:";X
720 IF X = 0 THEN 790
730 FOR J = 1 TO D
740 P = P + R(J + 1,D + 2) * X ^ J
750 NEXT J
760 PRINT TAB (10)" Y = ";P
770 PRINT
780 GO TO 680
790 END
```

```
C APPENDIX C.7
C ************ PROGRAM TO SOLVE FOR OVERALL MASS TRANSFER
C       COEFFICIENT USING THREE DIFFERENT CORRELATIONS
C       FIRST OF ROSE AND KINTINER
C       SECOND OF ANGELO . AT . EL
C       THIRD  OF ALHASSAN
        REAL M,KDR,KCR,KDRO,KDA,KDAO,KDT,KDTO
        PRINT*,'                           INPUT DATA'
        PRINT 100,R,ST,VEL,DENC,DEND,VISC,M,DD,DC,E
 100    FORMAT(//15X,'RADIUS OF DROP IN CM=',F7.4/15X,'SURFACE',
     *          'TENSION IN DYNE/CM =',F7.3/15X,'VELOCITY OF DROP',
     *          'IN CM/SEC =',F7.4/15X,'DENSITY OF CONTINEOUS',
     *          'PHASE IN G/CM3 =',F7.4/15X,'DENSITY OF DISPERESED',
     *          'PHASE IN G/CM3 =',F7.4/15X,'VISCOSITY OF',
     *          'CONTINUEOUS PHASE IN CP =',F7.4/15X,'(M) VALUE IN',
     *          'CORRELATIONS =',F7.3/15X,'DIFFUSIVITY OF DISPERESED',
     *          'PHASE IN (1/CM) =',E10.3/15X,'DIFFUSIVITY OF',
     *          'CONTINUEOUS PHASE IN (1/CM) =',E10.3/15X,
     *          'ECCINTRICITY =',F7.3///)
       READ*,R,ST,VEL,DENC,DEND,VISC,M,DD,DC,E
 20     DE=R*2
        N=2
        DO
          B=((DE)**0.225)/1.242
       W=(N*ST*B/R**3*(N+1)*(N-1)*(N+2)/((N+1)*DEND+N*DENC))**0.5
          SR=W*DE/VEL
          WEC=DE*(VEL**2)*DENC/ST
          ET=0.868*(SR**0.395)*(WEC**-0.229)*(ST**0.144)
          KDA=((4*DD*W*(1+E+(3/8)*E**2))/3.1416)**0.5
          KDAO=KDA*(1/(1+M*((DD/DC)**0.5)))
          KDR=0.45*((DD*W)**0.5)
          REC=DE*VEL*DENC/VISC
          SCC=VISC/(DENC*DC)
          KCR=(DC/DE)*(50+0.0085*REC*(SCC**0.7))
          KDRO=(KDR*KCR)/(KCR+M*KDR)
         EO=(9.81*(DENC-DEND)*DE**2)/(ST)
         KDT=4.3*(ET**2.69*EO**1.62*((DD*W)**0.5))
         KDTO=(KDT*KCR)/(KCR+M*KDT)
         PRINT 300,N,W,KDR,KDA,KDT,KCR,KDRO,KDAO,KDTO
 300     FORMAT(('*'),I4,('*'),F10.3,('*'),7(F8.5,('*'))/66('*'))
         PRINT 400
 400     FORMAT(66('*')///)
         N=N+1
        UNTIL(N.GT.4)
        PRINT*,'  INPUT NEW VALUES OF RADIUS,VELOCITY,ECCENTRICITY'
        READ *, R,VEL,ECC
        GOTO 20
        STOP
        END
```

APPENDIX C.8

```
************ TO SOLVE FOR MULTIPLE LINEAR REGRESSION
10 HOME : PRINT TAB(7) "MULTIPLE LINEAR REGRESSION"
14 REM  SET TEXT WINDOW TO LINES 2 THROUGH 24
15 POKE 34,1
20 PRINT
30 INPUT "NUMPER OF KNOWN POINTS:";N
39 REM DIMENSION ARRAYS ACCORDING TO KNOWN POINTS
40 DIM X(N + 1),S(N + 1),T(N + 1),A(N + 1,N + 2)
60 INPUT "NUMBER OF KNOWN VARIABLES:";V
70 IF V > N THEN PRINT CHR£(7): PRINT "NUMBER OF VARIABLES CANNOT
   EXCEED":PRINT "NUMBER OF KNOWN POINTS":CLEAR :GOTO 20
80 X(1) = 1
90 FOR I = 1 TO N
100 PRINT "POINT";I;
110 FOR J = 1 TO V
119 REM ENTER INDEPENDENT VARIABLES FOR EACH POINT
120 HTAB 11 : PRINT "VARIABLE ";J: HTAB 24
130 INPUT " : ";X(J + 1)
140 NEXT J
149 REM  ENTER DEPENDENT VARIABLE FOR EACH POINT
150 INPUT " DEPENDENT VARIABLE :";X(V + 2)
169 REM  POPULATE A MATRIX TO BE USED IN CURVE FITTING
170 FOR K = 1 TO V + 1
180 FOR L = 1 TO V + 2
190 A(K,L) = A(K,L) + X(K) * X(L)
200 S(K) = A(K,V + 2)
210 NEXT L
220 NEXT K
230 S(V + 2) = S(V + 2) + X(V + 2) ^ 2
240 NEXT I
248 REM STATEMEVTS 250 TO 500 FIT CURVE BY SOLVING THE SYSTEM
249 REM OF LINEAR EQUATIONS IN MATRIX A(*)
250 FOR I = 2 TO V + 1
260 T(I) = A(1,I)
270 NEXT I
280 FOR I = 1 TO V + 1
290 J = I
300 IF A(J,I) < 0 OR A(J,I) > 0 THEN 340
305 J = J + 1
310 IF J < V + 1 OR = V + 1 THEN 300
320 PRINT "NO UNIQUE SOLUTION"; CHR£ (7)
330 GOTO 810
340 FOR K = 1 TO V + 2
350 B = A(I,K)
360 A(I,K) = A(J,K)
370 A(J,K) = B
380 NEXT K
390 Z = 1 / A(I,I)
400 FOR K = 1 TO V + 2
410 A(I,K) = A * A(I,K)
420 NEXT K
430 FOR J = 1 TO V + 1
440 IF J = I THEN 490
```

```
450 Z = - A(J,I)
460 FOR K = 1 TO V + 2
470 A(J,K) = A(J,K) + Z * A(I,K)
480 NEXT K
490 NEXT J
500 NEXT I
510 HOME : PRINT
520 PRINT "EQUATION COEFFICIENTS:"
525 PRINT "CONSTANT = ";A(1,V + 2)
530 FOR I = 2 TO V + 1
540 PRINT "VARIABLE (";I - 1;") = ";A(I,V + 2)
550 NEXT I
560 P = O
570 FOR I = 2 TO V + 1
580 P = P + A(I,V + 2) * (S(I) - T(I) * S(I) / N)
590 NEXT I
600 R = S(V + 2) - S(1) ^ 2 / N
610 Z = R - P
620 L = N - V - 1
640 PRINT
650 I = P / R
655 PRINT
660 PRINT "COEFFICIENT OF":PRINT "DETERMINATION (R^2) = ";I
665 PRINT
670 PRINT "COEFICIENT OF MULTIPLE":PRINT "COEFFICIENT = "; SQR(I)
675 PRINT : ONERR GOTO 850
680 PRINT STANDARD ERROR OF ESTIMATE = "; SQR (ABS(Z / L))
690 PRINT
699 REM ESTIMATE DEPENDENT VARIABLE FROM ENTERED INDEPENDENT
    VARIABLES
700 PRINT "INTERPOLATION )0 TO END)"
710 P = A(1,V + 2)
720 FOR J = 1 TO V
730 PRINT "VALUE OF VARIABLE ";J:
740 INPUT " : " ; X
749 REM END OF PROGRAM?
750 IF X = 0 THEN 810
760 P = P + A(J + 1,V +2) * X
770 NEXT J
780 PRINT "DEPENDENT = ";P
790 PRINT
800 GOTO 700
810 TEXT : END
849 REM ERROR MESSAGE FOR DIVISION BY ZERO
850 PRINT CHR£ (7): PRINT "INVALID DATA - DIVISION BY ZERO"
860 GOTO 690
```

APPENDIX D.1

MASS TRANSFER DATA

APPENDIX D.1

RUN NO	Acetone Concentration *	 % w/w	Nozzles Used	t_f Sec	d_e m $\times 10^{-2}$	Average Area $m^2 \times 10^{-4}$	Terminal Velocity **	C_2 *	C_R * $\times 10^{-2}$	f_d ***	fc ***	C_E * $\times 10^{-2}$	Mass Transfer Rate Out of Drop	 Into Cont Phase
10 A	0.511	3.46	G1	3.00	0.77	1.86	9.76	0.38	10.00	0.08	1.25	2.85	80	87
B				1.50	0.74	1.72	9.85	0.41	6.01	0.14	1.30	3.61	88	64
C				1.00	0.69	1.50	8.38	0.44	5.80	0.17	1.23	4.84	89	68
D				0.76	0.68	1.45	10.10	0.46	5.42	0.22	1.33	6.36	89	76
E				0.58	0.65	1.33	10.81	0.47	4.86	0.25	1.47	6.97	90	81
11 A	1.01	6.85	G1	3.00	0.75	1.77	9.28	0.32	10.91	0.07	1.58	3.67	89	78
B				1.55	0.71	1.58	8.86	0.70	9.11	0.12	1.63	4.18	91	56
C				1.00	0.68	1.45	9.81	0.76	5.50	0.14	2.27	4.79	95	75
D				0.72	0.66	1.37	10.29	0.86	11.30	0.21	2.70	6.01	89	84
E				0.57	0.63	1.25	10.86	0.88	7.10	0.23	3.25	6.41	83	90
12 A	2.04	13.93	G1	3.00	0.72	1.63	10.25	1.29	4.87	0.06	3.50	3.61	97	95
B				1.50	0.69	1.50	10.85	1.52	4.35	0.11	4.80	5.08	97	104
C				1.00	0.66	1.37	11.11	1.65	3.87	0.13	4.17	5.41	98	80
D				0.68	0.63	1.25	11.23	1.73	3.66	0.18	4.67	5.89	98	70

APPENDIX D.1 continued

RUN NO	Acetone Concentration *	Acetone Concentration % w/w	Nozzles Used	t_f Sec	d_e m $\times 10^{-2}$	Average Area $m^2 \times 10^{-4}$	Terminal Velocity **	C_2 *	C_R * $\times 10^{-2}$	f_d ***	f_c ***	C_E * $\times 10^{-2}$	Mass Transfer Rate Out of Drop	Mass Transfer Rate Into Cont Phase
13 A	3.01	20.67	G1	3.10	0.68	1.45	9.95	1.72	4.65	0.05	3.60	4.13	98	93
B				1.51	0.65	1.33	11.29	1.86	4.00	0.10	4.33	6.00	99	93
C				1.00	0.62	1.21	10.83	2.34	3.72	0.11	3.67	6.71	99	92
D				0.62	0.58	1.06	12.00	2.42	3.21	0.16	5.00	8.29	99	84
14 A	0.511	3.46	G1	1.50	0.74	1.72	9.98	0.36	5.54	0.28	3.00	4.28	89	88
B				1.00	0.70	1.54	10.10	0.38	5.11	0.36	2.33	5.11	90	65
C				0.78	0.68	1.45	10.56	0.04	4.87	0.42	2.83	7.18	90	94
D				0.55	0.66	1.37	11.01	0.43	4.41	0.55	2.17	9.58	91	74
15 A	1.01	6.85	G1	1.62	0.72	1.63	9.73	0.61	5.46	0.24	2.50	5.48	95	56
B				1.00	0.69	1.50	10.11	0.73	5.18	0.34	3.00	7.88	95	68
C				0.82	0.67	1.41	10.29	0.79	4.28	0.38	3.42	7.27	96	64
D				0.61	0.65	1.33	12.15	0.82	4.08	0.47	3.17	12.64	96	84
16 A	2.11	14.41	G1	3.11	0.75	1.77	9.60	1.16	5.61	0.14	2.83	8.26	97	78
B				1.55	0.69	1.50	10.81	1.22	4.48	0.22	3.50	11.73	98	88
C				1.00	0.67	1.41	11.28	1.42	3.87	0.31	3.38	13.00	98	75
D				1.72	0.66	1.37	10.35	1.54	3.36	0.42	4.25	13.86	98	67

APPENDIX D.1 continued

	Acetone Concentration												Mass Transfer Rate	
RUN NO	*	% w/w	Nozzles Used	t_f Sec	d_e $m^2 \times 10^{-2}$	Average Area $m^2 \times 10^{-4}$	Terminal Velocity **	C_2 **	C_R * $\times 10^{-2}$	f_d ***	f_c ***	C_E * $\times 10^{-2}$	Out of Drop	Into Cont Phase
17 A	0.511	3.46	G2	3.15	0.83	2.16	10.75	0.34	5.81	0.19	1.67	4.47	89	81
B				1.50	0.79	1.96	11.29	0.22	5.30	0.34	2.63	5.18	90	78
C				1.00	0.75	1.77	10.25	0.40	5.00	0.44	2.87	7.20	90	91
D				0.72	0.72	1.63	10.86	0.43	4.24	0.54	3.30	9.70	92	115
18 A	1.01	6.85	G2	1.56	0.77	1.86	8.78	0.37	5.00	0.31	3.38	6.76	95	84
B				1.00	0.75	1.77	10.88	0.61	4.88	0.44	4.17	8.04	96	75
C				0.81	0.72	1.63	11.33	0.73	3.89	0.48	4.67	11.28	96	108
D				0.55	0.68	1.45	12.25	0.82	3.61	0.60	3.00	27.31	98	135
19 A	2.05	14.00	G2	1.51	0.75	1.77	8.91	1.21	4.00	0.29	5.67	7.80	98	74
B				1.00	0.72	1.63	9.28	1.35	3.36	0.39	4.67	13.83	98	81
C				0.81	0.70	1.54	10.23	1.38	3.11	0.44	3.42	15.05	98	57
D				0.55	0.67	1.41	11.10	1.46	2.11	0.57	3.00	31.07	99	79
20 A	3.00	20.60	G2	3.10	0.69	1.50	10.81	0.87	4.11	0.11	4.50	6.21	99	84
B				1.51	0.65	1.33	9.98	2.31	3.60	0.19	3.50	11.73	99	72
C				1.00	0.60	1.13	10.25	2.62	3.00	0.23	3.17	17.88	99	83
D				0.61	0.56	0.98	11.18	2.88	2.45	0.30	2.33	29.10	99	75

APPENDIX D.1 continued

RUN NO	Acetone Concentration		Nozzles Used	t_f	d_e	Average Area	Terminal Velocity	C_2	C_R	f_d	f_c	C_E	Mass Transfer Rate	
	*	% w/w		Sec	$m^2 \times 10^{-2}$	$m^2 \times 10^{-4}$	**	*	* $\times 10^{-2}$	***	***	* $\times 10^{-2}$	Out of Drop	Into Cont Phase
21 A	0.511	3.46	G3	3.15	0.91	2.60	8.67	0.31	5.05	0.25	2.25	5.15	90	91
B				1.56	0.84	2.22	8.93	0.28	4.87	0.40	3.00	5.97	90	88
C				1.00	0.80	2.01	9.43	0.37	4.60	0.54	3.17	8.00	91	92
D				0.65	0.77	1.86	10.10	0.40	3.89	0.74	2.50	9.86	92	66
22 A	1.08	7.33	G3	3.00	0.87	2.37	8.86	0.58	5.25	0.23	2.83	5.79	95	66
B				1.50	0.81	2.06	9.71	0.62	4.78	0.37	3.83	7.36	96	70
C				1.00	0.77	1.86	10.43	0.70	4.61	0.48	4.50	9.10	96	79
D				0.70	0.73	1.67	11.21	0.79	3.80	0.58	4.17	14.35	96	95
23 A	2.42	16.56	G3	3.15	0.78	1.91	8.74	0.86	4.63	0.16	4.50	6.26	98	74
B				1.60	0.72	1.63	9.91	1.50	4.10	0.24	4.83	9.20	98	75
C				1.00	0.70	1.54	10.87	1.64	3.15	0.36	4.17	16.11	99	77
D				0.60	0.68	1.45	12.15	1.99	2.90	0.55	3.83	19.34	99	56
24 A	0.511	3.46	G4	1.50	0.92	2.66	9.10	0.30	4.23	0.54	2.67	6.81	92	65
B				1.00	0.88	2.43	10.71	0.34	3.38	0.71	3.33	10.37	93	95

APPENDIX D.1 continued

RUN NO	Acetone Concentration		Nozzles Used	t_f Sec	d_e $m^2 \times 10^{-2}$	Average Area $m^2 \times 10^{-4}$	Terminal Velocity **	C_2 *	C_R * $\times 10^{-2}$	f_d ***	f_c ***	C_E * $\times 10^{-2}$	Mass Transfer Rate	
	*	% w/w											Out of Drop	Into Cont Phase
25 A	2.10	14.41	G4	1.55	0.80	2.01	9.21	1.38	3.60	0.35	3.50	11.38	98	55
B				1.05	0.75	1.77	10.36	1.52	2.75	0.42	3.33	18.79	99	71
26 A	3.50	24.11	PT1	1.00	0.71	1.58	10.28	2.34	2.28	0.37	5.33	17.01	99	69
B				0.78	0.64	1.28	11.61	2.67	1.87	0.35	6.33	20.21	99	103
27 A	3.42	23.56	PT2	0.86	0.69	1.50	10.83	2.58	1.80	0.40	4.33	24.28	99	77
B				0.55	0.61	1.17	11.19	2.98	1.63	0.43	3.83	27.34	100	71
28 A	3.36	23.15	PT3	1.10	0.76	1.81	9.28	2.21	1.65	0.42	4.83	21.61	99	74
B				0.75	0.68	1.45	10.10	2.61	1.48	0.44	5.00	25.83	100	88

* = kg × 10^{-3}.mol/L

** = m × 10^{-2}.sec^{-1}

*** = m^3 × 10^{-6}.sec^{-1}

APPENDIX D.2

EXPERIMENTAL AND THEORETICAL OVERALL MASS TRANSFER COEFFICIENTS OF SINGLE DROPS AND DROP PAIRS DURING:

I FORMATION

II TRAVEL THROUGH THE CONTINUOUS PHASE.

- a) Stagnant droplet
- b) With laminar circulating droplet
- c) With turbulent circulating droplet

III OSCILLATION

APPENDIX D.2A

Experimental Overall Mass Transfer Coefficients of Single Drops and Drop Pairs During Formation.

Run No		t_f s	d m x 10^{-2}	A m^2 x 10^{-4}	C_1 kg x 10^{-3}.mol/L	C_2	N_f x 10^{-2} kg x 10^{-3}.mols	k_{df} x 10^{-2} m x $10^{-2}s^{-1}$
10	A	3.00	0.77	1.86	0.51	0.38	1.04	1.09
	B	1.50	0.74	1.72	"	0.41	1.43	1.63
	C	1.00	0.69	1.50	"	0.44	1.22	1.59
	D	0.76	0.68	1.45	"	0.46	1.10	1.48
	E	0.58	0.65	1.33	"	0.47	1.02	1.50
11	A	3.00	0.75	1.77	1.01	0.72	2.14	1.20
	B	1.55	0.71	1.58	"	0.78	2.87	1.80
	C	1.00	0.68	1.45	"	0.83	2.96	2.02
	D	0.72	0.66	1.37	"	0.86	3.14	2.27
	E	0.57	0.63	1.25	"	0.88	2.98	2.36
12	A	3.00	0.72	1.63	2.04	1.29	4.89	1.47
	B	1.50	0.69	1.50	"	1.52	5.96	1.96
	C	1.00	0.66	1.29	"	1.65	5.87	2.23
	D	0.68	0.63	1.25	"	1.73	5.97	2.34
13	A	3.10	0.68	1.45	3.01	1.72	6.85	1.57
	B	1.51	0.65	1.33	"	1.86	10.93	2.74
	C	1.00	0.62	1.21	"	2.34	8.36	2.30
	D	0.62	0.58	1.06	"	2.42	9.72	3.05
14	A	1.50	0.76	1.81	0.51	0.36	4.63	5.01
	B	1.00	0.70	1.54	"	0.38	4.71	5.99
	C	0.78	0.71	1.58	"	0.40	5.33	6.60
	D	0.55	0.68	1.45	"	0.43	7.18	9.69

Appendix D.2A continued

Run No	t_f s	d m x 10^{-2}	A m^2 x 10^{-4}	C_1 kg x 10^{-3}.mol /L	C_2	N_f x 10^{-2} kg x 10^{-3}.mol/s	k_{df} x 10^{-2} m x $10^{-2}s^{-1}$
15 A	1.62	0.74	1.72	1.01	0.61	10.48	6.03
B	1.00	0.69	1.50	"	0.73	9.63	6.36
C	0.82	0.68	1.45	"	0.79	8.83	6.03
D	0.61	0.67	1.41	"	0.82	9.81	6.89
16 A	3.11	0.76	1.81	2.11	1.16	14.04	3.68
B	1.55	0.71	1.58	"	1.22	21.52	6.46
C	1.00	0.67	1.41	"	1.42	21.73	7.30
D	0.72	0.66	1.37	"	1.54	23.83	8.24
17 A	3.15	0.83	2.16	0.51	0.34	3.25	2.94
B	1.55	0.79	1.96	"	0.22	9.69	9.67
C	1.00	0.75	1.77	"	0.40	4.90	5.42
D	0.57	0.72	1.63	"	0.43	5.55	6.66
18 A	1.56	0.77	1.86	1.01	0.57	13.48	7.17
B	1.00	0.75	1.77	"	0.61	19.44	10.87
C	0.81	0.72	1.63	"	0.73	13.51	8.21
D	0.55	0.68	1.45	"	1.82	11.37	7.67
19 A	1.51	0.75	1.77	2.05	1.21	24.58	6.77
B	1.01	0.72	1.63	"	1.35	27.36	8.19
C	0.79	0.70	1.54	"	1.38	30.46	9.65
D	0.62	0.67	1.41	"	1.46	29.97	10.37
20 A	3.10	0.69	1.50	3.00	0.87	23.64	5.25
B	1.51	0.65	1.33	"	2.31	13.14	3.29
C	1.00	0.60	1.13	"	2.62	8.60	2.54
D	0.61	0.56	0.99	"	2.81	3.62	1.22

Appendix D.2A continued

Run No	t_f s	d m x 10^{-2}	A m^2 x 10^{-4}	C_1 kg x 10^{-3}.mol /L	C_2	N_f x 10^{-2} kg x 10^{-3}.mol/s	k_{df} x 10^{-2} m x $10^{-2}$$s^{-1}$
21 A	3.15	0.91	2.60	0.51	0.31	5.04	3.79
B	1.56	0.84	2.21	"	0.28	9.19	8.73
C	1.00	0.80	2.01	"	0.37	7.56	7.36
D	0.65	0.77	1.86	"	0.40	8.16	8.59
22 A	3.00	0.87	2.38	1.08	0.58	11.49	5.32
B	1.50	0.81	2.06	"	0.62	17.07	7.67
C	1.00	0.77	1.86	"	0.70	18.17	9.05
D	0.70	0.73	1.67	"	0.79	16.88	9.36
23 A	3.15	0.78	1.91	2.42	0.86	24.61	5.32
B	1.60	0.74	1.72	"	1.50	24.40	5.86
C	1.01	0.72	1.63	"	1.64	30.49	7.73
D	0.60	0.68	1.45	"	1.99	28.01	7.98
24 A	1.50	0.92	2.66	0.51	0.30	11.47	8.44
B	1.00	0.88	2.43	"	0.34	12.20	9.83
25 A	2.55	0.80	2.01	2.10	1.38	24.91	5.90
B	1.05	0.75	1.77	"	1.52	24.40	6.56
26 A	1.00	0.71	1.58	3.50	2.34	43.48	7.6
B	0.78	0.64	1.29	"	2.67	29.21	6.27
27 A	0.86	0.69	1.50	3.42	2.58	33.60	6.55
B	0.55	0.61	1.17	"	2.98	19.06	4.76
28 A	1.10	0.76	1.81	3.36	2.21	48.06	7.90
B	0.75	0.68	1.45	"	2.61	32.93	6.76

APPENDIX D.2B

Theoretical Overall Dispersed Phase Mass Transfer Coefficients of Single Drops and Drop Pairs During Formation

Run No	t_f s	m x 10^{-2}	C_1 kg x 10^{-3}.mol/L	E_m x 10^{-2}	C_2 kg x 10^{-3}.mol/L	A m^2 x 10^{-4}	N_f x 10^{-2} kg x 10^{-3}.mol/s	K_{df} theo x 10^{-2} m x 10^{-2}. s^{-1}
10 A	3.00	0.77	0.51	13.56	0.44	1.86	1.44	1.52
B	1.50	0.74	0.51	9.98	0.46	1.72	0.91	1.04
C	1.00	0.69	0.51	8.74	0.46	1.49	0.74	0.97
D	0.76	0.68	0.51	7.73	0.47	1.45	0.57	0.77
E	0.58	0.65	0.51	7.06	0.47	1.33	0.50	0.73
11 A	3.00	0.75	1.01	13.92	0.86	1.77	2.85	1.59
B	1.55	0.71	1.01	10.57	0.90	1.58	1.77	1.11
C	1.00	0.68	1.01	8.86	0.92	1.45	1.27	0.87
D	0.72	0.66	1.01	7.75	0.93	1.37	1.04	0.75
E	0.57	0.63	1.01	7.22	0.93	1.24	0.90	0.72
12 A	3.00	0.72	2.04	14.50	1.74	1.63	5.01	1.51
B	1.50	0.69	2.04	10.70	1.82	1.49	3.23	1.06
C	1.00	0.66	2.04	9.48	1.84	1.37	2.44	0.87
D	0.68	0.63	2.04	8.28	1.87	1.25	1.90	0.75
13 A	3.10	0.68	3.01	16.56	2.51	1.45	6.99	1.51
B	1.51	0.65	3.01	12.09	2.64	1.33	4.52	1.13
C	1.00	0.62	3.01	10.32	2.69	1.21	3.28	0.90
D	0.62	0.58	3.01	8.69	2.74	1.06	2.34	0.73
14 A	1.50	0.76	0.51	9.71	0.46	1.81	0.99	1.07
B	1.00	0.70	0.51	8.61	0.46	1.54	0.77	0.98
C	0.78	0.71	0.51	7.50	0.47	1.58	0.65	0.81
D	0.55	0.68	0.51	6.57	0.47	1.45	0.57	0.77

Appendix D.2B continued

Run No	t_f s	m x 10^{-2}	C_1 kg x 10^{-3}.mol/L	E_m x 10^{-2}	C_2 kg x 10^{-3}.mol/L	A m^2 x 10^{-4}	N_f x 10^{-2} kg x 10^{-3}.mol/s	K_{df} theo x 10^{-2} m x 10^{-2}. s^{-1}
15 A	1.62	0.74	1.01	10.66	0.90	1.72	2.01	1.16
B	1.00	0.69	1.01	8.73	0.92	1.49	1.33	0.88
C	0.82	0.68	1.01	8.03	0.92	1.45	1.28	0.87
D	0.61	0.67	1.01	7.03	0.93	1.41	1.08	0.76
16 A	3.11	0.76	2.11	13.99	1.81	1.81	5.87	1.55
B	1.55	0.71	2.11	10.57	1.88	1.58	5.05	1.51
C	1.00	0.67	2.11	9.34	1.91	1.41	2.68	0.90
D	0.72	0.66	2.11	7.75	1.94	1.37	2.18	0.75
17 A	3.15	0.83	0.51	12.89	0.44	2.16	1.81	1.64
B	1.55	0.79	0.51	9.50	0.46	1.96	1.11	1.11
C	1.00	0.75	0.51	8.04	0.47	1.77	0.76	0.84
D	0.57	0.72	0.51	6.32	0.47	1.63	0.64	0.77
18 A	1.56	0.77	1.01	9.90	0.91	1.86	2.06	1.10
B	1.00	0.75	1.01	8.14	0.92	1.77	1.71	0.95
C	0.81	0.72	1.01	7.63	0.93	1.63	1.35	0.82
D	0.55	0.68	1.01	6.66	0.94	1.45	0.99	0.67
19 A	1.51	0.75	2.05	10.36	1.83	1.77	4.17	1.15
B	1.00	0.72	2.05	8.78	1.87	1.63	3.02	0.90
C	0.79	0.70	2.05	8.03	1.88	1.54	2.62	0.83
D	0.62	0.67	2.05	7.43	1.89	1.41	2.16	0.75
20 A	3.10	0.69	3.00	16.24	2.51	1.49	7.16	1.60
B	1.51	0.65	3.00	12.03	2.63	1.33	4.52	1.13
C	1.00	0.60	3.00	10.61	2.68	1.13	3.07	0.91
D	0.61	0.56	3.00	8.88	2.73	0.98	2.48	0.84

Appendix D.2B continued

Run No	t_f s	m x 10^{-2}	C_1 kg x 10^{-3}.mol/L	E_m x 10^{-2}	C_2 kg x 10^{-3}.mol/L	A m^2 x 10^{-4}	N_f x 10^{-2} kg x 10^{-3}.mol/s	K_{df} theo x 10^{-2} m x 10^{-2}. s^{-1}
21 A	3.15	0.91	0.51	11.76	0.45	2.06	2.04	1.54
B	1.56	0.84	0.51	8.96	0.46	2.21	1.34	1.19
C	1.00	0.80	0.51	7.53	0.47	2.01	0.92	0.90
D	0.65	0.77	0.51	7.48	0.47	1.86	0.82	0.86
22 A	3.00	0.87	1.08	12.16	0.94	2.37	4.15	1.62
B	1.50	0.81	1.08	9.23	0.98	2.06	2.39	1.07
C	1.00	0.77	1.08	7.93	0.99	1.86	1.85	0.92
D	0.70	0.73	1.08	7.30	1.00	1.67	1.40	0.78
23 A	3.15	0.78	2.42	14.41	2.07	1.91	7.40	1.60
B	1.60	0.74	2.42	10.83	2.15	1.72	4.88	1.17
C	1.00	0.72	2.42	8.80	2.20	1.63	3.66	0.93
D	0.60	0.68	2.42	7.22	2.24	1.45	2.25	0.64
24 A	1.50	0.92	0.51	8.02	0.47	2.66	1.41	1.04
B	1.00	0.88	0.51	6.85	0.47	2.43	1.23	0.99
25 A	1.55	0.80	2.11	9.77	1.90	2.01	4.83	1.14
B	1.05	0.75	2.11	8.58	1.92	1.77	3.60	0.96
26 A	1.00	0.71	3.50	9.11	3.18	1.58	5.08	0.92
B	0.78	0.64	3.50	8.93	3.18	1.29	3.72	0.82
27 A	0.86	0.69	3.42	8.69	3.12	1.45	4.38	0.88
B	0.55	0.61	3.42	7.87	3.15	1.19	2.72	0.67
28 A	1.10	0.76	3.35	8.78	3.05	1.81	5.85	0.96
B	0.75	0.68	3.35	8.11	3.07	1.45	3.90	0.80

APPENDIX D.2C

Experimental Overall Mass Transfer Coefficients of Dispersed Phase Droplet During Ascent of Single Drops and Drop Pairs (n = 2).

Run No	ω rad.s^{-1}	ε	d_o m x 10^{-2}	A_o m^2 x 10^{-4}	$\bar{A}$ m^2 x 10^{-4}	N_f x 10^{-2} kg x 10^{-3}.mol/s	K_{dexp} x 10^{-2} m x 10^{-2}s^{-1}
10 A	38.99	0.191	0.79	1.96	2.15	2.23	2.73
B	41.20	0.193	0.75	1.77	1.94	4.95	6.22
C	45.40	0.228	0.72	1.63	1.82	6.57	8.20
D	46.33	0.196	0.70	1.54	1.81	8.79	10.56
E	49.32	0.191	0.68	1.45	1.59	10.45	13.98
11 A	39.03	0.193	0.78	1.54	1.70	1.55	7.84
B	42.11	0.203	0.73	1.67	1.84	7.36	5.71
C	44.71	0.213	0.70	1.54	1.69	10.13	7.89
D	46.60	0.190	0.68	1.45	1.59	15.61	11.42
E	49.71	0.187	0.66	1.37	1.50	18.58	14.08
12 A	36.05	0.165	0.74	1.72	1.86	8.09	3.37
B	38.25	0.162	0.80	1.54	1.66	16.93	6.71
C	42.46	0.172	0.63	1.25	1.36	22.13	9.86
D	43.39	0.163	0.60	1.13	1.22	31.08	14.73
13 A	35.78	0.159	0.70	1.54	1.66	8.90	3.12
B	38.09	0.150	0.68	1.45	1.56	17.32	5.97
C	42.56	0.156	0.58	1.06	1.45	26.06	7.68
D	43.39	0.163	0.60	1.02	1.14	39.36	14.27
14 A	41.20	0.191	0.76	1.81	2.10	8.62	12.09
B	44.50	0.194	0.75	1.77	2.04	11.82	16.52
C	46.33	0.190	0.71	1.58	1.73	14.83	16.03
D	48.28	0.188	0.68	1.45	1.59	21.12	30.89

Appendix D.2C continued

Run No	ω rad.s^{-1}	ε	d_0 m x 10^{-2}	A_o m^2 x 10^{-4}	$\bar{A}$ m^2 x 10^{-4}	N_f x 10^{-2} kg x 10^{-3}.mol/s	K_{dexp} x 10^{-2} m x 10^{-2}s^{-1}
15 A	41.30	0.190	0.74	1.72	1.88	13.39	11.68
B	43.81	0.189	0.72	1.63	1.78	23.33	17.95
C	45.64	0.189	0.68	1.45	1.59	28.69	22.84
D	47.60	0.173	0.67	1.41	1.53	36.73	29.28
16 A	34.07	0.168	0.77	1.86	2.02	15.58	6.69
B	38.25	0.162	0.72	1.63	1.76	26.09	12.15
C	44.31	0.159	0.70	1.54	1.66	43.49	18.45
D	40.68	0.169	0.64	1.29	1.40	62.88	29.17
17 A	35.13	0.176	0.84	2.22	2.42	5.36	6.51
B	37.62	0.174	0.82	2.11	2.29	12.05	23.92
C	40.44	0.187	0.78	1.91	2.09	15.46	18.49
D	42.79	0.184	0.75	1.77	1.93	21.04	25.35
18 A	37.63	0.198	0.79	1.96	2.15	9.80	8.00
B	39.03	0.176	0.78	1.91	2.08	24.08	19.55
C	41.30	0.174	0.75	1.77	1.92	33.34	23.79
D	44.71	0.169	0.71	1.58	1.71	46.93	33.47
19 A	34.07	0.177	0.76	1.81	1.97	34.22	14.36
B	36.05	0.175	0.74	1.72	1.87	51.45	20.38
C	37.49	0.167	0.72	1.63	1.77	59.80	24.48
D	39.84	0.161	0.68	1.45	1.57	82.40	35.95
20 A	35.06	0.150	0.71	1.58	1.70	9.20	6.22
B	38.09	0.161	0.67	1.41	1.52	43.32	12.34
C	42.56	0.163	0.63	1.25	1.35	58.58	16.56
D	46.84	0.159	0.58	1.06	1.14	82.40	25.10

Appendix D.2C continued

Run No	ω rad.s^{-1}	ε	d_0 m x 10^{-2}	A_o m^2 x 10^{-4}	$\bar{A}$ m^2 x 10^{-4}	N_f x 10^{-2} kg x 10^{-3}.mol/s	K_{dexp} x 10^{-2} m x 10^{-2}s^{-1}
21 A	30.92	0.194	0.92	2.66	2.92	6.50	7.18
B	34.55	0.196	0.86	2.32	2.55	9.20	12.89
C	36.97	0.193	0.83	2.16	2.37	17.37	19.81
D	38.99	0.187	0.80	2.01	2.20	26.56	30.18
22 A	31.76	0.189	0.88	2.43	2.66	12.12	7.86
B	35.07	0.183	0.83	2.16	2.36	21.23	14.51
C	37.63	0.178	0.78	1.91	2.08	31.26	21.47
D	40.52	0.174	0.75	1.77	1.92	43.77	28.86
23 A	32.26	0.176	0.81	2.06	2.24	12.83	6.66
B	36.05	0.168	0.75	1.77	1.92	35.65	12.38
C	37.49	0.161	0.72	1.63	1.76	57.77	20.01
D	39.03	0.151	0.70	1.54	1.66	54.88	16.61
24 A	30.46	0.187	0.93	2.72	2.97	14.01	15.72
B	32.39	0.173	0.89	2.49	2.71	21.85	23.71
25 A	31.15	0.169	0.82	2.11	2.29	46.48	14.71
B	34.07	0.161	0.78	1.91	2.06	62.78	20.05
26 A	32.79	0.150	0.75	1.77	1.90	86.86	19.54
B	37.87	0.144	0.70	1.54	1.65	93.33	21.18
27 A	25.14	0.136	0.74	1.72	1.84	102.48	21.59
B	46.74	0.156	0.67	1.41	1.52	128.08	28.28
28 A	29.84	0.155	0.80	2.01	2.17	91.65	19.11
B	34.82	0.154	0.73	1.67	1.80	113.93	24.25

APPENDIX D.2D

Theoretical Overall Mass Transfer Coefficients of Stagnant and Single Drops and Drop Pairs

Run No	t_f s	$\bar{A}$ $m^2 \times 10^{-4}$	C_2 kg. mol x 10^{-3}/L	E_m x 10^{-2} *	C_3 kg.mol x 10^{-3}/L	$N_f \times 10^{-3}$ kg x 10^{-3}.mol/s **	$K_{d\ theo} \times 10^{-3}$ m x 10^{-2}. s^{-1}
10 A	3.00	2.15	0.38	7.33	0.35	6.18	7.56
B	1.50	1.94	0.41	5.39	0.39	3.66	4.60
C	1.00	1.82	0.44	4.72	0.42	2.97	3.71
D	0.76	1.81	0.46	4.18	0.44	2.84	2.31
E	0.58	1.59	0.47	3.82	0.45	2.48	3.31
11 A	3.00	1.70	0.72	7.62	0.6	11.39	9.31
B	1.55	1.84	0.78	5.79	0.73	8.06	5.61
C	1.00	1.69	0.83	4.85	0.79	5.66	4.04
D	0.72	1.50	0.86	3.96	0.82	5.18	4.01
E	0.57	1.50	0.88	3.96	0.85	3.38	2.56
12 A	3.00	1.86	1.29	8.14	1.11	18.36	7.65
B	1.50	1.66	1.52	6.01	1.43	13.22	5.24
C	1.00	1.36	1.65	5.13	1.57	10.28	4.58
D	0.68	1.22	1.73	4.43	1.65	8.94	4.24
13 A	3.10	1.66	1.72	8.96	1.57	20.99	7.35
B	1.51	1.56	1.86	6.54	1.74	14.67	5.05
C	1.00	1.45	2.34	5.58	2.21	13.78	4.06
D	0.62	1.14	2.42	4.70	2.31	9.55	3.49
14 A	1.50	1.98	0.36	5.25	0.34	3.66	5.13
B	1.00	1.94	0.38	4.46	0.36	3.10	4.21
C	0.78	1.73	0.40	4.05	0.38	2.84	4.10
D	0.44	1.59	0.43	3.55	0.41	2.60	3.80

Appendix D.2D continued

Run No	t_f s	$\bar{A}$ $m^2 \times 10^{-4}$	C_2 kg. mol x 10^{-3}/L	E_m x 10^{-2} *	C_3 kg.mol x 10^{-3}/L	$N_f \times 10^{-3}$ kg x 10^{-3}.mol/s **	K_d theo x 10^{-3} m x 10^{-2}. s^{-1}
15 A	1.62	1.88	0.61	5.68	0.57	6.72	5.86
B	1.00	1.78	0.73	4.65	0.70	4.44	3.42
C	0.82	1.59	0.79	4.33	0.75	5.42	4.31
D	0.61	1.53	0.82	3.85	0.78	4.95	3.94
16 A	3.11	2.02	1.16	7.92	1.07	17.00	7.25
B	1.55	1.76	1.22	5.98	1.15	10.29	4.79
C	1.00	1.66	1.42	5.02	1.35	9.37	3.98
D	0.72	1.40	1.54	4.32	1.47	9.01	4.18
17 A	3.15	2.42	0.34	6.97	0.32	5.16	6.27
B	1.55	2.29	0.22	5.14	0.21	2.23	4.42
C	1.00	2.09	0.40	4.34	0.38	3.81	4.56
D	0.57	1.93	0.43	3.42	0.41	3.37	4.06
18 A	1.56	2.15	0.57	5.35	0.54	6.17	5.03
B	1.00	2.08	0.61	4.40	0.58	5.70	4.49
C	0.81	1.92	0.73	4.13	0.70	5.04	3.60
D	0.55	1.71	0.82	3.60	0.79	4.25	3.03
19 A	1.51	1.97	1.21	5.56	1.414	13.20	5.54
B	1.00	1.87	1.35	4.72	1.29	10.01	3.97
C	0.79	1.77	1.38	4.31	1.32	9.20	3.77
D	0.62	1.57	1.46	3.99	1.40	8.07	3.52
20 A	3.10	1.70	0.87	27.82	0.63	35.50	24.00
B	1.51	1.52	2.31	20.61	1.83	59.35	16.90
C	1.00	1.35	2.62	18.17	2.14	46.68	13.20
D	0.61	1.14	2.88	15.20	2.44	34.79	10.60

Appendix D.2D continued

Run No	t_f s	$\bar{A}$ $m^2 \times 10^{-4}$	C_2 kg. mol x 10^{-3}/L	E_m x 10^{-2} *	C_3 kg.mol x 10^{-3}/L	$N_f \times 10^{-3}$ kg x 10^{-3}.mol/s **	$K_{d\ theo} \times 10^{-3}$ m x 10^{-2}. s^{-1}
21 A	3.15	2.92	0.31	6.36	0.29	6.80	7.51
B	1.50	2.55	0.28	4.75	0.27	2.68	2.84
C	1.00	2.37	0.37	4.07	0.35	4.62	5.27
D	0.65	2.20	0.40	3.41	0.39	2.06	2.34
22 A	3.00	2.66	0.58	6.58	0.54	11.86	7.69
B	1.50	2.36	0.62	5.00	0.59	7.18	4.91
C	1.00	2.08	0.70	4.29	0.67	6.17	4.24
D	0.70	1.92	0.79	3.79	0.76	5.26	3.46
23 A	3.15	2.24	0.86	7.80	0.79	14.82	7.69
B	1.60	1.92	1.50	6.03	1.41	14.99	5.20
C	1.00	1.76	1.67	4.90	1.59	12.24	4.16
D	0.60	1.66	1.99	3.91	1.91	11.22	3.40
24 A	1.50	2.97	0.30	4.34	0.29	3.51	3.94
B	1.00	2.71	0.34	3.70	0.33	3.08	3.34
25 A	1.55	2.29	1.38	4.63	1.32	13.75	4.35
B	1.05	2.06	1.52	3.98	1.46	11.26	3.60
26 A	1.00	1.90	2.34	4.37	2.24	15.88	3.57
B	0.78	1.65	2.67	4.12	2.56	12.80	2.90
27 A	0.86	1.84	2.58	4.57	2.46	17.50	3.69
B	0.55	1.52	2.98	3.71	2.87	11.09	2.45
28 A	1.10	2.17	2.21	4.83	2.10	21.46	4.47
B	0.75	1.80	2.61	4.46	2.49	16.75	3.57

$\bar{A}$ = from Appendix D.2C   * = r from Appendix D.1   ** = d from Appendix D.1

APPENDIX D.2E

Theoretical Mass Transfer Coefficient of Dispersed Phase Single Drops and Droplet Pairs With Solute Circulating Inside the Drop.

Run No	t_f s	r m x 10^{-2}	C_2 kgx10^{-3}.mol/L	E_m x 10^{-2}	C_3 kgx10^{-3}.mol/L	N_t x 10^{-3} kgx10^{-3}.mol/s *	K_d theor x 10^{-} m x 10^{-2}.s^{-1} **
10 A	3.00	0.385	0.38	10.99	0.34	8.24	10.09
B	1.50	0.370	0.41	8.09	0.38	5.49	6.90
C	1.00	0.345	0.44	7.08	0.41	3.72	4.64
D	0.76	0.340	0.46	6.26	0.41	7.10	8.52
E	0.58	0.325	0.47	5.73	0.44	3.71	4.98
11 A	3.00	0.375	0.72	1.43	0.64	15.20	12.42
B	1.55	0.355	0.78	8.68	0.71	11.28	7.86
C	1.00	0.340	0.83	7.28	0.77	8.50	6.06
D	0.72	0.330	0.86	6.37	0.81	6.47	5.02
E	0.57	0.315	0.88	5.93	0.83	5.63	4.26
12 A	3.00	0.360	1.29	12.25	1.13	26.70	11.13
B	1.50	0.345	1.52	9.04	1.38	20.57	8.15
C	1.00	0.330	1.65	7.69	1.52	16.71	7.45
D	0.68	0.315	1.73	6.67	1.61	13.42	6.36
13 A	3.10	0.340	1.72	13.43	1.49	32.15	11.26
B	1.51	0.325	1.86	9.81	1.68	21.97	7.57
C	1.00	0.310	2.34	8.33	2.14	21.21	6.25
D	0.62	0.290	2.42	7.01	2.25	14.74	5.34
14 A	1.50	0.380	0.36	7.88	0.33	5.49	7.70
B	1.00	0.365	0.38	6.98	0.35	4.64	6.30
C	0.78	0.355	0.40	6.08	0.37	4.26	6.15
D	0.55	0.340	0.43	5.33	0.40	3.89	5.69

Appendix D.2E continued

Run No	t_f s	r m x 10^{-2}	C_2 kgx10^{-3}.mol/L	E_m x 10^{-2}	C_3 kgx10^{-3}.mol/L	N_t x 10^{-3} kgx10^{-3}.mol/s *	K_d theor x 10^{-} m x 10^{-2}.s^{-1} **
15 A	1.62	0.370	0.61	8.52	0.56	8.40	7.33
B	1.00	0.355	0.73	7.16	0.68	7.40	5.69
C	0.82	0.345	0.79	6.50	0.74	6.77	5.39
D	0.61	0.335	0.82	5.77	0.77	6.18	4.93
16 A	3.11	0.380	1.16	11.88	1.02	26.29	11.21
B	1.55	0.355	1.22	8.98	1.11	16.08	7.49
C	1.00	0.340	1.42	7.53	1.31	14.76	6.26
D	0.72	0.355	1.54	6.48	1.44	12.80	5.93
17 A	3.15	0.415	0.34	10.45	0.30	10.32	12.55
B	1.55	0.395	0.22	7.70	0.20	4.45	8.83
C	1.00	0.375	0.40	6.52	0.37	5.71	6.83
D	0.57	0.360	0.43	5.13	0.40	5.05	6.09
18 A	1.56	0.385	0.57	8.26	0.52	10.28	8.39
B	1.00	0.375	0.61	6.79	0.57	7.60	5.99
C	0.81	0.360	0.73	6.37	0.68	8.40	6.00
D	0.55	0.340	0.82	5.55	0.77	7.08	5.05
19 A	1.51	0.375	1.21	8.32	1.11	18.78	7.88
B	1.00	0.360	1.35	7.05	1.25	16.61	6.58
C	0.79	0.350	1.38	6.44	1.29	13.74	5.62
D	0.62	0.335	1.46	5.96	1.37	12.05	5.26
20 A	3.10	0.345	0.87	13.22	0.75	17.54	11.86
B	1.51	0.325	2.31	9.79	2.08	28.10	8.01
C	1.00	0.300	2.62	8.63	2.39	22.10	6.25
D	0.61	0.280	2.88	7.22	2.67	16.41	5.00

Appendix D.2E continued

Run No	t_f s	r m x 10^{-2}	C_2 kgx10^{-3}.mol/L	E_m x 10^{-2}	C_3 kgx10^{-3}.mol/L	N_t x 10^{-3} kgx10^{-3}.mol/s *	K_d theor x 10^{-} m x 10^{-2}.s^{-1} **
21 A	3.15	0.405	0.31	10.71	0.28	10.20	11.27
B	1.56	0.420	0.28	7.27	0.26	5.35	7.49
C	1.00	0.400	0.37	6.11	0.35	4.62	5.27
D	0.65	0.395	0.40	4.99	0.38	4.12	4.68
22 A	3.00	0.435	0.58	9.87	0.52	17.79	15.53
B	1.50	0.405	0.62	7.50	0.57	11.96	8.17
C	1.00	0.395	0.70	6.28	0.66	8.22	5.65
D	0.70	0.365	0.79	5.68	0.75	7.01	4.52
23 A	3.15	0.390	0.86	11.66	0.76	21.12	10.96
B	1.60	0.360	1.50	9.00	1.37	21.59	7.50
C	1.00	0.350	1.67	7.32	1.55	18.32	6.23
D	0.60	0.340	1.99	5.84	1.87	11.54	3.49
24 A	1.50	0.460	0.30	6.51	0.28	7.03	7.89
B	1.00	0.440	0.34	5.56	0.32	6.15	6.68
25 A	1.55	0.40	1.38	7.98	1.27	25.21	7.98
B	1.00	0.375	1.52	6.84	1.42	18.80	6.00
26 A	1.00	0.355	2.34	7.39	2.17	27.21	6.12
B	0.78	0.320	2.67	7.24	2.48	11.67	2.65
27 A	0.86	0.345	2.58	7.05	2.40	50.95	10.73
B	0.55	0.355	2.98	5.48	2.82	11.85	2.62
28 A	1.10	0.380	2.21	7.24	2.05	31.26	6.52
B	0.75	0.340	2.61	6.68	2.44	31.92	6.79

* d_e from Appendix D.1

** $\bar{A}$ from Appendix D.2C

APPENDIX D.2F

Theoretical Overall Mass Transfer Coefficient of single drops and drop pairs during Turbulent Circulation of Solute Inside

Run	t_f s	C_D kg x 10^{-3}.mol/L	Velocity m x 10^{-2} s^{-1}	k_c x 10^{-3} m x 10^{-2} s^{-1}	k_d x 10^{-2} m x 10^{-2} s^{-1}	K_d x 10^{-3} m x 10^{-2} s^{-1}
10 A	3.00	0.511	9.76	2.19	2.30	2.69
B	1.50	0.511	9.85	3.10	2.32	3.63
C	1.00	0.511	8.38	3.79	1.97	4.15
D	0.76	0.511	10.10	4.35	2.38	4.82
E	0.58	0.511	10.81	4.98	2.54	5.44
11 A	3.00	1.01	9.28	2.19	2.21	2.58
B	1.55	1.01	8.86	3.05	2.11	3.41
C	1.00	1.01	9.81	3.79	2.33	4.15
D	0.72	1.01	10.29	4.47	2.45	4.75
E	0.57	1.01	10.86	5.02	2.58	5.31
12 A	3.00	2.04	11.23	2.19	2.73	2.35
B	1.50	2.04	10.85	3.10	2.63	3.20
C	1.00	2.04	10.43	3.79	2.53	3.79
D	0.68	2.04	11.11	4.60	2.70	4.51
13 A	3.10	3.01	9.95	2.15	2.45	2.07
B	1.51	3.01	11.29	3.09	2.78	2.91
C	1.00	3.01	10.83	3.79	2.67	3.47
D	0.62	3.01	12.00	4.82	2.96	4.33
14 A	1.50	0.511	9.98	3.10	2.35	3.64
B	1.00	0.511	11.76	3.79	2.77	4.43
C	0.78	0.511	10.56	4.29	2.48	3.82
D	0.55	0.511	9.28	5.11	2.18	5.35

Appendix D.2F continued

Run	t_f s	C_D kg x 10^{-3}.mol/L	Velocity m x 10^{-2} s^{-1}	k_c x 10^{-3} m x 10^{-2} s^{-1}	k_d x 10^{-2} m x 10^{-2} s^{-1}	K_d x 10^{-3} m x 10^{-2} s^{-1}
15 A	1.61	1.01	9.73	2.99	2.32	3.40
B	1.00	1.01	10.11	3.79	2.41	4.18
C	0.82	1.01	10.29	4.19	2.45	4.55
D	0.61	1.01	12.15	4.86	2.89	5.29
16 A	3.11	2.11	9.60	2.15	2.35	2.24
B	1.55	2.11	10.81	3.05	2.64	3.09
C	1.00	2.11	11.28	3.79	2.76	3.76
D	0.72	2.11	10.35	4.47	2.53	4.27
17 A	3.15	0.511	10.75	2.14	2.53	2.66
B	1.55	0.511	11.29	3.05	2.66	3.65
C	1.00	0.511	9.98	3.79	2.35	4.30
D	0.57	0.511	10.10	5.02	2.38	5.39
18 A	1.56	1.01	8.78	3.04	2.09	3.39
B	1.00	1.01	10.88	3.79	2.59	4.23
C	0.81	1.01	11.33	4.21	2.70	4.65
D	0.55	1.01	12.25	5.11	2.91	5.52
19 A	1.51	2.05	8.91	3.09	2.16	3.11
B	1.00	2.05	9.28	3.79	2.25	3.72
C	0.79	2.05	10.23	4.27	2.48	4.18
D	0.62	2.05	11.10	4.82	2.69	4.68
20 A	3.10	3.00	10.81	2.15	2.67	2.11
B	1.51	3.00	9.98	3.09	2.46	2.90
C	1.00	3.00	10.25	3.79	2.53	3.48
D	0.61	3.00	11.18	4.86	2.76	4.35

Appendix D.2F continued

Run	t_f s	C_D kg x 10^{-3}.mol/L	Velocity m x 10^{-2} s^{-1}	k_c x 10^{-3} m x 10^{-2} s^{-1}	k_d x 10^{-2} m x 10^{-2} s^{-1}	K_d x 10^{-3} m x 10^{-2} s^{-1}
21 A	3.15	0.511	8.67	2.14	2.04	2.59
B	1.56	0.511	8.93	3.04	2.10	3.51
C	1.00	0.511	10.21	3.79	2.40	4.31
D	0.65	0.511	11.35	4.70	2.67	5.24
22 A	3.00	1.08	8.86	2.19	2.11	2.53
B	1.50	1.08	9.71	3.10	2.31	3.47
C	1.00	1.08	10.43	3.79	2.48	4.15
D	0.70	1.08	11.21	4.53	2.67	4.87
23 A	3.15	2.42	9.91	2.14	2.42	2.17
B	1.60	2.42	11.25	3.00	2.75	2.97
C	1.00	2.42	10.87	3.79	2.66	3.63
D	0.60	2.42	9.36	4.90	2.29	4.40
24 A	1.50	0.511	10.10	3.10	2.38	3.65
B	1.00	0.511	11.86	3.79	2.79	4.43
25 A	1.55	2.10	9.98	3.05	2.43	3.09
B	1.05	2.10	12.35	3.70	3.01	3.76
26 A	1.00	3.50	10.28	3.79	2.55	3.30
B	0.78	3.50	11.61	4.29	2.88	3.73
27 A	0.86	3.42	10.83	4.09	2.67	3.61
B	0.55	3.42	11.19	5.11	2.78	4.39
28 A	1.10	3.36	11.46	3.62	2.84	3.30
B	0.75	3.36	12.61	4.38	3.12	3.94

APPENDIX D.2G

Experimental Overall Mass Transfer Coefficients of Single Drops and Drop Pairs During Oscillation (n = 4).

Run No	ω rad.s^{-1}	ε	d_m m x 10^{-2}	A_o m^2 x 10^{-2}	$\bar{A}$ m^2 x 10^{-2}	N_f x 10^{-2} kg x 10^{-3}.mol/s	K_{dexp} x 10^{-2} m x 10^{-2}s^{-1}
10 A	112.18	0.117	0.61	1.17	1.24	2.23	4.73
B	118.54	0.118	0.56	0.98	1.04	4.95	11.57
C	130.62	0.134	0.53	0.88	0.94	6.57	15.86
D	133.29	0.120	0.50	0.79	0.84	8.79	22.75
E	141.90	0.117	0.47	0.69	0.73	10.45	30.46
11 A	112.28	0.119	0.58	1.06	1.12	1.15	4.32
B	121.16	0.124	0.53	0.88	0.93	7.36	11.30
C	128.64	0.119	0.51	0.81	0.87	10.13	15.32
D	134.09	0.117	0.48	0.72	0.76	15.61	23.88
E	143.02	0.115	0.45	0.64	0.68	18.58	31.05
12 A	103.72	0.101	0.55	0.95	1.00	8.09	6.27
B	110.03	0.099	0.51	0.82	0.86	16.93	12.94
C	117.03	0.099	0.48	0.72	0.76	22.13	17.65
D	124.83	0.100	0.46	0.66	0.69	31.08	26.04
13 A	102.91	0.097	0.52	0.85	0.89	8.90	5.81
B	109.56	0.092	0.48	0.72	0.75	17.32	12.42
C	116.83	0.096	0.40	0.50	0.53	26.06	21.01
D	128.32	0.092	0.38	0.45	0.47	39.36	34.61
14 A	118.54	0.117	0.57	1.02	1.08	8.62	22.17
B	128.04	0.119	0.50	0.78	0.83	11.81	37.44
C	133.29	0.117	0.47	0.69	0.73	14.83	50.79
D	138.90	0.115	0.43	0.58	0.61	21.12	80.52

Appendix D.2G continued

Run No	ω rad.s^{-1}	ε	d_m m x 10^{-2}	A_o m^2 x 10^{-2}	$\bar{A}$ m^2 x 10^{-2}	N_f x 10^{-2} kg x 10^{-3}.mol/s	K_{dexp} x 10^{-2} m x 10^{-2}s^{-1}
15 A	118.84	0.117	0.48	0.72	0.76	13.39	28.88
B	126.07	0.115	0.45	0.64	0.68	23.33	47.00
C	131.32	0.116	0.42	0.55	0.59	28.69	61.55
D	136.96	0.106	0.40	0.50	0.53	36.73	84.51
16 A	98.01	0.104	0.46	0.66	0.69	15.68	19.59
B	110.03	0.099	0.43	0.58	0.61	26.09	35.06
C	114.61	0.098	0.40	0.55	0.58	43.49	52.80
D	117.03	0.104	0.38	0.45	0.47	62.88	86.87
17 A	101.09	0.108	0.57	1.02	1.07	5.36	14.73
B	108.25	0.106	0.54	0.92	0.97	12.05	56.47
C	116.35	0.115	0.53	0.88	0.93	15.46	41.56
D	123.13	0.112	0.50	0.78	0.82	21.04	59.67
18 A	108.26	0.122	0.64	1.28	1.36	9.80	12.64
B	112.29	0.108	0.61	1.17	1.23	24.80	33.05
C	118.84	0.106	0.58	1.06	1.12	33.34	40.78
D	128.64	0.104	0.55	0.95	1.00	46.94	57.24
19 A	98.01	0.108	0.61	1.17	1.23	34.22	22.99
B	103.72	0.107	0.59	1.09	1.15	51.45	33.14
C	107.86	0.102	0.56	0.98	1.03	59.80	42.07
D	114.61	0.099	0.52	0.85	0.89	82.40	63.41
20 A	100.81	0.092	0.57	1.02	1.07	9.20	9.88
B	109.55	0.099	0.56	0.98	1.03	43.32	18.21
C	122.42	0.100	0.53	0.88	0.92	58.58	24.30
D	134.72	0.097	0.50	0.78	0.82	82.40	34.89

Appendix D.2G continued

Run No	ω rad.s^{-1}	ε	d_m m x 10^{-2}	A_o m^2 x 10^{-2}	$\bar{A}$ m^2 x 10^{-2}	N_f x 10^{-2} kg x 10^{-3}.mol/s	K_{dexp} x 10^{-2} m x 10^{-2}s^{-1}
21 A	88.97	0.119	0.66	1.37	1.45	6.50	14.46
B	99.42	0.120	0.62	1.21	1.28	9.20	25.67
C	106.38	0.118	0.58	1.06	1.11	17.37	42.29
D	112.18	0.115	0.54	0.92	0.97	26.56	68.45
22 A	91.39	0.116	0.63	1.25	1.32	12.12	15.83
B	100.92	0.112	0.58	1.06	1.12	21.23	30.57
C	108.26	0.109	0.55	0.95	0.95	31.26	47.01
D	116.58	0.107	0.51	0.82	0.86	43.77	64.42
23 A	92.82	0.108	0.59	1.09	1.15	12.83	12.97
B	103.72	0.103	0.56	0.99	1.04	35.65	22.85
C	107.86	0.098	0.52	0.85	0.89	57.77	39.58
D	112.28	0.093	0.47	0.69	0.72	54.88	38.30
24 A	87.63	0.115	0.71	1.58	1.67	14.01	27.96
B	93.20	0.106	0.67	1.41	1.48	21.85	43.42
25 A	89.61	0.104	0.61	1.17	1.23	46.48	27.38
B	98.01	0.099	0.56	0.98	1.03	62.78	40.10
26 A	94.32	0.092	0.38	0.45	0.47	86.86	78.98
B	108.93	0.089	0.34	0.36	0.38	93.33	91.99
27 A	72.30	0.083	0.41	0.53	0.55	102.48	72.22
B	134.42	0.095	0.37	0.43	0.45	128.08	95.51
28 A	85.83	0.096	0.41	0.53	0.56	91.65	74.05
B	100.15	0.094	0.38	0.45	0.47	113.93	92.88

APPENDIX D.3

OUTPUT OF AREA VELOCITY PROGRAM APPENDIX C.3

APPENDIX D.3

TYPICAL OUTPUT OF AREA VELOCITY PROGRAM APPENDIX C.3 THIS SUMMURISES THE RESULTS FROM THREE RUNS ONLY.THE COMPLETE SET OF RESULTS HAVE BEEN SUBMITTED AS UNBOUND MATERIAL.

1- SINGLE DROPS.
RUN (11E).

```
 TIME   Y/X    Y/Z    XZ/Y    DA     SA     AR      V      VEL    RXY
                               2      2             3
 SEC                          CM.    CM.           CM.   CM/SEC
-----  -----  -----  -----  -----  -----  -----  -----  ------  -----
0.016  0.963  1.444  0.623  4.956  6.141  1.239  0.245   3.000  0.019
0.031  0.962  1.471  0.589  4.747  5.484  1.155  0.214   3.200  0.020
0.047  0.964  1.688  0.553  4.956  5.626  1.135  0.235   3.840  0.018
0.062  0.963  1.529  0.588  4.886  5.738  1.174  0.231   5.760  0.019
0.078  0.955  1.105  0.663  4.328  4.985  1.152  0.170   5.120  0.023
0.109  0.957  1.294  0.592  4.328  4.820  1.114  0.167   4.663  0.022
0.125  1.000  1.053  0.633  4.119  4.668  1.133  0.147   6.240  0.000
0.156  0.952  1.053  0.665  4.188  4.561  1.089  0.155   5.888  0.024
0.187  0.950  1.000  0.667  4.049  4.036  0.997  0.140   6.560  0.026
0.219  0.966  2.333  0.414  4.817  4.680  0.972  0.189   6.903  0.018
0.250  0.963  1.733  0.519  4.747  5.007  1.055  0.204   6.800  0.019
0.281  0.964  1.929  0.484  4.817  4.941  1.026  0.205   6.578  0.018
0.312  0.958  1.353  0.591  4.468  5.031  1.126  0.182   6.976  0.021
0.344  0.960  1.500  0.555  4.537  4.900  1.080  0.186   6.982  0.020
0.375  0.957  1.222  0.627  4.398  5.107  1.161  0.177   6.987  0.022
0.406  0.963  1.733  0.519  4.747  5.007  1.055  0.204   7.655  0.019
0.438  0.962  1.563  0.555  4.677  5.118  1.094  0.202   8.046  0.020
0.469  0.966  2.154  0.449  4.886  4.935  1.010  0.205   8.256  0.018
0.500  0.964  1.800  0.518  4.886  5.266  1.078  0.220   8.420  0.018
0.547  0.968  2.500  0.413  5.096  5.370  1.054  0.216   8.521  0.016
0.625  0.966  2.000  0.483  4.956  5.228  1.055  0.220   8.896  0.018
0.703  0.967  2.231  0.448  5.026  5.258  1.046  0.219   8.676  0.017
0.750  0.964  1.800  0.518  4.886  5.266  1.078  0.220   8.800  0.018
0.781  0.966  2.154  0.449  4.886  4.935  1.010  0.205   8.973  0.018
0.859  0.962  1.471  0.589  4.747  5.484  1.155  0.214   8.809  0.020
0.938  0.963  1.733  0.519  4.747  5.007  1.055  0.204   8.416  0.019
0.969  1.000  1.050  0.667  4.328  5.094  1.177  0.171   8.599  0.000
1.016  1.000  1.158  0.633  4.398  5.377  1.223  0.178   8.350  0.000
1.063  1.000  1.053  0.633  4.119  4.668  1.133  0.147   8.122  0.000
1.094  0.958  1.353  0.591  4.468  5.031  1.126  0.182   8.027  0.021
1.172  0.957  1.222  0.627  4.398  5.107  1.161  0.177   7.561  0.022
1.219  0.958  1.437  0.556  4.398  4.700  1.069  0.171   7.344  0.021
1.250  0.955  1.105  0.663  4.328  4.985  1.152  0.170   7.368  0.023
1.328  0.964  1.800  0.518  4.886  5.266  1.078  0.220   7.371  0.018
1.375  0.963  1.625  0.554  4.817  5.358  1.112  0.218   7.273  0.019
1.406  0.964  1.800  0.518  4.886  5.266  1.078  0.220   7.189  0.018
1.484  0.962  1.471  0.589  4.747  5.484  1.155  0.214   7.646  0.020
1.531  1.000  1.929  0.467  4.747  4.704  0.991  0.198   7.837  0.000
1.563  0.955  1.105  0.663  4.328  4.985  1.152  0.170   8.070  0.023
1.641  0.957  1.294  0.592  4.328  4.820  1.114  0.167   8.753  0.022
1.719  0.950  1.056  0.632  3.979  4.184  1.052  0.133   9.728  0.026
```

1.750	0.952	1.176	0.595	4.049	4.389	1.084	0.138	10.446	0.024
1.797	1.000	1.053	0.633	4.119	4.668	1.133	0.147	10.780	0.000
1.875	0.955	1.167	0.629	4.258	4.843	1.137	0.161	10.821	0.023
1.953	0.952	1.053	0.665	4.188	4.561	1.089	0.155	11.581	0.024
2.000	0.966	2.154	0.449	4.886	4.935	1.010	0.205	12.205	0.018
2.031	0.964	1.800	0.518	4.886	5.266	1.078	0.220	12.736	0.018
2.109	0.967	2.417	0.414	4.956	5.003	1.009	0.202	12.663	0.017
2.156	0.966	2.154	0.449	4.886	4.935	1.010	0.205	12.823	0.018
2.219	0.968	3.000	0.344	4.956	4.986	1.006	0.180	12.674	0.016
2.266	0.963	1.733	0.519	4.747	5.007	1.055	0.204	12.535	0.019
2.344	1.000	2.000	0.467	4.886	4.960	1.015	0.213	12.215	0.000
2.422	0.962	1.563	0.555	4.677	5.118	1.094	0.202	11.883	0.020
2.500	0.964	1.800	0.518	4.886	5.266	1.078	0.220	11.600	0.018
2.531	0.963	1.857	0.485	4.677	4.687	1.002	0.191	11.587	0.019
2.578	0.966	2.154	0.449	4.886	4.935	1.010	0.205	11.551	0.018
2.656	0.952	1.053	0.665	4.188	4.561	1.089	0.155	11.298	0.024
2.734	0.955	1.167	0.629	4.258	4.843	1.137	0.161	11.761	0.023
2.813	1.000	1.053	0.633	4.119	4.668	1.133	0.147	11.666	0.000
2.891	0.957	1.294	0.592	4.328	4.820	1.114	0.167	11.579	0.022
2.969	0.952	1.111	0.630	4.119	4.545	1.104	0.147	11.490	0.024
3.047	0.955	1.235	0.594	4.188	4.610	1.101	0.152	11.389	0.023
3.125	1.000	1.053	0.633	4.119	4.668	1.133	0.147	11.203	0.000
3.203	0.955	1.235	0.594	4.188	4.610	1.101	0.152	11.330	0.023
3.250	0.950	1.000	0.667	4.049	4.036	0.997	0.140	11.963	0.026
3.281	0.960	1.500	0.555	4.537	4.900	1.080	0.186	11.950	0.020
3.313	0.958	1.353	0.591	4.468	5.031	1.126	0.182	11.964	0.021
3.359	0.962	1.786	0.485	4.537	4.461	0.983	0.176	11.907	0.020
3.438	0.960	1.500	0.555	4.537	4.900	1.080	0.186	11.668	0.020
3.469	1.000	1.929	0.467	4.747	4.704	0.991	0.198	11.650	0.000
3.516	0.962	1.563	0.555	4.677	5.118	1.094	0.202	11.881	0.020
3.594	0.964	1.929	0.484	4.817	4.941	1.026	0.205	11.687	0.018
3.672	0.962	1.667	0.520	4.607	4.776	1.037	0.189	11.724	0.020
3.719	0.963	1.857	0.485	4.677	4.687	1.002	0.191	11.724	0.019
3.750	0.955	1.167	0.629	4.258	4.843	1.137	0.161	11.763	0.023
3.828	1.000	1.353	0.567	4.398	4.929	1.121	0.174	11.959	0.000
3.875	0.950	1.000	0.667	4.049	4.036	0.997	0.140	11.954	0.026
3.906	0.952	1.053	0.665	4.188	4.561	1.089	0.155	12.073	0.024
3.984	0.958	1.437	0.556	4.398	4.700	1.069	0.171	11.992	0.021
4.031	1.000	1.294	0.567	4.258	4.752	1.116	0.160	12.078	0.000
4.063	1.000	1.667	0.500	4.537	4.592	1.012	0.182	12.089	0.000
4.141	0.952	1.053	0.665	4.188	4.561	1.089	0.155	12.049	0.024
4.188	1.000	1.437	0.533	4.328	4.577	1.057	0.164	11.955	0.000
4.219	0.950	1.056	0.632	3.979	4.184	1.052	0.133	11.973	0.026
4.297	0.962	1.563	0.555	4.677	5.118	1.094	0.202	12.139	0.020
4.375	1.000	1.412	0.567	4.537	5.115	1.127	0.190	12.194	0.000
4.453	0.960	1.500	0.555	4.537	4.900	1.080	0.186	12.126	0.020
4.500	0.979	1.424	0.562	4.468	4.897	1.096	0.180	12.024	0.011
4.531	0.963	1.857	0.485	4.677	4.687	1.002	0.191	12.385	0.019
4.609	0.960	1.600	0.521	4.468	4.568	1.022	0.174	12.340	0.020
4.688	1.000	1.857	0.467	4.607	4.477	0.972	0.183	12.448	0.000
4.766	0.958	1.353	0.591	4.468	5.031	1.126	0.182	12.319	0.021
4.844	0.960	1.600	0.521	4.468	4.568	1.022	0.174	12.156	0.020
4.922	0.952	1.111	0.630	4.119	4.545	1.104	0.147	12.030	0.024
5.000	0.955	1.235	0.594	4.188	4.610	1.101	0.152	12.000	0.023

```
5.078  0.950  1.000  0.667  4.049  4.036  0.997  0.140  12.056  0.026
5.156  0.963  1.857  0.485  4.677  4.687  1.002  0.191  11.912  0.019
5.234  0.958  1.533  0.522  4.328  4.380  1.012  0.161  11.803  0.021
5.281  0.960  1.333  0.625  4.677  5.607  1.199  0.209  11.740  0.020
5.313  0.957  1.375  0.558  4.258  4.514  1.060  0.157  11.710  0.022
5.391  0.962  1.667  0.520  4.607  4.776  1.037  0.189  11.589  0.020
5.438  0.960  1.412  0.590  4.607  5.250  1.140  0.198  11.546  0.020
5.469  0.980  1.563  0.544  4.642  5.024  1.082  0.198  11.520  0.010
5.547  0.962  1.786  0.485  4.537  4.461  0.983  0.176  11.457  0.020
5.625  1.000  1.353  0.567  4.398  4.929  1.121  0.174  11.378  0.000
5.703  0.960  1.500  0.555  4.537  4.900  1.080  0.186  11.504  0.020
5.750  0.958  1.437  0.556  4.398  4.700  1.069  0.171  11.442  0.021
5.781  0.962  1.667  0.520  4.607  4.776  1.037  0.189  11.420  0.020
5.844  0.958  1.353  0.591  4.468  5.031  1.126  0.182  11.335  0.021
5.875  0.960  1.500  0.555  4.537  4.900  1.080  0.186  11.297  0.020
5.906  0.955  1.167  0.629  4.258  4.843  1.137  0.161  11.259  0.023
5.938  0.958  1.437  0.556  4.398  4.700  1.069  0.171  11.222  0.021
5.969  0.957  1.294  0.592  4.328  4.820  1.114  0.167  11.182  0.022
6.000  0.963  1.857  0.485  4.677  4.687  1.002  0.191  11.145  0.019
6.031  0.960  1.500  0.555  4.537  4.900  1.080  0.186  11.109  0.020
6.250  0.962  1.667  0.520  4.607  4.776  1.037  0.189  10.806  0.020
6.328  0.958  1.533  0.522  4.328  4.380  1.012  0.161  10.746  0.021
6.406  0.960  1.600  0.521  4.468  4.568  1.022  0.174  10.736  0.020
6.484  0.957  1.294  0.592  4.328  4.820  1.114  0.167  10.641  0.022
6.563  0.958  1.533  0.522  4.328  4.380  1.012  0.161  10.546  0.021
6.641  0.955  1.235  0.594  4.188  4.610  1.101  0.152  10.481  0.023
6.719  0.957  1.333  0.575  4.293  4.668  1.087  0.162  10.378  0.022
6.797  1.000  1.167  0.600  4.188  4.864  1.161  0.154  10.280  0.000
6.844  0.962  1.786  0.485  4.537  4.461  0.983  0.176  10.215  0.020
6.875  0.958  1.533  0.522  4.328  4.380  1.012  0.161  10.182  0.021
6.953  0.960  1.714  0.486  4.398  4.259  0.969  0.163  10.086  0.020
7.031  0.957  1.467  0.523  4.188  4.208  1.005  0.147   9.998  0.022

                             X               Y               Z

  MEAN                   5.205E-01       5.025E-01       3.416E-01

  VARIANCE               6.236E-02       5.825E-02       2.714E-02



                         SLOPE           INTERCEPT       CORR.COFF.

  X-VS-T                -0.00873         0.84744        -0.19921
  Y-VS-T                -0.00870         0.81900        -0.20325
  Z-VS-T                -0.00179         0.54370        -0.05909
```

2- DROP PAIRS.
A.RUN (17C1).

```
TIME   Y/X    Y/Z    XZ/Y    DA     SA     AR     V      VEL     RXY
```

SEC				CM.^2	CM.^2		CM.^3	CM/SEC	
0.031	0.962	1.471	0.589	4.747	5.484	1.155	0.214	4.800	0.020
0.062	0.960	1.333	0.625	4.677	5.607	1.199	0.209	4.960	0.020
0.094	0.963	1.733	0.519	4.747	5.007	1.055	0.204	5.120	0.019
0.141	0.962	1.471	0.589	4.747	5.484	1.155	0.214	4.907	0.020
0.187	0.964	1.800	0.518	4.886	5.266	1.078	0.220	5.227	0.018
0.234	0.958	1.278	0.626	4.537	5.357	1.181	0.193	5.717	0.021
0.312	0.960	1.500	0.555	4.537	4.900	1.080	0.186	6.048	0.020
0.344	0.955	1.105	0.663	4.328	4.985	1.152	0.170	6.865	0.023
0.391	0.957	1.222	0.627	4.398	5.107	1.161	0.177	7.296	0.022
0.469	0.952	1.053	0.665	4.188	4.561	1.089	0.155	7.019	0.024
0.547	0.963	2.000	0.450	4.607	4.399	0.955	0.177	6.912	0.019
0.625	0.960	1.500	0.555	4.537	4.900	1.080	0.186	6.576	0.020
0.703	0.962	1.786	0.485	4.537	4.461	0.983	0.176	6.912	0.020
0.750	0.958	1.437	0.556	4.398	4.700	1.069	0.171	6.947	0.021
0.078	0.964	2.250	0.415	4.677	4.396	0.940	0.176	76.800	0.018
0.828	0.962	1.667	0.520	4.607	4.776	1.037	0.189	8.163	0.020
0.859	0.963	1.857	0.485	4.677	4.687	1.002	0.191	8.390	0.019
0.938	0.952	1.053	0.665	4.188	4.561	1.089	0.155	8.352	0.024
1.016	0.957	1.294	0.592	4.328	4.820	1.114	0.167	7.985	0.022
1.094	0.950	1.000	0.667	4.049	4.036	0.997	0.140	8.091	0.026
1.141	0.958	1.437	0.556	4.398	4.700	1.069	0.171	7.899	0.021
1.172	0.955	1.167	0.629	4.258	4.843	1.137	0.161	8.286	0.023
1.219	0.957	1.375	0.558	4.258	4.514	1.060	0.157	8.230	0.022
1.250	0.952	1.176	0.595	4.049	4.389	1.084	0.138	8.216	0.024
1.328	0.963	2.000	0.450	4.607	4.399	0.955	0.177	8.358	0.019
1.406	0.960	1.500	0.555	4.537	4.900	1.080	0.186	8.427	0.020
1.438	0.962	1.786	0.485	4.537	4.461	0.983	0.176	8.348	0.020
1.484	0.958	1.437	0.556	4.398	4.700	1.069	0.171	8.792	0.021
1.563	0.960	1.600	0.521	4.468	4.568	1.022	0.174	9.056	0.020
1.641	0.958	1.353	0.591	4.468	5.031	1.126	0.182	9.301	0.021
1.719	0.962	1.786	0.485	4.537	4.461	0.983	0.176	9.327	0.020
1.797	0.955	1.167	0.629	4.258	4.843	1.137	0.161	10.029	0.023
1.844	0.957	1.294	0.592	4.328	4.820	1.114	0.167	10.132	0.022
1.875	0.952	1.053	0.665	4.188	4.561	1.089	0.155	10.245	0.024
1.922	0.957	1.375	0.558	4.258	4.514	1.060	0.157	10.407	0.022
1.953	1.000	1.053	0.633	4.119	4.668	1.133	0.147	10.568	0.000
2.031	0.960	1.600	0.521	4.468	4.568	1.022	0.174	10.338	0.020
2.109	0.958	1.437	0.556	4.398	4.700	1.069	0.171	10.183	0.021
2.188	0.963	2.000	0.450	4.607	4.399	0.955	0.177	10.034	0.019
2.266	1.000	1.667	0.500	4.537	4.592	1.012	0.182	9.860	0.000
2.344	0.962	1.786	0.485	4.537	4.461	0.983	0.176	9.813	0.020
2.422	0.960	1.500	0.555	4.537	4.900	1.080	0.186	9.790	0.020
2.500	0.962	1.923	0.451	4.468	4.177	0.935	0.164	9.764	0.020
2.578	0.958	1.437	0.556	4.398	4.700	1.069	0.171	9.941	0.021
2.656	0.960	1.600	0.521	4.468	4.568	1.022	0.174	9.788	0.020
2.734	0.955	1.167	0.629	4.258	4.843	1.137	0.161	9.830	0.023
2.813	0.957	1.294	0.592	4.328	4.820	1.114	0.167	9.639	0.022
2.891	0.952	1.053	0.665	4.188	4.561	1.089	0.155	9.700	0.024
2.969	0.955	1.167	0.629	4.258	4.843	1.137	0.161	9.718	0.023
3.047	0.950	1.000	0.667	4.049	4.036	0.997	0.140	9.603	0.026
3.125	0.963	2.000	0.450	4.607	4.399	0.955	0.177	9.712	0.019

```
3.203   0.958   1.437   0.556   4.398   4.700   1.069   0.171    9.678   0.021
3.281   0.962   1.786   0.485   4.537   4.461   0.983   0.176    9.670   0.020
3.359   0.960   1.600   0.521   4.468   4.568   1.022   0.174    9.719   0.020
3.438   0.963   2.000   0.450   4.607   4.399   0.955   0.177    9.885   0.019
3.516   0.962   1.786   0.485   4.537   4.461   0.983   0.176    9.865   0.020
3.594   0.964   2.077   0.449   4.747   4.651   0.980   0.191    9.770   0.018
3.672   0.962   1.786   0.485   4.537   4.461   0.983   0.176   10.017   0.020
3.750   0.963   2.167   0.415   4.537   4.145   0.914   0.163    9.960   0.019
3.828   0.957   1.222   0.627   4.398   5.107   1.161   0.177    9.757   0.022
3.906   1.042   1.563   0.512   4.537   4.798   1.057   0.186    9.818   -.020
3.984   0.955   1.235   0.594   4.188   4.610   1.101   0.152    9.788   0.023
4.063   0.957   1.375   0.558   4.258   4.514   1.060   0.157    9.713   0.022
4.000   1.000   1.111   0.600   4.049   4.612   1.139   0.140   10.028   0.000
4.219   0.952   1.176   0.595   4.049   4.389   1.084   0.138    9.873   0.024
4.297   0.950   1.000   0.667   4.049   4.036   0.997   0.140    9.775   0.026
4.375   0.962   1.923   0.451   4.468   4.177   0.935   0.164    9.863   0.020
4.453   0.958   1.533   0.522   4.328   4.380   1.012   0.161    9.910   0.021
4.531   0.960   1.714   0.486   4.398   4.259   0.969   0.163    9.986   0.020
4.609   0.957   1.294   0.592   4.328   4.820   1.114   0.167   10.047   0.022
4.688   0.958   1.437   0.556   4.398   4.700   1.069   0.171   10.240   0.021
4.766   0.952   1.111   0.630   4.119   4.545   1.104   0.147   10.334   0.024
4.844   0.955   1.235   0.594   4.188   4.610   1.101   0.152   10.426   0.023
4.922   1.000   1.053   0.633   4.119   4.668   1.133   0.147   10.573   0.000
5.000   0.960   1.714   0.486   4.398   4.259   0.969   0.163   10.642   0.020
5.078   0.957   1.375   0.558   4.258   4.514   1.060   0.157   10.722   0.022
5.156   0.958   1.533   0.522   4.328   4.380   1.012   0.161   10.857   0.021
5.234   0.952   1.111   0.630   4.119   4.545   1.104   0.147   10.945   0.024
5.313   0.955   1.235   0.594   4.188   4.610   1.101   0.152   11.070   0.023
5.391   1.000   1.111   0.600   4.049   4.612   1.139   0.140   11.125   0.000
5.469   0.960   1.714   0.486   4.398   4.259   0.969   0.163   11.013   0.020
5.547   0.958   1.437   0.556   4.398   4.700   1.069   0.171   10.972   0.021
5.625   0.962   1.667   0.520   4.607   4.776   1.037   0.189   10.869   0.020
5.703   0.952   1.111   0.630   4.119   4.545   1.104   0.147   10.855   0.024
5.781   0.957   1.375   0.558   4.258   4.514   1.060   0.157   10.792   0.022
5.859   0.950   1.056   0.632   3.979   4.184   1.052   0.133   10.750   0.026
5.938   0.955   1.235   0.594   4.188   4.610   1.101   0.152   10.814   0.023
6.016   0.952   1.111   0.630   4.119   4.545   1.104   0.147   10.935   0.024
6.094   0.957   1.375   0.558   4.258   4.514   1.060   0.157   10.926   0.022
6.172   1.000   1.053   0.633   4.119   4.668   1.133   0.147   10.856   0.000
6.250   0.960   1.714   0.486   4.398   4.259   0.969   0.163   10.898   0.020
6.328   0.957   1.375   0.558   4.258   4.514   1.060   0.157   10.839   0.022
6.484   0.962   1.923   0.451   4.468   4.177   0.935   0.164   10.663   0.020
6.719   0.958   1.437   0.556   4.398   4.700   1.069   0.171   10.419   0.021
6.953   0.960   1.714   0.486   4.398   4.259   0.969   0.163   10.093   0.020

                              X                  Y                  Z

  MEAN                    3.770E-01          3.625E-01          2.540E-01

  VARIANCE                8.507E-02          7.871E-02          3.936E-02
```

	SLOPE	INTERCEPT	CORR.COFF.
X-VS-T	-0.01038	0.82513	-0.27690
Y-VS-T	-0.00964	0.79237	-0.26457
Z-VS-T	-0.00071	0.53684	-0.02204

B.RUN (17C2).

TIME SEC	Y/X	Y/Z	XZ/Y	DA CM.^{2}	SA CM.^{2}	AR	V CM.^{3}	VEL CM/SEC	RXY
0.031	0.960	1.500	0.555	4.537	4.900	1.080	0.186	4.800	0.020
0.062	0.962	1.667	0.520	4.607	4.776	1.037	0.189	4.960	0.020
0.094	0.957	1.222	0.627	4.398	5.107	1.161	0.177	5.120	0.022
0.141	0.958	1.353	0.591	4.468	5.031	1.126	0.182	4.907	0.021
0.187	0.955	1.105	0.663	4.328	4.985	1.152	0.170	5.227	0.023
0.234	0.962	1.786	0.485	4.537	4.461	0.983	0.176	5.717	0.020
0.312	0.958	1.353	0.591	4.468	5.031	1.126	0.182	6.048	0.021
0.344	0.964	2.077	0.449	4.747	4.651	0.980	0.191	6.865	0.018
0.391	0.963	1.857	0.485	4.677	4.687	1.002	0.191	7.296	0.019
0.469	0.966	2.545	0.380	4.747	4.462	0.940	0.173	7.019	0.018
0.547	0.957	1.294	0.592	4.328	4.820	1.114	0.167	6.912	0.022
0.625	0.960	1.500	0.555	4.537	4.900	1.080	0.186	6.576	0.020
0.703	0.958	1.353	0.591	4.468	5.031	1.126	0.182	6.912	0.021
0.750	0.962	1.667	0.520	4.607	4.776	1.037	0.189	6.947	0.020
0.781	0.955	1.167	0.629	4.258	4.843	1.137	0.161	7.680	0.023
0.828	0.958	1.437	0.556	4.398	4.700	1.069	0.171	8.163	0.021
0.859	0.957	1.294	0.592	4.328	4.820	1.114	0.167	8.390	0.022
0.938	0.966	2.545	0.380	4.747	4.462	0.940	0.173	8.352	0.018
1.016	0.963	2.000	0.450	4.607	4.399	0.955	0.177	7.985	0.019
1.094	0.967	2.900	0.345	4.817	4.611	0.957	0.169	8.091	0.017
1.141	0.962	1.786	0.485	4.537	4.461	0.983	0.176	7.899	0.020
1.172	0.964	2.250	0.415	4.677	4.396	0.940	0.176	8.286	0.018
1.219	0.963	1.857	0.485	4.677	4.687	1.002	0.191	8.230	0.019
1.250	1.000	2.900	0.333	4.747	4.324	0.911	0.163	8.216	0.000
1.328	1.000	1.437	0.533	4.328	4.577	1.057	0.164	8.358	0.000
1.406	0.962	1.786	0.485	4.537	4.461	0.983	0.176	8.427	0.020
1.438	0.958	1.437	0.556	4.398	4.700	1.069	0.171	8.348	0.021
1.484	0.962	1.786	0.485	4.537	4.461	0.983	0.176	8.792	0.020
1.563	0.957	1.294	0.592	4.328	4.820	1.114	0.167	9.056	0.022
1.641	1.000	2.000	0.433	4.537	4.192	0.924	0.170	9.301	0.000
1.719	0.958	1.353	0.591	4.468	5.031	1.126	0.182	9.327	0.021
1.797	0.964	2.250	0.415	4.677	4.396	0.940	0.176	10.029	0.018
1.844	0.963	2.000	0.450	4.607	4.399	0.955	0.177	10.132	0.019
1.875	0.966	2.545	0.380	4.747	4.462	0.940	0.173	10.245	0.018
1.922	0.963	2.000	0.450	4.607	4.399	0.955	0.177	10.407	0.019
1.953	0.967	2.900	0.345	4.817	4.611	0.957	0.169	10.568	0.017
2.031	1.000	1.667	0.500	4.537	4.592	1.012	0.182	10.338	0.000
2.109	0.962	1.786	0.485	4.537	4.461	0.983	0.176	10.183	0.020
2.188	0.957	1.294	0.592	4.328	4.820	1.114	0.167	10.034	0.022
2.266	0.958	1.437	0.556	4.398	4.700	1.069	0.171	9.860	0.021

2.344	1.000	1.500	0.533	4.468	4.749	1.063	0.179	9.813	0.000
2.422	1.000	1.786	0.467	4.468	4.276	0.957	0.170	9.790	0.000
2.500	0.958	1.437	0.556	4.398	4.700	1.069	0.171	9.764	0.021
2.578	0.962	1.923	0.451	4.468	4.177	0.935	0.164	9.941	0.020
2.656	0.958	1.437	0.556	4.398	4.700	1.069	0.171	9.788	0.021
2.734	0.964	2.250	0.415	4.677	4.396	0.940	0.176	9.830	0.018
2.813	0.963	2.000	0.450	4.607	4.399	0.955	0.177	9.639	0.019
2.891	0.966	2.800	0.345	4.677	4.281	0.915	0.157	9.700	0.018
2.969	0.964	2.455	0.380	4.607	4.176	0.907	0.161	9.718	0.018
3.047	0.967	2.900	0.345	4.817	4.611	0.957	0.169	9.603	0.017
3.125	1.000	1.437	0.533	4.328	4.577	1.057	0.164	9.712	0.000
3.203	0.962	1.786	0.485	4.537	4.461	0.983	0.176	9.678	0.020
3.281	0.958	1.533	0.522	4.328	4.380	1.012	0.161	9.670	0.021
3.359	0.960	1.500	0.555	4.537	4.900	1.080	0.186	9.719	0.020
3.438	1.000	1.437	0.533	4.328	4.577	1.057	0.164	9.885	0.000
3.516	0.958	1.533	0.522	4.328	4.380	1.012	0.161	9.865	0.021
3.594	0.955	1.235	0.594	4.188	4.610	1.101	0.152	9.770	0.023
3.672	1.000	1.600	0.500	4.398	4.408	1.002	0.168	10.017	0.000
3.750	0.957	1.222	0.627	4.398	5.107	1.161	0.177	9.960	0.022
3.828	0.963	2.167	0.415	4.537	4.145	0.914	0.163	9.916	0.019
3.906	0.962	1.786	0.485	4.537	4.461	0.983	0.176	9.818	0.020
3.984	0.964	2.250	0.415	4.677	4.396	0.940	0.176	9.788	0.018
4.063	0.963	2.000	0.450	4.607	4.399	0.955	0.177	9.713	0.019
4.141	0.967	2.900	0.345	4.817	4.611	0.957	0.169	9.687	0.017
4.219	0.966	2.545	0.380	4.747	4.462	0.940	0.173	9.873	0.018
4.297	0.967	2.900	0.345	4.817	4.611	0.957	0.169	9.775	0.017
4.375	0.958	1.533	0.522	4.328	4.380	1.012	0.161	9.863	0.021
4.453	0.962	1.786	0.485	4.537	4.461	0.983	0.176	9.910	0.020
4.531	0.958	1.437	0.556	4.398	4.700	1.069	0.171	9.986	0.021
4.609	0.963	2.000	0.450	4.607	4.399	0.955	0.177	10.047	0.019
4.688	0.962	1.786	0.485	4.537	4.461	0.983	0.176	10.240	0.020
4.766	0.966	2.333	0.414	4.817	4.680	0.972	0.189	10.334	0.018
4.844	0.964	2.077	0.449	4.747	4.651	0.980	0.191	10.426	0.018
4.922	0.967	2.900	0.345	4.817	4.611	0.957	0.169	10.573	0.017
5.000	0.960	1.600	0.521	4.468	4.568	1.022	0.174	10.642	0.020
5.078	0.963	2.167	0.415	4.537	4.145	0.914	0.163	10.722	0.019
5.156	0.962	1.786	0.485	4.537	4.461	0.983	0.176	10.857	0.020
5.234	0.966	2.545	0.380	4.747	4.462	0.940	0.173	10.945	0.018
5.313	0.964	2.250	0.415	4.677	4.396	0.940	0.176	11.070	0.018
5.391	0.966	2.800	0.345	4.677	4.281	0.915	0.157	11.125	0.018
5.469	0.960	1.500	0.555	4.537	4.900	1.080	0.186	11.013	0.020
5.547	0.962	1.923	0.451	4.468	4.177	0.935	0.164	10.972	0.020
5.625	0.958	1.437	0.556	4.398	4.700	1.069	0.171	10.869	0.021
5.703	0.964	2.250	0.415	4.677	4.396	0.940	0.176	10.855	0.018
5.781	0.963	2.000	0.450	4.607	4.399	0.955	0.177	10.792	0.019
5.859	0.964	2.455	0.380	4.607	4.176	0.907	0.161	10.750	0.018
5.938	0.963	2.167	0.415	4.537	4.145	0.914	0.163	10.814	0.019
6.016	0.964	2.077	0.449	4.747	4.651	0.980	0.191	10.935	0.018
6.094	0.962	1.667	0.520	4.607	4.776	1.037	0.189	10.926	0.020
6.172	0.964	2.455	0.380	4.607	4.176	0.907	0.161	10.856	0.018
6.250	0.960	1.500	0.555	4.537	4.900	1.080	0.186	10.898	0.020
6.328	0.962	1.786	0.485	4.537	4.461	0.983	0.176	10.839	0.020
6.484	0.960	1.600	0.521	4.468	4.568	1.022	0.174	10.663	0.020
6.719	0.962	1.923	0.451	4.468	4.177	0.935	0.164	10.419	0.020

```
6.953  0.958  1.437  0.556  4.398  4.700  1.069  0.171  10.093  0.021

                         X              Y              Z

MEAN                 4.125E-01      3.981E-01      2.206E-01

VARIANCE             1.012E-01      9.434E-02      3.104E-02


                       SLOPE        INTERCEPT       CORR.COFF.

X-VS-T                0.00738        0.84585         0.20214
Y-VS-T                0.00683        0.81737         0.19053
Z-VS-T               -0.01049        0.49648        -0.26998
```

APPENDIX D.4

OUTPUT OF COMPUTER PROGRAM APPENDIX C.4

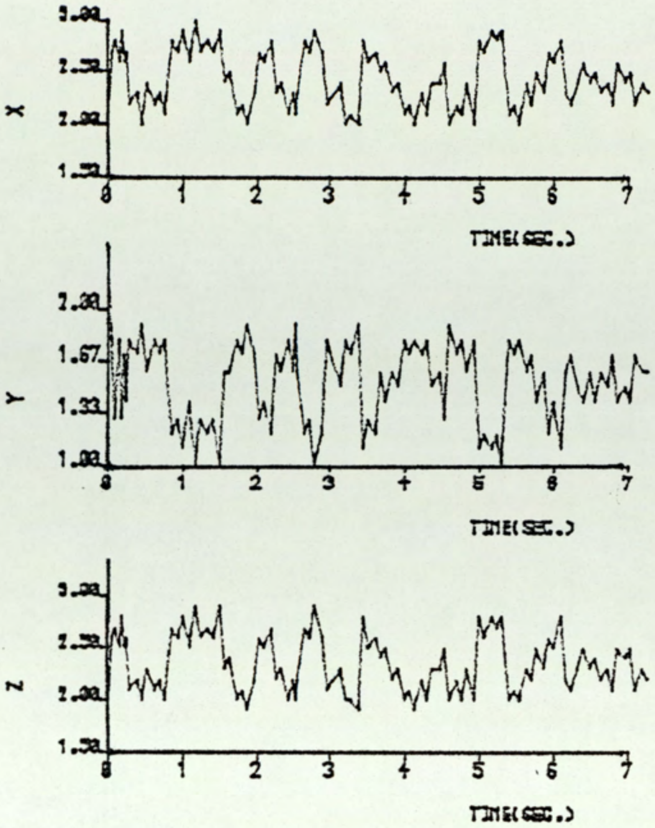

FIGURE D.37 X, Y, Z VS TIME RUN 18A1

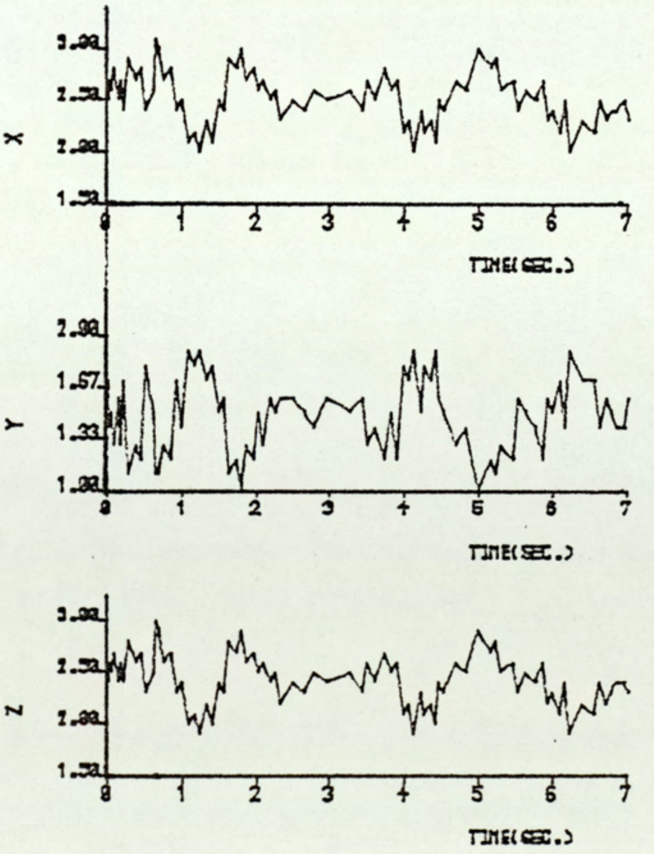

FIGURE D.36 X, Y, Z VS TIME RUN 17A1

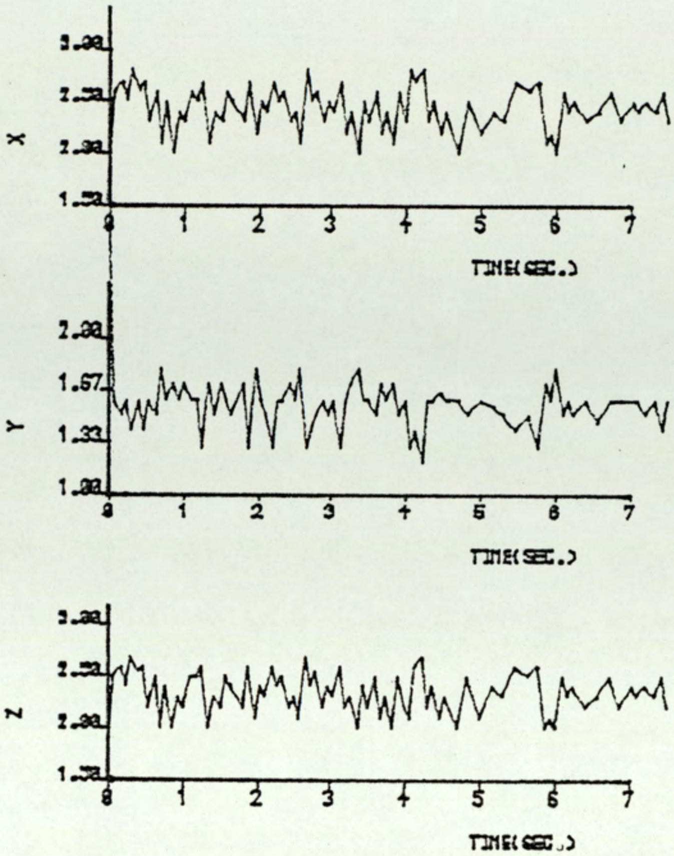

FIGURE D.39 X, Y, Z VS TIME RUN 28A1

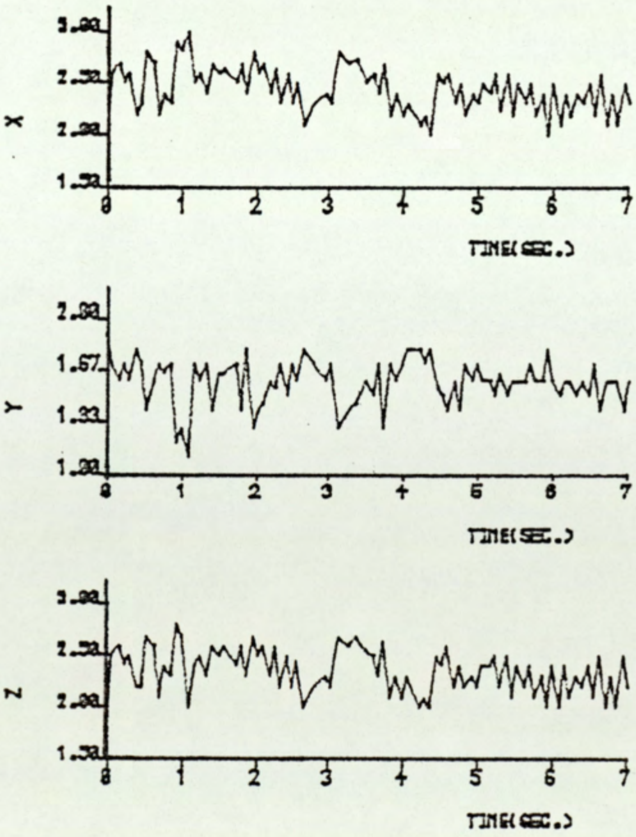

FIGURE D.38 X, Y, Z VS TIME RUN 26A1

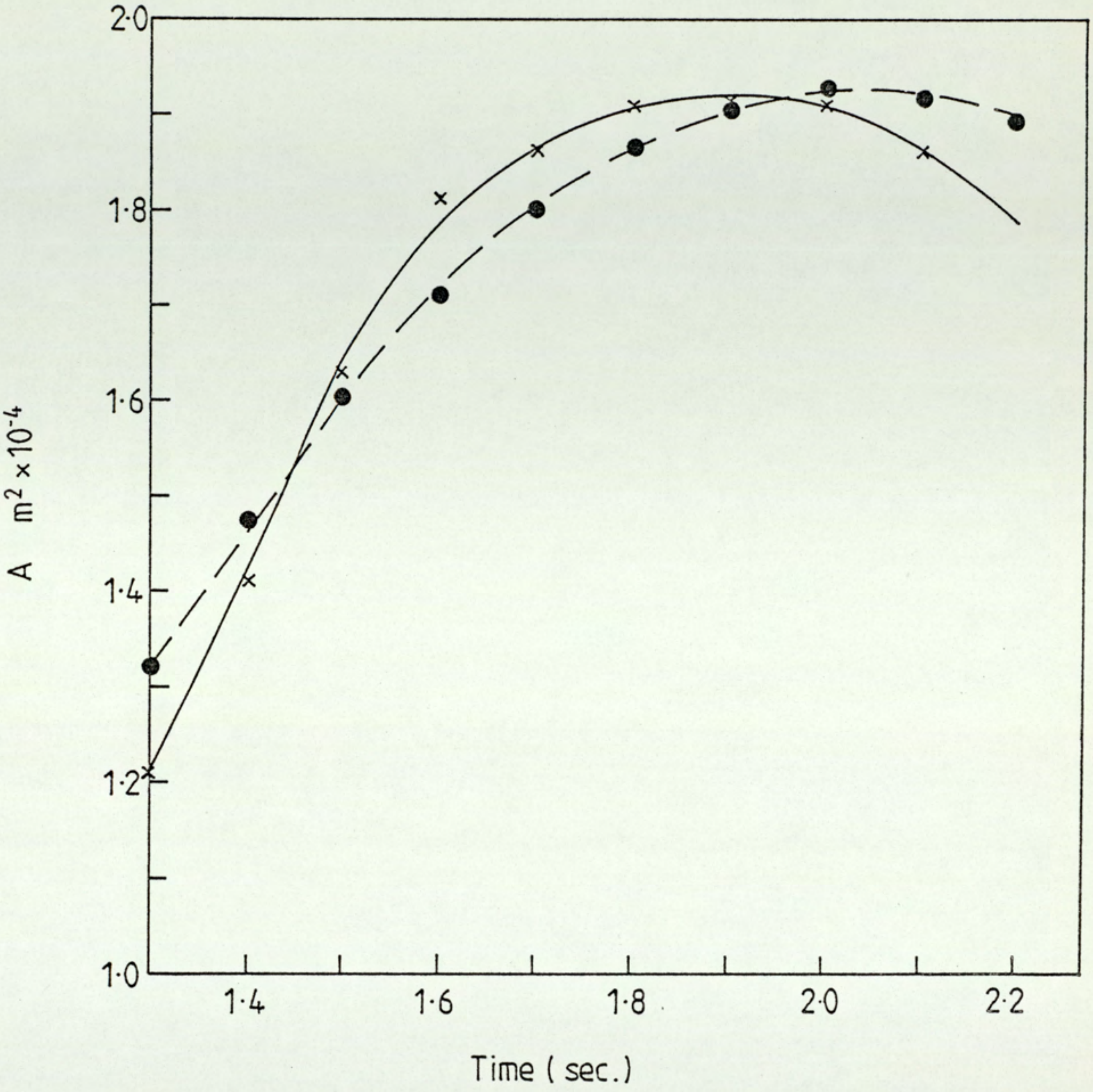

Figure D3. Droplet area during formation vs. time for (Run C)
× Observed, ● Calculated

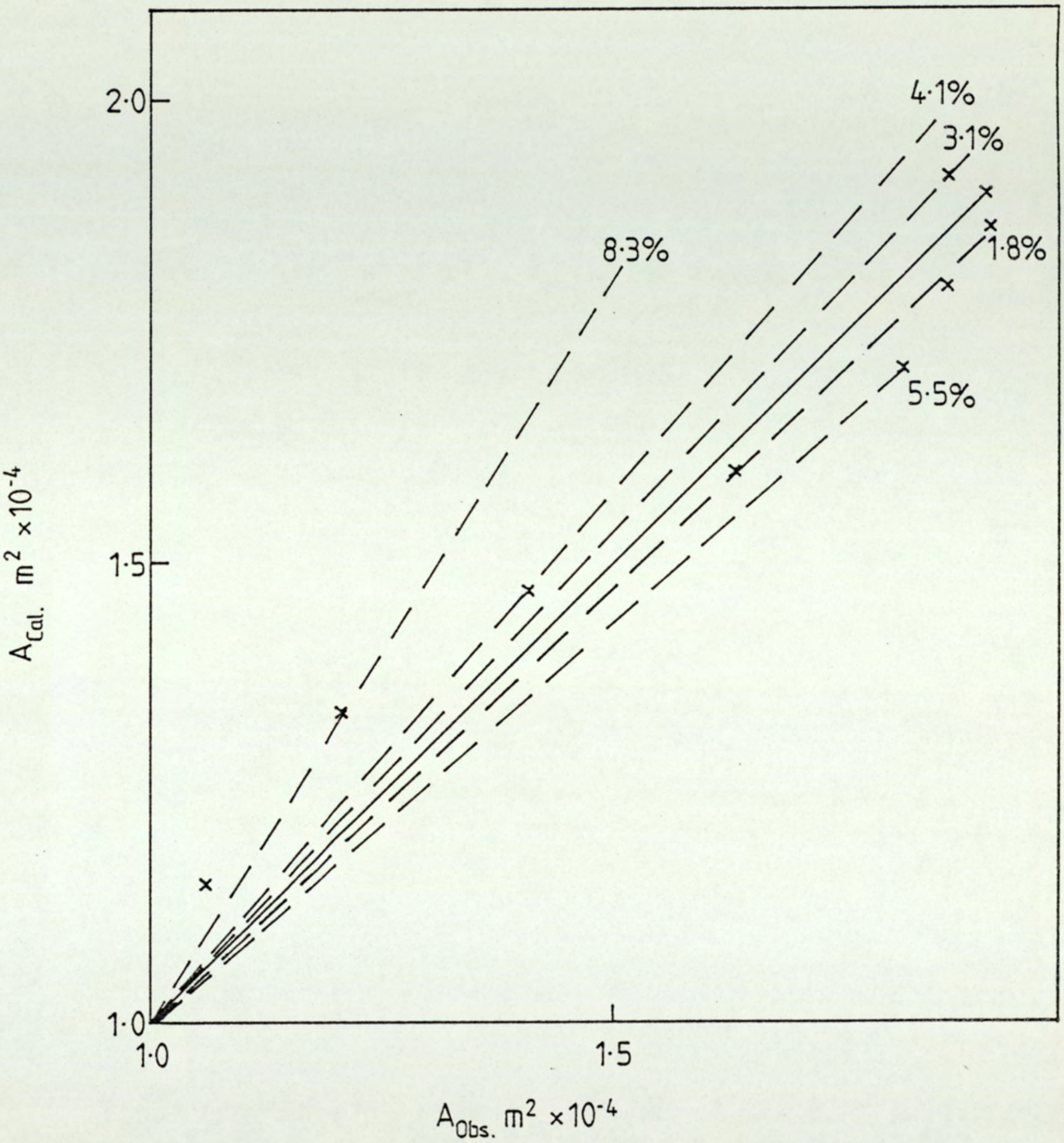

Figure D4. Comparison of the observed interfacial area with those predicted (Run C)

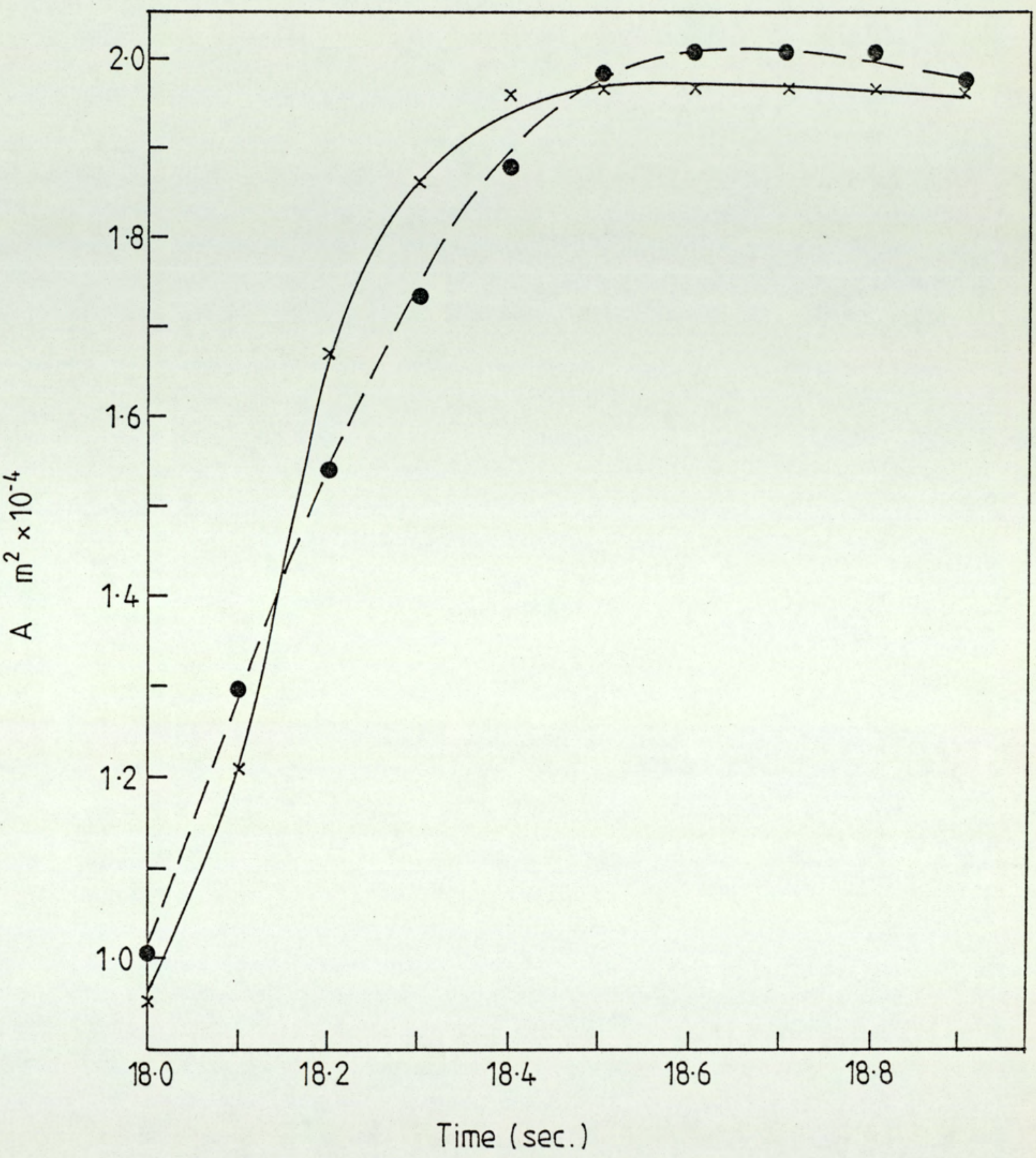

Figure D5. Droplet area during formation vs. time for (Run D)
× Observed, ● Calculated

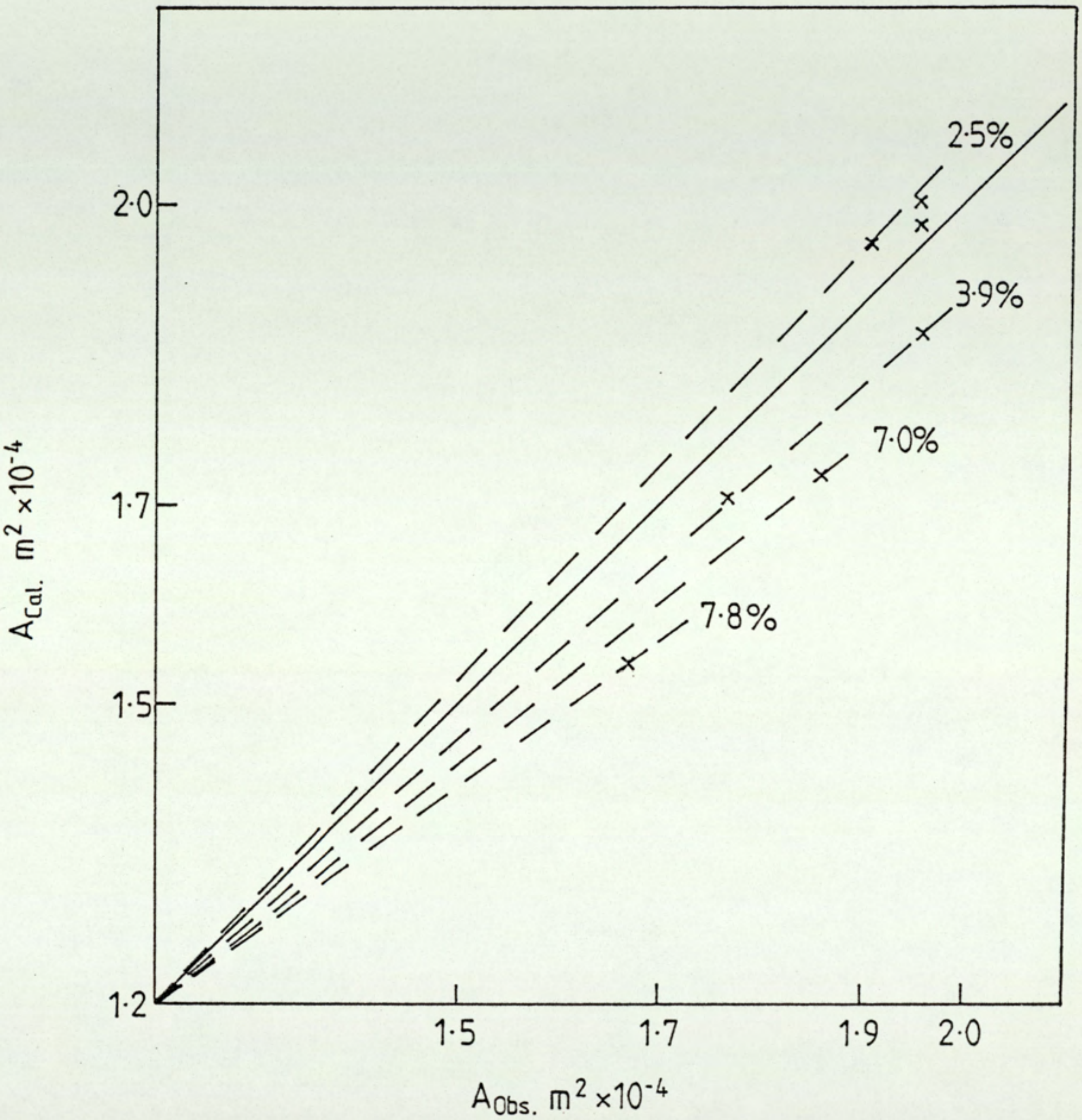

Figure D6 Comparison of the observed interfacial area with those predicted (Run D)

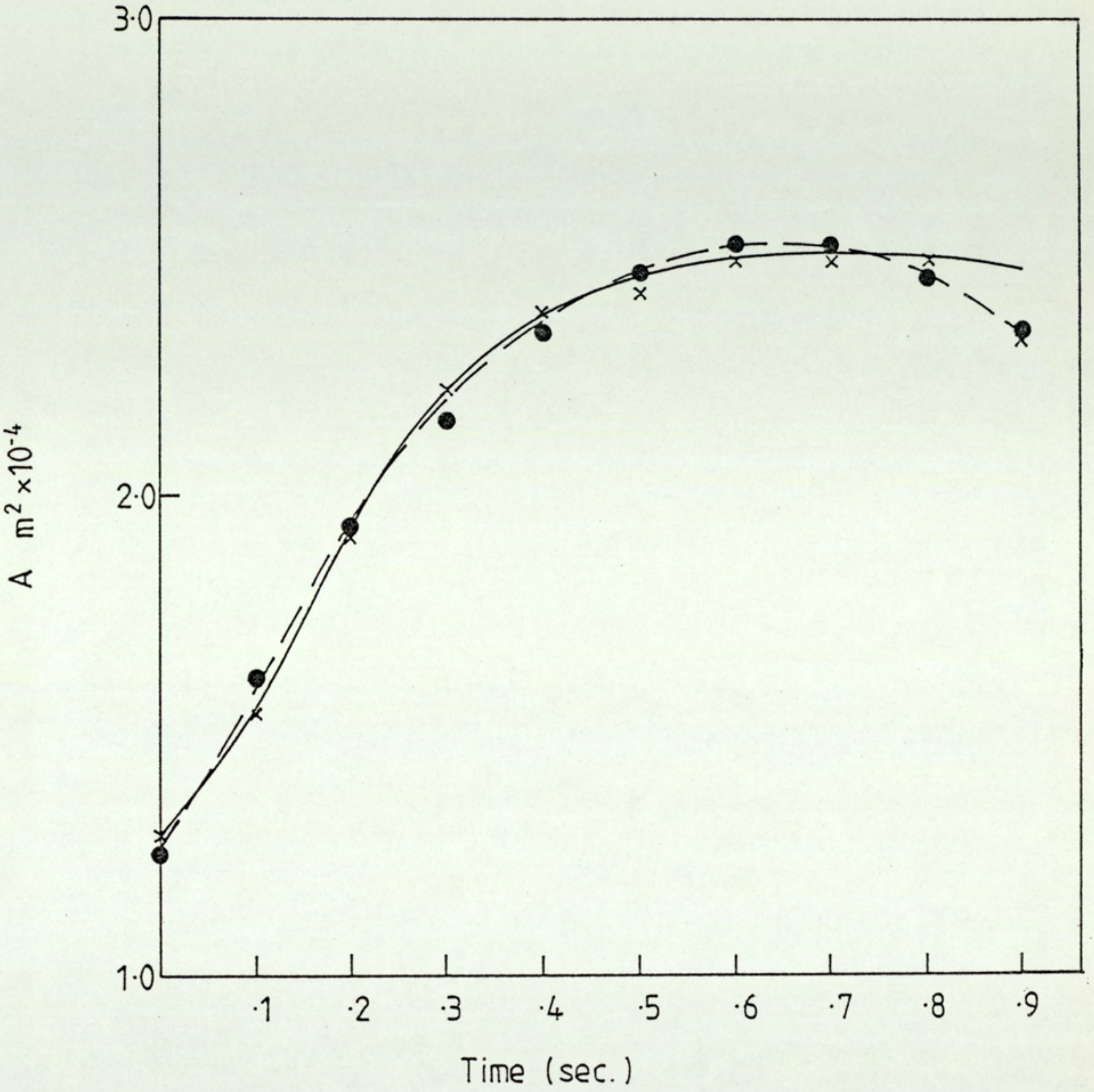

Figure D7. Droplet area during formation vs. time (Run E)
× Observed, ● Calculated

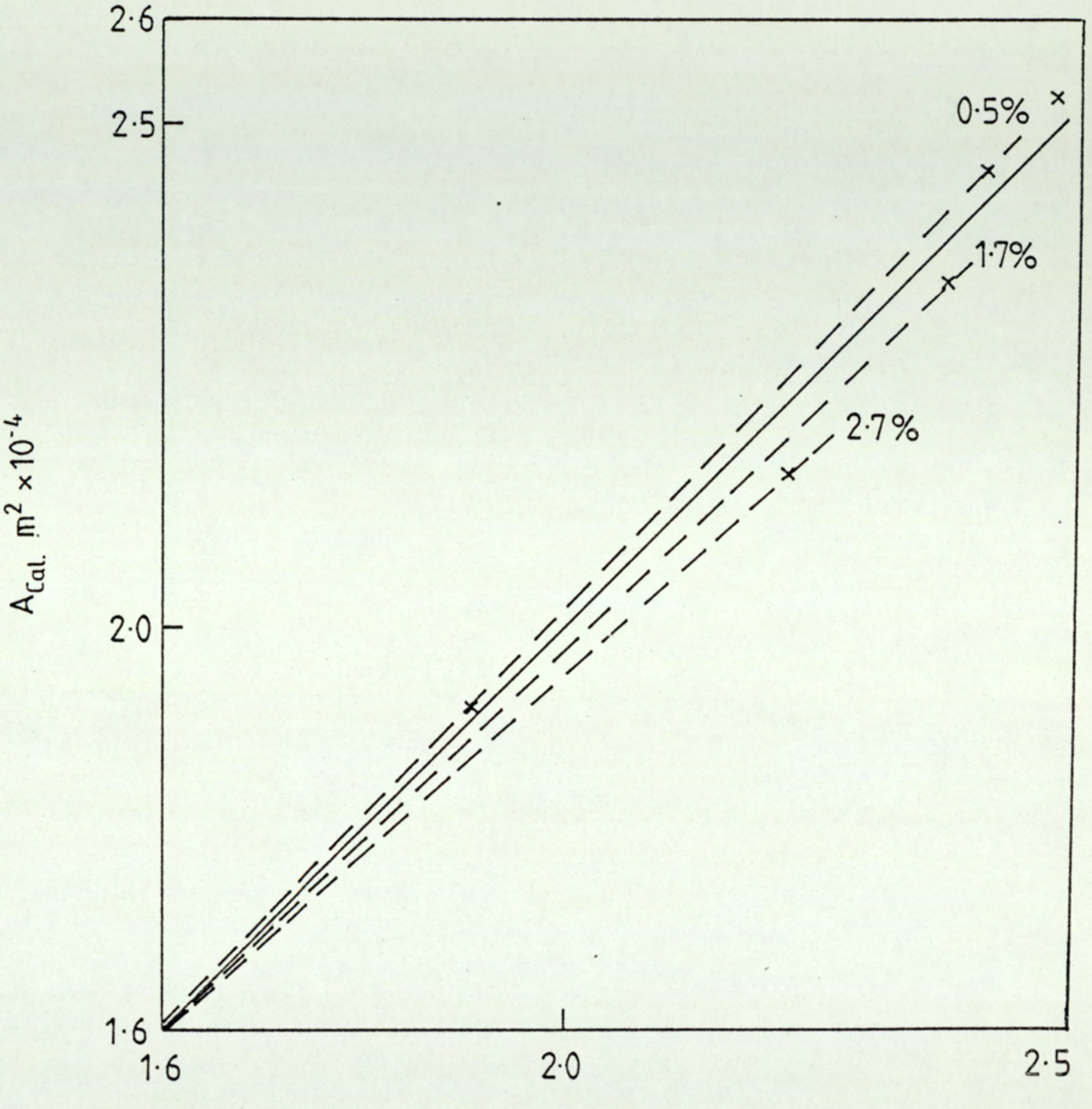

Figure D8. Comparison of the observed interfacial area with those predicted (Run E)

A complete set of this Appendix will be in Unbound Material

APPENDIX D.5

OUTPUT OF COMPUTER PROGRAM APPENDIX C.7

Appendix D.5

value of n = 2

value of ε from Table 7.7 and Appendix D.2C

Run No.	ω rad.s^{-1}	$k_{dR} \times 10^{-2}$ *	$k_{dA} \times 10^{-2}$ *	$k_{dT} \times 10^{-2}$ *	$k_{cR} \times 10^{-2}$ *	$K_{dRO} \times 10^{-3}$ *	$K_{dAO} \times 10^{-2}$ *	$K_{dTO} \times 10^{-3}$ *
10 A	38.99	1.46	5.88	0.23	1.33	8.17	2.78	1.99
B	41.20	1.49	6.05	0.21	1.34	8.34	2.86	1.85
C	45.40	1.57	6.35	0.27	1.16	7.99	3.01	2.30
D	46.33	1.59	6.41	0.17	1.38	8.72	3.04	1.57
E	49.32	1.64	6.62	0.14	1.48	8.46	3.13	1.84
11 A	39.03	1.48	6.10	0.25	1.28	7.94	2.76	2.14
B	42.11	1.53	6.23	0.25	1.23	7.95	2.87	2.17
C	44.71	1.58	6.42	0.18	1.35	8.46	2.95	1.68
D	46.60	1.61	6.55	0.16	1.42	8.71	3.02	1.50
E	49.71	1.67	6.77	0.15	1.43	8.54	3.12	1.66
12 A	36.05	1.46	5.82	0.20	1.43	7.14	2.46	2.52
B	38.25	1.50	5.99	0.16	1.52	7.58	2.54	2.02
C	40.68	1.55	6.18	0.14	1.55	8.05	2.62	1.58
D	43.39	1.60	6.77	0.13	1.57	8.06	2.70	1.60
13 A	35.78	1.48	5.89	0.20	1.42	6.61	2.30	2.72
B	38.09	1.53	6.07	0.14	1.60	7.10	2.38	2.15
C	40.66	1.58	6.14	0.14	1.54	7.68	2.40	1.58
D	44.61	1.65	6.57	0.10	1.71	8.04	2.57	1.34
14 A	41.20	1.50	6.45	0.20	1.36	8.38	2.86	1.81
B	44.50	1.56	6.23	0.18	1.38	9.17	2.98	1.34
C	46.33	1.59	6.41	0.16	1.44	8.89	3.04	1.43
D	48.28	1.62	6.55	0.14	1.50	8.51	3.10	1.78

* = m x 10^{-2}.sec^{-1}

Appendix D.5 continued

Run No.	ω rad.s^{-1}	k_{dR} x 10^{-2} *	k_{dA} x 10^{-2} *	k_{dT} x 10^{-2} *	k_{cR} x 10^{-2} *	K_{dRO} x 10^{-3} *	K_{dAO} x 10^{-2} *	K_{dTO} x 10^{-3} *
15 A	41.30	1.52	6.17	0.21	1.34	8.24	2.84	1.85
B	43.81	1.57	6.35	0.18	1.39	8.53	2.92	1.61
C	45.64	1.60	6.48	0.16	1.42	8.69	2.99	1.49
D	47.60	1.63	6.62	0.11	1.67	9.43	3.05	1.01
16 A	34.07	1.41	5.60	0.24	1.34	7.45	2.37	2.11
B	38.25	1.50	5.87	0.16	1.51	8.06	2.49	1.52
C	39.84	1.53	6.05	0.14	1.58	8.35	2.56	1.32
D	40.68	1.55	6.11	0.17	1.45	8.09	2.59	1.54
17 A	35.13	1.38	5.58	0.20	1.45	8.23	2.64	1.82
B	38.25	1.50	5.88	0.16	1.51	8.66	2.78	1.49
C	39.84	1.53	5.99	0.14	1.58	8.34	2.83	1.84
D	40.68	1.55	6.16	0.17	1.45	8.52	2.92	1.70
18 A	37.63	1.45	5.89	0.29	1.22	7.67	2.71	2.45
B	39.03	1.48	6.62	0.17	1.45	9.01	3.05	1.28
C	41.30	1.52	6.17	0.15	1.55	8.78	2.84	1.36
D	44.70	1.58	6.42	0.11	1.67	9.28	2.95	1.06
19 A	34.07	1.41	5.65	0.29	1.25	7.24	2.39	2.37
B	36.05	1.46	5.82	0.25	1.31	7.49	2.46	2.09
C	37.49	1.48	5.93	0.19	1.43	7.91	2.51	1.67
D	39.84	1.53	6.11	0.15	1.55	8.34	2.59	1.33
20 A	35.06	1.47	5.83	0.17	1.53	7.70	2.28	1.54
B	38.09	1.53	6.07	0.19	1.42	7.59	2.38	1.66
C	42.56	1.62	6.42	0.16	1.47	7.92	2.51	1.41
D	46.84	1.70	6.74	0.11	1.60	8.47	2.64	1.07

* = m x 10^{-2}.sec^{-1}

Appendix D.5 continued

Run No.	ω rad.s^{-1}	k_{dR}x 10^{-2} *	k_{dA} x 10^{-2} *	k_{dT} x 10^{-2} *	k_{cR} x 10^{-2} *	K_{dRO} x 10^{-3} *	K_{dAO} x 10^{-2} *	K_{dTO} x 10^{-3} *
21 A	30.92	1.29	5.24	0.38	1.18	7.26	2.48	3.07
B	34.55	1.37	5.54	0.32	1.22	7.59	2.02	2.64
C	36.97	1.42	5.73	0.26	1.29	8.19	2.71	1.92
D	38.99	1.46	5.88	0.21	1.38	8.68	2.79	1.47
22 A	31.76	1.33	5.41	0.34	1.21	7.34	2.49	2.81
B	35.07	1.40	5.68	0.25	1.33	7.85	2.62	2.17
C	37.63	1.45	5.89	0.20	1.43	8.26	2.71	1.76
D	40.52	1.51	6.11	0.15	1.54	8.69	2.81	1.41
23 A	32.26	1.38	5.11	0.32	1.23	7.26	2.07	2.10
B	36.05	1.46	5.40	0.21	1.39	7.92	2.20	1.47
C	37.49	1.48	6.13	0.16	1.52	8.38	2.49	1.22
D	39.03	1.51	5.62	0.12	1.69	7.46	2.29	1.95
24 A	30.46	1.29	5.20	0.35	1.234	7.68	2.46	2.37
B	32.39	1.33	5.39	0.22	1.44	8.32	2.54	1.62
25 A	31.15	1.35	5.41	0.29	1.29	7.42	2.28	2.09
B	34.07	1.41	5.65	0.20	1.45	8.32	2.39	1.17
26 A	32.79	1.44	5.25	0.21	1.47	7.27	1.98	1.78
B	37.87	1.54	5.64	0.13	1.65	8.00	2.12	1.21
27 A	25.14	1.26	5.36	0.24	1.53	7.53	2.02	1.55
B	46.74	1.71	5.83	0.11	1.61	8.01	2.20	1.22
28 A	29.84	1.37	5.01	0.29	1.33	7.51	1.89	1.50
B	34.82	1.48	5.41	0.20	1.44	8.10	2.04	1.11

* = m x 10^{-2}.sec^{-1}

APPENDIX D.6

OUTPUT OF COMPUTER PROGRAM APPENDIX C.6

APPENDIX D.6

Results of the regression analysis technique, least squares method, to fit, the changing droplet area during formation with time to a mathematical equation.

This appendix includes the following:

1. The results of ten runs by applying the program on a BBC micro computer, for a variety of glass and ptfe nozzles, with different solute concentrations and flow rates, as in Table 7.5.

2. The above results presented graphically as experimental and regress times, together with the closeness of fit, or the values of the correlation coefficients, and the estimation of error.

```
RUN NO. A
NTH-ORDER REGRESSION
BY LEAST SQUARES
DEGREE OF EQUATION : 2
NUMBER OF KNOWN POINTS : 10
X , Y OF POINT 1 : 1.00 , 0.75
X , Y OF POINT 2 : 1.10 , 0.95
X , Y OF POINT 3 : 1.20 , 1.29
X , Y OF POINT 4 : 1.30 , 1.54
X , Y OF POINT 5 : 1.40 , 1.63
X , Y OF POINT 6 : 1.50 , 1.63
X , Y OF POINT 7 : 1.60 , 1.63
X , Y OF POINT 8 : 1.70 , 1.63
X , Y OF POINT 9 : 1.80 , 1.58
X , Y OF POINT 10 : 1.90 , 1.45

             CONSTANT = -5.22305202
       1 DEGREE COEFFICIENT = 8.68856997
       2 DEGREE COEFFICIENT = -2.73106382

COEFFICIENT OF
DETERMINATION (R ^ 2) = 0.976155517
COEFFICIENT OF CORRELATION = 0.988005828
STANDERD ERROR OF ESTIMATE = 5.54476285E-2

INTERPOLATION  (0 TO END PROGRAM)
VALUE OF X: 1.10    Y = 0.734454138
VALUE OF X: 1.10    Y = 1.02978773O
VALUE OF X: 1.20    Y = 1.270500050
VALUE OF X: 1.30    Y = 1.456591090
VALUE OF X: 1.40    Y = 1.588060860
VALUE OF X: 1.50    Y = 1.664909350
VALUE OF X: 1.60    Y = 1.687136560
VALUE OF X: 1.70    Y = 1.654742500
VALUE OF X: 1.80    Y = 1.567727160
VALUE OF X: 1.90    Y = 1.426095500
END


RUN NO. (B)
NTH-ORDER REGRESSION
BY LEAST SQUARES
DEGREE OF EQUATION : 2
NUMBER OF KNOWN POINTS : 11
X , Y OF POINT 1 : 2.00 , 0.79
X , Y OF POINT 2 : 2.10 , 1.06
X , Y OF POINT 3 : 2.20 , 1.41
X , Y OF POINT 4 : 2.30 , 1.58
X , Y OF POINT 5 : 2.40 , 1.67
X , Y OF POINT 6 : 2.50 , 1.72
X , Y OF POINT 7 : 2.60 , 1.72
X , Y OF POINT 8 : 2.70 , 1.72
X , Y OF POINT 9 : 2.80 , 1.67
X , Y OF POINT 10 : 2.90 , 1.54
```

```
X , Y OF POINT 11 : 3.00 , 1.29
        CONSTANT = -16.8389088
    1 DEGREE COEFFICIENT = 14.3662161
    2 DEGREE COEFFICIENT = -2.77269788

COEFFICIENT OF DETERMINATION (R ^ 2) = 0.985944335
COEFFICIENT OF CORRELATION = 0.992947297
STANDERD ERROR OF ESTIMATE = 4.08762426E-2

INTERPOLATION (0 TO END PROGRAM)
VALUE OF X : 2.00      Y = 0.802731957
VALUE OF X : 2.10      Y = 1.102547440
VALUE OF X : 2.20      Y = 1.346908970
VALUE OF X : 2.30      Y = 1.535816540
VALUE OF X : 2.40      Y = 1.669270150
VALUE OF X : 2.50      Y = 1.747269790
VALUE OF X : 2.60      Y = 1.769815490
VALUE OF X : 2.70      Y = 1.736907230
VALUE OF X : 2.80      Y = 1.648545000
VALUE OF X : 2.90      Y = 1.504728820
VALUE OF X : 3.00      Y = 1.305458690
END


RUN NO. (C)
NTH-ORDER REGRESSION
BY LEAST SQUARES
DEGREE OF EQUATION : 2
NUMBER OF KNOWN POINTS : 12
X , Y OF POINT 1 : 1.00 , 0.88
X , Y OF POINT 2 : 1.10 , 0.92
X , Y OF POINT 3 : 1.20 , 1.06
X , Y OF POINT 4 : 1.30 , 1.21
X , Y OF POINT 5 : 1.40 , 1.41
X , Y OF POINT 6 : 1.50 , 1.63
X , Y OF POINT 7 : 1.60 , 1.81
X , Y OF POINT 8 : 1.70 , 1.86
X , Y OF POINT 9 : 1.80 , 1.91
X , Y OF POINT 10 : 1.90 , 1.91
X , Y OF POINT 11 : 2.00 , 1.91
X , Y OF POINT 12 : 2.10 , 1.86
        CONSTANT = -2.63195673
    1 DEGREE COEFFICIENT = 4.46735922
    2 DEGREE COEFFICIENT = -1.09515535

COEFFICIENT OF DETERMINATION (R ^ 2) = 0.964136549
COEFFICIENT OF CORRELATION = 0.981904552
STANDERD ERROR OF ESTIMATE = 8.63618513E-2
INTERPOLATION (0 TO END PROGRAM)
VALUE OF X : 1.00      Y = 0.740247146
VALUE OF X : 1.10      Y = 0.957000446
VALUE OF X : 1.20      Y = 1.15175064
VALUE OF X : 1.30      Y = 1.32479772
VALUE OF X : 1.40      Y = 1.47584170
```

```
VALUE OF X : 1.50        Y = 1.60498257
VALUE OF X : 1.60        Y = 1.71222034
VALUE OF X : 1.70        Y = 1.79755500
VALUE OF X : 1.80        Y = 1.86098654
VALUE OF X : 1.90        Y = 1.90251499
VALUE OF X : 2.00        Y = 1.92214032
VALUE OF X : 2.10        Y = 1.91986255
END


RUN NO. (D)
NTH-ORDER REGRESSION
BY LEAST SQUARES
DEGREE OF EQUATION : 2
NUMBER OF KNWON POINTS : 12
X , Y OF POINT 1 : 18.00 , 0.95
X , Y OF POINT 2 : 18.10 , 1.21
X , Y OF POINT 3 : 18.20 , 1.67
X , Y OF POINT 4 : 18.30 , 1.86
X , Y OF POINT 5 : 18.40 , 1.96
X , Y OF POINT 6 : 18.50 , 1.96
X , Y OF POINT 7 : 18.60 , 1.96
X , Y OF POINT 8 : 18.70 , 1.96
X , Y OF POINT 9 : 18.80 , 1.96
X , Y OF POINT 10 : 18.90 , 1.96
X , Y OF POINT 11 : 19.00 , 1.91
X , Y OF POINT 12 : 19.10 , 1.77
          CONSTANT = -754.649233
     1 DEGREE COEFFICIENT = 80.957236
     2 DEGREE COEFFICIENT = -2.16531013

COEFFICIENT OF DETERMINATION (R ^ 2) = 0.942200154
COEFFICIENT OF CORRELATION = 0.970669951
STANDERD ERROR OF ESTIMATE = 8.92131438E-2

INTERPOLATION (0 TO END PROGRAM)
VALUE OF X : 18.00       Y = 1.02053285
VALUE OF X : 18.10       Y = 1.29948688
VALUE OF X : 18.20       Y = 1.53513432
VALUE OF X : 18.30       Y = 1.72747612
VALUE OF X : 18.40       Y = 1.87651134
VALUE OF X : 18.50       Y = 1.98224044
VALUE OF X : 18.60       Y = 2.04466391
VALUE OF X : 18.70       Y = 2.06378078
VALUE OF X : 18.80       Y = 2.03959131
VALUE OF X : 18.90       Y = 1.97209573
VALUE OF X : 19.00       Y = 1.86129379
VALUE OF X : 19.10       Y = 1.70718575
END


RUN NO. (E)
NTH-ORDER REGRESSION
BY LEAST SQUARES
```

```
VALUE OF X : 1.50       Y = 1.60498257
VALUE OF X : 1.60       Y = 1.71222034
VALUE OF X : 1.70       Y = 1.79755500
VALUE OF X : 1.80       Y = 1.86098654
VALUE OF X : 1.90       Y = 1.90251499
VALUE OF X : 2.00       Y = 1.92214032
VALUE OF X : 2.10       Y = 1.91986255
END


RUN NO. (D)
NTH-ORDER REGRESSION
BY LEAST SQUARES
DEGREE OF EQUATION : 2
NUMBER OF KNWON POINTS : 12
X , Y OF POINT 1 : 18.00 , 0.95
X , Y OF POINT 2 : 18.10 , 1.21
X , Y OF POINT 3 : 18.20 , 1.67
X , Y OF POINT 4 : 18.30 , 1.86
X , Y OF POINT 5 : 18.40 , 1.96
X , Y OF POINT 6 : 18.50 , 1.96
X , Y OF POINT 7 : 18.60 , 1.96
X , Y OF POINT 8 : 18.70 , 1.96
X , Y OF POINT 9 : 18.80 , 1.96
X , Y OF POINT 10 : 18.90 , 1.96
X , Y OF POINT 11 : 19.00 , 1.91
X , Y OF POINT 12 : 19.10 , 1.77
         CONSTANT = -754.649233
    1 DEGREE COEFFICIENT = 80.957236
    2 DEGREE COEFFICIENT = -2.16531013

COEFFICIENT OF DETERMINATION (R ^ 2) = 0.942200154
COEFFICIENT OF CORRELATION = 0.970669951
STANDERD ERROR OF ESTIMATE = 8.92131438E-2

INTERPOLATION (0 TO END PROGRAM)
VALUE OF X : 18.00      Y = 1.02053285
VALUE OF X : 18.10      Y = 1.29948688
VALUE OF X : 18.20      Y = 1.53513432
VALUE OF X : 18.30      Y = 1.72747612
VALUE OF X : 18.40      Y = 1.87651134
VALUE OF X : 18.50      Y = 1.98224044
VALUE OF X : 18.60      Y = 2.04466391
VALUE OF X : 18.70      Y = 2.06378078
VALUE OF X : 18.80      Y = 2.03959131
VALUE OF X : 18.90      Y = 1.97209573
VALUE OF X : 19.00      Y = 1.86129379
VALUE OF X : 19.10      Y = 1.70718575
END


RUN NO. (E)
NTH-ORDER REGRESSION
BY LEAST SQUARES
```

```
DEGREE OD EQUATION : 2
NUMBER OF KNOWN POINTS : 11
X , Y OF POINT 1 : 1.00 , 1.29
X , Y OF POINT 2 : 1.10 , 1.54
X , Y OF POINT 3 : 1.20 , 1.91
X , Y OF POINT 4 : 1.30 , 2.22
X , Y OF POINT 5 : 1.40 , 2.38
X , Y OF POINT 6 : 1.50 , 2.42
X , Y OF POINT 7 : 1.60 , 2.49
X , Y OF POINT 8 : 1.70 , 2.49
X , Y OF POINT 9 : 1.80 , 2.49
X , Y OF POINT 10 : 1.90 , 2.32
X , Y OF POINT 11 : 2.00 , 2.16
        CONSTANT = -5.64911144
    1 DEGREE COEFFICIENT = 9.91034581
    2 DEGREE COEFFICIENT = -3.00466074

COEFFICIENT OF DETERMINATION (R ^ 2) = 0.989819684
COEFFICIENT OF CORRELATION = 0.994896821
STANDERD ERROR OF ESTIMATE = 4.617477244E-2

INTERPOLATION (0 TO END PROGRAM)
VALUE OF X : 1.00       Y = 1.25657364
VALUE OF X : 1.10       Y = 1.61662946
VALUE OF X : 1.20       Y = 1.91659207
VALUE OF X : 1.30       Y = 2.15646147
VALUE OF X : 1.40       Y = 2.33623766
VALUE OF X : 1.50       Y = 2.45592062
VALUE OF X : 1.60       Y = 2.51551037
VALUE OF X : 1.70       Y = 2.51500691
VALUE OF X : 1.80       Y = 2.45441024
VALUE OF X : 1.90       Y = 2.33372035
VALUE OF X : 2.00       Y = 2.15293724
END


RUN NO. (F)
NTH-ORDER REGRESSION
BY LEAST SQUARES
DEGREE OF EQUATION : 2
NUMBER OF KNOWN POINTS : 11
X , Y OF POINT 1 : 1.00 , 1.09
X , Y OF POINT 2 : 1.10 , 1.29
X , Y OF POINT 3 : 1.20 , 1.58
X , Y OF POINT 4 : 1.30 , 1.91
X , Y OF POINT 5 : 1.40 , 2.16
X , Y OF POINT 6 : 1.50 , 2.22
X , Y OF POINT 7 : 1.60 , 2.22
X , Y OF POINT 8 : 1.70 , 2.22
X , Y OF POINT 9 : 1.80 , 2.16
X , Y OF POINT 10 : 1.90 , 2.06
X , Y OF POINT 11 : 2.00 , 1.91
        CONSTANT = -5.69095303
    1 DEGREE COEFFICIENT = 9.62796833
```

```
    2 DEGREE COEFFICIENT = -2.9184137

COEFFICIENT OF DETERMINATION (R ^ 2) = 0.981460992
COEFFICICENT OF CORRELATION = 0.990687131
STANDERD ERROR OF ESTIMATE = 6.08578051E-2

INTERPOLATION (0 TO END PROGRAM)
VALUE OF X : 1.00       Y = 1.01860160
VALUE OF X : 1.10       Y = 1.36853156
VALUE OF X : 1.20       Y = 1.66009324
VALUE OF X : 1.30       Y = 1.89328665
VALUE OF X : 1.40       Y = 2.06811790
VALUE OF X : 1.50       Y = 2.18456865
VALUE OF X : 1.60       Y = 2.24265723
VALUE OF X : 1.70       Y = 2.24237755
VALUE OF X : 1.80       Y = 2.18372959
VALUE OF X : 1.90       Y = 2.06671335
VALUE OF X : 2.00       Y = 1.89132884
END


RUN NO. (G)
NTH-ORDER REGRESSION
BY LEAST SQUARES
DEGREE OF EQUATION : 2
NUMBER OF KNOWN POINTS : 11
X , Y OF POINT 1 : 2.00 , 0.88
X , Y OF POINT 2 : 2.10 , 1.09
X , Y OF POINT 3 : 2.20 , 1.41
X , Y OF POINT 4 : 2.30 , 1.63
X , Y OF POINT 5 : 2.40 , 1.81
X , Y OF POINT 6 : 2.50 , 1.86
X , Y OF POINT 7 : 2.60 , 1.91
X , Y OF POINT 8 : 2.70 , 1.91
X , Y OF POINT 9 : 2.80 , 1.91
X , Y OF POINT 10 : 2.90 , 1.86
X , Y OF POINT 11 : 3.00 , 1.58
         CONSTANT = -16.1613505
    1 DEGREE COEFFICIENT = 13.6382161
    2 DEGREE COEFFIVIENT = -2.56873424

COEFFICIENT OF DETERMINATION (R ^ 2) = 0.986510592
COEFFICIENT OF CORRELATION = 0.99323295
STANDERD ERROR OF ESTIMATE = 4.64179536E-2

INTERPOLATION (0 TO END PROGRAM)
VALUE OF X : 2.00       Y = 0.840144698
VALUE OF X : 2.10       Y = 1.15078527
VALUE OF X : 2.20       Y = 1.41005116
VALUE OF X : 2.30       Y = 1.61794236
VALUE OF X : 2.40       Y = 1.77445889
VALUE OF X : 2.50       Y = 1.87960071
VALUE OF X : 2.60       Y = 1.93336786
VALUE OF X : 2.70       Y = 1.93576033
```

```
VALUE OF X : 2.80       Y = 1.88677811
VALUE OF X : 2.90       Y = 1.78642119
VALUE OF X : 3.00       Y = 1.63468961
END


RUN NO. (H)
NTH-ORDER REGRESSUON
BY LEAST SQUARES
DEGREE OF EQUATION : 2
NUMBER OF KNOWN POINTS : 9
X , Y OF POINT 1 : 1.00 , 1.58
X , Y OF POINT 2 : 1.10 , 1.63
X , Y OF POINT 3 : 1.20 , 1.63
X , Y OF POINT 4 : 1.30 , 1.63
X , Y OF POINT 5 : 1.40 , 1.63
X , Y OF POINT 6 : 1.50 , 1.58
X , Y OF POINT 7 : 1.60 , 1.54
X , Y OF POINT 8 : 1.70 , 1.17
X , Y OF POINT 9 : 1.80 , 0.72
       CONSTANT = -3.2109725
   1 DEGREE COEFFICIENT = 7.80378564
   2 DEGREE COEFFICIENT =-3.08766154

COEFFICIENT OF DETERMINATION (R ^ 2) = 0.918556098
COEFFICIENT OF CORRELATION = 0.958413323
STANDERD ERROR OF ESTIMATE = 0.103054765

INTERPOLATION (0 TO END PROGRAM)
VALUE OF X : 1.00       Y = 1.50515160
VALUE OF X : 1.10       Y = 1.63712124
VALUE OF X : 1.20       Y = 1.70733765
VALUE OF X : 1.30       Y = 1.71580082
VALUE OF X : 1.40       Y = 1.66251077
VALUE OF X : 1.50       Y = 1.54746749
VALUE OF X : 1.60       Y = 1.37067097
VALUE OF X : 1.70       Y = 1.13212122
VALUE OF X : 1.80       Y = 0.83181825
VALUE OF X : 1.90       Y = 0.46976204
VALUE OF X : 2.00       Y = 4.59526032E-2
END
RUN NO. (J)
NTH-ORDER REGRESSION
BY LEAST SQUARES
DEGREE OF EQUATION : 2
NUMBER OF KNOWN POINT : 12
X , Y OF POINT 1 : 1.00 , 2.54
X , Y OF POINT 2 : 1.10 , 2.55
X , T OF POINT 3 : 1.20 , 2.54
X , Y OF POINT 4 : 1.30 , 2.54
X , Y OF POINT 5 : 1.40 , 2.20
X , Y OF POINT 6 : 1.50 , 2.20
X , Y OF POINT 7 : 1.60 , 2.10
X , Y OF POINT 8 : 1.70 , 2.05
```

```
X , Y OF POINT 9 : 1.80 , 2.05
X , Y OF POINT 10 : 1.90 , 1.98
X , Y OF POINT 11 : 2.00 , 1.74
X , Y OF POINT 12 : 2.10 , 0.98
          CONSTANT = 1.17603074
     1 DEGREE COEFFICIENT = 2.49632965
     2 DEGREE COEFFICIENT = -1.15909122

COEFFICIENT OF DETERMINATION (R ^ 2) = 0.863266349
COEFFICIENT OF CORRELATION = 0.929121278
STANDERD ERROR OF ESTIMATE = 0.182847688

INTERPOLATION (0 TO END PROGRAM)
VALUE OF X : 1.00     Y = 2.51326917
VALUE OF X : 1.10     Y = 2.51949298
VALUE OF X : 1.20     Y = 2.50253496
VALUE OF X : 1.30     Y = 2.46239512
VALUE OF X : 1.40     Y = 2.39907345
VALUE OF X : 1.50     Y = 2.31256997
VALUE OF X : 1.60     Y = 2.20288645
VALUE OF X : 1.70     Y = 2.07001752
VALUE OF X : 1.80     Y = 1.91396855
VALUE PF X : 1.90     Y = 1.73473777
VALUE OF X : 2.00     Y = 1.53232516
VALUE OF X : 2.10     Y = 1.30673072
END
RUN NO. (K)
NTH-ORDER REGRESSION
BY LEAST SQUARES
DEGREE OF EQUATION : 2
NUMBER OF KNOWN POINTS : 12
X , Y OF POINT 1 : 1.00 , 2.11
X , Y OF POINT 2 : 1.10 , 2.11
X , Y OF POINT 3 : 1.20 , 2.11
X , Y OF POINT 4 : 1.30 , 2.11
X , Y OF POINT 5 : 1.40 , 2.11
X , Y OF POINT 6 : 1.50 , 2.11
X , Y OF POINT 7 : 1.60 , 1.96
X , Y OF POINT 8 : 1.70 , 1.94
X , Y OF POINT 9 : 1.80 , 1.90
X , Y OF POINT 10 : 1.90 , 1.86
X , Y OF POINT 11 : 2.00 , 1.72
X , Y OF POINT 12 : 2.10 , 1.54
          CONSTANT = 1.10862509
     1 DEGREE COEFFICIENT = 1.67392779
     2 DEGREE COEFFICIENT = -0.689311237

COEFFICIENT OF DETERMINATION (R ^ 2) = 0.966503669
COEFFICIENT OF CORRELATION = 0.983109185
STANDERD ERROR OF ESTIMATE = 3.77404096E-2

INTERPOLATION (0 TO END PROGRAM)
VALUE OF X : 1.00      Y = 2.09324165
VALUE OF X : 1.10      Y = 2.11587907
```

```
VALUE OF X : 1.20       Y = 2.12473026
VALUE OF X : 1.30       Y = 2.11979523
VALUE OF X : 1.40       Y = 2.10107397
VALUE OF X : 1.50       Y = 2.06856649
VALUE OF X : 1.60       Y = 2.02227279
VALUE OF X : 1.70       Y = 1.96219286
VALUE OF X : 1.80       Y = 1.88832671
VALUE OF X : 1.90       Y = 1.80067433
VALUE OF X : 2.00       Y = 1.69923573
VALUE OF X : 2.10       Y = 1.58401090
END
```

APPENDIX E

CALCULATION OF MASS TRANSFER RATES AND COEFFICIENTS

This Appendix contains examples of the methods of calculation used for,

I Overall mass Transfer Coefficient During Drop Formation
  1. Experimental Values
  2. Predicted Values

II Overall mass Transfer Coefficient During Droplet Ascent
  1. Experimental Values
  2. Predicted Values
    a. Stagnant Drop
    b. Circulating Drop
      i) Laminar Circulation
      ii) Turbulent Circulation
    c. Oscillating Drop

APPENDIX E

E.1. OVERALL MASS TRANSFER COEFFICIENT DURING DROP FORMATION

All the calculations are, for example, based upon the data relevant to Run 14B (Table 7.1b).

a. Experimental

$$N_f = K_{df} A_{mf} \Delta C \qquad 1.1.$$

$$f_d (C_1 - C_2) = K_{df} A_{mf} \Delta C$$

$$A_{mf} = \pi d^2 = \pi (0.70)^2 = 1.54 \text{ m}^2 \times 10^{-4}$$

$$0.36 (0.511 - 0.38) = K_{df} \times 1.54 (0.511 - \text{zero})$$

$$K_{df} = 5.98 \times 10^{-2} \text{ m} \times 10^{-2}.\text{sec}^{-1}$$

b. Predicted

i) Johnson and Hamielec's (23) correlation to calculate the efficiency during drop formation;

$$E_m = \frac{C_1 - C_2}{C_1 - C^*} = \frac{20.6}{de} \left[\frac{D_d t_f}{\pi}\right]^{0.5}$$

$$= \frac{20.6}{0.70} \left[\frac{2.69 \times 10^{-5} \times 1.0}{3.14}\right]^{0.5}$$

$$= 8.61 \times 10^{-2}$$

$$8.61 \times 10^{-2} = \frac{0.511 - C_2}{0.511 - \text{zero}}$$

$$C_2 = 0.46 \text{ kg.} \times 10^{-3}\text{.mol/L}$$

ii) The overall mass transfer coefficient was estimated from equation 1.1.

$$N_A = K_d \; A \, \Delta C$$

while $$N_A = \frac{\pi \, d^3}{6t_f} \; (0.511 - 0.46)$$

$$= 0.179 \times 5.1 \times 10^{-2} \text{ at } t_f = 1.0 \text{ sec}$$

$$= 9.13 \times 10^{-3} \text{ kg} \times 10^{-3}\text{.mol/sec}$$

$$A = \pi \, d^2 = 1.54 \text{ m}^2 \times 10^{-4}$$

$$9.13 \times 10^{-3} = K_{df} \times 1.54 \; (0.511 - \text{zero})$$

$$K_{df} = 1.16 \times 10^{-2} \text{ m} \times 10^{-2}\text{.sec}^{-1}$$

E.2. OVERALL MASS TRANSFER COEFFICIENT DURING DROP ASCENT

a. Experimental

$$N_t = K_{dexp} \, \bar{A} \, (C_2 - C^*)$$

$$\bar{A} = (\frac{\varepsilon}{2} + 1)\, Ao$$

$$\varepsilon = 0.434\, S_r^{-0.46}\ We^{-0.53}\ \sigma_r^{0.11}$$

$$= 0.434 \left(\frac{44.5 \times 0.70}{11.76}\right)^{-0.46} \left(\frac{0.70 \times 11.76^2 \times 0.862}{21.8}\right)^{-0.53} (0.87)^{0.11}$$

$$= 0.31$$

$$Ao = \pi\, d_o^2 = (0.75)^2 \pi = 1.77\ m^2 \times 10^{-4}$$

$$\bar{A} = (\frac{0.31}{2} + 1)\ 1.77$$

$$= 2.04\ m^2 \times 10^{-4}$$

$$N_t = 0.36\ (0.38 - 0.0511)$$

$$= 11.82 \times 10^{-2}\ kg \times 10^{-3}.mol/sec$$

b. Predicted

b.1. Stagnant droplet

The efficiency of mass transfer was calculated using Newman's (149) correlation:

$$E_m = \frac{C_1 - C_2}{C_1 - C^*} = \pi \left(\frac{D_d\, t_f}{r^2}\right)^{0.5}$$

$$= 3.14 \left(\frac{2.69 \times 10^{-5} \times 1.0}{(0.35)^2} \right)^{0.5}$$

$$= 4.66 \times 10^{-2}$$

$$4.66 \times 10^{-2} = \frac{0.38 - C_3}{0.38 - \text{zero}}$$

$$C_3 = 0.36 \text{ kg.} \times 10^{-3}\text{.mol/L}$$

$$\frac{\pi d^3}{6t_f} (0.38 - 0.36) = K_d \pi d^2 (0.38 - 0.0)$$

$$\frac{\pi}{6} \times (0.70)^3 \times 0.02 = K_d (0.70)^2 \pi \times 0.38$$

$$K_d = 6.12 \times 10^{-3} \text{ m} \times 10^{-2}\text{.sec}^{-1}$$

b.2. Laminar circulation

$$E_m = \frac{C_2 - C_3}{C_1 - C^*} \pi \quad \frac{R D_d t_f}{r^2}^{0.5}$$

$$= 3.14 \left(\frac{2.25 \times 2.69 \times 10^{-5} \times 1.0}{(0.35)^2} \right)^{0.5}$$

$$= 6.98 \times 10^{-2}$$

$$6.98 \times 10^{-2} = \frac{0.38 - C_3}{0.38 - 0.0}$$

$$C_3 = 0.35 \text{ kg} \times 10^{-3}\text{.mol/L}$$

$$\frac{\pi d^3}{6t_f} (C_2 - C_3) = K_d \; \pi d^2 (C_2 - C^*)$$

$$5.37 \times 10^{-3} = K_d \times 0.58$$

$$K_d = 9.26 \times 10^{-3} \text{ m} \times 10^{-2}\text{.sec}^{-1}$$

b.3. Turbulent circulation

i) The dispersed phase mass transfer coefficient was evaluated by Handlos and Baron's (152) correlation:

$$k_d = \frac{\lambda V}{768\,(1 + (\mu_d/\mu_c))}$$

$$= \frac{2.88 \times 11.76}{768\,(1 + (0.00594/0.001))}$$

$$= 2.77 \times 10^{-2} \text{ m} \times 10^{-2}\text{.sec}^{-1}$$

ii) The continuous phase mass transfer coefficient was evaluated using Higbie's (65) equation:

$$k_c = \frac{4}{\pi} \cdot \left[\frac{D_c}{t_f}\right]^{0.5}$$

$$= 3.79 \times 10^{-3} \text{ m} \times 10^{-2}.\text{sec}^{-1}$$

$$\frac{1}{K_d} = \frac{1}{k_d} + \frac{m}{k_c}$$

$$= \frac{1}{2.77 \times 10^{-2}} + \frac{0.72}{3.79 \times 10^{-3}}$$

$$= 4.42 \times 10^{-2} \text{ m} \times 10^{-2}.\text{sec}^{-1}$$

E.3. OVERALL MASS TRANSFER COEFFICIENT DURING OSCILLATION

a. Experimental

This was calculated as described in section E.2a except $n = 4$ and Ao was calculated by measuring the minimum drop diameter during oscillation:

$$do = 0.50 \text{ m} \times 10^{-2}$$

$$Ao = de^2 \pi = 0.78 \text{ m}^2 \times 10^{-4}$$

$$\bar{A} = (\frac{0.12}{2} + 1)\ 0.78$$

$$= 0.83 \text{ m}^2 \times 10^{-4}$$

$$K_d = \frac{11.81 \times 10^{-1}}{0.83 \times 0.38} = 37.44 \times 10^{-2} \text{ m} \times 10^{-2}\text{.sec}$$

b. Predicted

b.1 By Rose and Kintner (80)

i) The dispersed phase mass transfer coefficient was estimated by:

$$k_d = 0.45\,(\omega D_d)^{0.5}$$

$$\omega^2 = \frac{n\,\sigma\,b}{r^3}\;\frac{(n+1)\,(n-1)\,(n+2)}{(n+1)\,\rho_d + n\rho_c}$$

$$b = \frac{de.^{0.225}}{1.242} = \frac{0.70^{0.225}}{1.242} = 0.74 \text{ m} \times 10^{-2}$$

$$\omega^2 = \frac{2 \times 21.8 \times 0.74}{(0.35)^3}\;\frac{(2+1)\,(2-1)\,(2+2)}{(2+1) \times 0.862 + 2 \times 0.996}$$

$$\omega = 44.50 \text{ rad.sec}^{-1}$$

$$k_d = 0.45\,(44.50 \times 2.69 \times 10^{-5})$$

$$= 1.56 \times 10^{-2} \text{ m} \times 10^{-2}\text{.sec}^{-1}$$

ii) The continuous phase mass transfer coefficient was evaluated by Garner et al's (21) correlation:

$$k_c = \frac{D_c}{de} \left[50 + 8.5 \times 10^{-3} (Re) (Sc)^{0.7}\right]$$

$$= \frac{1.13 \times 10^{-5}}{0.70} \quad 50 + 8.5 \times 10^{-3} \quad \frac{0.70 \times 11.76 \times 0.996}{0.00594}$$

$$\left[\frac{0.00594}{0.996 \times 1.13 \times 10^{-5}}\right]^{0.7}$$

$$= 1.61 \times 10^{-2} \text{ m} \times 10^{-2}.\text{sec}^{-1}$$

iii) Overall mass transfer coefficient:

$$\frac{1}{K_d} = \frac{1}{1.56 \times 10^{-2}} + \frac{0.72}{1.61 \times 10^{-2}}$$

$$= 9.18 \times 10^{-3} \text{ m} \times 10^{-2}.\text{sec}^{-1}$$

b.2 Angelo et al (69)

ii) The dispersed phase mass transfer coefficient was evaluated by:

$$k_d = \sqrt{\frac{4D_d\, \omega\, (1 + \varepsilon + 3/8\, \varepsilon^2)}{\pi}}$$

$$= \left[\frac{4 \times 2.69 \times 10^{-5} \times 44.50\ (1 + 1.60 + 3/8 \times 1.60^2)}{3.14}\right]^{0.5}$$

$$= 6.22 \times 10^{-2} \text{ m} \times 10^{-2}.\text{sec}^{-1}$$

ii) The overall mass transfer coefficient was calculated from,

$$K_d = k_d \frac{1}{1 + m\sqrt{\frac{D_d}{D_c}}}$$

$$= 6.22 \times 10^{-2} \frac{1}{1 + 0.72\left[\frac{2.69 \times 10^{-5}}{1.13 \times 10^{-5}}\right]^{0.5}}$$

$$= 2.95 \times 10^{-2}\ \mathrm{m} \times 10^{-2}.\mathrm{sec}^{-1}$$

b.3 Al-Hassan's Correlation (1)

i) The dispersed phase mass transfer coefficient was estimated by:

$$k_d = 4.3\ \varepsilon^{2.692}\ Eo^{1.672}\ (D_d\ \omega)^{0.5}$$

$$= 4.3\ (1.60)^{2.692} \frac{9.81 \times 0.134 \times 0.70^2}{21.8}^{1.672} \qquad (2.69 \times 10^{-5} \times 44.50)^{0.5}$$

$$= 1.46 \times 10^{-3}\ \mathrm{m} \times 10^{-2}.\mathrm{sec}^{-1}$$

ii) The continuous phase mass transfer coefficient was also evaluated by Garner et al's correlation (21)

$$K_c = 1.61 \times 10^{-2}\ \mathrm{m} \times 10^{-2}.\mathrm{sec}^{-1}$$

iii) The overall mass transfer coefficient is:

$$\frac{1}{K_d} = \frac{1}{1.46 \times 10^{-3}} + \frac{0.72}{1.61 \times 10^{-2}}$$

$$= 1.34 \times 10^{-3} \text{ m} \times 10^{-2}.\text{sec}^{-1}$$

APPENDIX F

DETAILED DESCRIPTION OF SUGGESTED TECHNIQUE TO MEASURE THE AMPLITUDE OF OSCILLATION

Six small platinum plates could be fitted in both sides of the column in a position that would not disturb the flow. These should be very thin of platinum (to prevent oxidation) with dimentions of eg. 1.0cm width and 2.0cm length. Each pair of parallel plates could be connected to measure the conductivity of the liquid passing through, ie. with the ends connected to either a conductivity cell, to measure the conductance directly, or an oscilloscope to measure the voltage.

The highest capacitance will occur when there is no drop in between the two plates of the capacitor. This capacitance will decrease with increase in drop size, Figure F.2.

The capacity of a given capacitor depends on its geometry and on the dielectric material. For a parallel-plate capacitor the capacitance C, in farads is given by:

$$C = \frac{k \varepsilon_o A}{d} \qquad (9.1)$$

Knowing the capacity as a function of drop size, the corresponding drop area could therefore be calculated from,

$$e = \frac{A_{max}}{A_1} - 1 \qquad (3.6)$$

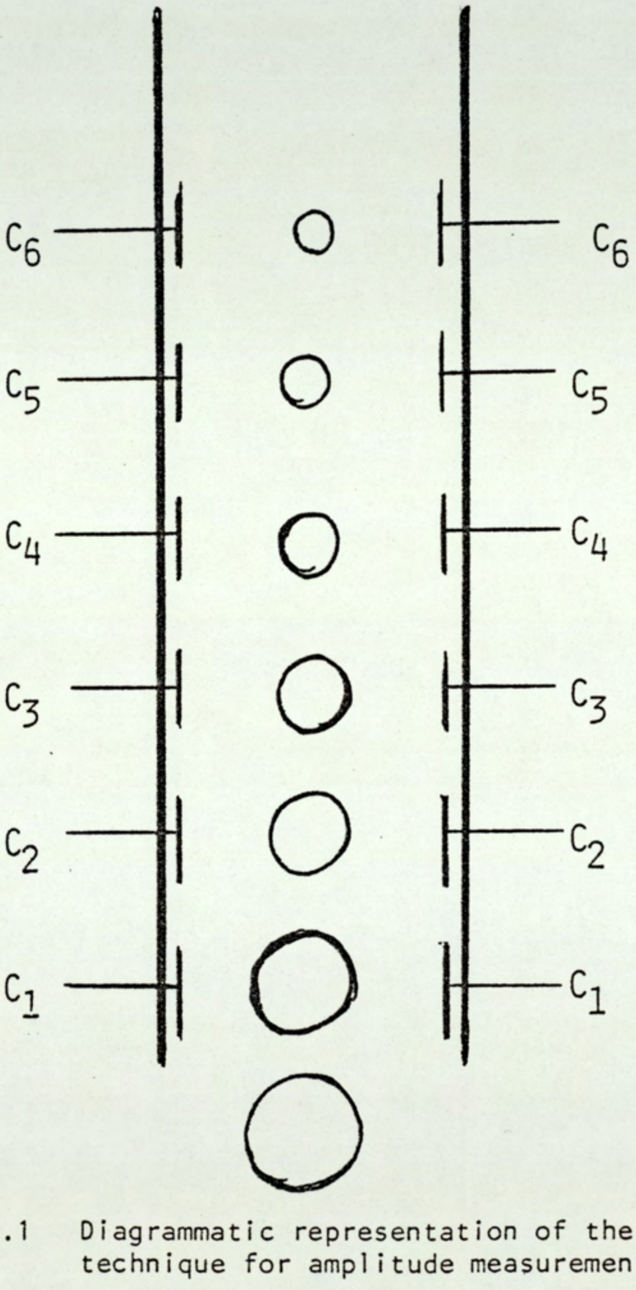

Figure F.1 Diagrammatic representation of the suggested technique for amplitude measurement.

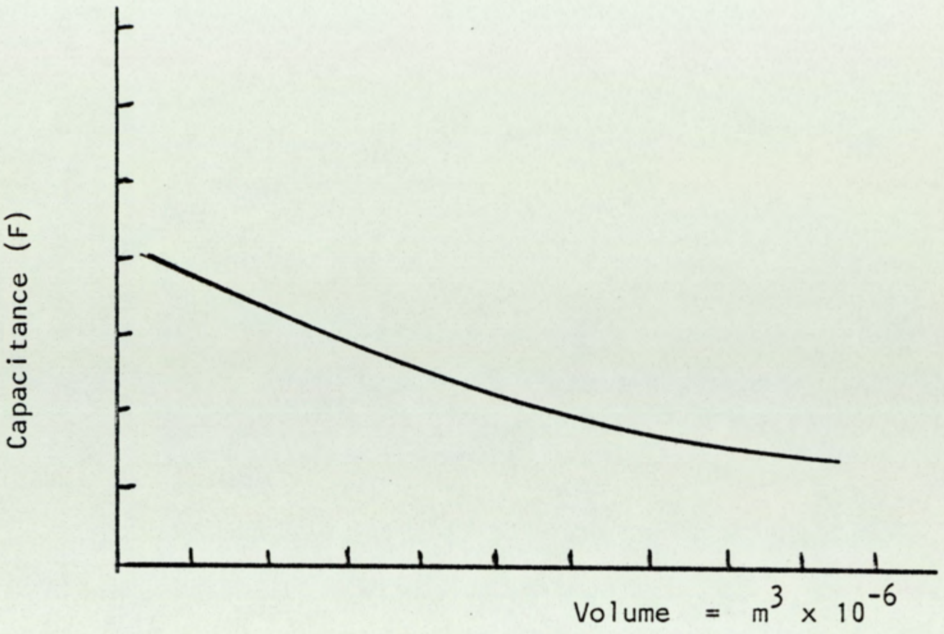

Figure F.2 Variation of the capacitance in Farad (F) with object volume (m^3)

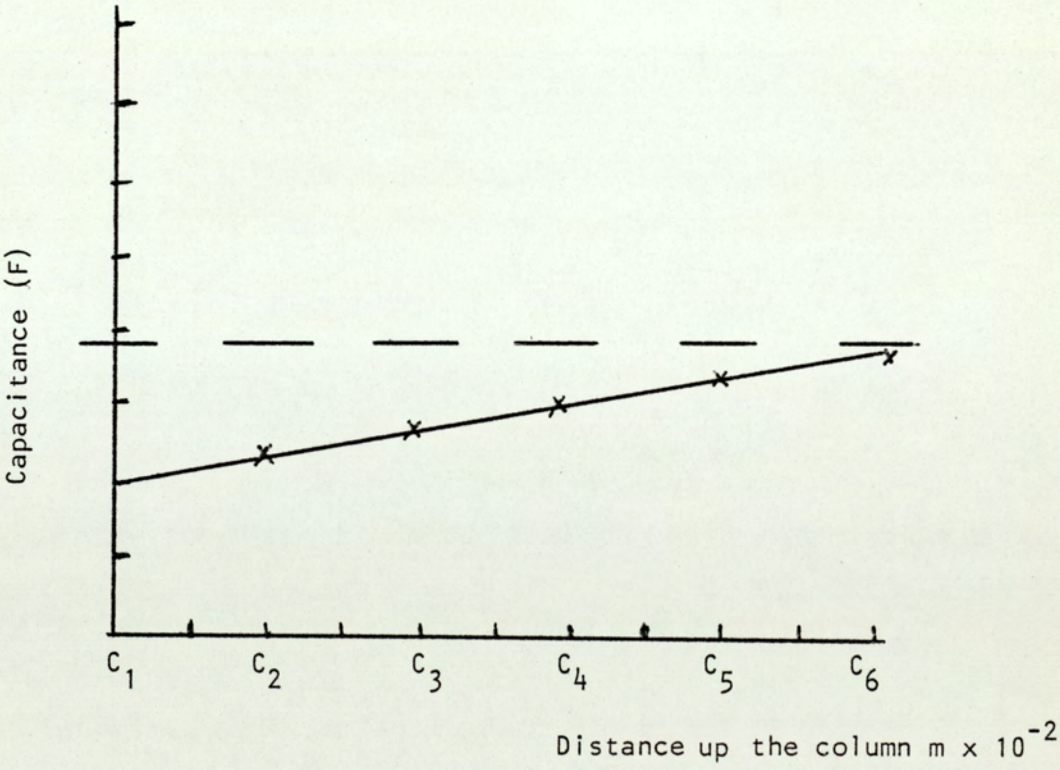

Figure F.3 Illustration of the difference in capacitance between C_1 and C_6

APPENDIX G

Paper presented at the Solvent Extraction and Ion Exchange Group Research meeting Soc. of Chem. Ind., Aston 8th May 1985

MASS TRANSFER CHARACTERISTICS OF LARGE OSCILLATING DROPS

Malalah, M and Mumford, C J
Department of Chemical Engineering
University of Aston in Birmingham

SUMMARY

The mass transfer characteristics of large oscillating toluene drops, d>5mm, were investigated (a) during formation and (b) during travel through a counter-current aqueous phase. A comparison was made between single drops and parallel-rising drop pairs, involving mutual interference and collision-rebound effects.

Compared with published correlations for overall mass transfer coefficient during formation, involving inherent assumptions regarding drop surface area, experimental coefficients were ≤ 22% greater for single drops and ≤ 55% greater for drop pairs.

Experimental data for single drops during travel also confirmed the limitations of existing models based on a symmetrical spheroid. Of significance for extractor operation involving drop swarms, an enhancement of overall mass transfer coefficient of up to 88% was observed due to collision-rebound effects with drop pairs compared with single drop models.

INTRODUCTION

In a gravity-operated extraction column contact between the dispersed and continuous phase proceeds in three distinct stages, namely drop formation, drop travel through the continuous phase, and coalescence at the bulk interface.

The present work was concerned only with the first two stages with drop diameters between 5 and 10mm such that they exhibited a cyclic oscillatory motion with Re = 200 to 1000, as they rose through the continuous phase.

In such an experimental study precise control is desirable over the volume of the drop formed at any flowrate, so that the initial interfacial area is as near constant as practicable. However, as summarised in Table 3, there is little agreement between investigators relating to the prediction of the overall mass transfer coefficient during formation, due in part to the difficulty in establishing a suitable experimental technique and also the difficulty of accounting for the effect of interfacial area changes. [Subsequent to the work reported here, a correlation has been developed for the change of interfacial area with time during formation (32)].

Drops exhibit several interesting phenomena when rising, or falling, through a continuous phase. The liquid inside may remain stagnant or possess internal circulation, or deform and oscillate. The terminal velocity and mass transfer rate are both related to these phenomena.

Whereas the behaviour of stagnant and internally circulating drops, d < 5mm, has been extensively investigated less data are available on larger oscillating drops. The hydrodynamics and rates of mass transfer associated with single large oscillating drops in an aqueous continuous phase have been studied by Al-Hassan (1) and this has been extended in the present work. Here, to approximate to the practical situation in an extraction column, a pair of drops released in parallel were also studied to account for the interactions affecting the oscillatory behaviour and, in some cases, involving collision and rebound or collision and coalescence.

BACKGROUND

Hydrodynamics

Numerous investigators (1, 2) have studied the behaviour of oscillating drops in the absence of mass transfer in order to derive correlations for their hydrodynamic behaviour in practical columns. Therefore only selected experiments were performed with the mutually-saturated system toluene-water to facilitate comparison of the effect of mass transfer on droplet oscillation and terminal velocities.

Mass Transfer Characteristics

The mechanism of solute transfer to, or from, a single drop is fundamental to extraction. The resistance to transfer, whether internal or external to the drop surface, depends upon the motion of the fluid particle. The most common single drop correlations for dispersed phase film coefficient are summarised in Table 1 and for the continuous phase film coefficient in Table 2, depending in each case upon the drop behaviour.

The fundamentals of oscillating drop mass transfer were set out by Rose and Kintner (6) who proposed a model based upon the concept of interfacial stretch and internal droplet mixing. This model considers both the amplitude and frequency of single drop oscillation, and oscillation was deduced to break up internal circulation streamlines and achieve turbulent internal mixing. The final equations are,

$$E_m = 1 - \exp\left[\frac{-2\pi D_E}{V}\int_{t_o}^{t_f}\frac{1}{f_1(t)}\left\{\left(\frac{3V}{4\pi W}\right)^2\frac{1}{2\alpha}\ln\left(\frac{1+\alpha}{1-\alpha}\right)+W\right\}dt\right]$$

where $$a = \frac{W - (3V/4\pi W)^2}{W}$$

$$W = (a_o + a_p\,|\sin 0.5\,\omega t\,|)^2$$

Table 1

Correlations for Dispersed Phase Mass Transfer Efficiency and Coefficient

Author and Ref	Correlation	State of Drops	Remarks
Newman A.B. (3)	$Em = \frac{C_1-C_o}{C_1-C^*} = \pi \left(\frac{D_d t_f}{r^2}\right)^{0.5}$	Stagnant	For small size drops
Calderbank et.al (30)	$Em = \frac{C_1-C_o}{C_1-C^*} = \pi \left(\frac{R D_d t_f}{r^2}\right)^{0.5}$	Laminar Circulating	R is the ratio of effective diffusivity to molecular diffusivity, = 2.25
Kronig & Brink (4)	$Em = 1-\frac{3}{8}\sum_{\eta=1}^{\alpha} A_n^2 \exp\left[\frac{-\lambda_n 16 D_d t}{r^2}\right]$	Laminar circulating	Values of A_n and λ_n for values of (n) from 1 to 7 presented by (10)
Handlos and Baron (5)	$Sh_d = 0.00375 Pe_d/(1+(\frac{\mu_d}{\mu_c}))$	Turbulent Circulating	Recommended when resistance to mass transfer exists in the continuous phase.
Skelland and Wellek (24)	$Sh_d = 31.4 \dot{T}m^{-0.338} Sc_d^{-0.125} We^{0.371}$	Circulating	Drops falling in a stationary continuous phase
Rose and Kintner (6)	$K_d = 0.45 (D_d \omega)^{0.5}$	Oscillating	For symmetrical spheriod droplet; widely accepted.
Angelo et al (8)	$K_d = \left[\frac{4D_d \omega (1+\varepsilon+\frac{3}{8}\varepsilon^2)}{\pi}\right]^{0.5}$	Oscillating	Correct only for integral number of complete oscillations
Brunson et al (25)	$Sh_d = \frac{2}{\pi}\left[\frac{d^2 \omega}{2D}(1+0.687\varepsilon^2)\right]^{0.5}$	Oscillating	With 26% absolute deviation
Yamaguchi et al (26)	$Sh_d = 1.14(Re')^{0.56}(Sc_d)^{0.5}$	Oscillating	For transfer of low solute concentation from aqueous drop to organic continuous phase
Al-Hassan (1)	$K_d = 4.3\,\varepsilon^{2.69} Eo^{1.62} (D_d \omega)^{0.5}$	Oscillating	Applicable only for Toluene-Acetone-Water system

able 2

orrelation for Continuous Phase Mass Transfer Coefficient

Author and Ref	Correlation	State of Drops	Remarks
Linton and Sutherland (16)	$Sh_c = 0.0582\ (Re)^{0.5}(Sc)^{0.33}$	Stagnant	Ignores diffusion and wake effects
Row et al (17)	$Sh_c = 2 + 0.76(Re)^{0.5}(Sc)^{0.33}$	Stagnant	Accounts for diffusion process
Kinard et al (18)	$Sh_c = 2 + (Sh_n) + 0.45(Re)^{0.5}(Sc)^{0.33}$	Stagnant	Includes diffusion and wake effects
Boussinesq (19)	$Sh_c = 1.13(Re)^{0.5}(Sc)^{0.5}$	Circulating	Claimed to be valid for many systems
Garner and Tayeban (20)	$Sh_c = 0.6(Re)^{0.5}(Sc)^{0.5}$	Circulating	Inapplicable to $Re > 450$
Garner et al (21)	$Sh_c = 126 + 1.8\ (Re)^{0.5}(Sc)^{0.42}$	Circulating	For partially miscible binary systems of low interfacial tension
Mekasut et al (22)	$Sh_c = 1.04(Ga)^{0.49}$	Circulating	Ga = Galileo number $= d^3\ \rho_c^2 g/\ \mu_c^2$
Garner and Tayeban (20)	$Sh_c = 50 + 0.0085(Re)(Sc)^{0.7}$	Oscillating	Successfully used by Thorsen et al (29)
Yamaguchi et al (23)	$Sh_c = 1.14(Re')^{0.5}\ (Sc)^{0.5}$	Oscillating	$Re' = \dfrac{\rho_c \cdot \omega\ d_e^2}{\mu_c}$
Mekasut et al (22)	$Sh_c = 6.74\ (Ga)^{0.34}$	Oscillating	Ignores the effect of frequency of oscillation

$$f_1(t) = \frac{(a_o^2 b - (a - X_o)^2 (b_o - X_o)) - 2abX_o + bX_o^2}{a^2 - 2aX_o - X_o^2} = X$$

$$a = a_o + a_p \,|\sin 0.5\,\omega t\,|$$

and $$b = \frac{3V}{4\pi a^2}$$

The correlation proposed for the dispersed phase mass transfer coefficient is,

$$K_D = 0.45\ (D_d\omega)^{0.5} \tag{2}$$

The equation proposed by Schroeder and Kintner (7) for the frequency of oscillation is,

$$\omega^2 = \frac{n\delta b}{r^3}\left[\frac{(n+1)(n-1)(n+2)}{(n+1)\rho_d + n\rho_c}\right] \tag{3}$$

while: $$b = \frac{de^{0.225}}{1.242}$$

and n is the mode of oscillation, for rigid body motion n = 0, 1. For fluid oscillating drops n > 1.

Angelo et al (8) also proposed a model involving surface stretch and internal mixing.

$$K_D = \left[\frac{4D_d\,\omega\,(1+\varepsilon_o)}{\pi}\right]^{0.5} \tag{4}$$

where, $$\varepsilon_o = \varepsilon + \frac{3}{8}\varepsilon^2$$

$$\varepsilon = \left[\frac{A_{max}}{A_o}\right] - 1 \tag{5}$$

$$A = A_o(1 + \varepsilon \sin^2 \omega t)$$

In their first study Rose and Kintner (6) assumed that the oscillating drop formed a symmetrical spheroid, ie it was either oblate, prolate or spherical. The amplitude was also determined from the actual change in area. Al-Hassan (1) later discounted the assumption of a symmetrical spheroid, based on experimental observations of the X, Y and Z axes of large oscillating drops, and estimated the amplitude from measuring these axes. Several dimensionless groups, eg We, Sc and S_r were found to have a marked effect on the oscillation characteristics in addition to Reynolds number (1).

Whilst previous work was based on the change of one axis of a drop Al-Hassan was able, by a system of mirrors, to observe all three axes simultaneously. The symmetrical spheroid assumption was hence shown to be invalid for d > 5.5mm (1). Furthermore the overall mass transfer coefficients were found to be considerably greater than those predicted by earlier models (10, 14). Agreement was only approximate for small oscillating drops, d < 5mm, and for low acetone concentrations. The empirical correlation of Yamaguchi (Table 1) gave the best fit. Therefore Al-Hassan proposed the correlation,

$$K_D = 4.3\ \varepsilon^{2.692}\ E_a^{1.672}\sqrt{D_d\omega} \qquad (6)$$

and for the amplitude of oscillation,

$$\varepsilon_{cal} = 0.868\ S_r^{0.395}\ We_c^{-0.229}\ \sigma_r^{0.144} \qquad (7)$$

EXPERIMENTAL INVESTIGATION

The equipment comprised a spray column of 5cm diameter industrial glass and 100cm in length, enclosed in a square jacket as shown in Figures A and B. Thermostatically controlled water was circulated through the jacket and the complete apparatus, including the phase reservoirs, was enclosed in a temperature controlled cabinet.

Table 3

Correlation of Mass Transfer Coefficient During Drop Formation

Author and Ref	Correlation	Remarks
Licht and Pensing (9)	$K_{df} = \frac{6}{7} \left(\frac{D_d}{\pi t_f}\right)^{0.5}$	The amount extracted was so small, that it could not be detected by experiment.
Heertjes et al (10)	$K_{df} = \frac{24}{7} \left(\frac{D_d}{\pi t_f}\right)^{0.5}$	Ratio of extraction was (2-5) times the value predicted by the model with $t_f = 0.24\text{-}1.18$ sec.
Groothuis et al (11)	$K_{df} = \frac{4}{3} \left(\frac{D_d}{\pi t_f}\right)^{0.5}$	With drop diameter between 0.035-0.085 cm the rate of absorption increase at $Re > 50$.
Coulson and Skinner (12)	$K_{df} = 2 \sqrt{\frac{3}{5}} \left(\frac{D_d}{\pi t_p}\right)^{0.5}$	Average time of exposure and average exposed surface are obtained by the fresh surface model (15).
Heertjes and de Nie (13)	$K_{df} = 2 \left[\frac{r_o}{a_d} + \frac{2}{3}\right] \left(\frac{D_d}{\pi t_f}\right)^{0.5}$	At slow Formation rates, the fresh surface model (15) was very successful.
Heertjes and de Nie (14)	$K_{df} = \frac{14}{3} \left[\frac{r_o}{a_d} + \frac{1}{3}\right] \left(\frac{D_d}{\pi t_f}\right)^{0.5}$	Growth of surface occurs by even stretching of the diffusion layer.
Ilkovic (15)	$K_{df} = 1.31 \left(\frac{D_d}{\pi t_f}\right)^{0.5}$	This model has been proved by many workers and used successfully (27,28)

A novel sampling probe, which withdrew samples of dispersed phase only, was used to collect drops immediately after formation or at 10cm increments up the column. Mirrors provided in the water jacket enabled front and side views of drops to be photographed simultaneously.

A conventional 3mm ground glass nozzle was used for single drop formation at acetone concentrations <20%wt/wt (1). For double drop studies pairs of nozzles, spaced at a critical distance to avoid coalescence during drop travel, were constructed of either glass (3mm to 6mm id) or ptfe (4mm to 7mm id) to cater for the variation in wetting phenomena associated with acetone concentrations >20%wt/wt.

The system investigated was toluene (Analar)-acetone-distilled water with toluene dispersed in all cases. This was chosen because of the ease of purification and the availability of earlier data for comparison purposes (1). Iodine at a concentration of 30ppm, which has been found to have no effect on the relevant system physical properties, was added to the toluene to provide a sharp contrast for photography. Acetone concentrations were determined by uv spectrophotometry with frequent checks using the iodoform titration method (31).

Droplet formation and hydrodynamics were recorded using cine-photography at 64 fps and 1000 fps or using video at 25 fps. Figure C shows typical drop shapes.

Both phases were prepared 24 hours prior to each experimental run and kept inside the cabinet. The column and cabinet temperature was controlled at 22± 1°C. In operation the column was filled with continuous phase and its flowrate adjusted to the required value; the flow of individual drops at the controlled rate was then introduced. Samples of extract and raffinate were collected and analysed at 5 minute intervals until steady-state was reached. Incremental dispersed and continuous phase samples were then collected after which the hydrodynamics were filmed. The volume of dispersed phase displaced over a period of 15 minutes was measured.

RESULTS

Amplitude of Oscillation

The amplitude of oscillation was determined from cine films of rising drops. The length of the major axis was measured at maximum drop distortion from frame to frame analysis. There was considerable scatter in the data and an average length from observations was calculated. The initial diameter of the drop after formation was also measured. The maximum and initial areas were then calculated.

A comparison between the observed amplitudes of oscillation calculated by equation 5 and those predicted from equation 7 is presented in Figures 1 and 2. (The data and Figures 3-12, typify 18 single drop and 50 drop pair results.)

Frequency of Oscillation

The experimentally observed and predicted frequencies of oscillation were determined using equation 3. The observed value was obtained from measurements of the drop diameter and mode of oscillation n after a set time of 4 to 5 seconds after release. The average value from 3 drops was recorded. The predicted value was obtained assuming n = 2 and an average drop diameter based on the displaced volume of dispersed phase. A comparison between the observed and the predicted frequencies is given in Figures 3 and 4; these demonstrate that the deviation for single drops was approximately 25% but for drop-pairs this increased to >50%. The modified behaviour of one drop in a pair is shown in Figure D (b).

Efficiency of Mass Transfer

During drop formation:

The experimental overall mass transfer coefficient during drop formation was evaluated using the equation

$$N_f = K_{df} A \Delta C \qquad (8)$$

The coefficient was predicted using Heertjes equation (10). The results are compared in

Figures 5 and 6.

During drop ascent:

The overall mass transfer coefficient during drop rise was calculated using equation 8 above. The coefficient was also predicted by the methods of Calderbank et al (30), Handlos et al (5) and Rose and Kintner (6). A comparison of the data for single drops is given in Figures 7 to 9 and for drop pairs in Figures 10 to 12.

DISCUSSION OF RESULTS

Mass transfer during formation was significantly greater than predicted by existing correlations, which are summarised in Table 3. The overall mass transfer coefficient was of the order of 22% greater for single drops and an improved correlation has therefore been developed, based upon more reliable surface area predictions (32). For drop pairs the deviation was of the order of 55%, indicative of turbulence transfer between the forming drops. This is of relevance to the design of distributors and sieve plates.

Clearly, from Figures 7 to 9, published models for the prediction of mass transfer from single large oscillating drops provide a poor correlation of the experimental data. Possible explanations for this are that,

a) The models were derived for d < 5mm.

b) A higher initial solute concentration, 25% w/w, was used in this work.

c) Most of the models attempt to approximate the shape of the drop to s spheroid or take average values to evaluate the variables eg surface area. The deviations from a symmetrical spheroid noted by Al-Hassan (1) have been confirmed, indeed some drops deformed to a spherical cap or an ellipsoidal cap.

No work has been published previously on the alteration to mass transfer when two or more drops travel together in a continuum. The results in Figures 10 to 12 demonstrate an enhancement of overall mass transfer coefficient by between 64%-88% due to mutual interference during travel and, in particular, to collision and rebound.

(Inter drop coalescence was avoided in all experiments.)

CONCLUSIONS

With the system studied, the mass transfer characteristics of single large drops during formation from projecting nozzles, and of large (ie >5mm) oscillating single drops during travel, are poorly correlated by published models. In particular an improved model is required for mass transfer during formation (32).

The situation of drop pairs, which is but the first step towards the real case of drop swarms, is not catered for at all by existing correlations. A model has subsequently been derived for predicting the frequency of oscillation of a large drop adjacent to a second equi-sized drop (32). A dimensionless equation has also been proposed for eccentricity in this case (32). However, further work is necessary before the implications for column design can be assessed.

ACKNOWLEDGEMENTS

The authors wish to express appreciation to Professor G V Jeffreys for his interest, encouragement and suggestions throughout this work.

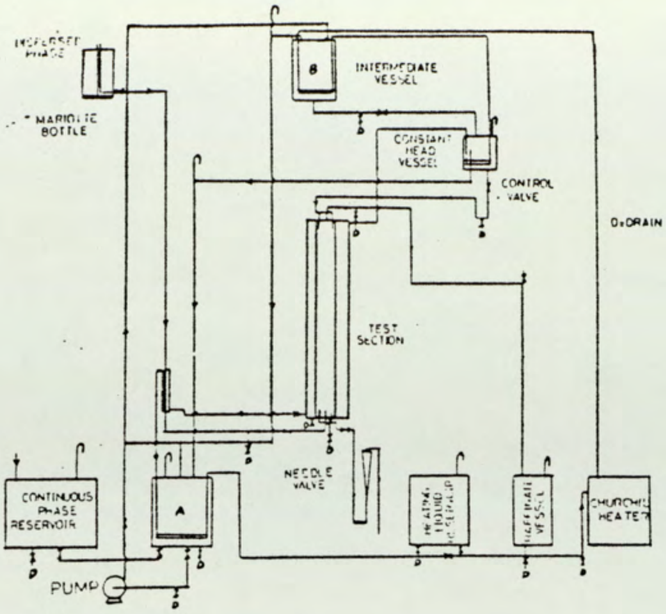

Figure A Flow Diagram of Apparatus

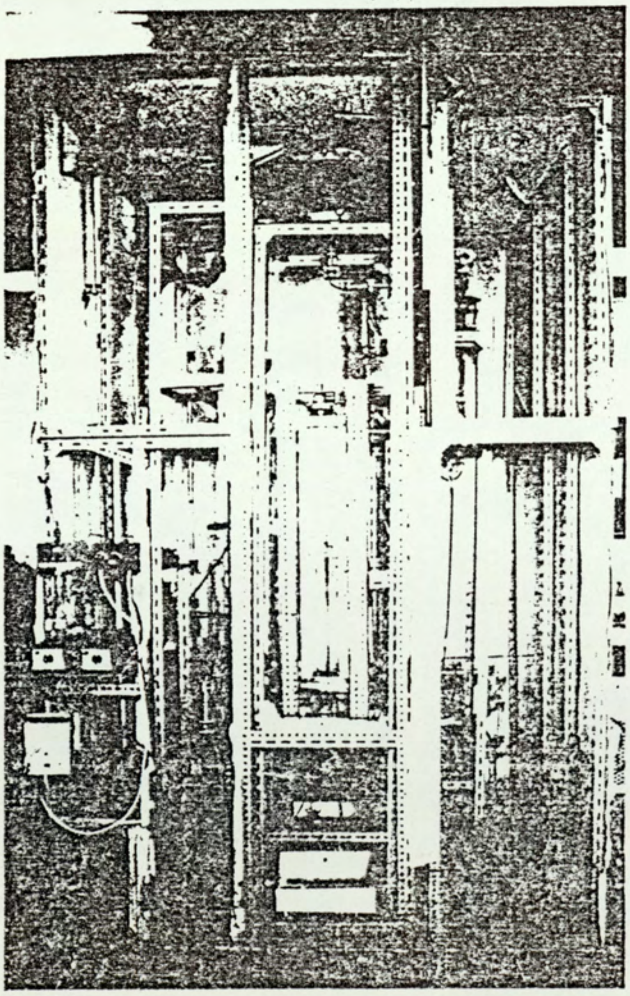

Figure B General Arrangement of Apparatus

Test section and mirror arrangement in the centre of enclosed cabinet. Heater circulator on the right.

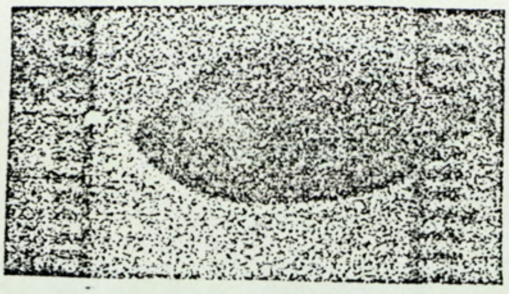

de = 0.75 cm
Re = 1333
n = 3

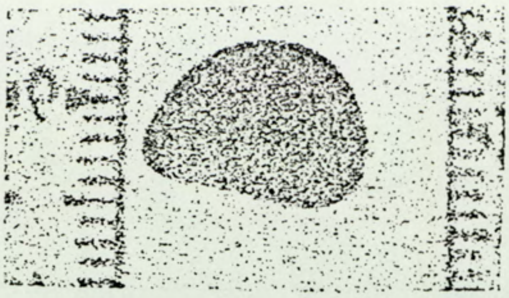

de = 0.55 cm
Re = 790
n = 2

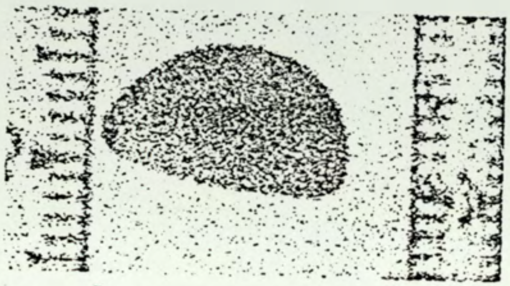

de = 0.57 cm
Re = 811
n = 2

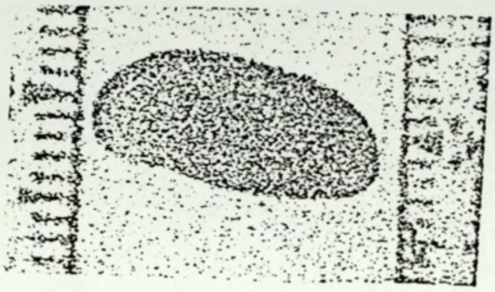

de = 0.61 cm
Re = 892
n = 4

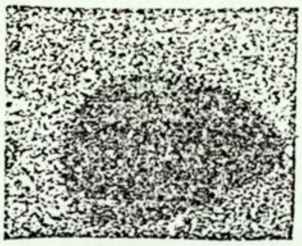

de = 0.52 cm
Re = 733
n = 3

de = 0.68 cm
Re = 958
n = 2

Figure C Relation between the shape of a drop and its mode of oscillation (n) and Reynolds Number.

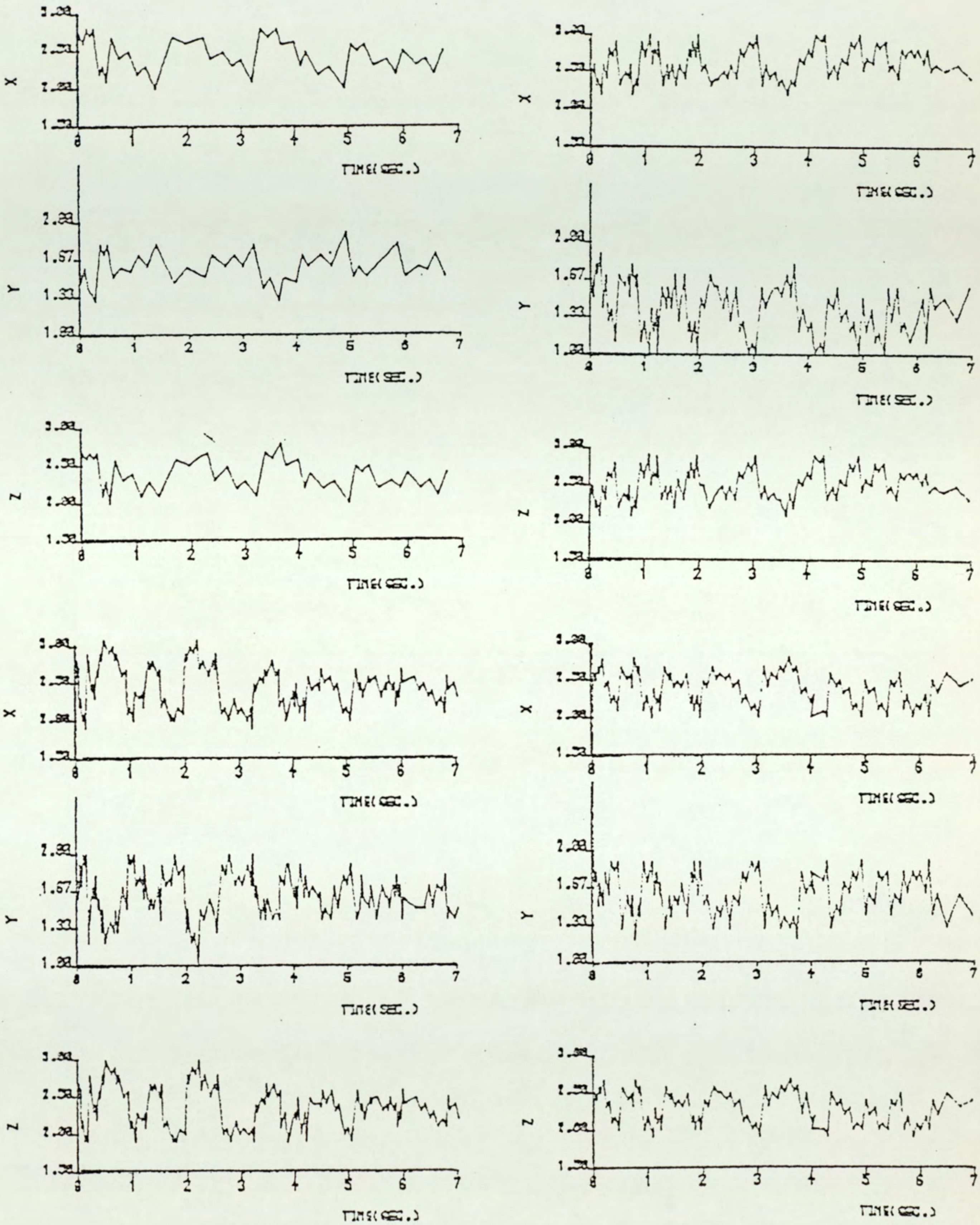

(a) Single drop

(b) Equi-sized drop pair

Figure D Fluctuations in single and drop pair dimensions (x, y and z - axes) with time

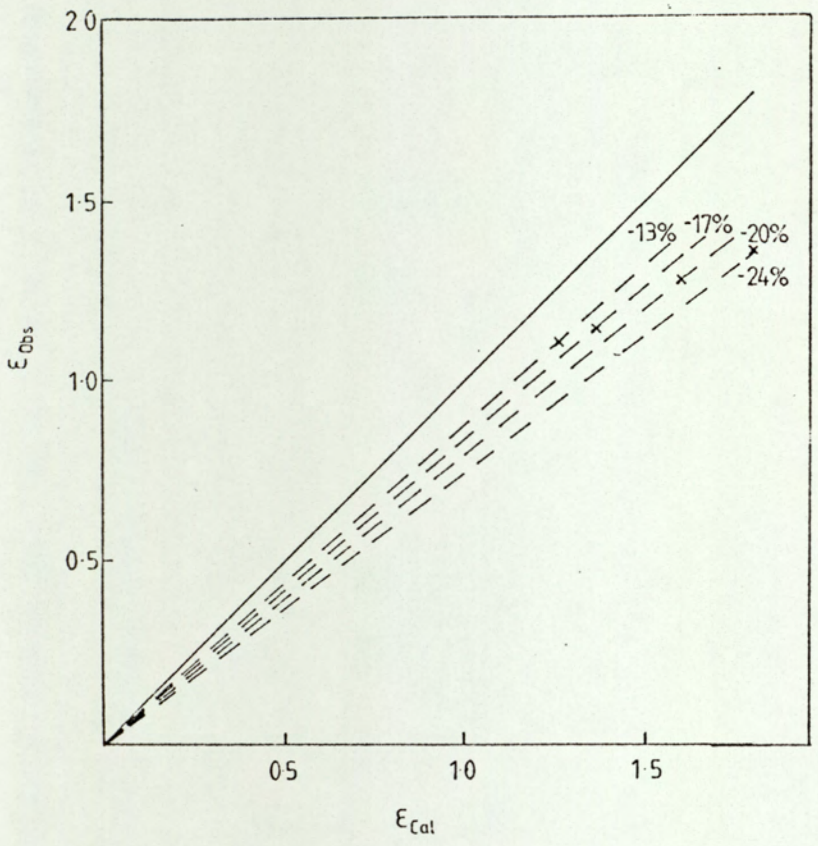

Figure 1 Observed and Calculated ε's of Single drops.

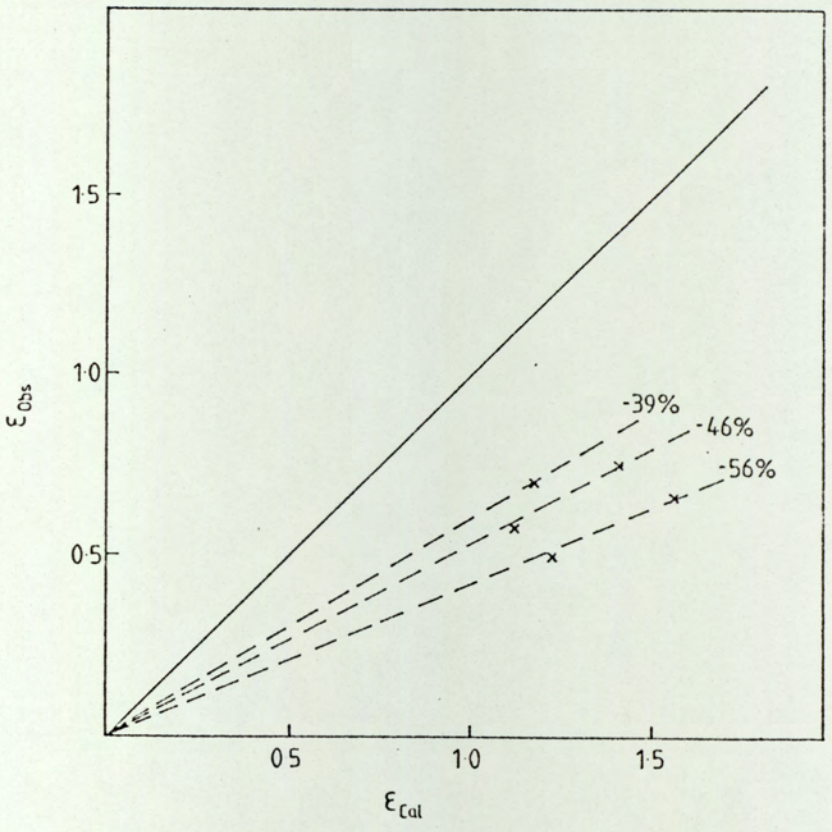

Figure 2 Observed and Calculated ε's of Drop pairs.

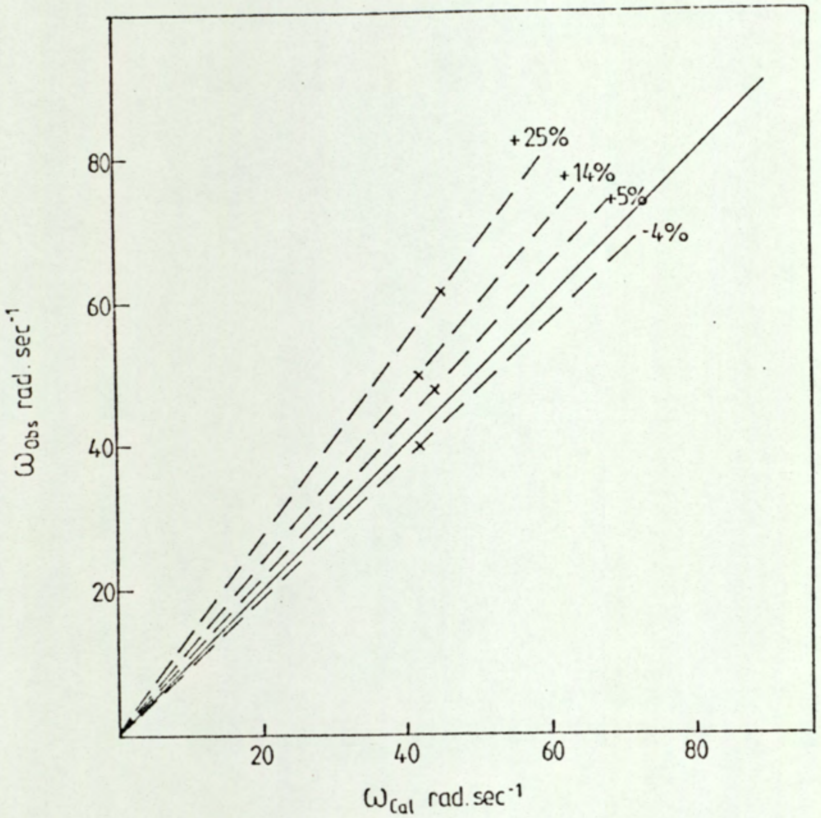

Figure 3 Observed and Calculated ω of single drops using equation (2·9), n = 2.

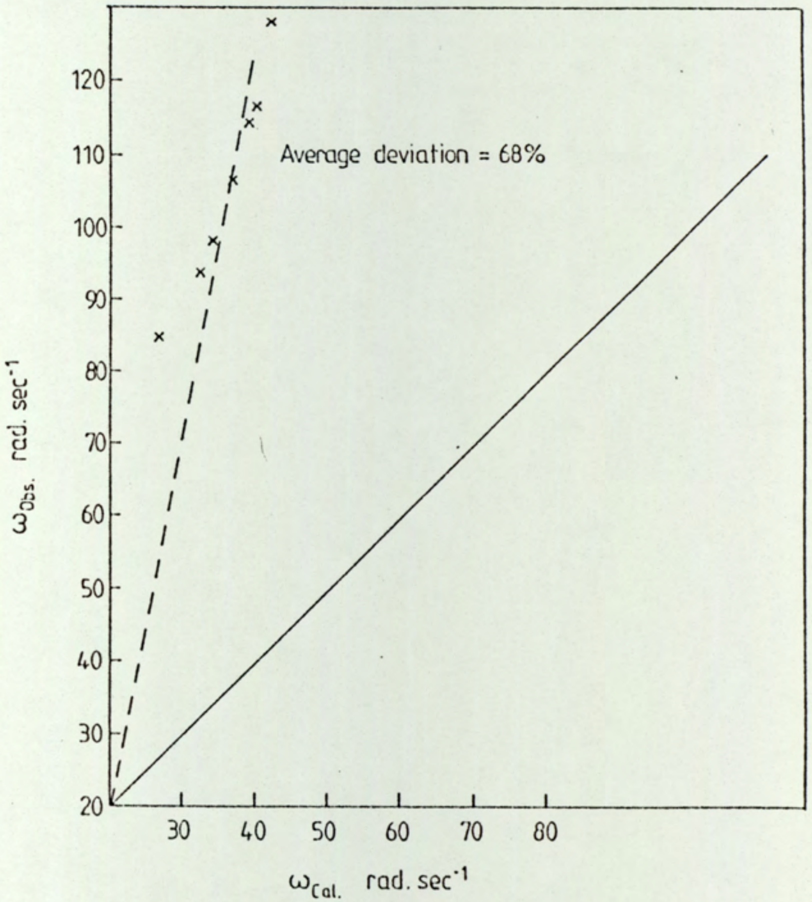

Figure 4 Observed and Calculated ω of drop pairs using equation (2·9). n = 4

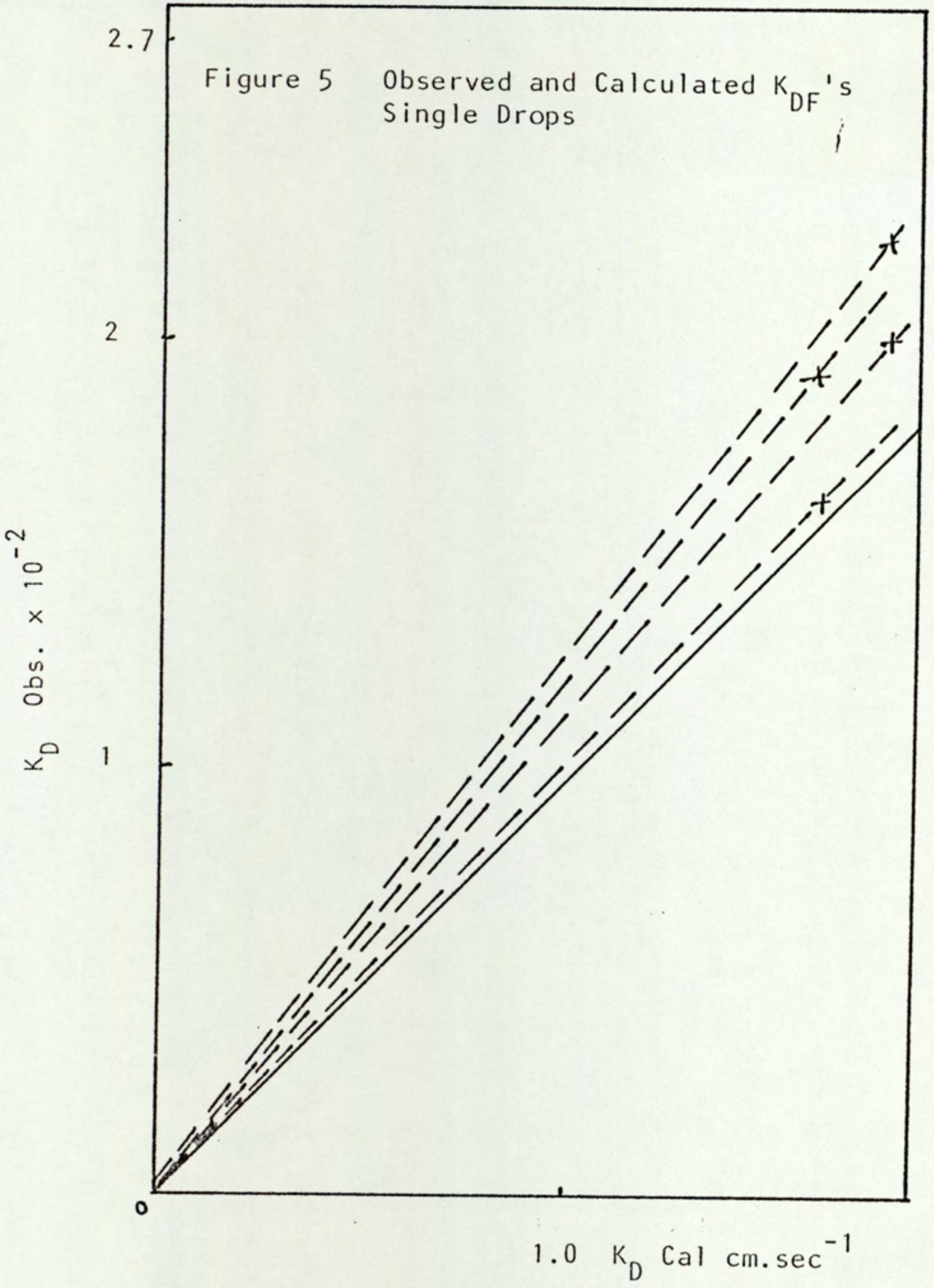

Figure 5 Observed and Calculated K_{DF}'s Single Drops

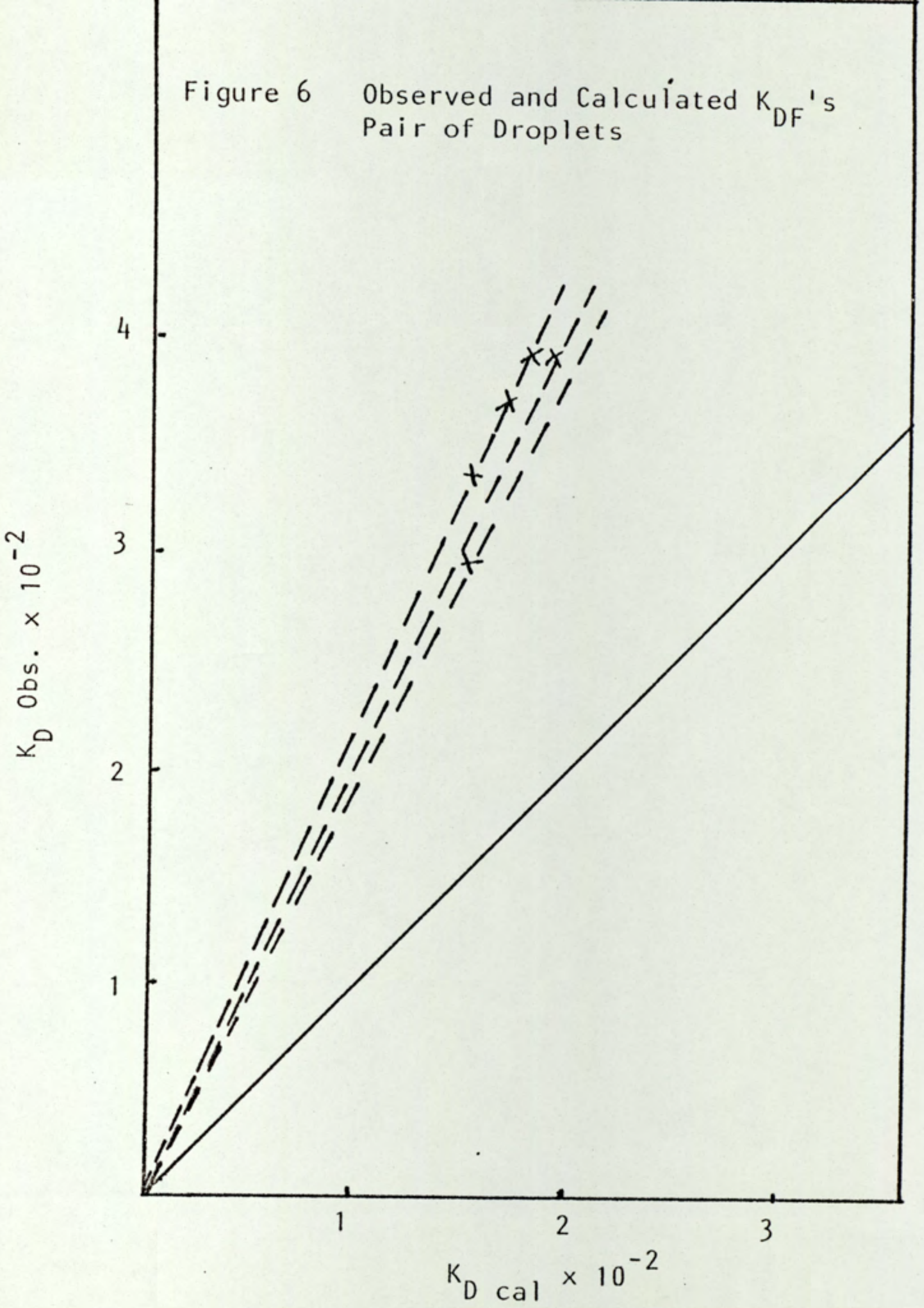

Figure 6 Observed and Calculated K_{DF}'s Pair of Droplets

Figure 7 Comparison between $K_{D\ exp}$ and $K_{D\ Cal}$ for single phase drops based on equation 6.

0 at n = 4 maximum deviation = 63%

X at n = 2 maximum deviation = 77%

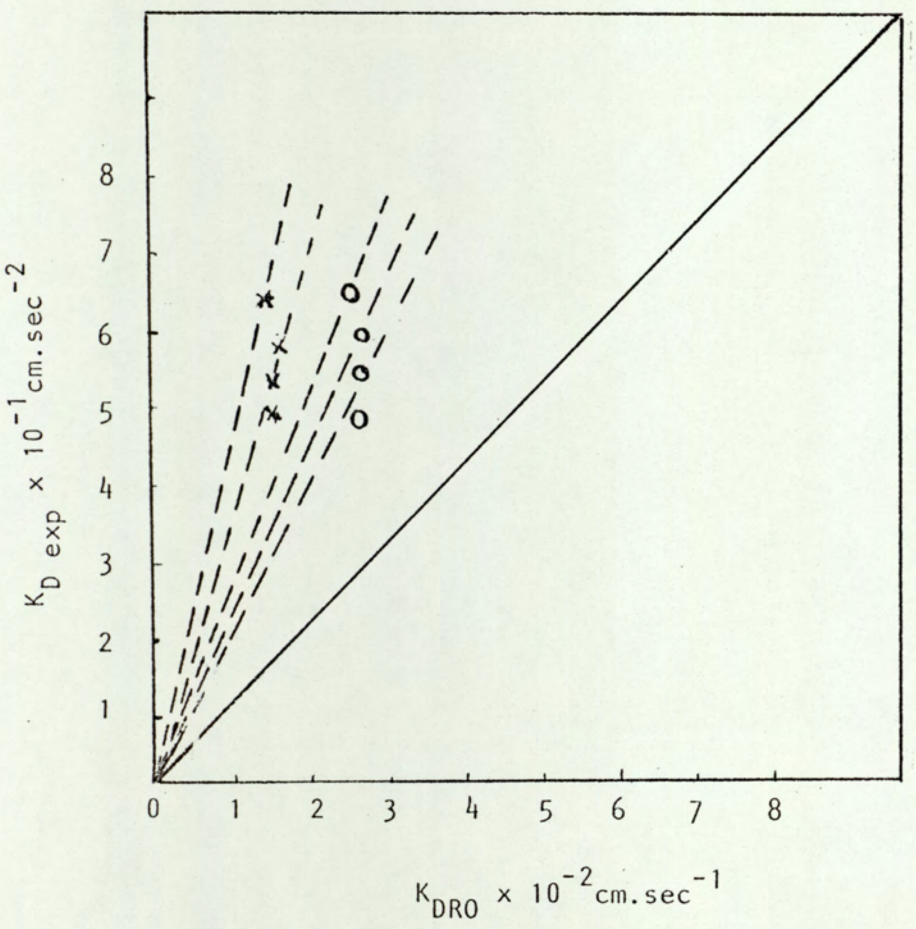

Figure 8 Comparison between $K_{D\ exp}$ and $K_{D\ cal}$ for single phase drops based on equation 8.

0 at n = 4 maximum deviation = -14%

X at n = 2 maximum deviation = +19%

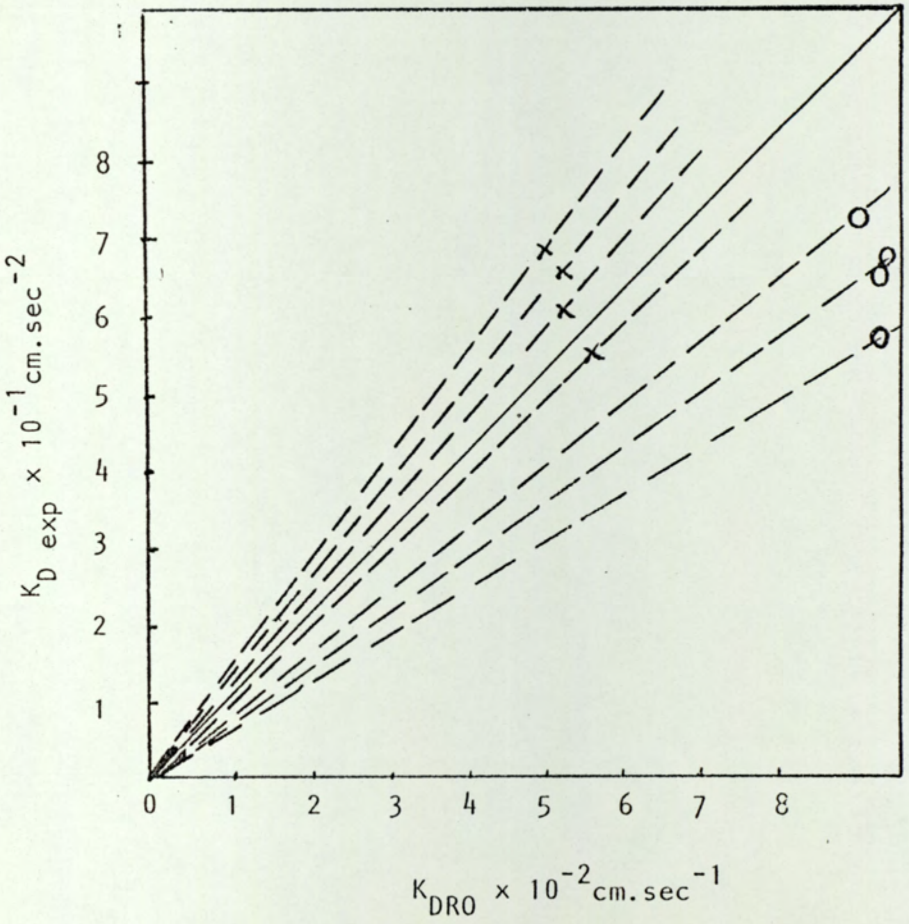

Figure 9 Comparison between $K_{D\ exp}$ and $K_{D\ cal}$ for single droplet based on equation 6

0 at n = maximum deviation = +30%
X at n = 2 maximum deviation = +82%

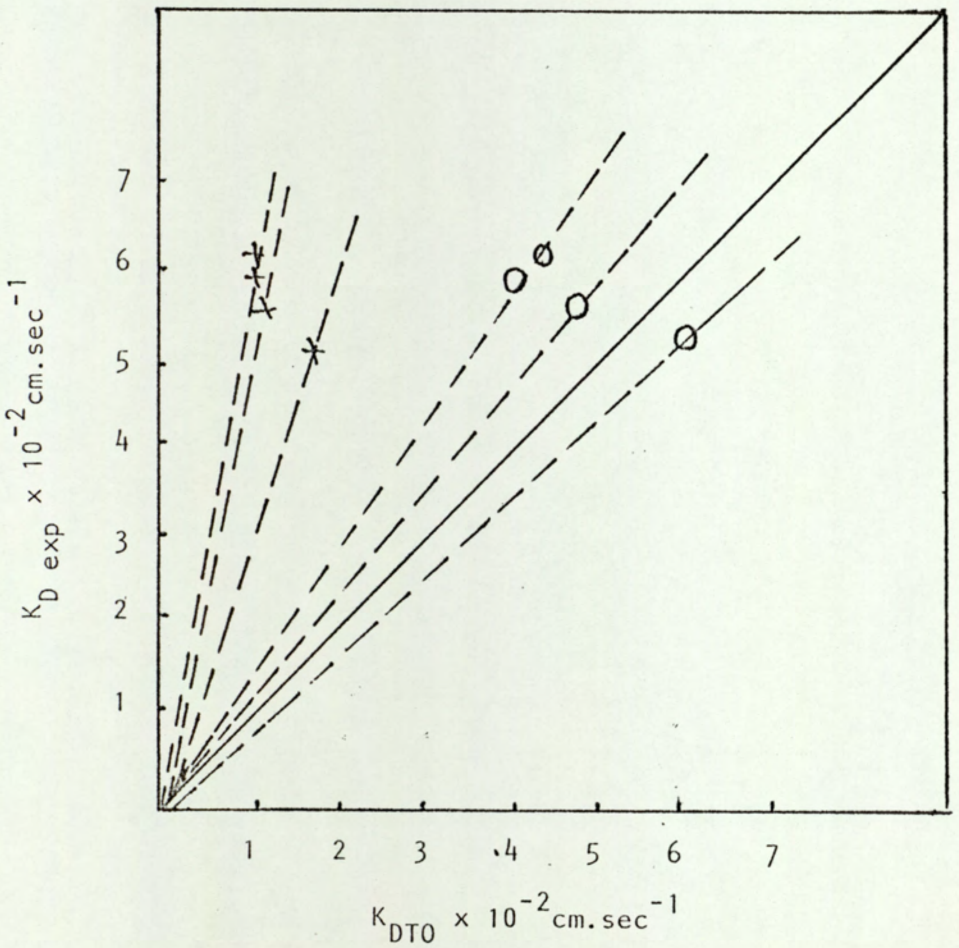

Figure 10 Comparison between $K_{D\ exp}$ and $K_{D\ cal}$ for pair of drops based on equation 3

0 at n = 4 maximum deviation = 88%
X at n = 2 maximum deviation = 92%

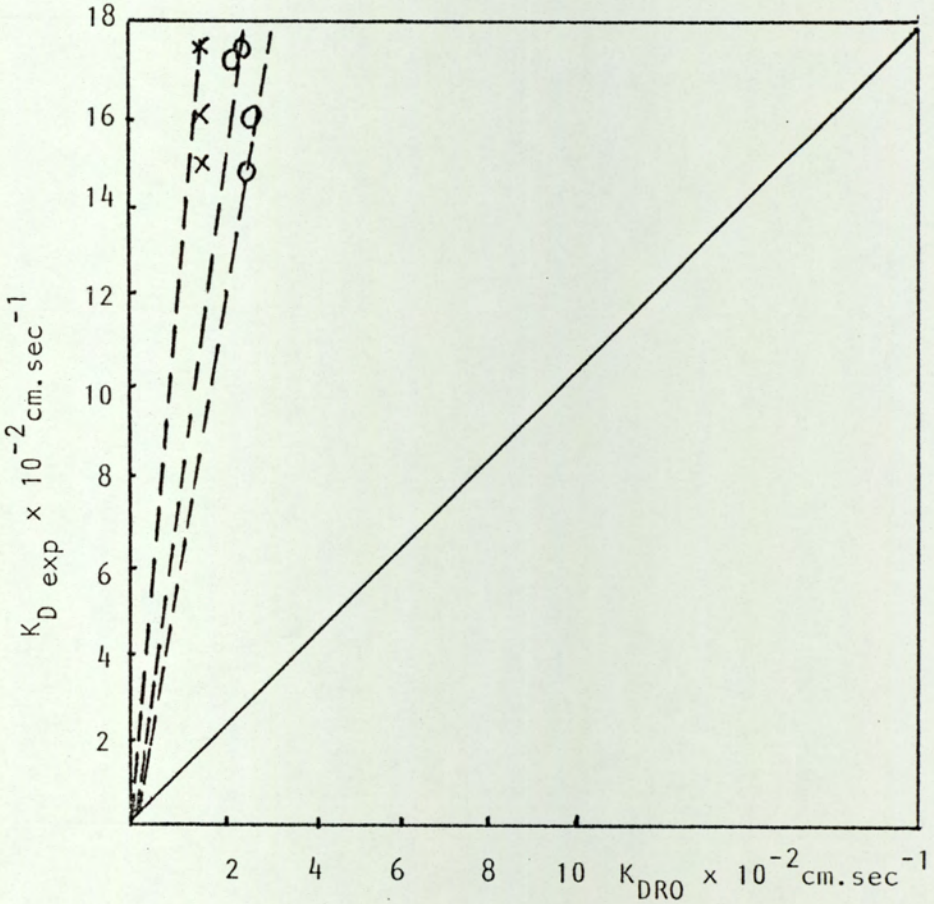

Figure 11 Comparison between $K_{D\ exp}$ and K_D for Drop Pairs based on equation 4

0 at n = 4 maximum deviation = 64%
X at n = 2 maximum deviation = 79%

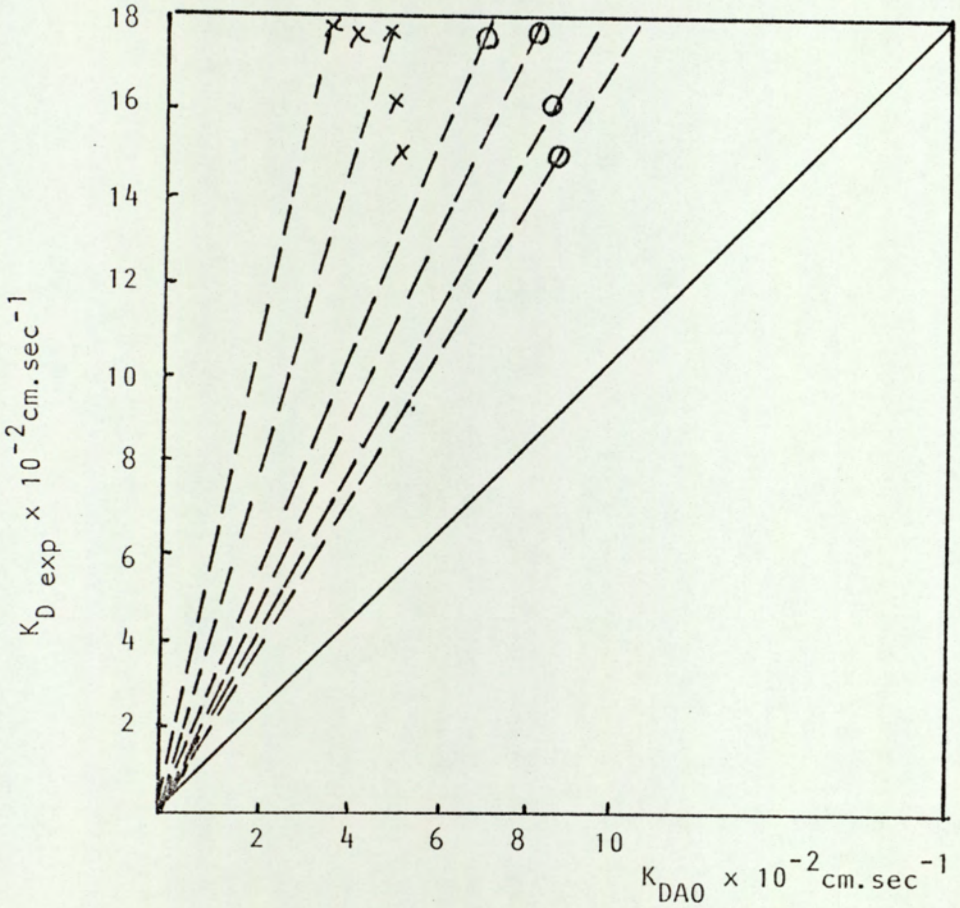

Figure 12 Comparison between $K_{D\ exp}$ and $K_{D\ cal}$ for Drop Pairs based on equation 6

0 at n = 4 maximum deviation = 65%
X at n = 2 maximun deviation = 93%

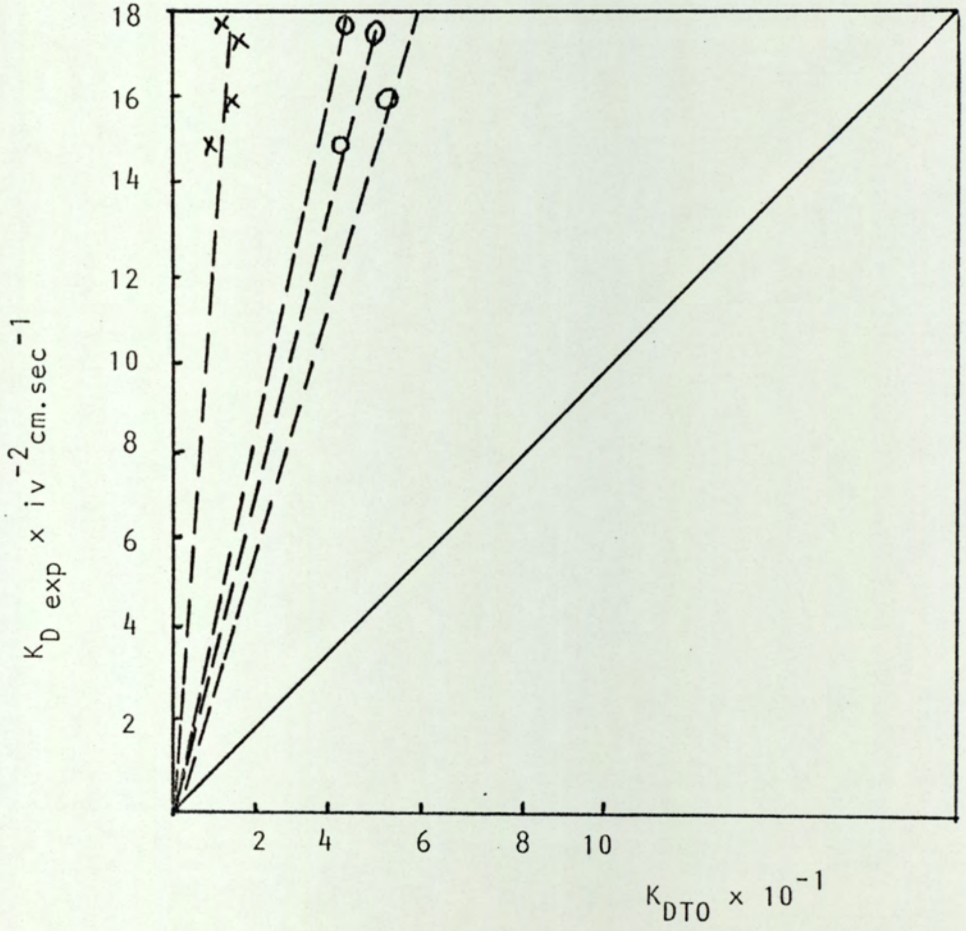

NOMENCLATURE

A	Interfacial area of droplet, cm^2
A_o	Initial area of droplet, cm^2
a	Horizontal radius, cm
a_o	Initial horizontal radius, cm
a_d	Surface area of drop, cm^2
a_p	Amplitude
b	Vertical radius of spheroid, cm
b_o	Initial vertical radius
C_1	Solute concentration, gm-mol/L
C_o	Initial solute concentration gm-mol/L
C^*	Equilibrium solute concentration gm-mol/L
C_D	Drag coefficient
d	Diameter of spherical droplet, cm
d_e	Diameter of sphere having the same volume of the droplet, cm
D	Molecular diffusivity, cm^2/sec
D_E	Effective diffusivity, cm^2/sec
D_d	Molecular diffusivity of solute in dispersed phase cm^2/sec
E_o	Eotvos Number = $\frac{g\Delta\rho de^2}{\sigma}$
Em	Fractional Extraction
f	Function, formation
g	Acceleration due to gravity cm/sec^2
K_{DF}	Dispersed phase mass transfer coefficient during drop formation
K_{DR}	Dispersed phase mass transfer coefficient, equation 3
K_{DA}	Dispersed phase mass transfer coefficient, equation 4
K_{DT}	Dispersed phase mass transfer coefficient, equation 6
K_{CR}	Continuous phase mass transfer coefficient, Rose and Kintner correlation
K_{DRO}	Overall mass transfer coefficient of dispersed phase due to Rose and Kintner
K_{DAO}	Overall mass transfer coefficient of dispersed phase due to Angelo et al
K_{DTO}	Overall mass transfer coefficient of dispersed phase due to Al-Hassan

σ	Interfacial tension ratio in dyne/cm
P_e	Peclet number deV/D
S_c	Schmidt number = $\mu/\rho D$
S_r	Strohel number = wd/V
S_h	Sherwood number = Kd/D
μ_c	Viscosity of continuous phase gm/cm sec
μ_d	Viscosity of dispersed phase gm/cm sec
ρ_c	Density of continuous phase gm/cm^3
ρ_d	Density of dispersed phase gm/cm^3
t	Residence time of droplet in the contactor, sec
t_f	Time of droplet formation, sec
t_o	Initial time, sec
V	Volume of drops, cm^3
Vel	Velocity of drops, cm-sec^{-1}
r_o	Initial radius, cm
ε	Eccentricity
ε_o	Initial eccentricity
n	Mode of oscillation
w	Frequency of oscillation, sec^{-1}
X	Radius of the drop in X-direction
Y	Radius of the drop in Y-direction
Z	Radius of the drop in Z-direction
W_e	Weber number = $\dfrac{d_e.V^2\rho}{\sigma}$
Sh_n	Contribution of Sherwood number due to natural convection
m	Distribution coefficient
T	Temperature °C
-	Average
*	Equilibrium

REFERENCES

1. Al-Hassan, T S, PhD Thesis, Aston University, (1979).
2. Johnson, A I and Hamielec, A E, A.I.ChemE. J, 6, 145, (1960).
3. Newman, A B, Trans. Am. Inst. Chem. Eng, 27, 203, (1931).
4. Kronig, Q and Brink, J C. Appl. Sci. Res, A-2, 142, (1950).
5. Handlos, A E and Baron, T. A.I.ChemE. J., 3, 127, (1957).
6. Rose, P H and Kintner, R C, A.I.ChemE. J., 12, 530, (1966).
7. Schroeder, R R and Kintner, R C, A.I.Chem.E. J., 11, 5, (1965).
8. Angelo, J B et al, A.I.Chem.E. J., 12, 751, (1966).
9. Licht, W and Pensing, W F, Ind. Eng. Chem., 45, 1885, (1953).
10. Heertjes, P A, Holve, W A and Talsma, H, Chem. Eng. Sci., 3, 122, (1954).
11. Groothuis, H and Kramers, H, Chem. Eng. Sci., 49, 17, (1955).
12. Coulson, J H and Skinner, S J, Chem. Eng. Sci., 1, 197, (1952).
13. Heertjes, P A and DeNie, L H, Chem. Eng. Sci., 21, 755, (1966).
14. Heertjes, P A and DeNie, L H, Mass Transfer to Drops, in "Recent Advances in Liquid-Liquid Extraction", C Hanson, ed. (1971).
15. Ilkovic, D, Colln. Czech. Chem. Commun., 6, 498, (1934).
16. Linton, M and Sutherland, Chem. Eng. Sci. Paris, 152, 1735, (1977).
17. Rowe, P N et al, Trans. Instn. Chem. Engrs., 43, 14, (1965).
18. Kinard, G E, Manning, F S and Manning, W P, Brit. Chem. Eng., 8, 326, (1963).
19. Boussinesq, J, C.R. Acad. Sci. Paris, 152, 1735, (1977).
20. Garner, F H and Tayeban, M. An. R. Soc. Esp. Fis. Quim., 563, 491, (1975).
21. Garner et al, Jnl. Appl. Chem., 9, 33, 821, (1978).
22. Mekasut, L, Molinier, J and Angilino, H, Chem. Eng. Sci., 33, 821, (1978).
23. Yamaguchi, M et al, Jnl. Chem. Eng. Japan, 8, 415, (1975).
24. Skelland, A H P and Wellek, R M, A.I.Chem.E. J., 10, 2191, (1964).
25. Brunson, R J and Wellek, R M, Can. Chem. Mag. J, 48, 267, (1970).
26. Yamaguchi, M, Fujimato and Katayama, T, J. Chem. Eng. Japan, 8, 361, (1975).
27. Popovich, A T, Jervis, R E and Trass, O, Chem. Eng. Sci, 19, 357, (1964).
28. Walia, D S and Vir, D, Chem. Eng. Sci. 31, 525, (1976).
29. Thorsen, G et al, Chem. Eng. Sci., 23, 413, (1968).
30. Calderbank, P H et al, Chem. Eng. Sci., 6, 65, (1956).
31. Goltz, G E et al, Anal. Chem., 29, 816, (1957).
32. Malalah, M, PhD Thesis, Aston University.

NOMENCLATURE

A	area of droplet, m^2 eq. (1.1)
A	area of one plate, m^2 eq. (9.1)
$\bar{A}$	mean area of drop during travel, m^2
A_{mf}	mean area of drop during formation, m^2
A_S	area of a sphere, m^2
A_{max}	area of droplet at maximum distortion eq. (3.6)
A_o	area of droplet at minimum distortion eq. (3.6)
A	a constant eq. (4.14)
AR	area ratio $\frac{DA}{SA}$ (Appendix D)
a	horizontal radius of spheriod, m
a_p	amplitude in x-axis, eq. (3.5) and (4.58)
a_o	initial radius, m eq. (4.58)
b	vertical radius of spheriod, m
b	amplitude coefficient eq. (3.7) and (2.11)
C	concentration kg.moles/L
C	constant eq. (4.13) and (4.52) and (7.7)
C_f	final concentration
C_o	initial concentration
C^*	equilibrium concentration
C_R	concentration in the raffinate phase
C_E	concentration in the extract phase
C_D	drag coefficient
ΔC	concentration difference
D	diffusivity, m^2/sec

DA	area of the drop (Appendix D)
D_c	diffusivity of continuous phase
D_d	diffusivity of dispersed phase
D_E	effective diffusivity
DR	diameter ratio, eq. (2.29)
d	diameter of droplet, m
d_e	equivalent diameter of droplet, m
E	eccentricity
E_m	extraction efficiency
F	drag force
f_c	correlation factor eq. (4.20)
f_c	flow rate of continuous phase
f_d	flow rate of dispersed phase
g	acceleration of gravity m/s^2
K	constant eg. (7.16)
K	overall mass transfer coefficient
k	individual mass transfer coefficient
k	dielectric constant eq. (9.1)
K_{od}	overall mass transfer coefficient, Figure 3.2
K_{df}	overall mass transfer coefficient of droplet during formation
K_{dc}	overall mass transfer coefficient of droplet during circulation
K_{ds}	overall mass transfer coefficient of droplet during oscillation
K_{dRO}	overall mass transfer coefficient by Rose and Kintner correlation
K_{dAO}	overall mass transfer coefficient by Angelo et al correlation
K_{dTO}	overall mass transfer coefficient by Al-Hassan correlation
m	constant eg. (4.14)
m, m'	distribution coefficient

n	constant eq. (4.14)
n	mode of oscillation
N, N_t, N_f	mass transfer rates kg.mols/s
N_A, N_{AO}	interfacial flux in solute kg.mols/s
P	physical property group
R	constant effective diffusivity eq. (4.37)
RXY	deformation ratio [(X - Y)/(X + Y)], Appendix D
SA	area of a sphere (Appendix D)
S	interaction of drops wake eq. (7.13)
T, t	time, droplet rise period, s
U	terminal velocity eq. (2.29)
V	terminal velocity, m/s
V	volume of drop (Appendix D)
VEL	instantaneous velocity (Appendix D)
v	volume of drop, m^3
x	time in seconds eq. (7.7)
X	length of droplet x-axis, m, film thickness in eq. 3.5, defined in eq. 4.49
X_o	initial drop diameter m x 10^{-2}, initial film thickness in eq. 3.5
Y	length of droplet y-axis, m
Z	length of droplet z-axis, m
conc$^{\underline{n}}$	concentration, kg.moles/L
$(Sh_c)_n$	Contribution of Sherwood number due to natural convection

Dimensionless Groups

Re	Reynolds number $\frac{V de\, \rho_c}{\mu_c}$
$\overline{Re}$	modified Reynolds number $\frac{\rho_c\, \omega\, de^2}{\mu_c}$

Sc	Schmidt number $\frac{\mu}{\rho D}$
Sh	Sherwood number $\frac{k\, de}{D}$
Sr	Strouhal number $\frac{\omega\, de}{V}$
We	Weber number $\frac{de\, V^2 \rho}{\sigma}$
Ga	Galileo number $\frac{de^3 \rho^2 g}{\mu^2}$
Pe	Peclet number $\frac{de\, V}{D}$
Eo	Eotvos number $\frac{g\, \Delta \rho\, d^2}{\sigma}$
M	Morton number $\frac{g\, \mu^4 \Delta \rho}{\rho^2 \sigma^3}$
Oh	Ohnesorge number $\left(\frac{\mu_d}{\rho_d \sigma\, de}\right)^{0.5}$
T_m	time dimensionless group $\frac{4 D t}{de^2}$

Functions

A_n	function of K_d eq. (4.35)
λ_n	function of K_d eq. (4.35)
h	function eg. (4.22)
$f_1(t)$	function of time eq. (4.49)
f	function eq. (7.10)
IF (I,ϕ)9Ei (I,ϕ)	elliptic integrals
b_1	empirical function eq. (2.11)

Greek Letters

ρ	density kg/m^3
μ	viscosity, cP
$\Delta\rho$	$(r_c - r_d)$, kg/m^3
σ	interfacial tension dyne/cm
ω	frequency of oscillation rad/s
ω'	1/2 ω
ω_t	transitional frequency rad/sec
θ	time, s
τ	dimensionless time
σ_r	ratio of interfacial tension $\frac{\sigma_i}{\sigma_f}$
μ_R	ratio of viscosity $\frac{\mu_d}{\mu_d}$

ε	amplitude of oscillation eq. (3.6)
ε_o	permativity of free space in mKS units, eq. (9.1)

Subscript

A	compound A
a	average
c	continuous phase
cal.	calculated value
D, d	dispersed phase
df	during drop formation
E	extract phase
e	equivalent
exp	experimental value
f	final, formation
h	horizontal
HB	Handlos and Baron
HG	Higbie
mf	mean during formation
max.	maximum
min.	minimum
obs.	observed value
Corr.	correlated value
o, i	initial, minimum
R	raffinate phase
S	sphere
T	column
theo	theoretical value
v	vertical eq. (2.21)

REFERENCES

(1) Al-Hassan, T S.
PhD Thesis, University of Aston in Birmingham, UK (1979).

(2) Al-Aswad, K K.
PhD Thesis, University of Aston in Birmingham, UK (1982).

(3) Dawodu, F A.
PhD Thesis, University of Aston in Birmingham, UK (1983).

(4) Stokes, G G.
Trans. Camb. Phil. Soc., 9, 8, (1850)

(5) Khandelwal, A N.
PhD Thesis, University of Aston in Birmingham, UK (1978).

(6) Hadamard, J S.
C R Acad. Sci. Paris, 152, 1735, (1911).

(7) Rybezynski, W.
Bull. Acad. Sci. Cracovie, Ser. A, 40, (1911).

(8) Boussinesq, J.
C R Acad. Sci. Paris, 156, 983, 1035, 1124, (1913).

(9) Kehat, E and Letan, R.
A.I.Ch.E.J., 17, 984, (1971).

(10) Magarvey, R H and Bishop R L.
Can. J. Phys., 39, 1418, (1961).

(11) Klee, A J and Treybal, R E.
A.I.Ch.E.J., 2, 444, (1956).

(12) Hendrix, C D, Dave, S B and Johnson, H F.
A.I.Ch.E.J., 13, 1072, (1967).

(13) Harriott, P.
Can. J. of Chem. Eng., 40, 60, (1962).

(14) Bond, W N and Newton, D A.
Phil. Mag., 794, (1928).

(15) Boussinesq, J.
C R Acad. Sci., 156, 1124, 1130, (1913). "Bubbles, Drops and Particles"
R Clift et al (ed.), Academic Press, NY, (1978).

(16) Garner, F H and Skelland, A H.
Chem. Eng. Sci., 4, 149, (1955).

(17) Kintner, R C, Horton, T J, Groumann, R E and Amberkar, S.
Can. J. of Chem. Eng., 39, 235, (1961).

(18) Grace, J R.
Tran. Instn. Chem. Engrs., 51, 116-120, (1973).

(19) Grace, J R, Wairegi, T and Nguyen, T H.
Tran. Instn. Chem. Engrs., 54, 167-173, (1976).

(20) Gunn, R.
J. Geophys. Res., 54, 383, (1949).

(21) Garner, F H and Tayeban, M.
An. R. Soc. Esp. Fis. Quim., 56B, 491, (1960).

(22) Garner, F H and Haycock, P J.
Proc. Roy. Soc., A252, 457, (1959).

(23) Johnson, A I and Hamielec, A E.
A.I.Ch.E.J., 6, 145, (1960).

(24) Elzinga, E R and Banchero, J T.
A.I.Ch.E.J., 7, 394, (1961).

(25) Hughes, R R and Gilliland, E R.
Chem. Eng. Progr., 48, 497, (1952).

(26) Winnikow, S and Chao, B T.
Phys. Fluid, 9, 1, 50, (1966).

(27) Foote, G B J.
Comput. Phys., 11, 507, (1973).

(28) Lamb, H.
"Hydrodynamics", Cambridge University Press, (1957).

(29) Rayleigh, Lord.
Proc. Roy. Soc., 29, 71, (1879).

(30) Schroeder, R R and Kintner, R C.
A.I.Ch.E.J., 11, 5, (1965).

(31) Miller, C A and Scriven, L E.
J. Fluid Mech., 32, 417, (1968).

(32) Subramanyan, S V.
J. Fluid Mech., 37, 715, (1969).

(33) Davies, J T.
"Turbulence Phenomena", Acad. Press, New York, (1972).

(34) Hartunian, R A and Sears, W R.
J. Fluid Mech., 3, 27, (1957).

(35) Hu, S and Kintner, R C.
A.I.Ch.E.J., 1, 42, (1955).

(36) Edge, R M and Grant, C D.
Chem. Eng. Sci., 26, 1001, (1971).

(37) Bond, W N.
Phil., Mag., Ser., 7, V5, 889, (1927).

(38) Licht, W and Narasimhamurty, G S R.
A.I.Ch.E.J., 1, 366, (1955).

(39) Thorsen, G, Stordalen, R M and Terjesen, S G.
Chem. Eng. Sci., 23, 413, (1968).

(40) Stapathy, R and Smith, W.
Fluid Mech. J., 10, 56, (1961).

(41) Mekasut, L, Molinie, J and Angelino, H.
Chem. Eng. Sci., 33, 821, (1978).

(42) Vignes, A.
Genic Chimique, 93, 173, (1965).

(43) Kintner, R C.
Advan. Chem. Eng., 4, 51, (1963).

(44) Calderbank, P H and Korchinski, I J O.
Chem. Eng. Sci., 6, 65, (1956).

(45) Johnson, A I and Braida, L.
Can. J. of Chem. Eng., 35, 165, (1957).

(46) Torobin, L B and Gauvin, W H.
Can. J. Chem. Eng., 37, 167, (1959).

(47) Yeheskel, J and Kehat, E.
Chem. Eng. Sci., 26, 223, (1971).

(48) Yeheskel, J and Kehat, E.
Chem. Eng. Sci.,26, 2037, (1971).

(49) Garner, F H and Grafton, R W.
Proc. Soc., A224, 64, (1954).

(50) Maxworth, T J.
Fluid Mech., 27, 367, 91967).

(51) Wegener, P P and Parlange, J Y.
Annu. Rev. Fluid Mech., 5, 79, (1973).

(52) Wellek, R M, Agrawal, A K and Skelland, A H P.
A.I.Ch.E.J., 12, 854, (1966).

(53) Heertjes, O M, Holve, W A and Talsma, H.
Chem. Eng. Sci., 3, 122, (1954).

(54) Raymond, D R and Zieminski, S A.
A.I.Ch.E.J., 17, 57, (1971).

(55) Griffith, R M.
Chem. Eng. Sci., 17, 1057, (1962).

(56) Frumkin, A and Levich, V G.
Zh. F12. Khim, 21, 1183, (1947).

(57) Levich, V G.
"Physicochemical Hydrodynamics", Prentice Hall, NY, (1962).

(58) Lochiel, A C.
Can. J. Chem. Eng., 43, 40, (1965).

(59) Haberman, W L and Sayre, R M.
David Taylor Model Basin Rep., Nu. 1143, (1958).

(60) Strom, J R and Kintner, R C.
A.I.Ch.E.J., 4, 153, (1958).

(61) Bird, R B.
Advances Chem. Eng., 1, 155, (1956).

(62) Lewis, W K.
Ind. Eng. Chem., 8, 8251, (1916).

(63) Lewis, W K and Whitman W G.
Ind. Eng. Chem., 16, 1215, (1924).

(64) Whitman, W G.
Chem. and Met. Eng., 29, 147, (1923).

(65) Higbie, R.
Trans. Am. Inst. Chem. Engrs., 31, 365, (1935).

(66) Brunson, R J and Wellek, R M.
Can. Chem. Eng. J., 48, 266, (1970).

(67) Haberman, W L and Morton, R K.
David Taylor Model Basin Rep., 802, (1953).

(68) Colburn, A P and Welsh, D G.
Tran. Inst. Chem. Eng., 38, 179, (1942).

(69) Angelo, J B, Lightfoot, E N and Howard, D W.
A.I.Ch.E.J., 12, 751, (1966).

(70) Ruckenstein, E.
Chem. Eng. Sci., 23, 363, (1968).

(71) Danckwerts, P V.
Ind. Eng. Chem., 43, 1460, (1951).

(72) Shulman, H L, Ullrich, C R and Wells, N.
A.I.Ch.E.J., 1, 247, (1955).

(73) Satoru Asai et al.
Soc. of Chem. Eng. of Japan, v.16 p.463, (1983).

(74) Toor, H L and Marchello, J M.
A.I.Ch.E.J., 4, 97, (1958).

(75) Kishinevskii, M K H and Pamfilov, A V.
J. Appl. Chem. USSR (Engl. Transl.), 22, 118, (1949).

(76) Kishinevskii, M K H.
J. Appl. Chem. USSR (Engl. Transl.), 24, 542, (1951).

(77) Kishinevskii, M K H and Keraivarenko, M A.
J. Appl. Chem. USSR (Engl. Transl.), 24, 413, (1951); Novik, 26, 673, (1953).

(78) Kishinevskii, M K H.
J. Appl. Chem. USSR (Engl. Transl.), 27, 359, (1953).

(79) King, C J.
Ind. Eng. Chem. Fundam., 5, 1, (1966).

(80) Rose, R M and Kintner, R C.
A.I.Ch.E.J., 12, 530, (1966).

(81) Ellis, S R M and Biddulph, M.
Chem. Eng. Sci., 21, 1107, (1966).

(82) Bakker, C A P, van Buytenen, P M and Beek, W J.
Chem. Eng. Sci., 21, 1039-1046, (1966).

(83) Sawistowski, H.
In "Recent Advances in Liquid-Liquid Extraction" (C Hanson, ed.), pp. 293-366, Pergamon, Oxford, (1971).

(84) Sterling, C V and Scriven, L E.
A.I.Ch.E.J., 5, 514, (1959).

(85) Sherwood, T K and Weir, J C.
Ind. Eng. Chem., 49, 1030, (1957).

(86) Thomson, J.
Phil. Mag., 10 (4), 330, (1855).

(87) Marangoni, C.
Annln. Phys., 143, 337, (1871).

(88) Olander, D R and Reddy, L B.
Chem. Eng. Sci., 19, 67, (1964).

(89) Takenchi, H and Numata Y.
Inter. Chem. Eng., 17, 468, (1977).

(90) Sawistowski, H and Goltz, G E.
Trans. Inst. Chem. Eng., 41, 174, (1963).

(91) Pearson, J R A.
J. Fluid Mech., 4, 489, (1958).

(92) Davies, J T and Rideal, E K.
"Interfacial Phenomena", 2nd ed., Academic Press, NY, (1963).

(93) Davies, J T.
Advances in Chemical Engineering, 4, 3, (1963).

(94) Brian, P L T.
A.I.Ch.E.J., 17, 765, (1971).

(95) Brian, P L T and Rose, J R.
A.I.Ch.E.J., 19, 582, (1972).

(96) Brian, P L T and Smith, K A.
A.I.Ch.E.J., 18, 231, (1971).

(97) Sherwood, T K, Pigford, R L and Wilke, C R.
"Mass Transfer Active Materials", Akademic Verlag, Berlin, (1967).

(98) Bakker et al.
Chem. Eng. Sci., 22, 1349-1355, (1967).

(99) Savic, P.
Natl. Res. Council Rep., Mt.22 Ottawa, Canada, (1953).

(100) Lindland, K P and Terjesen, S G.
Chem. Eng. Sci., 5, 1, (1956).

(101) Garner, F H and Hale A R.
Chem. Eng. Sci., 2, 157, (1953).

(102) Holm, A and Terjesen, S G.
Chem. Eng. Sci., 4, 265, (1955).

(103) Sawistowski, H and James, B R.
Proc. IIIrd International Conf. on Surface Active Materials, Akademic Verlag, Berlin, (1967).

(104) West, F B, Herman, A J, Chang, A T and Thomas, L E A.
Indus. Eng. Chem., 44, 625, (1952).

(105) Scheele, G F and Meister, B J.
A.I.Ch.E.J., 14, 9, (1968).

(106) Johnson, H F and Bliss, H.
Trans. Am. Inst. Chem. Eng., 42, 331, (1946).

(107) Logsdail, D H, Thornton, J D and Pratt, H R C.
Trans. Instn. Chem. Engrs., 35, 301, (1957).

(108) Groothuis, H and Zuiderweg, F J.
Chem. Eng. Sci., 12, 288, (1960).

(109) Jeffreys, G V and Lawson, G B.
Trans. Instn. Chem. Engrs., 43, 294, (1965).

(110) Humphrey, J A C, Hummel, R H and Smith, J W.
Chem. Eng. Sci., 29, 1496, (1974).

(111) Licht, W and Pensing, W F.
Ind. Eng. Chem., 45, 1885, (1953).

(112) Groothuis, H and Kramers, H.
Chem. Eng. Sci., 4, 17, (1955).

(113) Coulson, J H and Skinner, S J.
Chem. Eng. Sci., 1, 197, (1957).

(114) Heertjes, P M and de Nie, L H.
Chem. Eng. Sci., 21, 755, (1966).

(115) Ilkovic, D.
Colln. Czech, Chem. Commun., 6, 498, (1934).

(116) Hayworth, C B and Treybal R E.
Ind. Eng. Chem., 42, 1174, (1950).

(117) Null, H R and Johnson, H F.
A.I.Ch.E.J., 4, 273, (1958).

(118) Izard, J A.
A.I.Ch.E.J., 18, 634, (1972).

(119) Halligan, J E and Burkhart, L E.
A.I.Ch.E.J., 14, 411, (1968).

(120) Harkins, W D and Brown, F E.
J. Am. Chem. Soc., 41, 499, (1919).

(121) West, F B, Robinson, A, Morgenthalor, A C, Beck, T R and McGregor D K.
Ind. Eng. Chem., 43, 234, (1951).

(122) Licht, W and Conway, J B.
Ind. Eng. Chem., 42, 115, (1950).

(123) Sherwood, T K, Evans, J E and Longcar, J V A.
Ind. Eng. Chem., 31, 1146, (1939).

(124) Brounshtein, B I and Simakova, I V.
Chem. Abs., 87, 7988, (1977).

(125) Skelland, A H P and Minhans, S S.
A.I.Ch.E.J., 17, 1316, (1971).

(126) Popovich, A T, Jervis, R E and Trass, O.
Chem. Eng. Sci., 19, 357, (1964).

(127) Vrentas, J S, Liu, H T and Duda, J L.
Chem. Eng. J., 21, 155, (1981).

(128) Heertjes, P M and de Nie, L H.
"Mass Transfer to Drops, in Recent Advances in Liquid-Liquid Extraction",
ed.by C Hanson, pp. 367-400, Pergamon Press, (1971).

(129) Forsyth, J S et al.
Proc. Int. Solvent. Extr. Conf., Lyon, (ISEC), vol. 1, 417, (1974).

(130) Hughmark, G A.
Ind. Eng. Chem. Funds., 6, 408, (1967).

(131) Kinard, G E, Manning, F S and Manning W P.
Brit. Chem. Eng., 8, 326, (1963).

(132) Linton, M and Sutherland, K L.
Chem. Eng. Sci., 12, 214, (1960).

(133) Sideman, S and Shabtai, H.
Can. J. Chem. Eng., 42, 107, (1964).

(134) Griffith, R M.
Chem. Eng. Sci., 12, 198, (1960).

(135) Garner, F H and Suckling, R D.
A.I.Ch.E.J., 4, 114, (1958).

(136) Garner, F H, Jenson, V C and Keey, R T I.
Trans. Instn. Chem. Engrs., 37, 191, (1959).

(137) Rowe, P N, Claxton, K T and Lewis, J B.
Trans. Instn. Chem. Engrs., 43, 14, (1965).

(138) Kronig, R and Brink, J C.
Appl. Sci. Res., A.2, 142, (1950).

(139) Garner, F H and Skelland, A H P.
Ind. Eng. Chem., 46, 1255, (1954).

(140) Garner, F H, Foord, A and Tayeban, J.
Appl. Chem., 9, 315, (1959).

(141) Elizinga, E R and Banchero, J T.
Chem. Eng. Progr. Symposium, Ser., 55, 29, 149, (1959).

(142) Thorsen, G and Terjesen, S G.
Chem. Eng. Sci., 17, 137, (1962).

(143) Skelland, A H P and Cornish, A R H.
A.I.Ch.E.J., 9, 73, (1963).

(144) Yamaguchi, M, Fujamato and Katayama, T.
J. Chem. Eng. Japan, 8, 361, (1975).

(145) Skelland, A H P and Wellek, R M.
A.I.Ch.E.J., 10, 491, (1964).

(146) Yamaguchi, M, Watanabe, S and Katayama, T.
J. Chem. Eng. Japan, 8, 4151, (1975).

(147) Hendrix, C D, Dave, S B and Johnson, H F.
A.I.Ch.E.J., 13, 1072, (1967).

(148) Lochiel, A C and Calderbank, P H.
Chem. Eng. Sci., 19 471, (1964).

(149) Newman, A B.
Trans. Am. Inst. Chem. Eng., 27, 203, (1931).

(150) Vermeulen, T.
Ind. Eng. Chem., 45, 1664, (1953).

(151) Grober, H,
Z. Ver. dtsch. Ing., 69, 705, (1925).

(152) Handlos, A E and Baron, T.
A.I.Ch.E.J., 3, 127, (1957).

(153) Wellek, R M and Skelland, A H P.
A.I.Ch.E.J., 11, 557, (1965).

(154) Olander, D R.
A.I.Ch.E.J., 12, 1018, (1966).

(155) Patel, J M and Wellek, R M.
A.I.Ch.E.J., 13, 384, (1967).

(156) Treybal, R E.
"Liquid-Liquid Extraction", 2nd ed., McGraw-Hill Book Co., NY, (1963).

(157) Jeffreys, G V and Bonnet, J C.
J. Chem. Tech. Biotechnol, 33A, 176-186, (1983).

(158) West, R C.
"Handbook of Chemistry and Physics", 53rd Ed., The Chemical Rubber Co., (1972-1973).

(159) Seidell, A.
Solubilities of Inorganic and Organic Compounds, American Chemical Society, (1965).

(160) Wilke, C R and Chang, P.
A.I.Ch.E.J., 1, 264, (1955).

(161) Al-Hemiri, A A A.
PhD Thesis, University of Aston in Birmingham, UK, (1973).

(162) Sarkar, S.
PhD Thesis, University of Aston in Birmingham, UK, (1976).

(163) Goltz, G E and Glew, D N.
Analg. Chem., 29, 816, (1957).

(164) Vilhelm, V.
"Survey of Applicable Mathematics" by Rektorys, K. pp. 148, Iliffe Books Ltd., Czechoslovakia, (1969).

(165) Goldsmith, H L and Mason, S G.
J. of Colloid Science, 17, 448, (1962).

(166) Jeffreys, G V, Mumford, C J and Al-Aswad, K K.
A.I.Ch.E.J., pp. 1488, Sept. 1985.

(167) Othmar, D F, White, R E and Trueger, E.
Ind. Eng. Chem., 33, 1240, (1941).

(168) Ellis, W B.
PhD Thesis, University of Maryland, USA, (1966).

(169) Beek, W J and Kramers, H.
Chem. Eng. Sci., 17, 909, (1962).

(170) Lee, S Y.
F., Diss. Abst., 32B, 2140, (1971).

(171) Sternling, C V and Scriven, L E, A.I.Ch.E.J. 5, 514-423, (1959).